Folding and stability of Shikimate Kinase

Eleonora Cerasoli

A thesis submitted for the degree of Doctor of Philosophy

UNIVERSITY
of
GLASGOW

Institute of Biological and Life Sciences
October 2002

Declaration

The experimental work carried out in this thesis is my own work except where indicated.

This thesis is dedicated to my mother and my brother,
Luciana and Roberto.

Abstract

Shikimate kinase (SK; EC 2.7.1.71), an enzyme that catalyses the specific phosphorylation of the 3-hydroxyl group of shikimate using ATP as the phosphoryl donor, was chosen as a representative example of a subclass of α/β proteins with which to examine the unfolding, stability and mechanism of protein folding.

The equilibrium unfolding of the enzyme was monitored for SK in the absence and in the presence of shikimate and using both guanidinium chloride (GdmCl) and urea as denaturing agents. The changes in secondary and tertiary structure, monitored by far UV, circular dichroism (CD) and fluorescence respectively, could be fitted for both denaturants to a 2-state model giving an estimate of 17 kJ/mol as the stability of the folded state. The marked loss of activity and decrease in shikimate binding observed at low concentrations of GdmCl were found to be largely due to ionic strength effects associated with perturbation of the shikimate binding site.

The effects of different salts (NaCl, KCl, $CaCl_2$, $MgCl_2$, NaF, NaBr, $NaNO_3$ and Na_2SO_4) on the structure, activity, binding, and stability of SK have been investigated. The inclusion of salts leads to a marked stabilisation against unfolding of the enzyme by urea. Although the salts listed above have only small effects on far-UV CD and fluorescence spectra, NaCl and Na_2SO_4 were found to lead to a tightening of the structure of the enzyme as shown by the effect on the near-UV CD spectrum. All the salts studied have an effect on catalytic activity, which in general appears to be correlated with changes in ionic strength.

The refolding of SK after chemical denaturation using both urea and GdmCl has been studied in detail. This was performed using measurements of CD, fluorescence, activity, 8-anilino-1-naphthalene sulphonate (ANS) fluorescence, and employing both manual mixing and rapid reaction techniques. From these studies an outline pathway for the folding process has been formulated in which at least three intermediates are involved. The pathway described could act as a model for other members of the NMP kinase family of enzymes and the relevance of the results to the folding of other α/β domain proteins is discussed.

The unfolding of the enzyme by 4M urea could be prevented by inclusion of 1M NaCl or 0.33M Na_2SO_4, and the addition of these concentrations of salts to enzyme unfolded by 4M urea led to a slow but nearly complete regain of overall native secondary and tertiary structure, as judged by the regain of native-like CD and fluorescence. However, the refolded enzyme differs from the native form in terms of the degree of fluorescence quenching by iodide ions which suggests that the single Trp has only partially regained the positively charged environment provided by neighbouring Arg side chains and in terms of

the relatively weak binding of shikimate that can be observed by fluorescence quenching. While no binding of nucleotide could be detected directly there is some evidence for synergism in substrate binding which suggests that nucleotide may bind to some extent. However, the refolded enzyme does not possess detectable catalytic activity. During the refolding process brought about by addition of salt in the presence of 4M urea no change in the fluorescence of the probe ANS was observed, indicating that either an intermediate formed by hydrophobic collapse is unlikely to be significantly populated or that the concentration of the chaotropic agent used for denaturation displaces the dye by shear competition. The results point to both specific and general effects of salts on SK and are discussed in the light of the structural information available on the enzyme.

Additional experiments to investigate the effect of the residual ionic strength on the process of refolding after a denaturant jump were undertaken. In general the presence of NaCl and Na_2SO_4 lead to an increase in the refolding rate, while NaF seems to impair the efficiency of refolding.

Preliminary experiments to investigate the protection by substrates against inactivation of SK by the lysine-specific reagent pyridoxal-5'-phosphate (PLP) were carried out. The inclusion of shikimate, either alone or with ADP, does not appear to give any degree of protection against inactivation. The difference in the protection achieved in the presence of ADP or ATP points to the role of Lys 15 in the coordination of the γ-phosphate of ATP and that this interaction is necessary to achieve the conformational change in the enzyme required for catalysis.

Acknowledgments

First of all I would like to thank Professor Nicholas Price and the Universities of Stirling and Glasgow for giving me the opportunity to undertake these studies: Prof Price gave me the chance that neither the Italian Universities nor even the European community would have given to me.
I have learned a lot of things and for this reason I thank Prof. Price. I thank him for his patience and availability: whenever I needed help or advice he was always present, and if I have managed to finish my PhD on time it was mainly due to him. I thank him for all the things he taught me: I was really lucky to have him as a supervisor.

I would like to thank Dr. Sharon Kelly and John Greene for all the help they gave me. I thank my family for all the economic support and for the precious packs they sent me (Parmiggiano is very good when you have to think).

I thank Lewis and Bernard for their company in the university or when we met in the "research club" (nice name for a pub). I thank all the janitors for their help and information. Finally I thank Andy and my little fat dog Titch: I used to annoy her during my breaks while I was writing.

List of abbreviations used

2D-NMR, bi-dimensional nuclear magnetic resonance
AK, adenylate kinase
ANS, 8-anilino-1-naphthalene-sulphonate
Ap_5A, P^1,P^5-bis(5'-adenosyl)pentaphosphate
CD, circular dichroism
CDLs, caveolae-like domains
CMBF, classical mononucleotide-binding fold
DAHP, 3-deoxy-D-arabino-heptulosonic acid-7-phosphate
DEAE diethylaminoethyl
DHFRs dihydrofolate reductases
DHQ , dehydroquinate
DHQase, dehydroquinase
DHS, dehydroshikimate
DTT, dithiothreitol
EDTA ethylene diamine tetraacetic acid
EPSP, 5-enolpyruvoylshikimate 3-phosphate
ER, endoplasmic reticulum
FRET, fluorescence resonance energy transfer
GdmCl, guanidinium chloride
hCG-β, human chorionic gonadotropin β-subunit
HSP, heat shock protein
HX, hydrogen-exchange
LDH, lactate dehydrogenase
NADH nicotinamide adenine dinucleotide
NATA, N-acetyltryptophan amide
NBD, nucleotide binding domain
NMP, nucleoside monophosphate
ORD, optical rotary dispersion
PCDs, protein conformational disorders
PDB, protein data bank
PDI, protein disulphide isomerase
PEG, polyethylene glycol
PEP phosphoenolpyruvate
PK, pyruvate kinase
P-loop, phosphate-binding loop
PLP, pyridoxal-5'-phosphate
PPI, prolyl *cis-trans* isomerase
PrP, prion protein
RNase, ribonuclease
SF, stopped flow
SK, shikimate kinase
SRS, synchrotron radiation source
TNBS, 2,4,6-trinitrobenzenesulphonic acid
UK, uridylate kinase

CHAPTER 1: INTRODUCTION 6
1.1 Protein Folding *6*
1.1.1 The protein folding problem and its applications 6
1.1.1.1 The protein folding problem 6
1.1.1.2 Folding: industrial implications 6
1.1.1.3 Folding: clinical consequences and biological role of folding intermediates. 7
1.1.1.4 Folding in the cell 10
1.1.2 Kinetics and mechanism of protein folding. 15
1.1.2.1 Folding models 15
1.1.2.2 Folding funnels 16
1.1.2.3 Folding of small molecules 19
1.1.2.4 Folding of larger proteins 21
1.1.3 Protein structure, stability and cosolvent effects. 24
1.1.3.1 Protein structure and stability 24
1.1.3.2 Effect of co-solvent additives: salts 25
1.1.2 Methods for studying protein folding 27
1.2 The Shikimate pathway and Shikimate Kinase *29*
1.2.1 The Shikimate Pathway 29
1.2.1.1 An overview 29
1.2.1.2 The Steps of the pathway 31
1.2.2 Shikimate Kinase 34
1.2.2.1 The Shikimate Kinase reaction 34
1.2.2.2 The P-loop-containing nucleotide triphosphate hydrolases 35
1.2.2.3 The structure of shikimate kinase 38
1.2.2.4 Hinge-bending movements 43
1.2.2.5 Shikimate kinase as a model system for studying protein folding 44
1.3 Biophysical methods used in this work *46*
1.3.1 Circular Dichroism 46
1.3.1.1 Introduction 46
1.3.1.2 The CD of proteins 47
1.3.2 Fluorescence Spectroscopy 49
1.3.2.1 Theoretical background 49
1.3.2.2 Protein Fluorescence 51
1.3.2.3 Binding Studies 51
1.3.2.4 Quenching of Trp Fluorescence 52
1.3.3 Stopped flow CD and fluorescence 53
1.4 Aims of the project *53*
CHAPTER 2: MATERIALS AND METHODS 54
2.1 Enzyme purification *54*
2.2 Assay of enzyme activity *55*
2.3 Substrate binding studies *57*
2.4 Spectroscopic measurements *59*
2.5 Unfolding and refolding studies *62*
2.6 Chemical modification by pyridoxal-5'-phosphate (PLP) *65*
2.7 Studies of SK in the absence of chloride ions *68*
CHAPTER 3: THE FOLDING OF TYPE II SHIKIMATE KINASE 69
3.1 Abstract *69*
3.2 Introduction *70*
3.3 Unfolding of the enzyme *72*
3.3.1 Conformation of the enzyme in solution, kinetic parameters and aggregation 72
3.3.1.1 SK circular dichroism spectra 72
3.3.1.2 Specific activity and kinetic parameters. 75
3.3.1.3 Protein Stability 78
3.3.2 Equilibrium Unfolding with GdmCl and Urea 80
3.3.3 Denaturation of SK in the presence of substrates 86
3.3.4 Changes in K_d of substrates in the presence of denaturants 89

3.3.5 Changes of activity in the presence of denaturants 91
3.3.6 Effect of denaturants on quenching of Trp fluorescence 93
3.4 Refolding of the enzyme *94*
3.4.1 Refolding after unfolding in GdmCl 94
3.4.1.1 Regain of activity 94
3.4.1.2 Regain of fluorescence intensity 95
3.4.1.3 Refolding in the presence of shikimate 96
3.4.1.4 Refolding in the presence of NaI 96
3.4.1.5 Light scattering measurements and refolding in the presence of ANS 97
3.4.2 Refolding after unfolding in urea 99
3.4.2.1 Regain of activity. 99
3.4.2.2 Regain of secondary structure on refolding 100
3.4.2.3 Unfolding kinetics and effect of incubation time on the refolding kinetics 103
3.4.2.4 Regain of fluorescence intensity on refolding 105
3.4.2.5 Refolding in the presence of shikimate 107
3.4.2.6 Refolding in the presence of ADP and ATP 110
3.4.2.7 Refolding in the presence of sodium iodide 111
3.4.2.8 ANS as a probe for the formation of early intermediates. Preliminary experiments 114
3.4.2.9 ANS as a probe during refolding 119
3.4.3 Model of folding pathway and properties of intermediates 122
3.4.4 Comparison with studies on the refolding of adenylate kinase 124
Appendix 3.1: Chemical modification of SK by pyridoxal-5'-phosphate. *126*
CHAPTER 4: EFFECTS OF SALTS ON THE FUNCTION, CONFORMATIONAL STABILITY AND REFOLDING KINETICS OF SHIKIMATE KINASE 131
4.1 Abstract *131*
4.2 Introduction *133*
4.3 Fluorescence and CD spectra: the effect of salts *136*
4.3.1 UV and Fluorescence Spectra 136
4.3.2 Circular dichroism spectra 140
4.4 Effect of salts on the activity and the kinetic parameters *144*
4.5 Effects of salts on binding of shikimate *148*
4.6 Effects of salts on the binding of nucleotides *152*
4.6.1 ADP binding 152
4.6.2 ATP binding and comparison with ADP titration curves 154
4.7 Effects of salts on the quenching of fluorescence by NaI *158*
4.8 Equilibrium unfolding in the presence of different salts *159*
4.9 Conclusions *163*
4.10 Refolding of enzyme in 4M Urea by addition of salts *164*
4.10.1 Spectroscopic studies 165
4.10.1.1 Regain of secondary structure 165
4.10.1.2 Regain of fluorescence intensity 168
4.10.1.3 Refolding in the presence of ANS 169
4.10.1.4 Refolding in the presence of NaI 171
4.10.1.5 Comparison between the refolding traces obtained by different techniques. 174
4.10.2 Substrate binding and activity studies 176
4.10.3 The location of the chloride ions in shikimate kinase 179
4.10.4 Structural basis for effects of salts on shikimate kinase 181
4.11 Conclusions *182*
Appendix 4.1 Refolding of SK in the presence of salts *183*
A4.1.1 Regain of Activity 183
A4.1.2 Regain of secondary structure 184
A4.1.3 Regain of fluorescence intensity 186
A4.1.3.1 Preliminary Light scattering experiments 186
A4.1.3.2 Regain of fluorescence intensity in the presence of chloride 187
A4.1.3.3 Regain of fluorescence intensity in the presence of sulphate 190

A4.1.3.4 Refolding in the presence of fluoride 191
A4.1.4 Refolding with salts in the presence of sodium iodide 192
A4.1.5 Refolding in the presence of ANS 193
A4.1.5.1 ANS spectra in the presence of NaCl 193
A4.1.5.2 Refolding in the presence of ANS 195
A4.1.6 Conclusions 195
Appendix 4.2: Refolding in the presence of salts: fitting values *196*
CHAPTER 5: GENERAL DISCUSSION 198
5.1 Activity and ligand binding studies *198*
5.2 Stability studies: Chemical denaturation *200*
5.3 Refolding after denaturation *201*
5.4 Future work *203*

Table 1.1: List of some Protein Conformational Disorders and the protein involved 8
Figure 1.1: The energy landscape for a folding protein. 18
Figure 1.2: Scheme of models for folding of small and large proteins. 18
Figure 1.3: The reactions of the Shikimate Pathway 30
Figure 1.4: Position of dehydroquinase in the shikimate and quinate pathways. 34
Figure 1.5 Reaction catalysed by Shikimate Kinase. 35
Table 1.2: P-loop contacts in the classical mononucleotide-binding fold (CMBF) family: 38
Figure 1.6: The structure of shikimate kinase (Krell *et al.*, 1998). 41
Figure 1.7: Structure of SK: P-loop region and bound ADP 42
Figure 1.8: The adenosine binding motif 42
Figure 1.9: SK structure: position of the P-loop, adenine and shikimate binding domains 45
Figure 1.10: Position of the side chains of Arg11, Arg58 and Arg139. 45
Figure 1.11: Effect of an absorbing chiral medium on linearly polarised light. 47
Figure 2.1: Double coupled assay scheme 56
Figure 2.2 : First set of controls for the chemical modification experiments. 66
Figure 2.3: Effect of incubation time and stirring on SK activity 67
Figure 2.4: Effect of residual concentration of $NaBH_4$ on SK activity. 67
Figure 3.1: Comparison of the far- (a) and near- (b) UV CD spectra in Tris and MOPS 73
Figure 3.2: The far UV CD spectrum of SK. 74
Figure 3.3: Normalised fluorescence spectra (F_n/F_{350}) in Tris-HCl and MOPS 74
Table 3.1: Kinetic and binding parameters of shikimate kinase 76
Figure 3.4: Binding of substrates determined by fluorescence quenching experiments. 77
Table 3.2: Stability measurements. Activity 78
Figure 3.5: Fluorescence spectra effect of storage at room temperature (20°C) 79
Figure 3.6: Denaturation curves of SK using GdmCl and urea and spectra of native and denatured protein. 82
Figure 3.7: The unfolding of SK in the presence of urea and GdmCl. 84
Figure 3.8: Urea denaturation in MOPS buffer. 85
Figure 3.9: Quenching of the fluorescence due to the presence of shikimate 87
Figure 3.10: Effect of shikimate on the near-UV CD spectrum of SK.. Near UV spectra, protein concentration 0.5mg/ml, cell pathlength 0.5cm. The black and the red lines refer to enzyme in the absence of shikimate and in the presence of 2mM shikimate. 87
Figure 3.11: Unfolding of SK in the presence of shikimate. 88
Figure 3.12: The effect of denaturants and NaCl on the binding of substrates to SK. 90
Figure 3.13: Effect on the activity of denaturants and NaCl. 92
Figure 3.14: The kinetics of regain of activity of SK after denaturation in 2.8M GdmCl. 94
Figure 3.15: The kinetics of changes in protein fluorescence. 95
Figure 3.16: Normalised spectra of the solutions of the refolding experiment in GdmCl. 96
Figure 3.17: The kinetics of changes in quenching of fluorescence by iodide 97
Figure 3.18: The kinetics of changes in ANS fluorescence at 480nm 98
Figure 3.19: The kinetics of regain of activity of SK after denaturation in 4M urea. 99

Figure 3.20: The kinetics of changes in ellipticity at 225nm 100
Figure 3.21: CD spetra of the refolded solution after denaturation in 4M urea 101
Figure 3.22: The kinetics of changes in ellipticity at 225nm 102
Table 3.3: Effect on the incubation time on the kinetic parameters.....103
Figure 3.23: The kinetics of changes in protein fluorescence during unfolding 103
Figure 3.24: Effect of the incubation time on the refolding kinetics as monitored by fluorescence.....104
Figure 3.25: The kinetics of changes in protein fluorescence at 350nm using manual mixing 105
Figure 3.26:The kinetics of changes in protein fluorescence at 350nm using stopped flow mixing.....106
Figure 3.27: Fluorescence spectra before and after refolding in the presence of shikimate 108
Figure 3.28:The kinetics of changes in protein fluorescence at two different wavelegths....108
Figure 3.29:The kinetics of changes in protein fluorescence in the presence of shikimate..109
Figure 3.30: Kinetics of changes in protein fluorescence in the presence of nucleotides 110
Table 3.4: K_{sv} values for SK under different conditions.....111
Figure 3.31: Stern-Volmer plots of SK in different conditions.....112
Figure 3.32: The kinetics of changes in quenching of fluorescence by iodide.....113
Figure 3.33: Effect of ANS on the secondary structure of SK.....115
Figure 3.34: The kinetics of regain of activity of SK in the presence of 40μM ANS. 115
Figure 3.35: ANS spectra (40μM) in buffer, in 4M urea and in 0.36M urea. 117
Figure 3.36: SK.ANS spectra (40 μM) in in the presence of 2mM shikimate. 118
Figure 3.37: Shikimate titration in the presence of ANS.....118
Fig. 3.38: The kinetics of changes in ANS fluorescence at 480nm.....119
Figure 3.39: The kinetics of changes in ANS fluorescence at 480nm 120
Figure 3.40: The kinetics of changes in ANS fluorescence in the presence of shikimate. ...121
Table 3.5: Properties of intermediates in the refolding of shikimate kinase 123
Figure A3.1: Time-courses of inactivation of SK by PLP.....128
Figure A3.2: Pseudo-first-order plots of inactivation of SK at various PLP concentrations. 129
Figure A3.3: PLP inactivation:effect of shikimate, alone and with ADP. 129
Figure A3.4: PLP inactivation: effect of nucleotide substrates.....130
Figure A3.5: Effect of NaF and ADP on the time-course of inactivation of SK by PLP 130
Figure 4.1: Calculation of the light scattering contribution at 280nm. 136
Figure 4.2: Effect of added NaCl on the decrease in fluorescence intensity at 20°C.....137
Figure 4.3: Effect of NaCl on Trp fluorescence. 138
Figure 4.4: Effect of KCl, $CaCl_2$, NaF and NaBr on Trp fluorescence.....139
Figure 4.5: Effect of Na_2SO_4 on intrinsic Trp fluorescence. 140
Figure 4.6: Circular dichroism spectra of SK in the presence of NaCl.....141
Figure 4.7: Circular dichroism spectra of SK in the presence of NaCl , KCl and NaF.....142
Figure 4.8: Effects of other salts on the CD spectra of shikimate kinase.....143
Figure 4.9: Near-UV CD spectra of SK in the presence of 1M NaCl and 0.33M Na_2SO_4 143
Figure 4.10: Effects of salts on the activity of shikimate kinase.....146
Table 4.1: Controls of the quenched assay procedure 146
Table 4.2: Effects of salts on the activity of shikimate kinase 147
Table 4.3: Effects of salts on the kinetic parameters of SK.....147
Table 4.4: Binding of shikimate in the presence of different salts. 149
Table 4.5: Titration with salts in the presence of shikimate.....149
Table 4.6: Binding of shikimate in the absence and presence of ADP.....150
Figure 4.11: Titration with salts: effect on the shikimate binding. 150
Figure 4.12: Binding of shikimate in the presence of salts; effect of the presence of ADP. .151
Table 4.7: ADP binding 152
Figure 4.13: ADP binding in the presence of salts 154
Table 4.8: ATP binding in the presence of salts. 155
Figure 4.14: Titration curves for ATP obtained in buffers Tris and MOPS.....155
Figure 4.15: ATP titrations in the presence of salts.....157

Table 4.9: Stern-Volmer constants for the quenching of Trp54 fluorescence by NaI 158
Figure 4.16: Urea-induced unfolding in the presence of NaCl and KCl. 160
Figure 4.17: Urea-induced unfolding in the presence of Na_2SO_4 161
Figure 4.18: Urea-induced unfolding in the presence of NaBr, $MgCl_2$ $CaCl_2$, and NaF.....161
Table 4.10: Values of $[Urea]_{1/2}$ for unfolding of SK 162
Figure 4.19: Refolding of denatured SK by addition of salts monitored by CD. 165
Figure 4.20: Kinetics of changes in ellipticity at 225nm on addition of 1M NaCl to SK. 166
Figure 4.21: Kinetics of changes in ellipticity at 225nm on addition of 0.33M Na_2SO_4 167
Figure 4.22: Refolding of denatured SK by addition of salts monitored by fluorescence. ...168
Figure 4.23: Refolding of denatured SK by addition of salts monitored by fluorescence. 169
Figure 4.24: Tryptophan emission spectra of SK refolded in 4M Urea and salts. 170
Table 4.11: Stern-Volmer constants for the quenching of Trp54 fluorescence by NaI.....171
Figure 4.25: Refolding of denatured SK by addition of salts monitored by fluorescence. 172
Figure 4.26:Fluorescence emission spectra of refolded SK solution in the presence of NaI172
Figure 4.27: Comparison between salt-induced refolding in the absence and presence of NaI. 173
Figure 4.28: Comparison between salt-induced refolding in the absence and presence of NaI. 173
Figure 4.29: Comparison of different traces obtained after the salt-induced refolding.....175
Table 4.12: Binding of shikimate to SK in the absence and in the presence of ADP.....177
Figure 4.30: Binding of shikimate to refolded SK 177
Figure 4.31: Binding of shikimate to refolded SK in the absence and presence of ADP.....178
Figure 4.32: A stereoview of the native shikimate kinase structure. 180
Figure A4.1: The kinetics of regain of activity: effect of added NaCl and Na_2SO_4 183
Figure A4.2: Kinetics of changes in ellipticity in the presence of salts (manual mixing).....185
Figure A4.3: Kinetics of changes in ellipticity in the presence of 1M NaCl (stopped flow) ...186
Figure A4.4: Kinetics of changes in protein fluorescence in the presence of NaCl. 188
Figure A4.5: Protein concentration dependence of the kinetics of refolding. 188
Figure A4.6: Kinetics of changes in protein fluorescence in the presence of NaCl and KCl 189
Figure A4.7: Kinetics of changes in protein fluorescence in the presence of 1M NaCl. 189
Figure A4.8: The kinetics of changes in protein fluorescence in the presence of Na_2SO_4. ..190
Figure A4.9: Kinetics of changes in protein fluorescence in the presence of NaF 191
Figure A4.10: Normalised fluorescence spectra (refolded solution) in the presence of NaF192
Figure A4.11: Refolding of denatured SK in the presence of 1M NaCl (NaI 0.1M) 192
Figure A4.12: ANS spectra (40 μM) in buffer and in the presence of NaCl and Urea.....194
Figure A4.13: Changes in ANS fluorescence in the presence of 1M NaCl. 195
Table A4.1: Values of the fitting of refolding in the presence of salt (denaturant dilution) ...197
Table A4.2: Values of the fitting of the refolding traces (ionic strength jump experiments) 197

Chapter 1: Introduction

1.1 Protein Folding

1.1.1 The protein folding problem and its applications

1.1.1.1 The protein folding problem

A protein molecule is composed of a polypeptide sequence that meets both thermodynamic and kinetic folding requirements: it possesses a unique native state that is stable under physiological conditions, and it is able to find that state in a reasonable time (Levinthal, 1968). Understanding the mechanism by which proteins acquire this structure is known as "the protein folding problem" and the solution of this problem will require a detailed knowledge of the sequence of conformational events that leads from the ensemble of denatured states to the native protein. It is possible to divide this problem into a number of related questions: what is the physical basis of the stability of the folded protein conformation; what processes determine that a protein adopts its native conformation; what are the rules that link the amino acid sequence to the three-dimensional structure of a protein. If the three-dimensional structure of a protein can be predicted from its amino acid sequence (often referred as cracking the second half of the genetic code), this would provide the "missing link" in the flow of information between a gene sequence and the 3D structure of a protein (Creighton, 1990; 1994). Protein folding is no longer a purely academic research topic, as is illustrated by both biotechnological applications and by clinical consequences.

1.1.1.2 Folding: industrial implications

Transcription and translation of a recombinant gene do not always lead to the accumulation of a folded fully active protein. Instead, recombinant gene expression may lead to the production of protein in an inactive insoluble form known as an inclusion body, an extremely dense structure, different from amorphous precipitated protein. Inclusion bodies bear some similarities to true protein crystals in that, although not apparently ordered, they tend to be monocomponent and of extremely high packing density (Thatcher and Hitchcock, 1994). The reason for the formation of the inclusion bodies is probably associated with the particular environment in which the foreign protein accumulates, which can be quite different from the natural situation. In order to make a useful product this insoluble protein has first to be solubilized and then refolded artificially (Lilie *et al.*, 1998). Despite the possible disadvantages associated with the solubilization of inclusion bodies and *in vitro* renaturation, there are also advantages to their use as starting materials. In contrast to soluble products, the isolation steps for inclusion bodies are relatively simple and result in a concentrated and relatively pure protein. For this reason many studies have dealt with the

improvement of the refolding yield of recombinant proteins produced by overexpression in *Escherichia coli*. Most commonly, aggregates are solubilized in a strong chaotrope, such as 8M guanidinium chloride (GdmCl), which results in nearly complete unfolding of the protein molecules. Once soluble and unfolded, the proteins are first diluted with additional GdmCl solution and then refolded by removing the chaotrope by dialysis or additional dilution (De Bernardez Clark, 1998). The refolding step, however, is difficult and depends strongly on renaturing conditions. A number of variations have been proposed to the standard procedure (De Bernardez Clark, 2001). Some of these utilise standard chromatographic procedure (Batas *et al.*, 1999), others use high pressure in place of high concentrations of chaotrope agent (St. John *et al.*, 1999; Randolph *et al.*, Int. Appl. WO 00/02 901, 2001).
In the cases of proteins that do not refold using conventional methods, the use of mini-chaperones immobilized on agarose gel has been proposed (Altamirano *et al.*, 1997).
In many cases, folding has been achieved by manipulation with additives, such as salts, polyethylene glycol (PEG) or micelle-forming surfactants (Cleland and Wang, 1990; Wetlaufer and Xie, 1995). Since the efficiency of protein folding is largely determined by the rates of folding, unfolding and aggregation, it is important to know the influence of additives on these rate constants in order to obtain high folding yields (section 1.1.3.2). Refolding of denatured proteins is now recognised as a discrete and pivotal unit operation in the production of several products of industrial importance such as interferon beta 1-b (Betaferon® Schering), interleukin 2 (Proleukin® - Cetus (Chiron)) (Dorin *et al.*, 1998; U.S. patent 4,748,234) and the tissue plasminogen activator (Repilysin® - Roche) (De Bernardez Clark, 2001).

1.1.1.3 Folding: clinical consequences and biological role of folding intermediates.

Because the aqueous environment (pH, temperature, ionic strength, presence of chaotropic agents) strongly influences the conformation adopted by the polypeptide, it is an unanswered question which conformational changes proteins may experience upon migrating from one compartment to another of the cell. It is believed that folding and unfolding play an important role in the mechanisms and control of a broad spectrum of cellular processes, failures of which can lead to cellular malfunctions and to disease.
In particular it was demonstrated that compact folding intermediates (Christensen and Pain, 1994) (section 1.1.2 and 1.1.3) play an important role in processes such as: the recognition of proteins by chaperones (Martin *et al.*, 1991; Hendrick and Hartl, 1993); the interaction and penetration of proteins into membranes (Bychkova *et al.*, 1988; van der Goot *et al.*, 1991; Banuelos and Muga, 1995); the specificity of DNA-binding proteins (Hornby *et al.*, 1994); protein transport (Lindsay and Glover, 1992) and virus and phage caspid assembly processes (Kirkitadze *et al.*, 1998; Tume and Thomas, 1997). In addition, some evidence

indicates that certain mutations could be connected with incomplete protein folding, blocking it at the stages of compact intermediates (Lascu *et al.*, 1997), and this could lead to mislocation of proteins in a cell and may provoke genetic diseases (Bychkova and Ptitsyn, 1995). Misfolding of proteins does not need to involve mutations, but can be triggered by a variety of factors, such as protein overexpression, temperature, oxidative stress and activation of various signalling pathways linked to protein folding and quality control machinery. In the last few years, a variety of diseases have been shown to arise from protein misfolding. This group of diseases correlated with protein misfolding are now grouped together under the name of "protein conformational disorders" (PCDs) (Soto, 2001); some of these are reported in Table 1.1.

Protein Involved	Disease
β-Amyloid	Alzheimer's disease
α-Synuclein	Parkinson disease
Amylin	Diabetes Type 2
Superoxide dismutase	Amyotrophic lateral sclerosis
β_2-Microglobulin	Haemodialysis-related amyloidosis
CFTR protein	Cystic fibrosis
Hemoglobin	Sickle cell anemia
Huntingtin	Huntington disease
PrP	Creutzfeldt-Jakob disease and related disorders

Table 1.1: List of some Protein Conformational Disorders and the protein involved (Soto, 2001)

A common feature of most conformational diseases is the conversion of the soluble proteins into insoluble tertiary and quaternary structures with extensive β-sheet content (Kaytor and Warren, 1999). The conformational change can contribute to pathology through a variety of inter-related mechanisms that include loss of function of the misfolded protein, gain of a toxic activity or damage triggered by the accumulation of the misfolded form inside or outside cells. The latter can interfere with the normal cell function by a variety of possible mechanisms including apoptosis (Sanders and Nagy, 2000). The ability to form fibrils *in vitro* is not limited to the disease-associated proteins (Glenner *et al.*, 1974; Guijarro *et al.*, 1988; Chiti *et al.*, 1999b; Fandrich *et al.*, 2001): this has led to the idea that aggregation can

be viewed as a general property of polypeptide chains. In fact, as already mentioned, a common feature of these diseases is the formation of a β-sheet core which involves interactions between the atoms of main-chain amino acids that occur in all proteins (Ellis and Pinheiro, 2002).

The prion diseases provide an interesting example of the connection between protein folding and neurodegenerative disease (Cohen, 1999). It is believed that the prion protein (PrP), from a benign cellular conformation (PrP^{c}) (bound to the external surface of the plasma membrane by a glycosylphosphatidylinositol (GPI)-anchor), is transformed to a neurotoxic form (PrP^{sc}) that self-propagates by recruiting and inducing the conformational change in additional PrP^{c} molecules (Prusiner, 1997; Dagget, 1998; Westaway *et al.*, 1998). This hypothesis, known as the "protein-only" hypothesis, is supported by strong experimental evidence (Prusiner, 1998; Aguzzi and Weismann, 1997; Saborio *et al.*, 2001). The molecular details of the replication process are not completely known, and a large number of studies have been carried out both on the recombinant protein in solution and in a membrane environment. PrP displays intrinsic plasticity in its conformations (Hope *et al.*, 1996; Kelly, 1998): it is thought that portions of the PrP^{c} may posses a relatively open conformation which makes it susceptible to conversion into PrP^{Sc} under appropriate conditions (Baskakov *et al.*, 2002; Zhang *et al.*, 1997).

Since sub-cellular compartmentalisation implies different chemical environments and the PrP^{c} conformation depends on the phase composition, it is possible that this protein is able to assume various conformations in different cell compartments (Kelly, 1998; Pergami *et al.*, 1999). The hypothesis was advanced that, while the funnel model (section 1.1.2.2) generally considers the end point of folding a unique, native state, corresponding to the global free-energy minimum of the system, the inclusion of possible multiple conformers at the bottom of the energy funnel would be more appropriate (Ma *et al.*, 1999; Ferreira *et al.*, 2001). The membrane environment plays an important role in determining the conformation of the prion protein (Morillas *et al.*, 1999): some domains of the plasma membrane, caveolae-like domains (CDLs) (Kurzchalia and Patron, 1999; Campbell *et al.*, 2001), might be the sites where prions are propagated (Vey *et al.*, 1996; Massimino *et al.*, 2002). Moreover it has been proposed that folding intermediates may have a role in the conformational transition. In fact it was demonstrated that the PrP^{c} form while under native conditions shows very little tendency to undergo a transition to a β-sheet-rich structure, at a given concentration of NaCl (50-150mM), the rate of the α-helix → β-sheet transition increases as the concentration of urea is increased up to approximately 3.5M. Since urea increases the population of the unfolded protein, there is the possibility that one or more monomeric folding intermediates of prion protein may be involved in the transition to the oligomeric scrapie-like form (Morillas *et al.*, 2001).

Other studies on secreted oligomers of amyloid β-protein (Walsh *et al.*, 1999; 2002) and on aggregates formed by non-disease related proteins (Bucciantini *et al.*, 2002), suggest that early aggregates may be the primary toxic species (Lansbury Jr., 1999; Ellis and Pinheiro, 2002). This is supported also by the experimental finding that significant tissue damage and clinical symptoms of most of the conformational diseases appear before protein aggregates can be detected (Soto, 2001). In this scenario, the formation of large protein aggregates deposited in the tissue could even be considered a protective device because this allows the deposition and isolation of the toxic abnormally folded proteins (Lansbury Jr., 1999).

The knowledge of the folding process that leads to the formation of fibrillar inclusions could help in finding ways to inhibit the transition from native structures or drive proteins away from non-productive or disease-forming states (Kelly, 1998; Guerois and Serrano, 2001). The fact that this strategy could be a useful approach towards the treatment of these kinds of diseases, is demonstrated by recent findings that synthetic peptides, called "mini-chaperones", designed to be similar to the sequence of the protein region responsible for the self-association, dissolved amyloid aggregates *in vitro* and in animal models of Alzheimers' disease (Soto *et al.*, 1998, Sigurdsson *et al.*, 2000).

1.1.1.4 Folding in the cell

Many proteins require assistance to fold in the cell, although the basic principle remains that the amino acid sequence of a protein is sufficient to specify its three-dimensional structure. There are two major differences between the refolding of a denatured protein chain in a test tube and the folding of a newly synthesised chain inside the cell. Firstly, protein chains are made inside cells in a vectorial fashion by ribosomes. In many cases the rate of this process is slower than the rate of protein folding, thus there is the possibility that the elongating chain will misfold before it is complete and either be degraded or form aggregates. Secondly, the environment in which the folding takes place *in vivo*, is a complex one. High concentrations of different kinds of molecules (as well as the nascent chain) and ions are present, and this highly crowded macromolecular environment might lead to formation of potentially toxic aggregates (Ruddon and Bedows, 1997). Moreover the cellular compartmentalisation implies that the protein may be subject to various processing events important not only for function, but also for determining its extra- or intra-cellular location (Frydman, 2001; Ellis and Hartl, 1999).

In the cell there are at least two classes of proteins involved in polypeptide folding: the first class includes enzymes that catalyse specific isomerization steps or covalent changes essential for the formation of the native and functional conformations of the proteins concerned. A second class consists of families of proteins known as molecular chaperones

that modulate and promote protein folding, assembly and disassembly, and facilitate the degradation of misfolded polypeptides (Gething and Sambrook, 1992). To the first class belong enzymes such as the protein disulphide isomerase (PDI, EC 5.3.4.1) (Gilbert, 1994) and the prolyl *cis-trans* isomerase (PPI, EC 5.2.1.8) (Nall, 1994): these lead to an increase in the refolding rate for many proteins *in vitro* (Weissman and Kim, 1993; McClelland *et al.*, 1995).

The PPIs are enzymes that catalyses Xaa-Pro isomerization *in vitro* accelerating the refolding of proteins in which the *cis-trans* isomerization is responsible for an observed slow kinetic phase. Three families of PPI exist which do not show sequence similarity: the cyclophilins (Fischer *et al.*, 1984), the FK506-binding proteins (Siekierka *et al.*, 1989; Harding *et al.*, 1989) and the parvulins (Rahfeld *et al.*, 1994). Some members of the PPI family are thought to be involved in some important processes such as cell signalling and regulation (Brazin *et al.*, 2002), protein trafficking and transcription (Schiene-Fischer and You, 2001; Harrar *et al.*, 2001).

PDI is an enzyme which is present in the lumen of the endoplasmic reticulum (ER) and which catalyses the rate-limiting reactions of disulphide-bond formation, isomerization and oxidation within the ER; it displays chaperone activity both *in vitro* and *in vivo* (McClelland *et al.*, 1995; Ferrari and Soling, 1999; Winter *et al.*, 2002). The chaperone and the isomerase activities are in a way independent from each other but function in collaboration, possibly at consecutive stages of the folding process of the target protein (Freedman *et al.*, 2002). Under the reducing condition of the cytoplasm, endosomes and cell surface, PDI catalyses the reduction of protein disulphides. At those locations, PDI has been demonstrated to participate in the regulation of various physiological processes such as cell adhesion (Pariser *et al.*, 2000), platelet activation (Essex *et al.*, 1995; 1999; 2001) and integrin-dependent adhesion, at least in one cell type, namely the lymphocyte (Lahav *et al.*, 2000), leading to the hypothesis that disulphide exchange takes place during the process.

The molecular chaperones (heat shock protein (HSP), so called because their expression is induced under condition of cellular stress, such as an increase in temperature) are proteins that bind to and stabilize an otherwise unstable conformer of another protein (Hlodan and Hartl, 1994). HSPs are involved in a multitude of processes in different cellular compartments, wherever the folded state of a protein has to be achieved *de novo*, stabilized under stress conditions, or modulated to regulate its activity. HSPs are involved in the folding and assembly of proteins within cellular organelles, in the disassembly of oligomeric structures (Price, 1994) and in preventing incorrect interactions within and between non-native polypeptides, thus typically increasing the yield but not the rate of folding reactions (Hartl, 1996; Ellis and Hartl, 1999). At present, the two best understood chaperones are the

hsp70 and hsp60 families (Hendrick and Hartl, 1993). The hsp70s are 70 kDa ATPases found in the cytosol which bind to the nascent polypeptide chain avoiding aggregation.

The hsp60 chaperones, called "chaperonins", play a role in folding once the synthesis of the polypeptide chain is complete. They prevent aggregation of partially folded chains, allow folding in a protected environment, and also play a role in complex assembly and polypeptide translocation. The best-studied member of the family is GroEL, the *E. coli* chaperonin (Ranson *et al.*, 1998). The chaperonin GroEL and its ring shaped cofactor GroES facilitate protein folding in an ATP-regulated manner, forming the so-called GroE system (Houry *et al.*, 1999). GroEL recognizes non-native states in protein folding pathways and acts to prevent aggregation, which principally results from the exposure of hydrophobic surfaces in the early folding stages (Martin *et al.*, 1991; Wang *et al.*, 1999). Some proteins require several rounds of interaction with GroEL to reach their native state (iterative annealing) (Horovitz, 1998). GroEL interacts *in vitro* with almost any non-native model protein. However, *in vivo* GroEL is involved in the folding of only 10% of newly (so not under stress condition) translated polypeptides, indicating a preference for a subset of *E.coli* proteins. Structural analysis revealed that these proteins have a complex domain architecture, mostly containing two or more domains with α/β-folds (Houry *et al.*, 1999).

The role of HSPs is not restricted to assisting folding. They have an essential role in the mantainance of the translocation-competent state of precursor proteins. Because the formation of stable folded structure inhibits translocation of proteins across membranes, it was proposed that the "translocation-competent" conformations may resemble the "molten globule" or collapsed intermediate forms observed in the refolding of proteins *in vitro*. This provides a protein with the conformational flexibility necessary to adopt an extended structure during membrane transit.

HSPs are also involved in the degradation of misfolded proteins as well as in regulatory processes (Hartl, 1996; Horwich *et al.*, 1999). Because the events of cell stress and cell death are linked, HSPs induced in response to stress appear to function at key regulatory points in the control of apoptosis. HSPs include anti-apoptotic and pro-apoptotic proteins that interact with a variety of cellular proteins. They are commonly overexpressed in human tumours and their expression in certain cancer types correlates with poor prognosis and resistance to therapy: the ability of HSPs to prevent apoptosis induced by several anticancer drugs as well as other apoptotic stimuli suggests that they could enhance tumorigenesis and limit the efficency of cancer therapy (Jaattela, 1999). This has lead to the hypothesis that apoptosis-inhibitory HSPs may participate in carcinogenesis (Garrido *et al.*, 2001). It was demonstrated that the high expression of Hsp70 is required for the survival of tumorigenic breast cancer cells, and abrogation of Hsp70 synthesis results in extensive cell death (Nylandsted *et al.*, 2000).

In addition HSPs seem to have a role in the activation of integrins (Barazi *et al.*, 2002) and in prion diseases (Talzelt *et al.*, 1998; Stockel and Hartl, 2001). Recent studies have demonstrated that HSPs exit the mammalian cells, interact with the cells of the immune system and exert immunoregulatory effects (Asea *et al.*, 2002). Some findings indicate that certain HSPs can function as effective vaccines against the same tumour from which they are purified by virtue of their ability to bind tumour-specific peptides (Bremers and Parmiani, 2000); some of these vaccines are already in clinical trials (no author listed - BioDrugs 2002).

The "steric chaperones" (e.g.: the pro-region of some proteases), are another kind of chaperones that work in a different way from the molecular chaperons (Ellis, 1998) having as a distinguishing feature a high substrate specificity (Braun and Tommassen, 1998).
The folding-related roles of the pro-region may be classified into two types: in the first, the pro-region acts as an intramolecular chaperone to overcome kinetic barriers to folding, as in the case of substilin (Shinde and Inouye, 1995 a, b); in the second the pro-region acts as a thermodynamic stabilizer, through uncleaved disulphide bonds, as in the case of zymogens (Ma *et al.*, 2000). As an example of the first type are substilin and α-lytic protease pro-regions. When the mature enzymes are purified and denatured they fail to refold into active enzymes on removal of the denaturant. Instead, they adopt compact, partially folded conformations approximating the molten globule state. Such states are stable until the specific pro-sequence is added, when conformational changes occur resulting in the appearance of the correct tertiary structure for enzymic activity (Baker *et al.*, 1992; Eder *et al.*, 1993). Each pro-sequence is likely to act only on the molecule to which it is attached and it is then degraded. The pro-sequence seems to impart steric information for the folding of the protease domain, but after folding it is no longer required to maintain that particular conformation. In fact it was demonstrated that a mutation in the pro-sequence causes a conformational change in the mature substilin (Shinde and Inouye, 1997). Although identical in sequence to the wild type, this form of substilin shows slight differences in circular dichroism spectra, thermal stability and K_m for a synthetic substrate.
Because these pro-peptides are necessary for the correct folding of these classes of proteins they were termed "intramolecular chaperones". Summarising, the mechanism of maturation of intramolecular chaperones consists of three steps: 1) folding of the mature region, which is mediated by the intramolecular chaperone 2) cleavage of the intramolecular chaperone (autoprocessing) to give a non-covalently attached 1:1 pro-peptide-mature protein complex 3) removal of the pro-peptide by an autoproteolytic degradative process (Shinde and Inouye, 1995 a, b).
A covalent interaction of a steric chaperone with its target protein is not a prerequisite for substrate specificity. For example the folding of many lipases from *Pseudomonas spp.*

requires the activity of a lipase-specific foldase, Lif, which is produced as a separate polypeptide (Braun and Tommassen, 1998).

Because of the difficulties in applying high resolution structural techniques to the acquisition of structure accompanying or following translation *in vivo*, the usual experimental approach has been to study the refolding of denatured proteins when conditions have been changed to promote folding. Several lines of evidence indicate that this approach can give valid insights into the process of protein folding *in vivo* (Jaenicke, 1987; Huth *et al.*, 1993).
In fact the rate of folding of small proteins *in vitro* seems to match the rate of folding *in vivo*, and the final product results to be the same (e.g.: for enzymes there is the recovery of catalytic activity). More importantly there are evidences that the steps of protein folding do not change when the refolding is carried out inside the cell or *in vitro*. Studies on structurally homologous dihydrofolate reductases (DHFRs) show that the kinetics of folding are the same in the presence and absence of GroEL, indicating that chaperonins increase the probability of correct folding simply by decreasing the probability of aggregation in bulk solution (Horovitz, 1998). Another example in which the folding process was studied and compared both *in vivo* than *in vitro* is the human chorionic gonadotropin β-subunit (hCG-β): for this protein was found that the two pathways are indistinguishable because both the rate limiting step, than the other steps of the folding process are the same in both folding environment. The presence of PDI increases the rate of folding *in vitro* without changing the order of disulphide bond formation from that of intracellular folding pathway (Huth *et al.*, 1993).

1.1.2 Kinetics and mechanism of protein folding.

1.1.2.1 Folding models

Anfinsen's original experiments (1973), on the oxidative refolding of bovine pancreatic ribonuclease (RNase) to a native, biologically active enzyme *in vitro* after reduction of disulphide bridges and disruption of tertiary structure, demonstrated that proteins fold spontaneously and reversibly into their native conformation. While, in reaction involving a small molecule, one or at most a small number of strong covalent bonds are broken or made, in the folding reaction not only there is the reorganisation of a very large number of weak non-covalent interactions but also the denatured state is extremely heterogeneous (Creighton, 1994; Pande *et al.*, 1998; Dobson and Karplus, 1999). Moreover the number of possible conformations of a polypeptide chain is astronomically large: a protein randomly searching all avalilable conformational space to find the lowest energy state will never fold on physiological time scales (Levinthal paradox). The initial suggestions to solve this paradox involved the proposal that there must be specific pathways for folding (Levinthal, 1968), where the protein molecules would pass through well-defined partially structured states. Different models were proposed, each of which gave a major role to a particular aspect of the refolding process (Creighton, 1994; Radford, 2000).

The nucleation growth model (Wetlaufer, 1973) proposed that residues adjacent in sequence form a nucleus from which the native structure then develops in a sequential manner. In this model the nucleation event is the rate-limiting step. This nucleus would serve as a template upon which the remainder of the polypeptide chain would fold rapidly. Thus, tertiary structure would form as a necessary consequence of the formation of secondary structure.

The framework model (Baldwin, 1989) suggested that the folded structure is formed by packing together pre-existing individual elements of secondary structure (that could form independently of tertiary structure) and that these then dock into the native tertiary structure of the protein, possibly by a diffusion-collision mechanism (Karplus and Weaver, 1979; 1994). Ptitsyn (1973) proposed a folding model which involves an early compact transient intermediate, the kinetic "molten globule" (Ptitsyn, 1995b), which is characterized by being condensed, containing native-like secondary structure, but still lacking the tight packing of the native structure. The absence of tight packing in these kinds of intermediates results in the high accessibility to the solvent of the non-polar groups within the hydrophobic core of the protein, and therefore leads to a strong binding of hydrophobic probes such as 1-anilino-8-naphthalene sulphonate (ANS) (section 1.3.3). In these two models the rate limiting step is considered the packing of these elements of secondary structure.

By contrast in the hydrophobic collapse model (Dill, 1985), it is hypothesised that a protein would rapidly collapse around its hydrophobic side chain early during folding. From this

collapsed intermediate the native state develops by searching within this conformationally restricted space. In this model, the secondary structure would be directed by native-like tertiary interactions.

Finally, the jigsaw model (Harrison and Durbin, 1985) suggests that each protein molecule could fold by a different path. For this model, as in a jigsaw puzzle, the pieces are joined together in a different order each time the puzzle is assembled, yet the final result is always the same. If there is a distinctive pattern to the puzzle, certain parts may tend to be assembled before others.

The hydrophobic collapse mechanism and the framework model imply the existence of folding intermediates, whereas nucleation does not. Kinetic intermediates of folding are sometimes sensitive to aggregation because they still have an increased amount of exposed hydrophobic surface. These compact imtermediates may represent not only important intermediates in folding pathways (Christensen and Pain, 1994) but they may be involved in number of cellular processes (section 1.1.1).

From theoretical and experimental results it is now clear that there is not necessarily a single specific folding pathway and that a multidimensional energy landscape or folding funnel better describes the folding process (Radford, 2000). Features of the models described above are relevant in the context of present ideas concerning energy landscapes.

1.1.2.2 Folding funnels

In this new context the transition from denatured to native state is considered in terms of a "folding landscape" in which kinetic flow can occur through a series of states of progressively lower energy in a "folding funnel" the slope of which effectively guides the protein down towards the energy minimum (Bryngelson *et al.*, 1995; Dobson and Karplus, 1999). This view is based on a description of protein folding in terms of a statistical ensemble of protein conformations, which fold via parallel multi-pathway diffusion-like processes (Baldwin, 1994; Wolynes *et al.*, 1996; Dill, 1999). The accessible free energy surface has a "funnel-like" shape that guides the system along increasing contacts as it progresses toward the native conformation (Dobson and Karplus, 1999) (Fig.1.1- Brooks, 1998). In this picture each conformation is represented as a point on the landscape where the vertical axis is the internal free energy and the two horizontal axes represent the many degrees of freedom (one axis is correlated with the fraction of native contacts and the other with the total number of contacts, native and non-native). So, while the width of the funnel is related to the configurational entropy of the polypeptide chain, the depth of the funnel depicts a free energy function (Dobson and Karplus, 1999; Honig, 1999). Considering a folding reaction, the starting point is the "unfolded" state composed of many conformations of similar free energy, so the accessible free-energy surface is very broad. As folding

progresses (under conditions in which the native state is stable) there is increasing formation of native contacts, which are generally more stabilising than the non-native ones, leading to a decrease of the energy of the system. A funnel implies that, for protein folding, there is a decrease in energy and concomitant loss of entropy with increasing structure (Brooks, 1998). It is this global bias in the landscape guiding diffusion between non-native configurational traps toward the native configuration that gives a "solution" to the Levinthal paradox (Dill and Chan, 1997). The funnel therefore leads to a huge increase in folding rate (compared to the expected rate for a random diffusional process) and prevents entrapment in partially folded states (local energy minima). Thus there are potentially a number of routes to the native state and which pathways are populated will depend on the details of the system being studied (e.g. the amino acid sequence, the topology, and the experimental conditions) (Plaxo *et al.*, 1998).

While the folding landscape theory has provided an elegant way out of the Levinthal paradox, the nature of the driving force leading to the native conformation it is still not completely understood. There are two different main models proposed: the hierarchical and non-hierarchical model (Baldwin and Rose, 1999a,b; Fersht, 1997). A schematic representation is given in figure 1.2 and these models will be discussed in the next two sections.

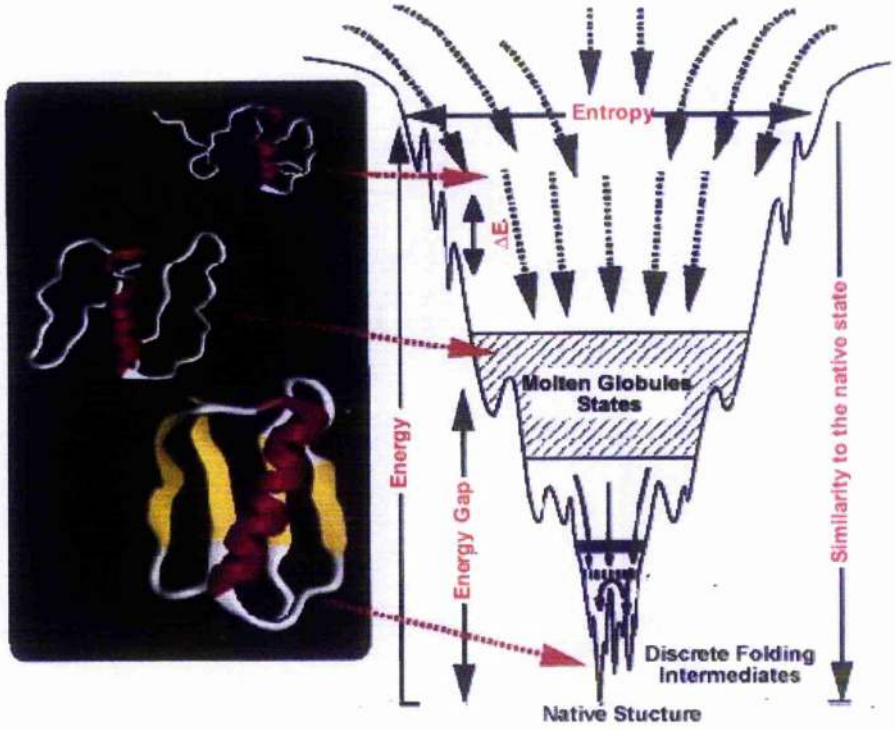

Figure 1.1: The energy landscape for a folding protein.

Schematic representation of a "folding funnel". Each conformation is represented as a point on the landscape where the vertical axis is the internal free energy and the width of the funnel is related to the configurational entropy of the polypeptide chain (Brooks, 1998).

Small Proteins	*Nucleation-condensation model*: co-operative formation of all native interactions
	Hierarchical model: intermediates not detectable
Large proteins (> 100 aa)	1. Hydrophobically collapsed state 2. Rearrangment of folded regions
	1. Formation of the first folding domain 2. Formation of remaining structure

Figure 1.2: Scheme of models for folding of small and large proteins.

Scheme of the two different main models for folding, the hierarchical and non-hierarchical model (Radford, 2000; Baldwin and Rose, 1999 a,b) for both small and large proteins.

1.1.2.3 Folding of small molecules

Small proteins generally fold with a monoexponential kinetic indicative of a two state process (U → N), but there are some exceptions. This has led to the division of small proteins into two classes that fold by different mechanisms: class I, that fold by a hierarchic process in which native-like secondary structure forms rapidly and is stabilized in molten globules-like intermediates, and class II, that do not involve intermediates.
While it is widely believed that some sort of nucleation event is central to the mechanism of protein folding, the detailed nature of this nucleation mechanism, the existence of these two classes and the types of models to apply to protein folding is still under debate (Baldwin and Rose, 1999a,b; Fersht, 2000; Galzitskaya *et al.*, 2001). A large number of studies have identified proteins that fold without accumulation of any detectable intermediates during folding (Fersht, 1995; Dobson and Karplus, 1999). These are generally small proteins of less than 100 amino acids that present the simple case of a one-step reaction, with a single kinetic phase. From the results on these " two state" folding systems a nucleation-condensation mechanism (non-hierarchic) has been proposed (Fersht, 1997). This is different from the classical nucleation model in that a large, more diffuse, nucleus is formed in the ground state. This nucleus develops in the transition state and is composed of both neighbouring residues in local secondary structure and long-range tertiary interactions. Nucleation-condensation is a coupled process in which the formations of the nucleus and of structure elsewhere are concerted. It is this view that has lead to the division of the small proteins between class I and class II folding mechanisms. Another view is the "hierarchic process" hypothesis (Baldwin and Rose, 1999a,b), that is to say a process in which folding begins with structures that are local in sequence and marginal in stability. These local structures then interact to produce intermediates of increasing complexity until the native conformation is formed. This hypothesis is opposed to the non-hierarchic models where the tertiary interactions not only stabilise local structures but also actually determine them. In the view of the hierarchic process hypothesis, the differences between class I and class II folding reactions lie not in the mechanism of their folding but only in the stability of their intermediates (Baldwin and Rose, 1999a,b).

This scenario has been compared to the old philosophical paradigm, "which was first - the chicken or the egg?". A correlation analysis between the decrease in hydrodynamic volume and increase in secondary structure content for different globular proteins in native and partially folded conformational states has shown that a good correlation exist between these parameters (Uversky and Fink, 2002). This suggests that hydrophobic collapse and the formation of secondary structure occur simultaneously, rather than representing two independent and sequential processes.

This conclusion is in agreement with recent findings on the structural features of unfolded proteins (Hammarstrom and Carlsson, 2000). In fact there is evidence that, even in concentrated solutions of strong denaturant, stabilising interactions may occurs reducing in this way the conformational space available. These structures in the unfolded state would probably guide the folding process and function as folding initiation-sites (Hammarstrom and Carlsson, 2000; Uversky and Fink, 2002).

Moreover it appears that different proteins may use different mechanisms to search the energy landscape for folding. In fact recent results have shown that for single domain proteins, which display a two-state folding behaviour, there is a good correlation between folding rate and the "contact order" (i.e.: the average sequence separation of contacting residues in the native state) (Plaxo *et al.*, 1998; Fersht, 2000; Grantcharova *et al.*, 2001). This is consistent with the dominant role of native state topology in determining folding rates. Thus the way in which different small proteins fold may be related to the predominance of one or another kind of secondary structure in the protein. The hypothesis that non-local interactions can determine the secondary structure is not new (Honig, 1999). An experiment carried out by Minor and Kim (Minor and Kim, 1996) with an 11-amino acid sequence, shows that this "chameleon" sequence folds as an α-helix when in one position but as a β-sheet when in another position of the primary structure of the IgG-binding domain of protein G. From this work it was concluded that the topology of the protein native state influences the folding mechanism. However it has been argued (Baldwin and Rose, 1999b) that by performing a molecular dynamic simulation on the chameleon sequence with long-range interactions suppressed, it is possible to obtain a similar situation to the experimental one. This finding leads to the conclusion that interactions that are local, but extend beyond the boundaries of the chameleon sequence itself, are sufficient to account for the observed position-dependent differences in conformation of this particular sequence.

For these reasons it would be interesting to undertake a large-scale systematic study of the folding properties of proteins belonging to different structural classes and to study the effect of factors such as amino acid sequence, chain topology, pH, co-solvent concentration and temperature on the folding process.

1.1.2.4 Folding of larger proteins

In the refolding of proteins consisting of 100-200 residues it is often found that there is a multi-exponential course of the folding reaction. This could be either due to the existence of slowly interconverting states or to the presence of folding intermediates. For a number of proteins slow phases observed in folding reactions have been attributed to the interconversion of *cis* and *trans* isomeric states of Xaa-Pro residues (Nall, 1994). Double jump experiments, mutational studies and/or the use of PPI are means of identifying a slow phase with Pro isomerization. When this is ruled out the observed multi exponential course is an indication of the accumulation of intermediates during the early stages of folding (Heidary *et al.*, 2000). The nature of the intermediate(s) depends on the nature of the driving force of the initial steps.

In general two different kinds of mechanism are observed (Radford, 2000 - Fig. 1.2). In the first, protein folding is initiated by hydrophobically driven collapse of the unfolded polypeptide followed by the formation of local structure. This leads to the formation of a compact intermediate in the first stage of folding (non-hierarchic) (Chan and Dill, 1990). The second mechanism considers the formation of local secondary structure as the driving force of folding: folding is initiated by local elements which gradually assemble to yield the final native fold through the interaction between these elements (hierarchic) (Baldwin and Rose, 1999a, b). Some of the observed intermediates seem to be fundamental for the folding process (on-pathway) while others (off-pathway) seem to arise by non-specific collapse of the polypeptide chain or to accumulate because they are trapped by non-native interactions (Weissman, 1995). Although the role that these off-pathways intermediates play in the folding process is still a matter of controversy (Roder and Colon, 1997), they are nonetheless important. In fact they form part of the energy landscape for folding and might be substrates for chaperones or precursors to aggregation (section 1.1.1) (Radford, 2000). It has been reported that discrete structural elements of the native proteins are sometimes present in incompletely folded intermediates (Panchenko *et al.*, 1996), pointing to their intrinsic stability in the absence of specific native interactions with the rest of the proteins (hierarchic). However there are some other findings which demonstrate the importance of the tertiary interactions in the formation of the "native" structure. These findings are both experimental (Arai *et al.*, 1998; Capaldi and Radford, 1998) and theoretical (Dinner *et al.*, 1996; Dobson and Karplus, 1999). For example, β-lactoglobulin, a predominantly β-sheet protein with a markedly high helical propensity, forms non-native α-helical intermediates during refolding. Both the compaction and the secondary structure formation are quite rapid processes (millisecond time scale)(Arai *et al.*, 1998). The burst phase intermediate was characterized as having a compact size, a globular shape, a hydrophobic core, substantial β-sheet and non-native α–helical structure, but little tertiary structure. These findings

suggest that both local interactions and non-local hydrophobic interactions are important forces early in protein folding (Uversky and Fink, 2002). Hence the local interactions that stabilize the non-native helices in the β-sheet regions of this protein persist in the environment of the collapsed intermediate and can only be overcome when the precise tertiary interactions of the native state develop. From lattice simulation calculations it has been found that, for larger proteins, long-range contacts are important, but for other proteins a mixture of short-range contacts for initiation and long-range contacts for cooperativity lead to efficient folding. It has been proposed that these core residues are particularly important for defining both the protein fold and the folding rate and, hence, that they have been conserved during evolution (Shakhnovich *et al.*, 1996; Mirny *et al.*, 1998; Ptitsyn, 1998).

Modular assembly was made a very attractive proposal by the discovery of split genes consisting of exons and introns. It was suggested that exons encode structural and functional modules. These modules or "foldons" are considered kinetically competent, quasi-independent folding units of a protein, and a large protein has to be considered structurally as a concatenation of domains, each comparable in size to smaller proteins which folds readily and having, in many cases, distinct physiological functions (Panchenk *et al.*, 1996). The foldons can separately fold by nucleation-condensation and then dock together (Fersht, 1997) proceeding *via* a variety of mechanisms, depending on the stability of the individual foldons and how nucleation and docking are coupled. The folding of barnase is an example of the folding of a modular structure (Fersht, 1993), where the individual foldons are so stable that they can form independently and produce a stable folding intermediate. The rate-limiting step is then the docking and rearrangement of the foldons.

Another point of view on the folding of larger molecules is in the framework of the "hierarchical" model. The main objection to the hierarchical model is how the secondary structures fold reliably into tertiary structures. To solve this question it was proposed that the missing step of the hierarchic folding model could be the existence of a segment in the protein chains that, acting like an intramolecular chaperone (section 1.1.1.4), can mediate and guide the final assembly of the protein tertiary structure. This segment is referred as "critical building block" (Ma *et al.*, 2000). The mechanism proposed for the "building block" is different from the concept of "folding nuclei" (the "folding nucleus" is the structure formed in the transition state by the protein chain). While the concept of folding nuclei focuses on a non-sequential distribution of the folding information along the entire protein chain, the chaperone-like building block fragment proposal focuses on a segmental distribution of the folding information. This segmental distribution controls the distributions of the populations throughout the hierarchical folding process (Ma *et al.*, 2000). Though this model has similarities to the more general hierarchic model, it reconciles the hydrophobic collapse

model and the hierarchic model by considering the hydrophobic collapse of the local elements, with subsequent binding of these units: the hydrophobicity is considered as the driving force of this process. According to this model protein folding can be viewed as a process of intramolecular recognition. Hence, protein folding and protein-protein association, which involves intermolecular recognition, are similar processes. Both involve conformational selection, with the driving force being the hydrophobic effect, although charge and polar complementarity are also important contributors. The process of intermolecular recognition occurs between the "building blocks". Some of the building blocks turn out to be important both for folding and for function: these particular building blocks are referred as "critical building blocks" (Kumar *et al.*, 2001; Tsai and Nussinov, 1997a; Tsai *et al.*, 1998; 1999a). It is these critical building blocks that have to be considered as "intramolecular-like" chaperones. These building blocks themselves may have not a stable, well-defined conformation in solution, but their conformations are stabilized by mutual interactions. A critical building block may be expected to fulfil three conditions: it should be in contact with most other building blocks in the structure; it is likely to be inserted between sequentially connected building blocks; in its absence the remaining building blocks are likely to mis-associate with each other. Moreover the amino-acid sequence of a critical building block is likely to be conserved in different organisms. An example of "critical building block" appear to be the P-loop in *Adenylate kinases*, a structural feature common also to *Shikimate kinase*, the protein studied in this thesis (Ma *et al.*, 2000).

What is clear from the experimental data is that proteins larger than 100 amino acid residues form populated intermediates early in folding and their existence is reflected in a rugged funnel landscape (Bai and Englander, 1996). These species vary in their conformational properties and stabilities; some are native-like, whereas others contain native-like structure in regions corresponding to domains or sub domains of the native protein, or may even contain highly non-native structures. The stability and nature of these on-pathway species would depend not only on the native topology but also on additional energetic factors. As a consequence it is not yet possible to make generalizations about these intermediates (Brockwell *et al.*, 2000). Although in the case of larger proteins a correlation has not been observed between a topological parameter, such as the contact order, and the folding rate, there is evidence from theoretical and experimental studies showing the importance of the topology for the folding process (Clementi *et al.*, 2000).
The pivotal importance of some modules or "building blocks" in folding should direct attention toward the study of these "larger" proteins. In particular it seems important to understand how key modules in larger proteins influence the folding of the neighbouring "modules" and how this interaction drives the folding process to the "native state".

1.1.3 Protein structure, stability and cosolvent effects.

1.1.3.1 Protein structure and stability

The folded conformations of proteins exhibit marginal stabilities equivalent to only a small number of weak intramolecular interactions (Dill, 1990; Jaenicke, 2000): the values for Gibbs free energy of stabilization of a medium size globular protein are in the range of 20-60 kJ mol^{-1} (Pfeil, 1998; Price, 2000). This is correlated to a high flexibility of the polypeptide chain, a prerequisite for the proper functioning of most proteins (Fischer and Schmid, 1990; Pace and Scholtz, 1997). In fact a folded protein does not exist in a single conformation but in a set of conformations whose inter-conversion involves the making and breaking of non-covalent interactions. The term "native" conformation refers to the most populated conformational ensemble (macrostate) under conditions similar to the physiological conditions where the protein performs its biological activity.

The concept of folding funnels (section 1.1.2.2) can be used not only to describe the folding of the polypeptide chain but also for understanding the function of the folded protein (Ma *et al.*, 1999). The more flexible the molecule, the larger is the ensemble of conformers, more "rugged" will be the bottom of the funnel. Hence the function of a protein and its properties are determined by the redistribution of its conformational sub-states in response to events like binding or a change in solvent conditions (Kumar *et al.*, 2000). The observed three-dimensional structure in solution (e.g.: using circular dichroism) has to be considered as a weighted average of all the conformations accessible, and this conformation depends on a number of experimental variables such as ionic strength, pH and temperature. Usually the native state is the thermodynamically most stable state, though there are some exceptions, such as, for example, in the case of protein presenting post translational modifications (Price, 2000), or when the refolding process is under kinetic control such in the case of some proteases (section 1.1.1) or their inhibitors (Price, 2000; Baker *et al.*, 1992).

Two approaches have been used for the estimates of the stability of proteins, chemical and thermal denaturation (Privalov, 1979) and the unfolding process is followed monitoring the changes in a chosen parameter varying the denaturant concentration or the temperature. Urea and GdmCl offer several advantages over other means of unfolding a protein such as acid, heat, or detergents. First, the product is better defined because the degree of unfolding is maximised. Second, unfolding is more likely to approach a two-state mechanism. Finally denaturation is more likely to be completely reversible (Pace and Scholtz, 1997). Urea is preferred to GdmCl when salt effects on the protein have to be investigated (Pace and Scholtz, 1997; Pace and Grimsley, 1988).

Generally single domain proteins give a two-state unfolding transition, while multi-domain proteins usually fold step-wise due to the separate unfolding of the single domains

(Creighton, 1994). Multi-subunit proteins usually dissociate first, and then the subunits unfold (Price, 1994). For some proteins, folding intermediates have been found which are stable in the presence of intermediate concentrations of denaturant and/or in the acid or alkaline region (Fischer and Schmid, 1990). Such equilibrium intermediates are frequently observed for proteins with a low overall stability and they usually have some native-like secondary structure and lack of rigid tertiary structure (stable "molten globules") (Jaenicke, 1991; Christensen and Pain, 1991; 1994). Because the difference in stability between these flexible intermediates and the native state is small, a weak perturbation, such as binding to a partner protein or a membrane (section 1.1.1), will be sufficient to arrest a folding protein in that state or to convert back it to a molten globular conformation (Fischer and Schmid, 1990).
When the unfolding mechanism can be described in terms of a two-state unfolding reaction it possible to give an estimate of the conformational stability of the protein determining the equilibrium constant and the free energy change for the reaction: N→ D as described in section 2.5.

1.1.3.2 Effect of co-solvent additives: salts

As has been recognised for many years, co-solvents, in general, and salts, in particular, are known to have a number of effects on the properties of proteins. Peptides and proteins could display different conformations in different solvent systems and these can be correlated with their biological functions (Siligardi *et al.*, 1991; Hope *et al.*, 1996; Barteri *et al.*, 1996; Damaschun *et al.*, 1999). Co-solvents and salts are used in protein purification procedures (Scopes, 1994; Arakawa, 1986) and can affect enzyme activity (Cacace *et al.*, 1997).
The ionic strenght of the solution is an important parameter affecting enzyme activity. Both the binding of charged substrates to enzymes and the movement of charged groups within the catalytic active site will be influenced by ionic composition of the medium. If charges are opposite then there is a decrease in the reaction rate with ionic strength whereas there will be an increase in the opposite situation. Moreover enzyme activity can be dependent on the type of ion present in solution. Generally kosmotrope anions (section 4.2) enhance enzyme activity. An example for the correlation between the enzyme activity and the Hofmeister series (section 4.2) is given by the herpex simplex virus type I protease which undergoes an increase in activity in the presence of salts in a way dependent on the position in the Hofmeister series (Cacace *et al.*,1997). Other organic solutes and metabolites were found to enhance the protease activity, linking the activation to the presence of a suitable subcellular microenvironment such as that of the nucleus, with its abundance of nucleotide polyanions.
Probably the most important effects of salts are on the solubility and stability of proteins (Von Hippel and Schleich, 1969; Timasheff and Arakawa, 1997). Generally salts stabilise the protein structure against thermal and chemical denaturation (Oobatake *et al.*, 1979; Pace

and Grimsley, 1988; Batalia *et al.*, 2000; Deswarte *et al.*, 2001) and stabilising ions are widely used as protective agents (Timasheff and Arakawa, 1997; Price, 2000). The mechanism of stabilisation can be different ranging from preferential hydration to preferential binding (Timasheff and Arakawa, 1997; Muzammil *et al.*, 2000) (section 4.2). This could well be of importance in maintaining the structural and functional integrity of, for example, recombinant therapeutic proteins on storage. On the other hand, destabilising salts could be useful in solubilising over-expressed proteins which have formed inclusion bodies (Thatcher and Hitchcock, 1994; De Bernardez Clark, 2001), or for undertaking unfolding/refolding studies of proteins (Jaenicke, 1987).

In addition, salts are used in many protocols for the growth of crystals for X-ray diffraction analysis (McPherson, 1982). As has been well documented, the presence of salts in the crystallisation medium can interfere with the properties of macromolecules such as ligand binding and the ability to undergo conformational changes associated with function (Chothia *et al.*, 1983; Busch and Ho, 1990; Yonath, 2002). In the case of the apo-form of AK it is suggested that the average structure in solution is different to that found in the crystal (Sinev, 1996). In fact the enzyme structure derived from the X-ray analysis of one of the crystalline forms (crystal A) of the apo-AK from pig muscle contains two sulphate ions, one of which is tightly bound to the enzyme in the vicinity of the β- phosphate of the ATP binding site. Therefore it can be assumed that this structure does not represent the real structure of the apo-enzyme. The crystal B form had no bound sulphates and had the widest cleft.

Salts that favour the compact protein conformation by means of preferential exclusion from the protein surface (Timasheff and Arakawa, 1997) stabilise the native state and also provide a useful tool for characterizing partially structured states in the refolding process (Bieri *et al.*, 1999; Otzen and Oliveberg, 1999; Krantz and Sosnick, 2000; Low *et al.*, 2000).

For many proteins refolding experiments in the presence of salts have been carried out at acidic pH (acid denatured state) and the salt-induced refolding was generally lead to a molten globule state (Goto *et al.*, 1990; Eder *et al.*, 1993; Hamada *et al.*, 1994; Nishii *et al.*, 1995; Uversky *et al.*, 1998b; Staniforth *et al.*, 1998; Nishimura *et al.*, 2000) though not always (Bedell *et al.*, 2000). In these cases the effect of the anions is attributed to their minimizing the charge repulsion by binding to the positively charged groups. The study of the refolding in these conditions is interesting because the acid-denatured states are thought to be the starting points for the misfolding in some conformational disorders (section 1.1.1.3). In fact it has been found that addition of salts to these acid-unfolded proteins leads to the formation of amyloid-like fibers (Damaschun *et al.*, 1999).

Effects at neutral pH are more difficult to elucidate because the influence of salts on the refolding properties of proteins is complex and a number of different effects, including electrostatic screening, protein stabilization, alteration of the properties of water (Jelesarov *et*

al., 1998), and binding can all play a role (Kulkarni *et al.*, 1999). Therefore salts could be useful in revealing insights into the roles that electrostatic interactions and anion binding play in the refolding: changing the refolding environment, the energy landscape of the refolding can be varied (Ferguson *et al.*, 1999; Jaspard, 2000; Kulkarni *et al.*, 1999). In fact the type of amino acid side chains in contact with the surrounding medium, and therefore the charge distribution of the molecule, greatly changes during the refolding and each transient conformation of the polypeptide chain must establish a unique pattern of interactions with the solvent. Therefore, it is likely that protein-solvent interactions are of major importance for the outcome of the refolding (Wiggins, 1997).

1.1.2 Methods for studying protein folding

One way of studying the unfolding-refolding process is by establishing equilibria between native and unfolded states. However, equilibrium studies give little insight into the mechanism of folding, since folding-unfolding transitions are often highly co-operative and partially folded intermediates states are not well-populated at equilibrium.

In order to monitor the kinetics of folding the refolding reaction is triggered by rapid dilution of a denaturing agent or by a pH or temperature jump, and the refolding can be followed by monitoring the regain of the activity or the resulting conformational changes can be monitored by spectroscopic techniques. Some of the time-resolved spectroscopic techniques that can be used are summarised in the following lines: this will be only a short overview of the different techniques and, the ones actually used in this work are analysed in more detail in section 1.3.

After the protein is transferred into a "refolding" environment, the initial stages of refolding involve changes in size, secondary, and tertiary structure content. The formation of the environment of aromatic residues or co-factors can be obtained following the changes in the absorbance in the near-UV region (Eaton *et al.*, 2000; Roder and Shastry, 1999). Another technique used to monitor the regain of secondary (far-UV) and tertiary (near-UV) structure is circular dichroism (CD; section 1.3.1)(Kelly and Price, 1997; Goldbeck *et al.*, 1997; Akiyama *et al.*, 2000). While the near-UV CD monitors the formation of the rigid environment of the aromatic side chains, the intrinsic fluorescence can be used to obtain information on the environment of aromatic side-chains as they become involved in tertiary structure interactions during folding and also provides a tool to assess the formation of the active site during the refolding process (section 1.3.2). The use of some fluorescent probes, as ANS, that are thought to bind to exposed hydrophobic regions, has been found to be very useful in the detection of early intermediates (section 1.3.3). Pulsed hydrogen-

exchange techniques (HX) combined with the bi-dimensional nuclear magnetic resonance (2D-NMR) (Englander *et al.*,1996; Englander, 2000) and mass spectrometry (pulsed HX-ESI-MS) (Miranker *et al.*, 1993) have provided information respectively on hydrogen-bond formation in specific residues and on folding populations (Deng and Smith, 1999). The role of individual residues in stabilizing intermediates and transition states could be explored by protein engineering: side-chains are modified by site-directed mutagenesis and the kinetics and equilibria of folding of each mutant measured (Matouschek *et al.*, 1994; Fersht, 1998). One example is the case of barnase were this strategy was applied and structural information on the intermediate and transition state were obtained (Matouschek *et al.*, 1994). Finally techniques like fluorescence resonance energy transfer (FRET), can be used to monitor changes in the distance between donor and acceptor probes that are close together in the native state and well separated in the unfolded state, giving information on the rate of collapse during folding (Eaton *et al.*, 2000; Roder and Shastry, 1999). The protein compaction process could be monitored by small-angle-X-ray-scattering combined with stopped flow mixing (Pollack *et al.*, 1999).
In parallel with the developments in the experimental techniques a number of theoretical methods have been developed to simulate protein folding (Dobson and Karplus, 1999).

The application of different techniques coupled with the theoretical developments have allowed the pathways of folding of a number of small proteins, such as barnase (Fersht, 1993), dihydrofolate reductase (Gegg *et al.*, 1997), chymotrypsin inhibitor 2 (Itzhaki *et al.*, 1995), lysozyme (Radford *et al.*, 1992) and CheY (Lopez-Hernandez and Serrano, 1996) to be mapped out and understood in reasonable detail.

1.2 The Shikimate pathway and Shikimate Kinase

1.2.1 The Shikimate Pathway

1.2.1.1 An overview

The shikimate pathway is a seven step biosynthetic route that converts erythrose-4-phosphate to chorismic acid, the major precursor of aromatic amino acids (Haslam, 1993) (Fig.1.3). Chorismate itself is a precursor not only for the aromatic amino acids but also for several other important aromatic compounds required in plants and micro-organisms: folate, *via* 4-aminobenzoate, the iron-binding compound enterochelin, *via* 2,3-dihydroxybenzoate, and ubiquinone, a component of the electron transport chain, and menaquinone, *via* 4-hydroxy-benzoate (Gibson, 1999; Roberts *et al.*, 2002). All pathway intermediates can also be considered branch point compounds that may serve as substrates for other metabolic pathways (Hermann, 1999). The pathway is named after one of the intermediates, shikimic acid, which was isolated by Eykmann from the fruits *Illicium religiosum* (Eykmann, 1885). The importance of this pathway resides in the fact that it is found in microorganisms and plants, but not in higher animals. The existence of the shikimate pathway was recently demonstrated in apicomplexan parasites such as *Plasmodium falciparum* and *Toxoplasma gondii* (Roberts *et al.*,1998), which causes toxoplasmosis. So compounds that target the enzymes of this pathway may also be effective as herbicides (Coggins, 1989; Kishore and Shah, 1998), antibiotics (Davies, 1994) and against other disease-causing bacteria or fungi that rely on the pathway. These include *Mycobacterium tuberculosis*, which causes tuberculosis, *Staphylococcus aureus*, a common and increasingly drug-resistant cause of serious post-operative infections, and *Pneumocystis carinii*, the most frequent cause of pneumonia in patients with AIDS (Roberts *et al.*, 2002).

The shikimate pathway operates in the cytosol of bacteria and fungi, but in plants it is also known to operate in plastid organelles (Roberts *et al.*, 2002). In micro-organisms the regulation of the pathway is achieved by feedback inhibition and by repression of the first enzyme. In higher plants, no physiological feedback inhibitor has been identified, suggesting that pathway regulation may occur exclusively at the genetic level.

This difference between microorganisms and plants is reflected in the unusually large variation in the primary structures of the respective first enzymes. Several of the pathway enzymes occur in isoenzymic forms whose expression varies with changes in environmental conditions and, within the plant, from organ to organ (Herrmann, 1999).

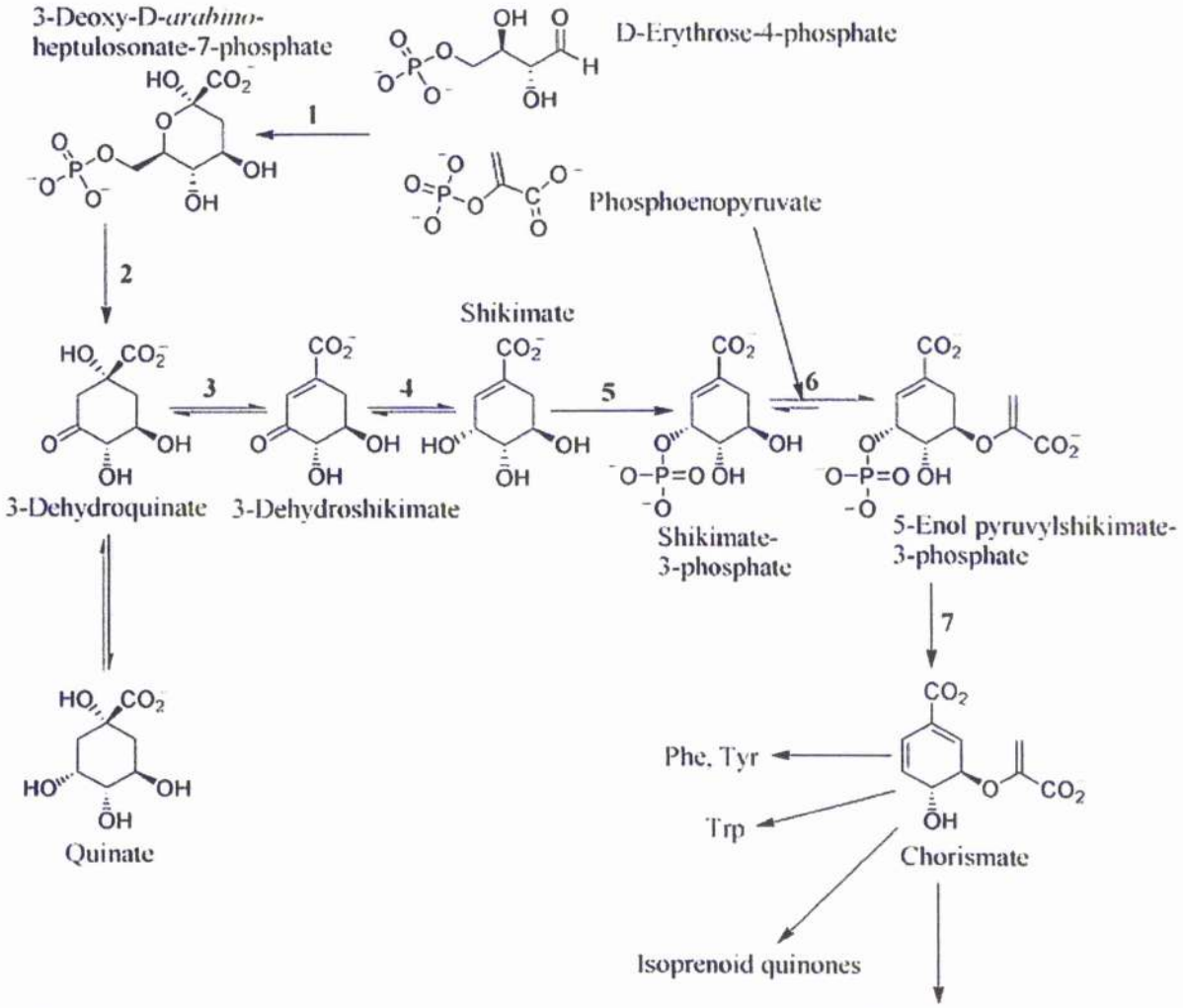

Figure 1.3: The reactions of the Shikimate Pathway

1.2.1.2 The Steps of the pathway

The 1st step is the condensation between erythrose-4-phosphate and phosphoenolpyruvate to form 3-deoxy-D-arabino-heptulosonic acid-7-phosphate (DAHP).The enzymatic synthesis of DAHP is catalysed by DAHP synthase (EC 4.1.2.15). The DAHP synthase studied in most detail is the enzyme from *E. coli* (Hermann, 1995), which produces three feedback inhibitor-sensitive DAHP synthase isoenzymes: a Tyr-sensitive, a Phe-sensitive, and a Trp-sensitive enzyme. These enzymes are oligomers with a subunit molecular weight of about 39 kDa. DAHP synthase in *E. coli* is a metalloprotein that is inhibited by chelating agents (McCandliss and Hermann, 1978). *In vitro* analysis of pure enzymes indicates that the metal requirement can be satisfied by several divalent cations (Stephens and Bauerle, 1991). Plant DAHP synthases have been obtained in pure form from carrot (Suzich *et al.*, 1985) and potato (Pinto *et al.*, 1986) as oligomers with subunit molecular weights of about 54 kDa. Because of the large differences in the primary structure, Walker and co-workers made a distinction between a small bacterial type I DAHP synthase of 39kD and a large plant type II enzyme of 54 kDa. However the "plant type II" DAHP synthase is also found in prokaryotes and the "bacterial type I" in eukaryotic microorganisms (Walker *et al.*, 1996; Paravicini *et al.*, 1989). DAHP synthase in *E. coli* is regulated at the transcriptional level by repression and at the protein level by feedback inhibition.

In bacteria, reactions two to six of the shikimate pathway are catalysed by five separate enzymes, but in fungi, a single polypeptide called the multifunctional AROM complex serves the same purpose. In these complexes, the enzymes do not appear (in terms of the amino acid sequence) in the order of the pathway reactions. Protein domains for DHQ synthase and EPSP synthase form the amino terminal part, domains for shikimate kinase, DHQ dehydratase, and shikimate dehydrogenase the carboxy terminal part (Hawkins and Smith, 1991). It appears that the *arom* locus evolved by gene fusion. DNA encoding the entire AROM complex has been cloned and sequenced from *A. nidulans* (Charles *et al.*, 1986), yeast (Duncan *et al.*, 1987) and *P. carinii* (Banerji *et al.*, 1993). In higher plants, a bifunctional enzyme catalyses reactions three and four of the pathway. The remaining three reactions of the shikimate pathway are catalysed by separate enzymes that are structurally rather similar to their prokaryotic homologues.

The 2nd step is the formation of highly substituted cyclohexane derivative, 3-dehydroquinate by the exchange of the ring oxygen of DAHP for the exocyclic C of DAHP with the elimination of phosphate. The reaction is catalysed by Dehydroquinate (DHQ) synthase (EC 4.6.1.3), a monomeric enzyme with a molecular weight of 39 kDa. The enzyme from *E. coli* requires divalent cations and NAD^+ for activity (Frost *et al.*, 1984) and it is activated by inorganic phosphate. The mechanism of this reaction was elucidated by Barlett and

Knowles (Bartlett and Satake, 1988; Bender *et al.*, 1989; Widlanski *et al.*, 1989). The true substrate for the enzyme is apparently the pyran form of DAHP (Garner and Hermann, 1984). The β-elimination of phosphate proceeds with *syn* stereochemistry and there is compelling evidence that the enzyme is a simple oxidoreductase (Bartlett and Satake, 1988; Bender *et al.*, 1989; Widlanski *et al.*, 1989). The phosphate monoester may either mediate its own elimination or may be aided by the enzyme. The remaining partial reactions proceed spontaneously. The enzyme itself provides a potential conformational template to prevent formation of undesirable side products (Bartlett *et al.*, 1994; Parker *et al.*, 1997).

The 3-dehydroquinate forms 3-dehydroshikimate by the elimination of water (3rd step). This step is catalysed by dehydroquinate dehydratase (Dehydroquinase, EC 4.2.1.10). The dehydration of 3-dehydroquinic acid to 3-dehydroshikimic acid is a central step in two separate metabolic pathways: one is the shikimate pathway in micro-organisms and plants, the other is involved in catabolism and is the quinate pathway in fungi which allows the use of quinate as the sole carbon source (Fig.1.4). DHQase exist in two forms: type I and type II, depending on the bacterial source (Deka *et al.*, 1992; Moore *et al.*, 1993; White *et al.*, 1990; Garbe *et al.*, 1991). Type I DHQase catalyses *syn*-elimination and type II *anti*-elimination of water (Shneier *et al.*, 1993). The mechanistic differences are reflected in the structures of these proteins; there is no sequence similarity between type I and II enzymes, a rare example of convergent or parallel evolution. Type I enzymes, the most studied of which is the *E.coli* enzyme, are dimers of 25 kDa subunits and catalyse the dehydration of dehydroquinate by a Schiff base mechanism (Kleanthous *et al.*, 1992). On the other hand the type II enzymes (the best studied example of which is the enzyme from *Streptomyces coelicor*) are dodecamers of 16-18 kDa monomeric molecular mass, which appear to catalyse the dehydration reaction via an enolate intermediate (Kleanthous *et al.*, 1992; Harris *et al.*, 1996; Leech *et al.*, 1998).

The 4th step is the reduction of dehydroshikimate (DHS) to shikimate. In *E. coli*, the reaction is catalysed by an NADP-dependent shikimate dehydrogenase (EC 1.1.1.25) of molecular weight 29 kDa. The pyridine nucleotide-dependent dehydrogenases are of two kinds: those with catalytically active metal ions such as Zn^{2+} and Fe^{2+} and those without (Aronson *et al.*, 1989). Shikimate dehydrogenase is thought to be of the metal-independent kind because the presence of EDTA does not give inhibition of the enzyme. A histidine residue has an essential role in pyridine nucleotide-dependent dehydrogenases: it forms a hydrogen bond with the carbonyl group of the substrate (Adams *et al.*, 1987), which then initiates the hydride ion transfer by polarization of the carbonyl group. In the metal-dependent kind, the hydride ion transfer is initiated by the bound metal ion.

The 5th step is the phosphorylation of shikimate to give shikimate 3-phosphate and is catalysed by shikimate kinase (EC 2.7.1.71). This reaction will be discussed separately in section 1.2.2.1, since shikimate kinase is the subject of this thesis.

The 6th step involves an esterification reaction to give 5-enolpyruvylshikimate 3-phosphate. This irreversible reaction is catalysed by 5-enolpyruvylshikimate 3-phosphate (EPSP) synthase (EC 2.5.1.19) a monomeric enzyme of molecular weight 48 kDa. Several studies proposed an ordered (Anderson and Johnson, 1990) or a random (Gruys *et al.*, 1993) kinetic mechanism for the enzyme-catalysed reaction that proceeds through a tetrahedral intermediate. This tetrahedral intermediate had already been suggested by Srinson and co-workers and was verified through extensive physicochemical investigations (Seto and Bartlett, 1994; Sikorski and Gruys, 1997). EPSP synthase is the only cellular target for the herbicide glyphosate (Steinrucken and Amrhein, 1980). Glyphosate binds to the enzyme-S3P complex, and is competitive with respect to phosphoenolpyruvate (PEP). Though initially the ternary complex enzyme-S3P-Glyphosate had been considered a transition state analogue, a number of experimental results have demonstrated that glyphosate and PEP binding are not totally equivalent. Since glyphosate is a competitive inhibitor with respect to PEP but does not bind in the same fashion as PEP, the inhibition is now termed an "adventitious allosteric interaction" (Sikorski and Gruys, 1997). Under specific *in vitro* conditions the EPSP synthase from *Bacillus subtilis* is an oligomeric protein with two non-equivalent PEP binding sites. Glyphosate binding is competitive with respect to one site only: thus this enzyme has been considered a classical allosteric protein (Majumder *et al.*, 1995).

The final step of the main trunk of the shikimate pathway is the *trans*-1,4 elimination of phosphate from EPSP to form chorismate (Hermann, 1995; Balasubramanian *et al.*, 1990, Hawkes *et al.*, 1990). In this reaction, the second of the three double bonds of the benzene ring is introduced. The reaction is catalysed by chorismate synthase (EC 4.6.1.4) and requires reduced flavin for activity even though the overall reaction is redox neutral. In the chorismate synthase catalysed reaction, the reduced flavin is apparently directly involved in the mechanism of the reaction (Ramjee *et al.*, 1991; 1992). Depending upon the organism, chorismate synthase is either monofunctional, requiring the addition of reduced flavin to *in vitro* enzyme assays, or bifunctional, with an associated NADP-driven flavin reductase within the same polypeptide chain.

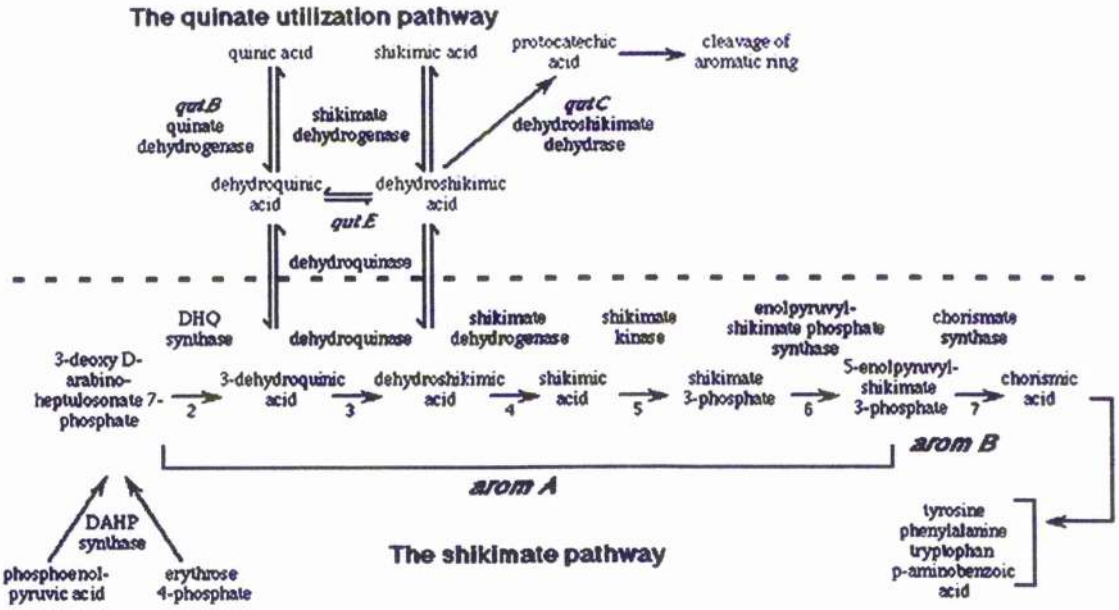

Figure 1.4: Position of dehydroquinase in the shikimate and quinate pathways.

The formation of 3-dehydroshikimic acid is a central step in two separate metabolic pathways: the shikimate pathway and the quinate pathway.

1.2.2 Shikimate Kinase

1.2.2.1 The Shikimate Kinase reaction

Shikimate kinase (EC 2.7.1.71) catalyses the fifth step in the biosynthesis of the aromatic amino acids (the shikimate pathway) in bacteria (gene aroK or aroL), plants and in fungi (where it is part of a multifunctional enzyme which catalyses five consecutive steps in this pathway (Duncan *et al.*, 1987)). SK catalyses the specific phosphorylation of the 3-hydroxyl group of shikimic acid using ATP as substrate (Fig.1.5). In *E. coli* this reaction is catalysed by two different isoforms: types I and II that have 30% sequence identity (Griffin and Gasson, 1995; Whipp and Pittard, 1995). This unusual situation led to the suggestion that shikimate may be a branch-point intermediate for two different pathways (Weiss and Edwards, 1980). The two isoenzymes also have a different affinity for the shikimate: the type I has a K_m of 20mM while the type II a K_m of 200μM. The role of SKI is unclear but it has been suggested that it may have another function in the cell, possibly in the process of cell division (DeFeyter and Pittard, 1986a; 1986b; Vinella *et al.*, 1996) and that it phosphorylates shikimate only fortuitously. By analogy with other kinases the conserved Lys15 residue (section 1.2.2.2) is thought to be involved in the stabilization of the

pentavalent transition state of the γ-phosphoryl group during the phospho-transfer reaction (Sigal *et al.*, 1986; Reinstein *et al.*, 1990; Muller-Dieckmann and Schulz, 1994).

Understanding the mechanism of the phospho-transfer reaction is of great interest because this occurs in many biological processes such as energy transfer, signal transduction, protein biosynthesis, activation of metabolites, and cell growth (Bossemeyer, 1995; Mildvan, 1997). By comparing the structure of adenylate kinase (AK) in the presence of P^1, P^5-bis (5'-adenosyl) pentaphosphate (Ap_5A), considered as reproducing the geometry before the phospho-transfer, with the structure of the uridylate kinase (UK) complexed with ADP: ADP/AMP, considered to represent the geometry after the phospho-transfer Muller-Dieckmann and Schulz (Muller-Dieckmann and Schulz, 1994) gave a model for the transition state of the phospho-transfer that corresponds to a trigonal bipyramidal transition state expected for the in-line S_N2 reaction. A similar mechanism has been proposed for AK on the base of NMR studies (Fry *et al.*, 1987). A recent quantum mechanical study on the phosphoryl transfer in the NMP kinases has proposed a synchronous shift of a proton from the monophosphate to the transferred PO_3^{2-} group (Hutter and Helms, 2000).

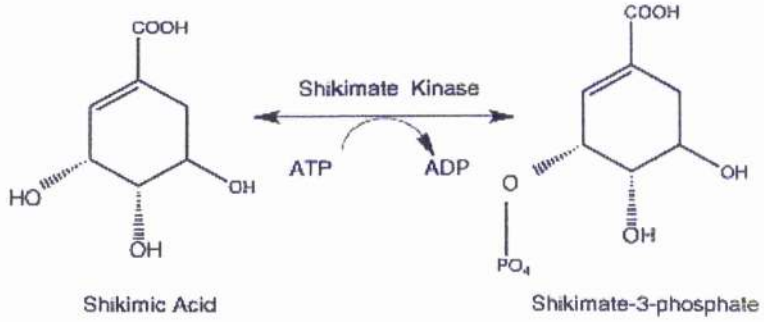

Figure 1.5 Reaction catalysed by Shikimate Kinase.

1.2.2.2 The P-loop-containing nucleotide triphosphate hydrolases

The overall 3-dimensional structures of proteins are much better conserved than their amino acid sequences, giving rise to families of proteins having related folds but varying widely in sequence similarity. There are four main structural classes observed in proteins: mainly α, mainly β, α+β and alternating α/β (Murzin *et al.*, 1995; Orengo, 1994). The α/β and α+β proteins differ in that the α/β proteins mainly are built up of parallel strands connected by helices (βαβ motifs), while the α + β proteins have strands and helices connected in a more irregular fashion. Various physical constraints on the packing of secondary and super secondary motifs gives rise to groups of folds within each class, containing common or favoured secondary structure arrangements (Murzin *et al.*, 1995). Studies of these groups

can generate valuable information on secondary structure packing, thereby identifying restrictions on fold topologies and improving *ab initio* fold predictions.

The most structurally diverse of the four classes of proteins is the α/β class which contains nearly 100 different kinds of protein folds. One of these subclasses is the P-loop-containing nucleotide triphosphate hydrolases. Amongst the mononucleotide triphosphate binding proteins only a few distinct calsses have been recognised: the cAMP-dependent kinase fold; the actin fold; the glutathione sinthetase; the type II tRNA synthetase; the nucleotide diphosphate kinase and, finally, the adenylate kinase fold, to which SK belongs. The core of this class forms a classical mononucleotide-binding fold (CMBF) found in a number of structurally diverse proteins such as myosin, elongation factor EF-Tu, $p21^{ras}$, the nucleotide binding domain (NBD) of the ABC transporter, Rec A and adenylate kinase (Yoshida and Amano, 1995). The family of nucleoside monophosphate kinases (NMP- e.g.: adenylate kinase, guanylate kinase, uridylate kinase and thymidine kinase) includes enzymes that catalyse the phospho-transfer to molecules other than NMPs, such as the kinase domain of the rat testis 6-phosphofructo-2-kinase/fructose-2,6-bisphosphatase and shikimate kinase (Hasemann *et al.*, 1996). The members of this class show a high degree of three-dimensional structural similarity although the sequence identity between the members is very low except for two conserved peptide sequences named the Walker A (or "P-loop", consensus sequence: GXXXXGKS/T, where X is a not conserved residue) and Walker B motifs (consensus sequence: ZZ-D-XX-G; Z= hydrophobic) (Walker *et al.*, 1982) that were proposed to be responsible for the binding of triphosphate and Mg^{2+}. On the basis of further work the Walker A consensus motif has been renamed kinase 1 motif and has the following fingerprint G(X)XXXXGKS/T (the X in parenthesis has been added to account for an insertion found in the sequence of the dethiobiotin synthetase) (Dever *et al.*, 1987; Traut, 1994). The NMP kinases are generally composed of three domains: the central CORE domain, which contains the P-loop and consists of parallel strands flanked by helices; the LID domain, which closes over the bound ATP during catalysis; and the NMP binding domain (Milner-White *et al.*,1991; Story and Steitz, 1992; Vonrhein *et al.*, 1995).
The structural conservation of the CORE within this group of proteins is illustrated by the fact that superimposition of the P-loops from proteins such as Rec A, adenylate kinase (AK), the elongation factor, G-proteins, and myosin results in root mean square deviations in alpha C atoms of only 0.3-0.4 Å (Krell *et al.*, 2001). In this family the kinase 1 motif is always found on a loop which typically forms a flexible connection between the first β-strand (β1) and the first α-helix (α1), that generates an anionic environment within which the β-phosphate of ATP can be accommodated (Smith and Rayment, 1995; Dreusicke and Schulz, 1996). The Lys in the P-loop is an essential lysine which is thought to be involved in nucleotide binding by direct interaction with the β-phosphate of ATP (Saraste *et al.*, 1990).

The last Ser/Thr residue of the kinase 1 motif is directly or indirectly involved in the coordination of Mg^{2+}, the cation essential for enzyme activity associated with the nucleotide. Another essential residue is a conserved aspartic acid, located in the kinase 2 motif (Walker B) (Dever *et al.*, 1987; Traut, 1994). This aspartate residue is usually found at the C-terminal segment of the second strand of the central β-sheet (Smith and Rayment, 1996), in the immediate vicinity of the kinase 1 motif, on the Walker B (kinase 2) motif, ZZ-D-XX-G, (Walker *et al.*, 1982). Not all ATP- or GTP-binding proteins contain this motif, but in these cases other residues fulfill the role of the kinase 2 Asp residue (section 1.2.2.3). The relative positions of the residues involved in catalysis are well conserved in the available structures, probably reflecting the precise adjustment needed for the proper function of the binding site. In fact it appears that the network of interactions that the residues of the P-loop establish with the rest of the protein play a crucial role in folding and activity. It was demonstrated, by engineering the kinase 1 and 2 motifs into a protein, namely CheY (that has the overall topology of this class of proteins but does not contain these motifs), that the structure of the P-loop is strongly influenced by the tertiary contacts (Cronet *et al.*, 1995). The P-loop is maintained in its active conformation through a network of contacts with the rest of the structure (Table 1.2). The first contact is a van der Waals' contact between the side-chain of a buried hydrophobic residue on the β-strand adjacent to the P-loop (e.g. Val81 in $p21^{ras}$) and the backbone of the three residues before the S/T of the kinase 1 motif; the second is a hydrogen bond between the S/T of the kinase 1 motif and the Asp of the kinase 2 motif (it should be noted that in the case of adenylate kinase, in which there is a single deviation from the P-loop pattern, Gly is found instead of Ser or Thr in the C-terminal position). The last observed contact is due to the main-chain carbonyl group of the Gly of the GKS/T that forms a hydrogen bond with a side-chain amide group of an Asn residue (in $p21^{ras}$ and EF-Tu) or a van der Waals' contact with an Arg from an adjacent loop (AK). The hydrophobic cluster formed by the packing of conserved hydrophobic residues (mainly Val) with the P-loop, and the other two interactions that could help in a synergistic fashion, could play a central role in determining its structure (Cronet *et al.*, 1995) and could have a role as a nucleation point during the folding of these kinds of proteins (Kumar *et al.*, 2001).

This work, together with other studies (Kinoshita *et al.*, 1999), indicates that sequence or protein fold information is not sufficient to understand the variety of the binding modes with substrates: instead structural comparisons at the atomic level must be made.

	$P21^{ras}$ (PDB entry: 5P21)	EF-Tu (PDB entry: 1ETU)	AK (PDB entry: 3ADK)
G	*N116*	*N135*	*R128*
	V81	*V104*	*V118*
	K117		
K	D57	D80	
	T58		I192
	A59	Y87	N193
	G60		
	V81	*V104*	*V118*
S/T	T35		
	D57	*D80*	*D93*

Table 1.2: P-loop contacts in the classical mononucleotide-binding fold (CMBF) family: the residues in italics and on the same line make conserved contacts with the corresponding residue of the P-loop throughout the whole CMBF family (Cronet *et al.*, 1995).

1.2.2.3 The structure of shikimate kinase

The shikimate kinase (E.C.2.7.1.71) of *E. chrysanthemi*, which was cloned and sequenced by Minton *et al.* (1989), is a type II enzyme. It is a small α/β protein of 173 residues and molecular mass of 18,955 Da, with a theoretical isoelectric point (calculated by EXPasy) of 5.58. From the X-ray structure of SK (Krell *et al.*, 1998), it is clear that the ordering of the strands, 23145 in the parallel β-sheet core, places the enzyme in the same structural family as the NMP kinases (Fig.1.6a, b). Adenylate kinases (AKs) have served as a template structure for previous modelling of 6-phosphofructo-2-kinase/fructose -2, 6-bisphosphatase enzyme (Bertrand *et al.*, 1997) as well as for shikimate kinase (Matsuo and Nishikawa, 1994), although SK possesses only 19% sequence identity with AK. Four structures of shikimate kinases are available: two of the *E. chrysanthemi* wild type enzyme (PDB entry: *1shk* and *2shk* - Krell *et al.*, 1998)[1,2], one of the K15M mutant (PDB entry *1e6c* – Krell et al., 2001) and finally the structure of SK from *Mycobacterium tuberculosis* (Gu *et al.*, 2002). The central five stranded parallel β-sheet core is flanked by α-helices, two on one side (α1 and

[1] Though the enzyme functions as a monomer, the two structures available for the WT are dimers: there is a disulphide bond between the Cys 162 residues, probably due to the crystallization procedure, which was carried out in the absence of DTT.

[2] **1 shk**: mol. A – with shikimate; mol. B-no ligand ; **2shk**: mol.A- with shikimate; mol.B- with ADP

α8) and three on the other (α4, α5 and α7) as shown in the figure 1.6 a and b (Krell *et al.*, 1998), with a topology similar to adenylate kinase.

Common to all proteins of the adenylate kinase family are three structural regions termed CORE, LID domain, and NMP_{bind} (section 1.2.2.2), that in SK is the shikimate binding domain (SB)(Vonrhein *et al.*, 1995; Krell *et al.*, 1998; Gu *et al.*, 2002 – Fig. 1.6 c).

The central rigid CORE region includes the central parallel β-sheet and the P-loop (GXXXXGKT/S - Fig. 1.7), which forms a giant anion hole that accommodates the β-phosphate of the ADP by donating hydrogen bonds from several backbone amides.

The conserved P-loop lysine, Lys15, is thought to have both a catalytic and structural function. The structure of the K15M mutant shows that the mutation causes perturbations in the region of the P-loop (Krell *et al.*, 2001). This, together with binding, activity and chemical modification data, confirms the role of K15 not only in stabilization of the pentavalent transition state, but also in mantaining the conformation of the P-loop. While AK does not have the T or S residue on the C-terminal side of the P-loop Lysine, this residue is present in SK (Thr16) and is involved in providing a hydrogen bonding ligand to maintain the Mg^{2+} cofactor in an octahedral coordination in the catalytic site. The importance of this hydroxyl residue has been investigated by site-directed mutagenesis on other P-loop containing proteins: the removal of the hydroxyl group often leads to substantially decreased affinity for substrate MgATP (Urbatsch *et al.*, 2000).

The kinase 2 motif is usually located on the C-terminal segment of the second β-strand of the sheet but does not appear to be present in SK at a sequence level. SK has a modified kinase 2 motif; compared to other NMP kinases, it retains the Gly (Gly79) but the Asp is replaced by Ala76. The functions performed by the conserved Asp in the kinase 2 motif are accomplished in the SK by Asp32 (formation of H-bond to Thr16) and Asp34 (H-bond to a water molecule coordinated to the active site) (Krell *et al.*, 1998). The D34N mutant of SK was expressed and purified (Krell *et al.*, 2001), but it was found to be unstable under standard storage conditions and lacked enzyme activity. These pieces of evidence suggest that D34 may play an important role in maintaining the conformation of the enzyme.

The adenosine binding pocket in shikimate kinase II from *E. chrysanthemi* extends from residue 148 to residue 168 and is very similar to the adenine-binding motif found in bacterial shikimate kinase II, AK type II isoenzymes and also to the AK type I isoenzyme from yeast (Fig. 1.8), although only backbone interactions are responsible for adenine recognition. This motif has a consensus sequence Val/Ile-Asp-X-Gln/Asn-X-Pro, or more generally Val/Ile-Asp-XXX(X)-Pro (Gu *et al.*, 2002), and is restricted to a small group of ATP-binding proteins. The adenine is sandwiched between Arg110, whose side-chain is parallel to the adenine ring, and Pro157, that forms part of a loop, which wraps around the bound adenine.

The LID domain is one of the domains involved in the large hinged movement that characterizes the NMP kinases (section 1.2.2.4), where it closes over the bound ATP. The size of the LID domain in AKs varies between the small cytosolic variant (11 residues) and the large mitochondrial variant (38 residue). The LID domain of SK contains 15 residues, which makes it more similar to the cytosolic variant of AK and it is thought to close over bound ATP. This domain, which is disordered in the wild type shikimate kinase structure, is instead stabilised by contacts with neighbouring lid domains in the K15 mutant structure (PDB entry 1e6c) (Krell *et al.*, 2001). The mutation does not have an effect on the overall conformation of the LID domain; a result which is very similar to the other NMP kinases with a short LID domain (Muller-Dieckmann and Schulz, 1994).

Shikimate binds at a site, which follows the β-strand 2; this binding site involves the α2 and α3 helices and the N-terminal region of the α4 helix and corresponds precisely with the AMP-binding site of adenylate kinase (Fig. 1.9 gives a schematic representation of the different binding regions of SK). Shikimic acid is a six membered ring with a carboxylate group (position 1) and three hydroxyl groups (positions 3, 4 and 5). The residues likely to be involved in binding the carboxyl group are Arg58 and 139 and there could be also a contribution from the backbone NH-groups Gly78 and 80, probably *via* a water molecule. The co-ordination of the hydroxyl groups is achieved by the charged side chain of Asp34 which is positioned to allow binding of hydroxyls at C3 and/or C4. In addition, Glu61 is in the correct orientation for binding the hydroxyl at C5 of shikimate (Krell *et al.*, 1998).

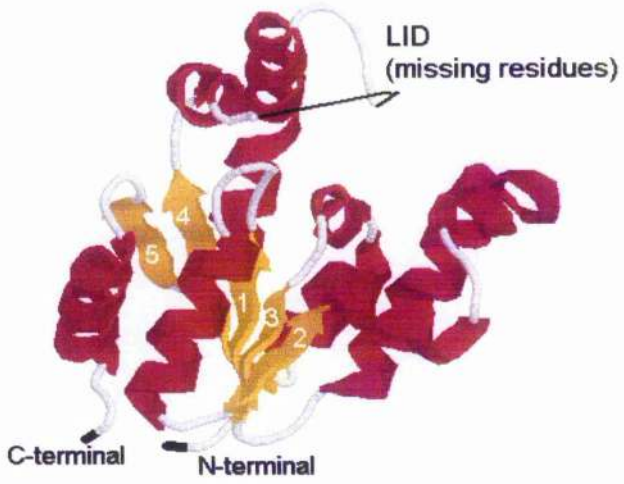

a)

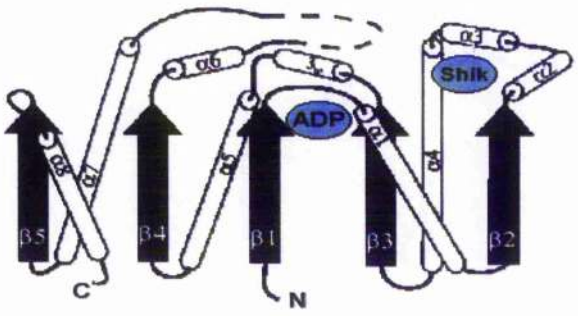

b)

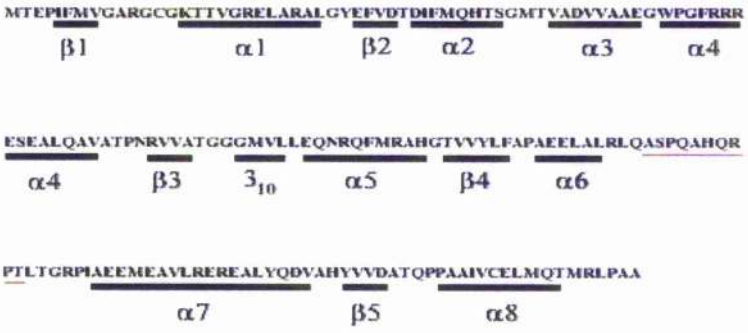

c)

Figure 1.6: The structure of shikimate kinase (Krell *et al.*, 1998).

a) Ribbon structure of SK; the order of β-strands is reported on each strand: the ordering 23145 in the parallel β-sheet classifies SK as belonging to the same structural family as the NMP kinases.
b) General topology of SK; the α-Helices and the single 3_{10} helix are represented as cylinders; β-Strands are represented as arrows; the approximate position of bound ADP and shikimate are indicated.
c) Sequence of SK from *Erwinia chrysanthemi*; the yellow region indicates the position of the P-loop (kinase 1 motif); the red line indicate the missing residues of the LID domain.

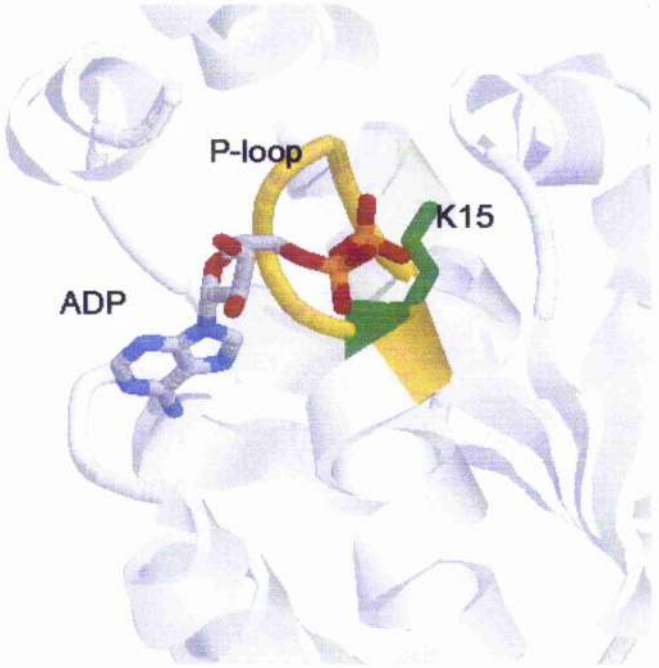

Figure 1.7: Structure of SK: P-loop region and bound ADP

Particulars of the structure of SK complexed with ADP (PDB code: 2shk). The P-loop, the area of the active site that interact directly with the phosphate group, is coloured in yellow. The P-loop lysine, K15, is coloured in green. This residue has both an essential structural and mechanistic role for the activity of the enzyme (Krell *et al.*, 1998; 2001)

SKII	*E.chrysanthemi*	148	HYVVDATQPP	AAIVCELMQT 168
SKII	*E.coli*		HIIIDATNEP	SQVISEIRSA
AKII	*Bos taurus*		HSAIDASQTP	DVVFASILAA
AKII	*Homo sapiens*		HSAIDASQTP	DVVFASILAA
AKII	*Rattus norvegicus*		HCAIDASQTP	DVVFASILAA
AKI	*S.pombe*		WAAVDAAQKP	EQVWEQIVAI
AKI	*S.cerevisiae*		WAAVDASQPP	ATVWADILNK

Figure 1.8: The adenosine binding motif.

Sequence alignment of shikimate kinases (isoensymes II) and adenylate kinases (isoenzymes II and yeast isoenzyme I) in the region of the adenine binding pocket. Conserved residues are highlighted. (Krell *et al.*, 1998).

1.2.2.4 Hinge-bending movements

In solution proteins exist in an ensemble of conformational isomers whose distribution is a function of the degree of their molecular flexibility and of external conditions. It is widely accepted that structural flexibility of enzymes plays an important role in their function (Price and Stevens, 1996; Price, 2000). This role is most evident in the case of transferases. In order to avoid abortive hydrolysis and to facilitate transfer of charged groups, transferases must undergo substrate-induced structural changes or "induced fit" (Koshland, 1958) to screen the active centre from water. Molecules exhibiting large flexibility may be described by folding funnels with rugged bottoms.

Of special interest are hinge-bending movements, where rigid domains are connected by flexible joints, such as in the case of NMP kinases, which tether the domains and constrain their movement. These motions may be considered to manifest relatively rugged bottoms, with low energy barriers separating the minima wells (Sinha *et al.*, 2001). The low energy barriers, corresponding to low energy transitions, enable the molecule to flip and interconvert between the different "open" and "closed" conformations. The conformer that is most favourable for binding is the one that is selected, shifting the equilibrium in its favour. These changes are large hinged movements around two flexible regions, which in the NMP kinases are the NMP binding site and the LID domain. Based on the comparison of AK crystal structures representing the enzyme in different ligand forms, apo-form from pig-muscle (Dreusicke *et al.*, 1988), enzyme-AMP binary complex from beef heart mitochondrial matrix (Diederichs and Schulz, 1990) and enzyme -Ap_5A complex from *E. coli* (Muller and Schulz, 1992), Schulz and co-workers suggested that AK undergoes large structural changes upon substrate binding (Schulz *et al.*, 1990; Gerstein *et al.*, 1993). Domain closure in solution was confirmed recently by time-resolved energy transfer studies of AKeco derivatives, labelled with fluorescent probes in both ligand-free and Ap_5A-bound forms (Sinev, 1996), and by ^{15}N NMR relaxation (Shapiro *et al.*, 2000). The observed structural changes involved domain displacements and resulted in the closure (or partial closure) of the enzyme interdomain cleft. This was followed by a dramatic reduction of solvent-accessible surface area of substrate bound inside the cleft and reduced flexibility.

The crystal structure of a mutant of AK in the presence of the ATP analogue $AMPPCF_2P$ (Schlauderer *et al.*, 1996) indicates that the domain motions occur largely independently from each other in agreement with the kinetic studies indicating a *random bi-bi* mechanism (Rhoads and Lowenstein, 1968). In this structure the LID had closed over the ATP analogue while the NMP binding site remained open consistent with the absence of AMP. By analogy with AK, the LID domain of SK is thought to close over bound ATP. Similarly, the shikimate-binding domain, which is in the same position as the AMP-binding site of AK, is thought to undergo a significant movement associated with the binding of shikimate.

The LID domain is disordered in the ligand-free structure of wild type SK (*2shk* – molecule A), but becomes slightly more ordered when ADP is bound (*2shk* – molecule B). In the closed state this domain should form a short loop folded over the bound nucleotide. Probably the absence of the γ-phosphate in the structure of the SK-ADP complex leads to an incomplete closure of the LID: this could be the reason for the high flexibility of the LID, and so account for the missing residues even in the presence of ADP. The structure of the K15 mutant of SK represents an open conformation, in contrast to the structure obtained for the wild type enzyme. The orientation of the two helices around the LID domain (α6 and α7) differs from that in the native structure because of hinge movements at A102 and R139. These hinge regions are in exactly the same structural position as the joints I and IV identified for the large variant of AK (Gerstein *et al.*, 1993). Movements around the hinge regions can be observed not only in the LID domain but also in the shikimate binding region (Krell *et al.*, 2001). These differences between the wild type and mutant structures are a result of the absence of ligands in the structure of the K15M mutant that is stabilised by favourable crystal contacts between the two molecules of the asymmetric unit and result from the displacement of the plane of the β-sheet by hinge movements at I35 and R39.

1.2.2.5 Shikimate kinase as a model system for studying protein folding

SK has a number of experimental advantages as a system for establishing the mechanism of protein folding. First of all it is a monomeric enzyme without disulphide bonds and with a molecular mass of 19 kDa is amongst the smallest kinases so far reported, and much of the progresses toward understanding the mechanism of folding has been achieved by the analysis of the folding of monomeric proteins. Moreover, SK has a single Trp residue (Trp54) which is located in the region near the shikimate binding site (Krell *et al.*, 1998 - Fig. 1.9). Binding of shikimate leads to quenching of Trp fluorescence (Idziak *et al.*, 1997), thereby providing a convenient probe to check for the integrity of the shikimate binding site. An additional feature of SK is that the side chains of Arg11, Arg58 and Arg139 provide a highly positively charged environment around the Trp side chain and the shikimate binding site (Fig. 1.10) (Krell *et al.*, 1998). This allows the use of the iodide ion as a quencher of protein fluorescence as an additional means of investigating the integrity of this region of the protein.

For all these reasons SK was chosen as a convenient representative example of the subclass of P-loop containing proteins with which to examine the mechanism of protein folding.

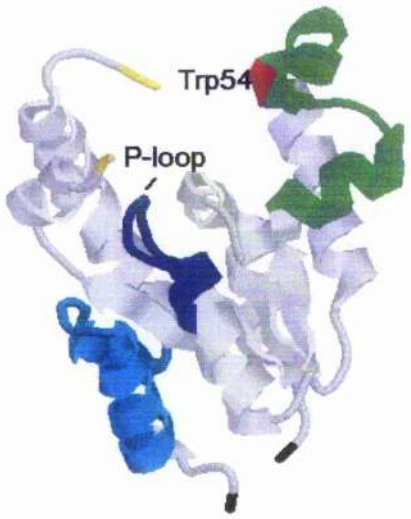

Figure 1.9: SK structure: position of the P-loop, adenine and shikimate binding domains

The figure shows in green the shikimate binding domain; in blue the P-loop and in cyan the adenine binding domain (Krell *et al.*, 1998).

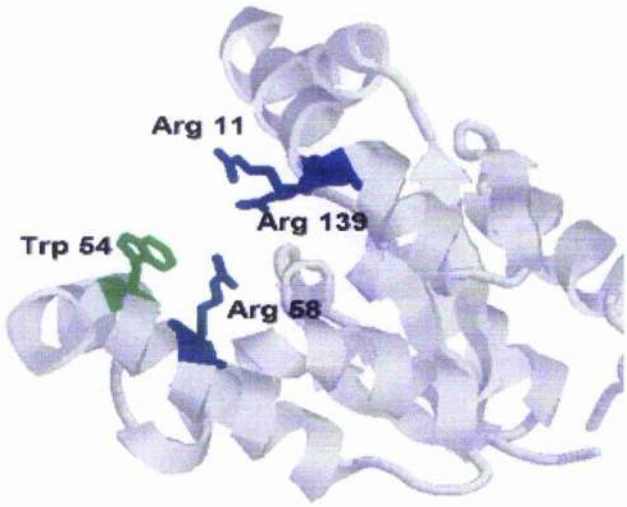

Figure 1.10: Position of the side chains of Arg11, Arg58 and Arg139.

The figure shows the three arginines around the Trp side chain that provide a highly positively charged environment around this residue and the shikimate binding site (Krell *et al.*, 1998).

1.3 Biophysical methods used in this work

1.3.1 Circular Dichroism

1.3.1.1 Introduction

The term Circular dichroism (CD) refers to the difference in absorption between left- and right handed circularly polarized light and the term optical rotatory dispersion (ORD) to the wavelength dependence of the optical rotation. These are two manifestations of optical activity, which is related to the asymmetry of the molecule, that may be caused by covalently bound groups or, in case of a macromolecule, by conformation.

In monochromatic, plane polarised, radiation the electric field and the magnetic field oscillate with a certain frequency along a fixed direction in the space. The oscillating direction of these two vectors is perpendicular to the propagation direction. The plane-polarised light can be divided in two circularly-polarised vectors, right (E_R) and left (E_L) respectively. While in an ordinary (achiral) medium E_L and E_R rotate with the same velocity, in a chiral medium these two components have different velocities. This is due to the different indices of refraction for the right- and left- circularly polarised light, n_r and n_l. The delay of the passage of the light passing throught a medium is explained by considering that the refractive index is correlated with the molecular polarizability. The light propagation can be considered as the radiation induces a dipolar oscillating moment that subsequently irradiates by itself. This radiation will have the same frequency of the incident light but, as it will be at a lower frequency than an absorption band, the phase will be delayed from the interaction. The delay of the phase, growing with the molecular polarizability, delays the passage of the light. This delay corresponds to the increase of the refractive index (the refractive index is correlated to the velocity of the light in a medium, $n_r = c/v$ where c is the velocity of the light *in vacuo* and v in the medium). This is called optical rotation. The variation of the optical rotation as a function of wavelength is called optical rotary dispersion (ORD). When the light passes throught a chiral medium and is absorbed there is the variation of two characteristics of the light: first the maximum amplitude is no longer confined in the plane, but it will form an ellipse in the plane x-y. This is due to the difference in the absorbance of the right or left circularly polarised light. The second difference is in the orientation of the ellipse due to the difference in the refractive index. When right- and left-cicularly polarised light is absorbed to different extents at some wavelengths the result is circular dichroism (CD) (Fig. 1.11) (Cantor and Schimmel, 1980; Woody, 1995). Since CD is an absorption difference, it is only observed in absorption bands.

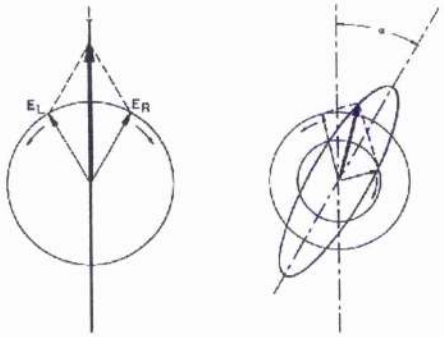

Figure 1.11: Effect of an absorbing chiral medium on linearly polarised light.

A linearly polarised light can be divided in two circularly-polarised vectors, right (E_R) and left (E_L) respectively, where the E_L and E_R components rotate with the same velocity. When the light passes through a chiral medium, and this medium present an absorption band, these two components have different velocities and amplitudes. The results is that the maximum amplitude is no longer confined in the plane and it will form an ellipse in the plane x-y.

1.3.1.2 The CD of proteins

CD is a solution technique that provides rapid determinations of protein secondary structure and it is a way to rapidly assess conformational changes resulting from different conditions eg.: protein concentration, pH, temperature and co-solute conentrations (if they do not absorb in the specific spectral region). CD has been used, in conjunction with other techniques, to study the kinetics and the intermediates of protein folding and unfolding (Labhardt, 1986; Kelly and Price, 1997; 2000). Finally CD is a useful tool for examining proteins made by site directed mutagenesis for structure-function studies, where it is important to know to what extent the conformation has been affected by the mutation. The far-UV spectrum will tell whether the mutant has folded with a backbone conformation similar to that of the wild-type protein, whereas the near-UV spectrum will detect many minor changes in conformation or dynamics.

The circular dichroism of biopolymers is usually measured in the region of electronic absorption (CD can be measured for any type of transition, for example vibrational CD is measured in the amide I and II region corresponding to the C=O stretch and N-H bend/CN stretch modes). The absorption bands that are optically active result from chromophores that are inherently asymmetric or symmetric chromophores that become asymmetric as a result of interaction with an asymmetric environment, as in the case of peptide bond.
The far-UV region (240-180nm) is dominated by the contribution of peptide bonds for which the CD band position and intensity depend on their conformation. Hence this part of the spectrum can be used to determine the secondary structure content of proteins (Woody, 1995; Kelly and Price, 2000).

The α-helix has two negative bands (222nm, transition n → π* and 208nm, transiton π→π* with the transition dipole parallel) and one positive band (190nm, transition π→π* with the transition dipole perpendicular to the helix axis). The β sheet has a negative band in the region 216-217nm, due to a n→π* transition, and a positive band at 195nm, due to a π→π* transition but the position and magnitude of these bands are variable. Finally the random coil has a weak positive band at 218nm (n→π*) and a more intense negative band at 197nm (π→π*).

An analysis of the secondary structure with CD is based on the idea that the mean residue ellipticity at any wavelength is a linear combination of the mean residue ellipticity of the individual secondary structures. The modern methods involve the use of databases of CD spectra and corresponding secondary structure contents derived from X-ray structure determination. A linear combination of these spectra is used to give a result that best fits the experimental spectrum for the test protein. The most accurate methods employ selection criteria in which only spectra similar to that of the experimental spectrum form the basis set (Johnson, 1988; Sreerama and Woody, 1994; Greenfield, 1996). It should be stressed that the far-UV CD of the peptide bond essentially reflects the dihedral angles so, when helices have strongly distorted angles, like those of transferrins, CD will underestimate the helical content (Bloemendal and Curtis Johnson Jr., 1995; Kelly and Price, 2000). Moreover the aromatic amino acid side chain or disulphide bonds can contribute to the CD spectrum in this region (Kelly and Price, 2000). Another source of error is when the spectra are not measured down to at least 184nm; although the α-helical content is reasonably reliable when deduced from spectra truncated at 200nm, estimates of the β-sheet content are not accurate (Bloemendal and Curtis Johnson Jr., 1995; Kelly and Price, 2000).

Since CD measures absorption differences highly sensitive detectors and bright light sources are prerequisites for good signal-to-noise ratios, expecially in the region below 200nm where many buffer components may absorb. Synchrotron radiation sources are especially useful at these lower wavelengths. In a synchrotron charged particles, in particular electrons or positrons, are forced to move in a circular orbit, leading to the emission of photons. When these charged particles are moving close to the speed of light, accelerated through magnetic fields, photons are emitted in a narrow cone in the forward direction at a tangent to the orbit. In a high energy electron or positron storage ring these photons are emitted over a wide range of wavelength from X-rays to the IR. This radiation is called synchrotron radiation. Synchrotron radiation has a number of unique properties, e.g.: high brightness (it is extremely intense and highly collimated), a wide energy spectrum and it is highly polarised. As far as CD is concerned the key advantage of the synchrotron is the very large increase in intensity (over 1000-fold) in the far-UV region (below 200nm) compared with the xenon arc sources in conventional CD instruments (Kelly and Price,

2000). In the near-UV (above 250nm), only the aromatic residues (and to some extent cysteine) absorb light. The tertiary fold of the polypeptide chain can place these side chains in chiral environments thus giving rise to CD spectra which can serve as characteristic fingerprints of the native structure (Kelly and Price, 1997; 2000). The position and sharpness of near-UV CD bands is influenced by the environment: hydrogen bonding usually yields a red shift, which can be up to 7nm, while hydrophobic environments tend to sharpen peaks. When an absorbing residue is highly mobile, CD from the different orientations will cancel each other (averaging of asymmetric environment) (Bloemendal and Johnson, 1995; Kelly and Price, 1997). This can be used to indicate flexibility changes in proteins. A slight loosening of a protein structure may not result in any change in solvent accessibility to aromatic residues and therefore will not change the maximum fluorescence wavelength of tryptophan. Such a change may also be outside the resolution of X-ray crystallographic analysis. The resulting change in dynamics of the residue, and hence in the asymmetry and detailed interactions with the immediate protein environment, will however affect the near-UV CD spectrum, usually quite markedly (Coligan *et al.*, 1997).

Non-protein chromophores or cofactors, such as flavin and haem moieties, may absorb in the regions of the spectrum well separated from those of aromatic amino acids or peptide bonds giving rise to CD signals which depend on the precise environment of the chromophore concerned (Kelly and Price, 1997). If in solution an equilibrium exists between two or more conformations, as in the case of denaturation, the CD gives an average indication of the conformational state of the protein. What will be observed, in the case of a two state transition, will be a sigmoidal transition that is a characteristic of these structural changes.

1.3.2 Fluorescence Spectroscopy

1.3.2.1 Theoretical background

Interaction of photons with molecules results in the promotion of valence electrons from ground state orbitals to higher energy level orbitals. Following excitation by absorption of energy, a molecule loses energy as heat by cascading through the closely spaced vibronic levels of the excited singlets (*internal conversion*). The molecule remains at the lowest vibrational level of the first singlet for a fraction of time because a relatively large amount of energy must be lost to go to the ground state. During this interval one of three things may happen: the molecule may convert to the triplet (*intersystem crossing*), it may revert to the ground state without emitting a photon, for example by collisional energy transfer to solvent or other molecules in the solution (*non-radiative transition*), or it may return to the ground state by emitting the excess energy as light. This process is called *fluorescence*.

The fluorescence emission and the non radiative transition are competitive and the fluorescence intensity depends upon the relative importance of each process (Lakowicz, 1983a; van Holde *et al.*, 1998; Sheehan, 2000). Fluorescence spectroscopy provides a powerful methodology for investigating the dynamic properties of solutions of biological interest. This is because the lifetime of the excited state is long and a broad range of interactions can influence this state and thereby the emission spectrum. These interactions include: collision with quenchers, rotational and translational diffusion, formation of complexes with solvents or solutes, and reorientation of the environment surrounding the excited fluorophore.

The fluorescence intensity is often defined in terms of quantum yield, Q (Lakowicz, 1983a; van Holde *et al.*, 1998; Sheehan, 2000) :

Q= number of photons emitted / number of photons absorbed

The basic requirement for fluorescence in a molecule is a highly delocalised system of electrons in fact most fluorescent molecules are aromatic (but note that not all aromatic molecules are fluorescent). Fluorophores are conveniently divided into "intrinsic" (i.e. those which are naturally occurring in the biological systems, or are very close analogues of parts of the system), and "extrinsic" (i.e. those which are added to the system and have no necessary structural relationship to the biological molecules) (Lakowic, 1983a). In both categories the fluorophores can be linked covalently or non-covalently to the biological system. Two types of factors may affect the intensity of fluorescence, internal and external (environmental) influences. Internal factors, such as the number of vibrational levels available for transition and the rigidity of the molecules are associated with the properties of the fluorescent molecules themselves. The external factors that affect Q give information about the macromolecule conformation and molecular interactions between small molecules (ligand) and larger biomolecules. Chromophores can be divided into those having a strongly polar excited state, in which separation of charge is much larger than in the ground state, and apolar fluorophores, in which there is a much more regular electronic distribution in both ground and excited states (Weber, 1997). The spectral changes of the first class of chromophores (to which the side chain of Trp residue belong- section 1.3.2.2) exhibit sensitivity to the environment. There could be two kinds of solvents effects: general and specific. General solvent effects depend on the polarizability of the solvent, and an increase in the dielectric constant usually shifts the fluorescence to longer wavelength. Specific solvent effects are the results of chemical reaction of the excited state with the solvent. Important chemical reactions include hydrogen-bonding, acid-base chemistry, and the formation of a charge transfer complexes where an electron in the fluorophore is transferred to another group on excitation (van Holde *et al.*, 1998).

1.3.2.2 Protein Fluorescence

The fluorescence spectrum of protein is usually dominated by the indole side chain of Trp residues, with the Tyr side chain also contributing, though fluorescence from tyrosine side chains is normally effectively quenched by energy transfer to Trp (Lakowicz, 1983b).
The fluorescence maximum of Tyr residue remains at 303nm irrespective of its molecular environment: the unfolding of proteins containing only Tyr is often accompanied by changes in intensity but not in emission wavelength. Decreased Tyr fluorescence in the native state is frequently observed. It is thought to originate from hydrogen bonding of the tyrosyl hydroxyl group and/or proximity of quenchers, such as disulphide bonds, in the folded state.
The environment of the tryptophan residue can be selectively investigated by exciting the protein at a wavelength of 295nm or greater because, at this wavelength, the fluorescence emission is essentially due to tryptophan residues (Eftink, 1991). The fluorescence spectrum of tryptophan appears to be sensitive to both specific and general solvent effects so, in proteins containing Trp residues, both shift in wavelength and changes in intensity are generally observed during unfolding. In a hydrophobic environment, such as in the interior of a folded protein, Trp emission occurs at lower wavelength (308nm for the deeply buried Trp in azurin) and is usually shifted to about 356nm in the unfolded state (Lakowicz, 1983b). Fluorescence from other reporter groups, intrinsic or extrinsic, can also be monitored. One example of this kind of probes is ANS, that binds non-covalently to proteins interacting mainly with hydrophobic surfaces. This probe has been used in protein folding studies to characterise structural features of folding intermediates (sections 3.4.2.8 and 9).

1.3.2.3 Binding Studies

The characterization of the ligand-binding interaction is of pivotal interest because the function of almost all proteins is related to their ability to bind ligands. Though there are several methods that can be used, fluorescence, because it is a solution method, allows us to study the effects of varying solution conditions, pH, ionic strength, and temperature.
To study ligand binding by fluorescence spectroscopy (Ward, 1985), it is necessary that a change in quantum yield be consequent upon ligand binding, whether one is observing ligand fluorescence or intrinsic protein fluorescence. The binding of a ligand to a protein affects the fluorescence in different ways: the ligand could act as a quencher (collisional mechanism), or it can interact physically with the fluorophore changing its environment or accessibility to solvent, or the binding can bring about a conformational change which leads to a change in the Trp environment (Eftink, 1997). In this work, the variation of the fluorescence intensity of SK on binding substrates has been used to determine their dissociation constants (section 2.3).

1.3.2.4 Quenching of Trp Fluorescence

Tryptophan appears to be uniquely sensitive to quenching by a variety of substances. This allows the determination of the accessibility of the Trp residue in proteins by quenching measurements. Fluorescence quenching can occur by a variety of mechanisms. One of the most important is that of collisional quenching which involves physical contact between the quencher and an excited indole ring. Certain compounds and ions are known to be particularly effective quenchers of fluorescence, usually by forming short lived collisional complexes with the excited state; in these complexes the energy of the excited state is dissipated as heat. The extent of quenching will not only depend on the nature of the quencher, but also on the accessibility of the fluorophores. While small molecules (e.g. oxygen) can penetrate *via* small crevices in the structure to the interior of the protein and so can quench the fluorescence of even deeply buried Trp side chains, other larger quenchers, such as acrylamide and succinimide, quench to a more limited extent. There is a strong relationship between the extent of quenching and the accessibility of the fluorophore (Eftink and Ghiron, 1976; 1981). Succinimide has proved particularly useful in this respect, e.g to examine the flexibility of the enzyme dehydroquinase (Moore *et al.*, 1993).

In addition to sensing the degree of exposure of the tryptophanyl residues, quenching studies can be used to reveal certain details concerning the microenvironment of the Trp residues. This can be done by comparing the quenching profiles for a protein obtained using quenchers of different charge or polarity. The local concentration of the quencher in the vicinity of the fluorophore may, in some cases, be affected by interactions between the quencher and the protein, thereby enhancing or reducing the effectiveness of the quencher leading to an under- or over-estimation of the exposure of a fluorophore. For example charged quenchers, such as iodide and caesium ions, are very suitable for examining the nature of the charged environment of fluorophores: a tryptophan that is flanked by positive charges (Lys or Arg residues), such as the W54 in SK (Fig. 1.10), might be quenched to a much greater degree by an anionic quencher than would normally be expected (Eftink and Ghiron, 1981).

1.3.3 Stopped flow CD and fluorescence

The stopped flow apparatus employs a rapid mixing and detection system that allows early events during a reaction to be examined. The dead time of a stopped flow instruments is usually of 5 msec (Kelly and Price, 2000). To detect changes, which occur in this time range, it is necessary to use low time constants and so, to improve the signal-to-noise ratio is then necessary to accumulate a certain number of traces. The high sensitivity and rapid response of fluorescence spectroscopy make it an ideal technique for stopped flow studies, which have been widely used in studies of protein folding (Eftink and Shastry, 1997). Coupling CD to stopped flow systems gives much higher noise and so it is necessary to employ low time constants and to accumulate a significant number of individual measurements to increase the signal-to-noise ratio (Kelly and Price, 2000). SF-CD data can provide useful information about the recovery/loss of secondary structure during the folding /unfolding transitions, reporting information over the entire protein, whereas the SF-fluorescence data provides information that is specific to the fluorescent sites. For this reason the two methods are complementary (Eftink and Shastry, 1997). Fast reactions, which occur within the dead time of most stopped-flow instruments, can be detected by the existence of "missing amplitude" in a kinetic experiment. SF-CD and fluorescence, (including the use of the fluorescent probe ANS; section 3.2 and 3.4.2), make SF a very useful approach to detect the accumulation of early transient intermediates in folding (Kuwajima *et al.*, 1987).

1.4 Aims of the project

The project involved the study of the unfolding and refolding of the enzyme to define the refolding pathways and the intermediates involved in this process. For this purpose spectroscopic techniques (fluorescence and CD) were used and activity and binding studies were undertaken. The refolding pathway was analysed using urea as denaturant (Chapter 3) and a study of the effect of salts on the conformation, stability, activity, binding, and refolding of SK was undertaken (Chapter 4; Appendix 4.1). Finally some experiments on the reactivity of the Lysine 15 side chain were performed to study the reactivity of this important side chain at the active site (Appendix 3.1).

Chapter 2: Materials and Methods

2.1 Enzyme purification

The purification protocol used for purifying the SK from *E. chrysanthemi* is based on the previous purification of the enzyme (Krell *et al.*, 1997) and was carried out largely by John Greene. This method was adapted from the one used for the purification of SK from *E. coli* (Millar *et al.*, 1986) by reducing the salt concentration so as to prevent protein precipitation. After cell breakage, all steps were performed at 4°C. *E. coli* BL21(DE3) pLysS cells (10g) were resuspended in 10 ml of buffer (20mM Tris/HCl, pH 7.5 containing 0.4mM dithiothreitol (DTT) plus one tablet of "Complete™" (Boehringer) to inhibit protease action). Cells were broken by two passes through a French pressure cell at 6.9 MPa and the resulting mixture was centrifuged at 100,000g for 1h. The supernatant was dialysed for 4h against buffer A (20mM Tris-HCl, pH 7.5 containing 0.4mM dithiothreitol and 1mM $MgCl_2$) and loaded on to a pre-equilibrated DEAE-Sephacel anion exchange column (30cm x 2.6 cm diameter, flow rate 50 ml/h). The column was then washed with buffer A until the absorbance at 280nm was less than 0.1. Elution of shikimate kinase was achieved using a linear gradient of 0-300 mM KCl in 600 ml buffer A with a flow rate of 50 ml/h and a fraction volume of 14ml. Pooled fractions were dialysed against buffer A. Before adding the solution to a Phenyl Sepharose CL-4B column (4 x 2cm), solid $(NH_4)_2SO_4$ was added to 30% saturation (164g/l). The solution was stirred for 20min and then centrifuged at 20,000g for 15min. The supernatant was loaded onto the column pre-equilibrated in buffer B (100mM Tris-HCl, pH 7.5 containing 0.4mM dithiothreitol and 1.2M $(NH_4)_2SO_4$). The column was washed overnight with buffer B at low flow rate (5ml/h) and 10ml fractions were collected. The enzyme was eluted using a linear gradient of 400ml 1.2-0.0 M $(NH_4)_2SO_4$ in buffer B with a flow rate of 20ml/h and a fraction volume of 10ml. At the end of the gradient the column was washed with 250ml of 100mM Tris-HCl, pH 7.5 containing 0.4mM dithiothreitol until residual shikimate kinase had been eluted. Active fractions were dialysed overnight against buffer A containing 10% (v/v) glycerol to concentrate the enzyme sample. After this step, the sample was loaded on to a pre-equilibrated Sephacryl S200 (superfine grade) column (120cm x 2.5 cm) and eluted at a flow rate of 10ml/h in buffer C (50mM Tris-HCl, pH 7.5 containing 0.4mM dithiothreitol, 5mM $MgCl_2$ and 500mM KCl) with a fraction volume of 4ml.

Active fractions were pooled and dialysed overnight against 50mM Tris-HCl, pH 7.5 containing 0.4mM dithiothreitol, 5mM $MgCl_2$ and 50% (v/v) glycerol. The purified SK was stored at –20°C. Before use, SK was dialysed against buffer D (35mM Tris-HCl, pH 7.6 containing 5mM KCl, 2.5mM $MgCl_2$ and 0.4mM dithiothreitol) and used within a two-day period. Enzyme activity, fluorescence and CD measurements showed that the protein is stable if stored at –20°C in this buffer (section 3.3.1).

The concentration of SK was determined spectrophotometrically using a value of 0.62 for the A_{280} of a 1mg/ml solution in a cuvette of 1cm pathlength. This value was calculated from the amino acid composition of the enzyme (Gill and von Hippel, 1989), using the observed ratio (1.09) of absorbances in buffer and in 6M GdmCl. This value was within 10% of that obtained using the dye-binding method (Bradford, 1976; Sapan *ef al.*, 1999). The ratio of absorbances at 280nm and 260nm was greater than 1.8, confirming the absence of significant contaminant by nucleotide.

2.2 Assay of enzyme activity

The activity of the shikimate kinase was determined by a double-coupled assay involving pyruvate kinase (PK) and lactate dehydrogenase (LDH). The production of ADP in the shikimate kinase-catalysed reaction leads ultimately to the conversion of NADH to NAD^+, which is monitored by the decrease in A_{340}. The assay was carried out at 25°C in a buffer consisting of 50mM triethanolamine hydrochloride containing 50mM KCl and 5mM $MgCl_2$, titrated to pH 7.2 with KOH (assay buffer). The reaction scheme is shown in figure 2.1. Concentrations of the assay components were 1.6mM shikimate, 5mM ATP, 1mM PEP, 0.2mM NADH, 1 unit of each of PK and LDH. Stock solutions of the substrates were stored at -20°C after neutralisation with KOH (except NADH prepared fresh daily). Under these conditions, the specific activity of the enzyme was 350µmol/min/mg (average of 5 assays).

In order to measure the activity of SK in the presence of denaturants or salts it was necessary to use a quenched assay because of the possible effects of these agents on the coupling enzymes (Johnson and Price, 1987). The SK-catalysed reaction was carried out in an assay solution containing 5mM ATP, 1.6mM shikimate and the appropriate concentration of GdmCl, urea or salts in the assay buffer. The stock solutions of salts used were prepared as described in section 2.7. At chosen times, after the start of the reaction, aliquots of this solution were diluted 30-fold into a quench mixture containing the appropriate concentrations of PEP, NADH, PK and LDH. From the decrease in A_{340}, the concentration of ADP produced in the SK-catalysed reaction at the chosen times can be determined, and hence the rate of this reaction calculated. Controls were performed to check that the conditions used had no influence on the coupling enzymes. For these was used an ADP stock solution which concentration was controlled spectrophotometrically using the absorbance at 260nm ([ADP]= 1mM → A_{260} =15). This stock solution was diluted in the proper conditions in an "incubation solution" and then assayed. The calculated and theoretical values were then compared to check any interference.

The apparent K_m values for each substrate, in buffer and in the presence of salts, were determined as follows: for ATP the concentration of shikimate was maintained at 3mM and

the ATP concentration was varied in the range from 0.1mM to 3mM; for shikimate the concentration of ATP was maintained at 5mM and the shikimate concentration varied in the range from 0.1mM to 4mM. The appropriate range of ATP or shikimate for each salt concentration was determined by a preliminary experiment. Kinetic parameters were obtained by direct fitting to the hyperbolic saturation curves using Microcal Origin software. All the salt and denaturants used were of analytical grade.

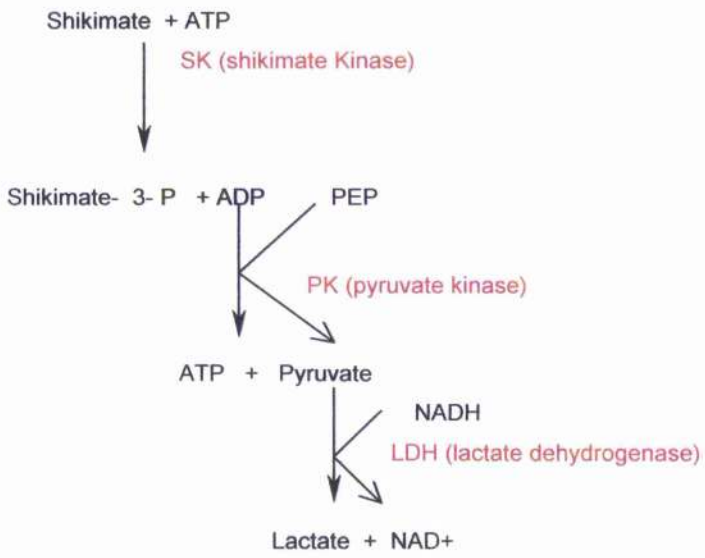

Figure 2.1: Double coupled assay scheme

The production of ADP in the shikimate kinase-catalysed reaction leads to the conversion of NADH to NAD^+, which is monitored by the decrease in absorbance at 340nm. The assay was carried out at 25°C in assay buffer (50mM triethanolamine hydrochloride containing 50mM KCl and 5mM $MgCl_2$, pH 7.2).

2.3 Substrate binding studies

Shikimate kinase undergoes conformational changes upon substrate binding (section 1.2.2.4). This leads to a quenching of the fluorescence intensity (Fig. 3.9) and allows the binding of ligands to be studied using fluorescence spectroscopy (section 1.3.2.3).
Assuming equivalent and independent binding sites and a consistent change in fluorescence on ligand binding the binding constant can be calculated by means of titration of a protein solution with ligands. Considering the binding equilibrium the dissociation constant can be expressed as follows:

$$AX \Leftrightarrow A + X$$

$$K_d = [A]_{eq}[X]_{eq}/[AX]_{eq}$$

Were A is the protein and X the ligand at the equilibrium. Titrating in conditions where

$$[X]_T >> [A]_T \text{ and so } [X]_T = [AX]_{eq} + [X]_{free} \approx [X]_{free}$$

K_d can be expressed in this way:

$$K_d = [A]_{eq}[X]_T/[AX]_{eq} \rightarrow [AX]_{eq} = [A]_{eq}[X]_T/K_d \quad (3)$$

The binding of the ligand causes a change in the fluorescence so:

$$\Delta F = F_n - F_0 \propto [AX]_{eq}$$

$$\Delta F_{max} = F_f - F_0 \propto [A]_T$$

were F_n is the fluorescence intensity after n-addition of ligand, F_0 is the initial fluorescence and F_{max} is the fluorescence of the solution after saturation. So:

$$\Delta F/\Delta F_{max} = [AX]_{eq}/[A]_T$$

This corresponds to the fraction of protein molecules bound ($[A]_T = [A]_{eq} + [AX]_{eq}$):

$$\Delta F/\Delta F_{max} = [AX]_{eq}/[A]_{eq} + [AX]_{eq}$$

Substituting the (3) in this expression it is obtained:

$$\Delta F/\Delta F_{max} = [X]_T/K_d + [X]_T$$

So the plot of $1 - F_n/F_0$ *vs* [X] (M) will give a rectangular hyperbola from which the values of K_d and $(1 - F_{max}/F_0)$ the limiting degree of quenching (between 0 and 1; zero in the case of no quenching, and so no detectable binding, and one, in the case of complete quenching) could be determined.

Experimentally the binding of substrates (shikimate, ADP and ATP) to SK, monitored by the quenching of protein fluorescence (Idziak *et al.*, 1997), was performed by titrations. These were carried out using the "CONCENTRATION" mode setting on the Perkin-Elmer LS50B

spectrofluorimeter (with the parameters modified for the purpose) and adding aliquots of the substrate stock solution, usually 10x10µl of the 10mM stock solution, of shikimate or ADP, followed by 3x10µl of the 50mM stock solution, measuring the fluorescence intensity at 350nm (excitation wavelength 295nm; T= 20°C). The stock solutions of substrates were made up in buffer D (35mM Tris-HCl, pH 7.6, 5mM KCl, 2.5mM $MgCl_2$, 0.4mM DTT) or in buffer E (MOPS - section 2.7). The protein concentration used in the titration experiments was in the range 0.04-0.06mg/ml and the volume of the SK solution was 1ml. The results were expressed as K_d (dissociation constant) and Q_{max} (fluorescence of the limiting quenching). In the case of ADP or ATP, a correction for the inner filter effect (Ward, 1985) was made using a parallel titration with the model compound N-acetyltryptophan amide (NATA). Each recorded intensity, F_n, was multiplied by the factor $F_{0\ (nata)} / F_{n\ (nata)}$, as described previously (Price, 1972). The concentration of the NATA stock solution was determined spectroscopically noting that a 100µM NATA solution has an absorbance at 280nm of 0.564. A control experiment was carried out for every set of titration experiments when the effects of denaturants or salts on binding parameters were investigated. The dissociation constants were determined by fitting the saturation curve ($1- F_n/F_0$ *vs* [substrate] (M)) to a hyperbolic function (Microcal Origin software) giving the K_d and Q_{max} values.

The binding of substrates (shikimate and ADP) to SK at different salt concentrations was monitored by the quenching of protein fluorescence as described before. The solutions were made up in the same range of protein concentration in buffer D (0.04-0.06mg/ml) and in the presence of the stated concentration of salt or denaturant. The binding of shikimate under these conditions was also measured in the presence of 2mM ADP. In the case of ADP, a correction for the inner filter effect was made using a parallel titration with the model compound NATA, as described previously. The dissociation constants were determined by direct fitting to a hyperbolic saturation curve.

Some of the titration experiments were performed by titrating a protein solution (0.04-0.06mg/ml) in the presence of shikimate (2mM) with stock solutions of salts. The instrument settings were the same as for the other type of titrations, while the addition of salts was usually 10 x 11µl of the salt stock solution. The concentrations of the salts stock solution used are reported in section 2.7.

2.4 Spectroscopic measurements

Except where indicated, all spectroscopic measurements were made on enzyme samples in buffer D (35 mM Tris-HCl, pH 7.6, 5 mM KCl, 2.5 mM $MgCl_2$, 0.4mM DTT). Spectroscopic measurements, such as CD and Fluorescence used in this work, are widely employed to study protein conformation (Price, 2000).

CD spectroscopy is useful to obtain information on the secondary structure and tertiary packing (section 1.3.1). The parameter used in CD is $\Delta\varepsilon$, the molar absorption difference, which is directly correlated to normal absorption and follows from the Lambert-Beer law:

$$\Delta\varepsilon = \Delta A/cd = (A_L - A_R)/ Cd$$

where C is the concentration in mole/litre (M), d is the pathlength in cm and $\Delta\varepsilon$ is the molar absorption differences in M^{-1} cm^{-1} between the absorption of left- and right-handed polarized light. Thus CD bands can be either positive or negative, depending on which type of light is absorbed more strongly. All commercially available CD instruments measure ΔA. The ellipticity is an angular measure that is related to ΔA as follows:

$$\theta = 32.98\ \Delta A$$

where θ is in degrees.
To eliminate the effects of pathlength and concentration, the molar ellipticity (deg. cm^2 $dmol^{-1}$) is defined as:

$$[\theta]_\lambda = MRW\ \theta/10\ d\ C$$

where θ is the observed ellipticity (degrees), d is the pathlength (cm) and C is the concentration (g/ml). At any wavelength the relation between the mean residue ellipticity and the difference in molar absorbance is:

$$[\theta]_\lambda = 100\ \theta/dc = 3298\ \Delta\varepsilon$$

(Cantor and Schimmel, 1980; Woody, 1995; Kelly and Price, 2000).
Most CD measurements were made using a Jasco J-600 spectropolarimeter, using cells of pathlength 0.05 or 0.5cm and protein concentrations in the range 0.1 to 0.5mg/ml, depending on the spectral region. Some CD data were obtained on experimental station 3.1 of the CLRC Daresbury Laboratory's Synchrotron Radiation Source (SRS). This facility comprises a vacuum-UV 1m Seya-Namioka monochromator, which provides a high flux of linearly polarised light in the wavelength range 120 to 300nm, which is converted to circularly polarised light (Clarke and Jones, 1999). The SRS CD facility was particularly useful when spectra were recorded in the presence of high concentrations of NaCl or urea which absorb

strongly in the far UV (Kelly and Price, 1997). Spectra were recorded using cells of pathlength 0.1 or 0.01mm and protein concentrations in the range 1 to 2mg/ml.

The other spectroscopic technique used is Fluorescence spectroscopy (section 1.3.2). Fluorescence data were obtained using a Perkin Elmer LS50B spectrofluorimeter and protein concentrations in the range 0.1-0.15mg/ml. Protein fluorescence was excited at 295nm, and emission spectra obtained over the range 300 to 400nm. ANS fluorescence was excited at 380nm, and emission spectra obtained over the range 400-600nm. The concentration of ANS stock solution was checked spectrophotometrically using a value of 6.0 for the A_{350} of a 1mM solution in a cuvette of 1cm pathlength (Dodd and Radda, 1968).

The degree of fluorescence quenching of Trp residues is a valuable means of obtaining information about the microenvironment and dynamics of the Trp side chain (section 1.3.2.4). The quenching reaction between the excited state of an indole ring, M^*, and a quencher, Q, can be described by the following scheme:

$$M^* + Q \underset{k_{-d}}{\overset{k_d}{\Leftrightarrow}} (M^* - - -Q) \xrightarrow{K_i} M + Q + \Delta$$

$(M^* - - -Q)$ is the complex formed by diffusional encounter between M^* and Q with rate constant k_d. The experimentally observed rate constant for the quenching reaction, k_d, is equal to $\gamma\, k_d$, where γ is the efficiency of the quenching process. The classical relationship often employed to describe the collisional quenching process is the Stern-Volmer equation:

$$F_0/F = 1 + K_{sv}[Q]$$

Where F_0 and F are the fluorescence intensities at an appropriate emission wavelength in the absence and presence of quencher, K_{sv} is the collisional quenching constant (Stern-Volmer constant) (Eftink and Ghiron, 1981; 1984). The magnitude of the Stern-Volmer constants is a valuable tool for monitoring the environment, mobility and accessibility of the Trp side chain. If the quenching yields a linear Stern-Volmer plot, this implies that the fluorescence quenching takes place on a simple collisional basis.

The quenching of the intrinsic fluorescence of Trp54 in SK by sodium iodide and succinimide in the presence of salts or salts and urea was analysed by Stern-Volmer plots (Moore *et al.*, 1993). Sodium iodide was chosen because it is sensitive to the environment of the single Trp present in the SK due to the presence of three positively charged arginines that surround this residue in the native conformation (Fig. 1.11). The concentration of enzyme used for the quenching experiment was about 0.1mg/ml (1ml). The stock concentration of quencher (2M) was made up in buffer D or E, aliquots were added and the intensity recorded after each addition (10µlx10 additions). The "CONCENTRATION" mode

setting was used with the excitation wavelength 295nm, the emission wavelength 350nm (band width 3nm; integration time 5sec). To study the effect of denaturants and salts (over the range of quencher concentrations from 0 to 0.2M) the K_{sv} was measured and the K_{sv} for the model compound NATA was calculated to assess the influence of the solution conditions on the changes in K_{sv}. The values reported in different solvent conditions were corrected for the values obtained for NATA :

$K_{sv(SK+x)} * K_{sv\ (nata)} / K_{sv(nata+x)}$ or $[F_0/F_n * (F_0/F_n)_{(nata)} / (F_0/F_n)_{(natacond.x)}]$.

Stern-Volmer constants (K_{sv}) were determined from the slope of the Stern-Volmer plot (F_0/F_n *vs.* [Q]) over the quoted range of quencher concentrations.

Light scattering was measured using the Perkin Elmer LS50B spectrofluorimeter with excitation and emission wavelengths of 320nm. This measurement gives a qualitative indication as to whether aggregation has occurred.

Stopped flow measurements (section 1.3.3) were made using an Applied Photophysics SX-17MV apparatus using a 10:1 mixing ratio. The dead times for the fluorescence and CD modes have been determined as 1.7ms and 8ms respectively (McClelland and Price, 1998). Kinetic analysis was undertaken using the Pro/K software supplied with the instrument. Unless otherwise stated, the errors in the amplitudes and rate constants derived were less than 10% of the stated values. The concentration of enzyme during refolding was in the range 60-110µg/ml in different experiments, with no significant variation in rate constants observed over this range.

2.5 Unfolding and refolding studies

The unfolding of SK was studied using chemical denaturation (GdmCl and urea) and the changes monitored by far-UV CD (loss of secondary structure) and fluorescence (loss of tertiary interactions).

Stock solutions of GdmCl (8M) and urea (10M) (both ultra pure grade) were made by weight and the concentration checked measuring the refracting index. To study the unfolding process, SK was incubated in the appropriate buffer and in the stated concentration of denaturant for 1h at 20°C, before the CD and fluorescence data were recorded. The unfolding was followed by monitoring the change at 222nm in the CD spectra and the change at 350nm in the fluorescence spectra (Price *et al.*, 1999). The far-UV CD and fluorescence spectra were recorded at 20°C as described in section 2.4. Protein concentration was approximately 0.1mg/ml and pathlength 0.05cm. The results were expressed as a percentage of total change of CD or fluorescence signal or as relative fluorescence:

$$\%\text{Total change} = (F_n - F_0)/(F_f - F_0) * 100$$

$$\text{Relative Fluorescence} = F_n/F_0 * 100$$

where F_n is the signal at a certain concentration of denaturant, F_0 is the signal at zero concentration of denaturant, and F_f is the signal at the higher concentration of denaturant used. A set of experiments was performed including different salts in the Tris buffer and another experiment was done using a chloride-free buffer system, namely MOPS, 3-[N-Morpholino] propanesulphonic acid. The salts concentrations were chosen to have comparable ionic strength, calculated as follows: $\mu = \frac{1}{2} \Sigma_i c_i z_i^2$ (section 2.7).

Since many globular proteins that have been found to approach closely a two state mechanism this kind of treatment was applied to SK in order to estimate of the free energy of stabilisation of native state (Pace, 1986):

$$N \Leftrightarrow D \qquad K_D = [D]_{eq} / [N]_{eq}$$

In which only the native state, N and the denatured state, D, are present at significant concentrations in the transition region. For a two state mechanism

$$f_n + f_d = 1 \quad \text{and} \quad Y = Y_n f_n + Y_d f_d \quad (3)$$

where Y is the observable parameter, and f_n and f_d represent the fraction of the protein present in the native and denatured states respectively. Combining the equations (3), it follows that:

$$f_d = (Y - Y_n)/(Y_d - Y_n) \text{ and } f_n = (Y_d - Y)/(Y_d - Y_n).$$

Thus, an equilibrium constant, K_D, and a free energy for unfolding, ΔG_D , can be calculated using:

$$K_D = e^{-\Delta G_D/RT} = f_d / f_n = (Y - Y_N) / (Y_D - Y)$$

The simplest method of estimating ΔG_D^{H2O} is to assume that the linear dependence of ΔG_D on denaturant concentration observed in the transition region continues to zero concentration, i.e. that the data obey an equation of the form:

$$\Delta G_D = \Delta G_D^{H2O} - m\ (\text{denaturant}) = -RT \ln K_{unf}$$

The kinetics of unfolding were determined in manual mixing mode by performing a 1/10 dilution into a buffer containing 4M urea, and monitoring the unfolding at 350nm (fluorescence) after excitation at 295nm.

The refolding was monitored by measuring the regain of the Fluorescence signal at 350nm (excitation at 295nm) or the regain of ellipticity at 225nm using both manual mixing and stopped flow techniques. When ANS was present in the refolding buffer the fluorescence was measured at 480nm (excitation at 380nm).

Refolding was initiated after unfolding in the presence of either 2.8M GdmCl or 4M urea for 1 hour (protein concentration about 1.1mg/ml), by dilution with 10 volumes of the specified buffer. The residual concentrations of denaturant were thus 0.25M GdmCl or 0.36M urea respectively while the protein concentration was in the range of 0.1mg/ml after dilution.

Other concentrations of proteins were tested to check for any concentration dependence of the refolding reaction. Each refolding curve is an average of at least 3 experiments (in the manual mixing mode) and of at least 10 shots in the stopped flow mode. The refolding curves were fitted with a single or double exponential as appropriate. The spectra of the start, end and refolded solutions were acquired each time.

When appropriate ANS, NaI, shikimate or salts were included in the refolding mixtures at a concentration of 40 µM, 0.1M, 2mM respectively and as specified for the salts, and a proper control (end point) was prepared in the stated condition.

ANS is used in the refolding experiments (section 3.4.2) to identify compact intermediates, especially during the early stages of folding. The ANS stock solution (10 mM) was made up in buffer D and its concentration checked spectrophotometrically after a 50-fold dilution as described previously (section 2.4). When different conditions were employed controls were performed to check the integrity of the protein solution used. In the case of refolding in the presence of ANS, spectra in both the Trp and ANS region were acquired.

In the case of refolding in the presence of shikimate the refolding was monitored by fluorescence at 330nm and not at 350nm because the fluorescence change at 350nm,

between the end and start point, was very small due to the shikimate quenching of Trp fluorescence (section 3.4.2.5). A control was performed at this wavelength (normal refolding without shikimate) in order to show that the kinetics were the same when monitored at 330nm or 350nm.

In order to study the salt-induced refolding of enzyme in the presence of 4M urea (an ionic strength jump), the unfolded enzyme was diluted with 10 volumes of buffer containing 4M urea and salt at a concentration of 1.1M for NaCl or 0.36M for Na_2SO_4. After dilution, the concentrations of denaturant and added salts were thus 4M urea and either 1M NaCl or 0.33M Na_2SO_4 (to give equivalent ionic strengths).

To monitor the regain of activity during the refolding, an unfolding solution was prepared, generally at a protein concentration of 1.1mg/ml. To start the refolding 100µl of this solution were diluted in 1ml of refolding buffer (buffer D alone or with different concentration of co-solutes) and the time was started. At different intervals of time 50µl of this solution was diluted into 950µl of assay buffer and immediately 20µl of this solution was assayed for enzyme activity. In the calculation of the refolding curve the delay due to the mixing and to the assay was considered. In these experiments, when appropriate, ANS or NaI were also included in the refolding mixtures.

2.6 Chemical modification by pyridoxal-5'-phosphate (PLP)

Chemical modification experiments represent one of the means, together with site directed mutagenesis, to investigate the role of single amino acid residues in catalysis. Chemical modification experiments have been performed on SK, using a lysine specific reagent (PLP) to investigate the role of the conserved P-loop lysine (K15) which, using site directed mutagenesis, has been demonstrated to have both a catalytic and structural role in SK (Krell *et al.*, 2001 - section 1.2.2.2).

The experimental situation considered here is when there is a considerable excess of modification reagent with respect to the residues that are modified: under these conditions the reaction can be regarded as pseudo-first order. The modification can be monitored either by following directly the appearance of product (the pyridoxyl derivatives of lysine possess characteristic white-blue fluorescence and they have an absorption maximum at 325nm with ε_M= 9710 $M^{-1}cm^{-1}$) or by following the effect of modification on some parameter of the enzyme (e.g. activity), as was done here.
The rate of inactivation, V_{inact} is given by

$$V_{inact} = -d[E]/dt = k_{inact}[E]$$

Rearrangement and integration between the limits 0 and t for time and E_o and E_t for [E] gives

$$\ln\{[E_t]/[E_o]\} = -k_{inact}\, t$$

where E_t is the activity at time t and E_o is the initial activity. Since $\ln\{[E_t]/[E_o]\}$ is the log of the residual activity at any time t, a semi-log plot of log (residual activity) *versus* time should give a straight-line plot, from the slope of which the values of the rate constant of inactivation, k_i can be determined. This analysis of the time dependence of inactivation assumes that the modification process is the only one utilizing the modification reagent. If the reagent is subject to a competing process, such as hydrolysis, this process will contribute to a decrease in reagent concentration as a function of time.

Pyridoxal phosphate (PLP) has been used in the modification of lysine residues. Generally PLP inhibits enzymes by formation of a Schiff base with a reactive Lys residue. This linkage is rapidly hydrolysed, so the Schiff base is often trapped by reduction with sodium borohydride ($NaBH_4$) (Valinger *et al.*, 1993). A number of protocols have been devised for the reduction; in the present work the procedure was chosen taking into account the fact that a double-coupled assay was used to determine enzyme activity. To set up a reliable method, controls and test reactions with and without reduction by $NaBH_4$ were performed. The first sets of controls were performed to check the feasibility of this kind of experiment using a double-coupled assay (section 3.3.6).

A control, using a stock solution of ADP was set up (Fig. 2.2). The stock solution of ADP (12mM) was diluted so that in a final volume of 2ml ("incubation volume") the concentration of ADP was 8mM. After dilution, the final concentration of ADP in the assay solution was 20μM. Three assays were performed: for the first one, performed to check the precision of the dilutions, 10μl of the "incubation" solution was diluted in 30μl of assay buffer and then 10μl was assayed (see section 2.2 for details of the assay solution). An experimental value of ADP concentration of 22.6μM was obtained, close to the calculated value (20μM).

The second assay was performed to assess the influence of the $NaBH_4$ (used to reduce the PLP-protein complex), on the coupling enzymes. For this purpose 10μl of the 8mM ADP solution were mixed with 30μl of $NaBH_4$ (5mg/ml) and 10μl of this solution assayed. There was no detectable activity: this experiment showed that any remaining trace of $NaBH_4$ could seriously affect the coupling enzymes.

The third assay was performed to check the influence on the activity of the coupling enzyme of an excess of PLP which had not been reduced. For this purpose 50μl of PLP 2mM was added to the ADP solution (8mM) and 10μl of this solution mixed with 30μl of $NaBH_4$ (5mg/ml). The concentration of ADP determined in this experiment was similar to the theoretical one (Fig. 2.2).

A second control experiment was done to check the effect of incubation at room temperature and stirring on the SK activity. A solution of SK (0.046mg/ml) was incubated at room temperature and assayed at time intervals (Fig. 2.3).

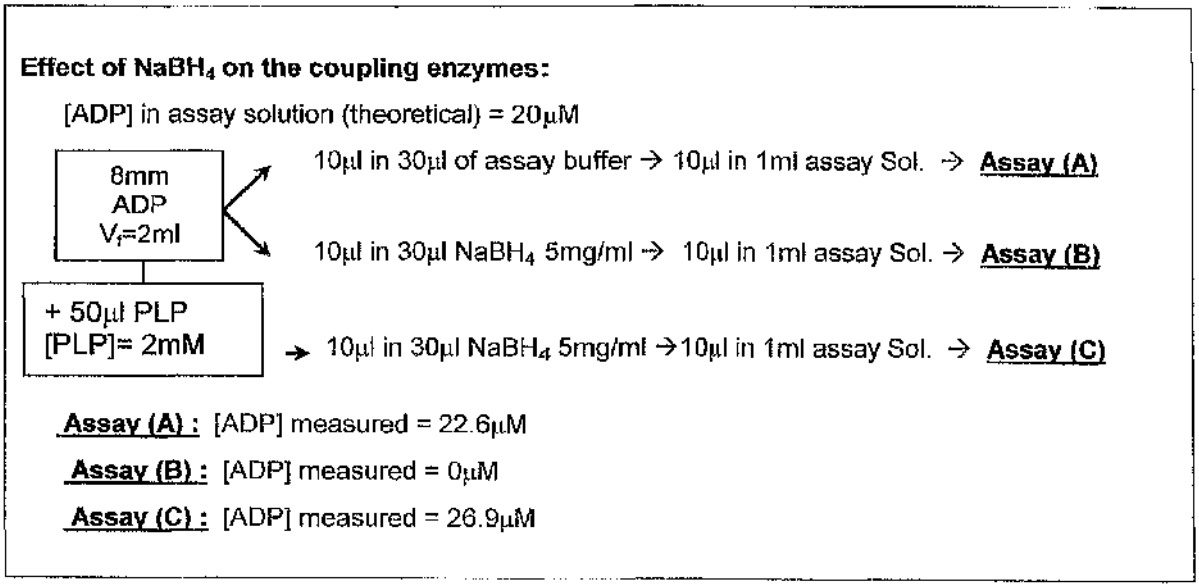

Figure 2.2 : First set of controls for the chemical modification experiments.

These controls were performed to check the feasibility of this type of experiment involving a double-coupled assay using a stock solution of ADP of known concentration.

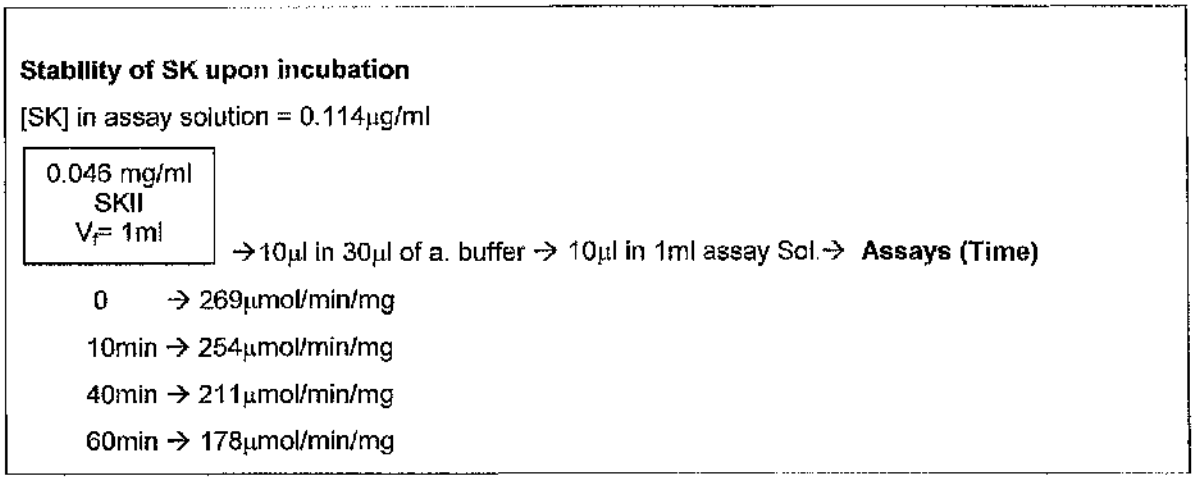

Figure 2.3: Effect of incubation time and stirring on SK activity .

The final control was performed to check the effect of different concentrations of $NaBH_4$ on SK activity. Three assays were performed by dilution of 10µl of the SK solution (0.046 mg/ml) with 30µl of buffer or water containing $NaBH_4$ and assaying 10µl of the resulting solution (Fig. 2.4). In this case there is an effect on the activity. So an eventual excess of $NaBH_4$ will have an effect on the SK activity leading, probably, to an overestimation of the inactivation, especially for the first data points in the time-course inactivation curve.

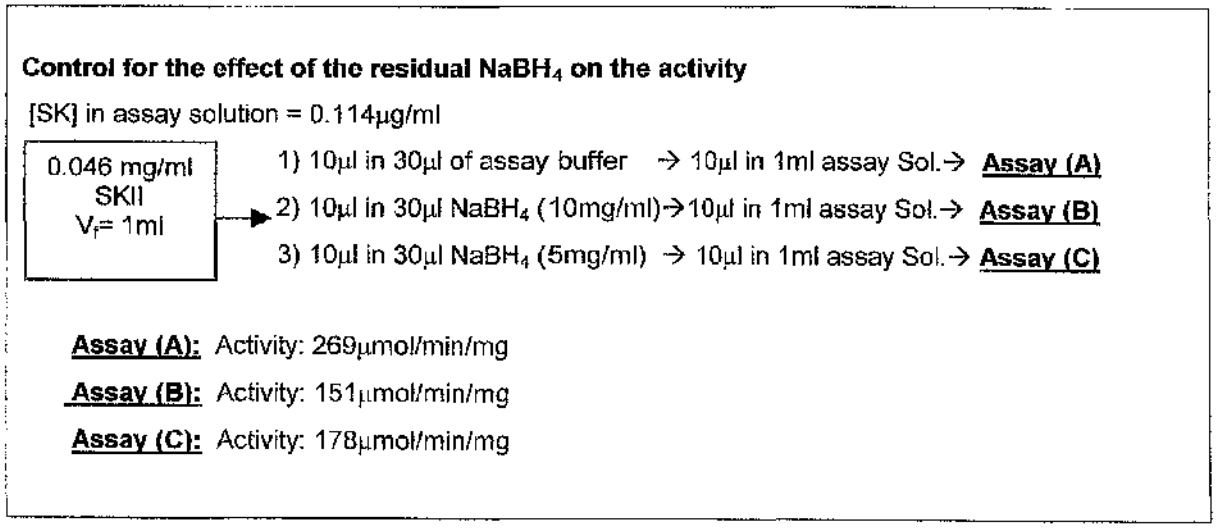

Figure 2.4: Effect of residual concentration of $NaBH_4$ on SK activity.

For inactivation experiments SK (0.046mg/ml) was incubated at room temperature (20°C) while stirring in test tubes (2ml) protected from the light with metal foil (protection from light sources was necessary to avoid photolytic degradation of PLP). Reactions were carried out in assay buffer (section 2.2) containing various concentrations of PLP (0.5; 1; 1.4mM). Zero time activity was determined by sampling prior to PLP addition; the effect of dilution (by addition of PLP) was taken into account. At chosen time intervals, samples (10µl) were added to 30µl of water (non-reduced samples) or to a solution of 5mg/ml of $NaBH_4$ in water (reduced samples), mixed, and immediately assayed (10µl of the resulting solution in 1ml of assay solution).

Some equilibrium protection experiments were carried out to check the effect of ligand binding on the inactivation reaction (Chen and Engel, 1974 ;1975). The effect of ligands on inactivation of SK by PLP was investigated by incubating the enzyme with PLP (1.4mM) in the presence of certain concentration of ligands (2mM shikimate, 2mMATP or 2mM ADP; 2mM shikimate and 2mM ADP; 2mM shikimate and 0.1M NaF). The zero-time activity was measured on the sample, containing the ligand, before the addition of PLP.

2.7 Studies of SK in the absence of chloride ions

In order to assess the effect of low concentrations of chloride on the conformational stability and function of the enzyme, some studies were performed in a chloride-free buffer (Buffer E), consisting of 50mM MOPS (3-[N-Morpholino]propanesulphonic acid), pH 7.6, containing 2.5mM K_2SO_4, 2.5mM $MgSO_4$ and 0.4mM dithiothreitol. A range of unfolding, refolding studies and binding experiments were carried out in this buffer.

The salts and the concentration of the stock solutions used were: NaCl (5M), Na_2SO_4 (1M), NaF (1M), KCl (4M), $MgSO_4$ (2.5M), NaBr (5M), $CaCl_2$ (2.5M), $MgCl_2$ (1M), $Ca(NO_3)_2$ (2.5M), $NaNO_3$ (5M). All the salts used were of analytical grade and the stock solutions were prepared by weight.

Chapter 3: The folding of type II shikimate kinase

3.1 Abstract

Shikimate kinase was chosen as a convenient representative example of the subclass of α/β proteins with which to examine the mechanism of protein folding (section 1.2.2.5).

A study of the unfolding and refolding of the type II SK, using studies of CD, protein fluorescence, activity and ANS fluorescence, and employing both manual mixing and rapid reaction techniques (sections 1.3.1-1.3.3) has been undertaken. The secondary structure content in solution was determined analysing CD data acquired over a more extended range of wavelengths using the SRS CD facility (section 3.3.1.1). When excited at 295nm, the fluorescence emission maximum of SK is 346nm, indicating that the single Trp (W54) is significantly exposed to the solvent, a conclusion consistent with the high value of the Stern-Volmer constant for quenching of the fluorescence by succinimide (Idziak *et al.*, 1997). For quenching experiments the quenching agents used were both succinimide and NaI, the latter giving information on the charged Trp environment (section 3.3.6) and providing reference values of K_{sv} when NaI was used in the refolding experiments (sections 3.4.1.4 and 3.4.2.6). When incubated in 4M GdmCl or 6 M urea, the fluorescence emission maximum shifts to 356nm, indicating that the Trp has become completely exposed to solvent, and there is a complete loss of secondary structure, with the ellipticity at 225nm reduced to less than 10% of the value characteristic of native enzyme. The equilibrium unfolding was performed both with SK alone and in the presence of shikimate (sections 3.3.2 and 3.3.3) and using both guanidinium chloride (GdmCl) and urea as denaturing agents. For both the denaturants used the unfolding curves were analysed in terms of the 2-state model and the stability of the folded state could be estimated as 17 kJ/mol. The activity (section 3.3.1.2 and 3.3.5) and the dissociation constants (K_d) for substrates (sections 3.3.1.2 and 3.3.4) were also studied in the presence of denaturants. Differences were found between the two denaturants used, especially when comparing the variation of the activity profile or the K_d with the denaturant concentration and the degree of unfolding measured by CD and fluorescence. This led to subsequent studies on the effects of different salts on the enzyme activity, binding of ligands, structure and folding kinetics (Chapter 4). The refolding experiments were at first carried out using GdmCl as denaturant (section 3.4.1). Due to the high extent of aggregation, highlighted by elevated light scattering during the refolding and by the anomalous pattern of the refolding in the presence of ANS (section 3.4.1.5), urea was used for further characterisation of the refolding kinetics (section 3.4.2). On the basis of these results a model of folding pathway was proposed (section 3.4.2.10). The relevance of the results to the folding of other α/β domain proteins is discussed (section 3.4.2.11).

3.2 Introduction

The determination of the secondary structure content in solution reflects the conformation of the protein under the actual experimental conditions: analysis of the CD spectrum in the far-UV region gives this estimation (section 1.3.1.2). To facilitate a reliable analysis, especially of the β-sheet content, it is very useful to obtain a good signal-to-noise ratio below 184nm. This is not always possible with commercial spectropolarimeters because, in this region, several components used in the most common buffer systems absorb strongly. Data below 200nm can be obtained using a bright light source (synchrotron radiation), and for this purpose the SRS facility in Daresbury (section 3.3.1.1) has been used. The effects of the storage conditions on the activity and conformation of the enzyme have been investigated to find the best storage conditions to avoid experimental artefacts (section 3.3.1.3). Shikimate kinase, as other kinases, is thought to undergo conformational changes upon substrate binding (hinge bending movements - section 1.2.2.4). The conformational changes can be investigated by studying the binding of substrate (section 1.3.2.3). Because the binding of shikimate, ADP and ATP give a quenching of the intrinsic Trp fluorescence (W54), this can be used to calculate the K_d by titration (sections 2.3; 3.3.1.2 and 3.3.4).

The study of the unfolding transition should be undertaken before studying the refolding reaction: it gives information on the eventual existence of stable intermediates in the unfolding process, provides an estimation of the stability of the enzyme and allows a determination of the conditions to use in the refolding experiment. The unfolding was measured following the CD change at 222nm, the fluorescence at 350nm and the change in the ratio F_{356}/F_{337} (used to measure the degree of exposure of Trp because of the change in emission maxima). The ratio F_{355}/F_{337} has the advantage of being independent of small variations of protein concentration between different experiments and reflects mainly the shifts in emission maxima upon denaturation or varied solvent composition, due to changes in polarity of the local environment surrounding tryptophan (Kleppe *et al.*, 1999). The unfolding transition has been studied using two denaturants, GdmCl and urea, with different chemical properties. In some cases estimates of protein stability obtained using both denaturants has revealed mechanistic differences (Gianni *et al.*, 2001) or has revealed insights on the properties of intermediates on the unfolding pathway (Hung and Chang, 2001). It has been suggested that these differences depend on the electrostatic and hydrophobic interactions in the particular protein. In fact urea, apart from the hydrogen bond breaking effect, also acts on hydrophobic bonds, while ions arising from GdmCl modulate electrostatic interactions. The chemical denaturation was also performed in the presence of substrate (section 3.3.3). This together with the data on the dissociation constants (K_d) of substrates and activity measurements in the presence of

denaturants (or salts) permit the possibility of quantifying the effects of these co-solvents on the active site and can give useful information about the kind of interactions responsible for binding substrates. These kinds of experiments can give useful insights into the unfolding process: for many proteins it has been demonstrated that the presence of the substrate protects the enzymes against chemical or thermal denaturation (Kleanthous *et al.*, 1991; Ribas de Pouplana *et al.*, 1991) while other reports (Wang *et al.*, 2000) have shown that during the denaturation of a number of enzymes by GdmCl, urea or heat, inactivation occurs before noticeable conformational changes of the enzyme molecule as a whole can be detected. It was suggested in these cases that the active site of the enzyme is usually situated in a limited region of the molecule that is more flexible than the enzyme as a whole (Tsou, 1986; 1993).

The refolding studies involved the study of the folding kinetics using CD and fluorescence with manual and rapid mixing techniques and the kinetics of refolding were monitored by activity, amide CD, intrinsic fluorescence, ANS fluorescence and changes in fluorescence due to binding of ligands. This allows one to monitor, respectively, the regain of the specific three-dimensional structure of the active site, the generation of the backbone conformation, burial of aromatic groups in the interior of the protein, formation of compact intermediates and formation of the substrate binding site (McClelland and Price, 1997). Finally the use of NaI, a quencher the Trp fluorescence (section 2.4), in the refolding buffer allowed an assessment of the regain of the charged Trp environment.

The P-loop lysine (K15) is one of the conserved residues in the family to which SK belongs and is involved in the binding of nucleotide (section 1.2.2). On the way to investigate the importance of a residue for catalysis is by chemical modification. Experiments on SK carried out using TNBS (2,4,6-trinitrobenzenesulphonic acid) as modifier showed an enhanced chemical reactivity toward this compound, with a second order rate constant of inactivation calculated as $6.15 \times 10^4\ M^{-1}min^{-1}$ (Krell *et al.*, 2001). This seems to be due to the proximity of the side chain of C13 to K15, with the formation of an ion pair between these residues. It was suggested that the TNBS cause a rapid modification of C13 followed by intramolecular transfer of the TNBS group to the lysine residue (Krell *et al.*, 2001). Though TNBS is a reagent selective toward the α and γ amino group, some reaction with the sulphydryl group may occur. The use of PLP (pyridoxal-5'-phosphate) seemed to be a good solution to this problem, this reagent being more lysine-specific than TNBS: in fact the reaction with the Cys SH group would form an hemithioacetal, an unstable compound rapidly hydrolysed in an aqueous environment. For this reason some preliminary experiments of chemical modification using PLP as modifier were carried out (Appendix 3.1).

3.3 Unfolding of the enzyme

3.3.1 Conformation of the enzyme in solution, kinetic parameters and aggregation

3.3.1.1 SK circular dichroism spectra

The far-UV CD spectrum of SK in buffer D (35mM Tris-HCl, pH 7.6, 5mM KCl, 2.5mM $MgCl_2$, 0.4mM DTT) in the absence of denaturants shows pronounced double minima at 208nm and 222nm and a maximum at 193nm (Fig. 3.1a). An initial analysis of the spectrum over the range 240nm to 195nm by the CONTIN procedure (Provencher and Glöckner, 1981) gave 28% α-helix, 34% β-sheet, 15% turn and 23% remainder, while using the SELCON procedure (Sreerama and Woody, 1993) over this range of wavelengths, the values were 30% α-helix, 19% β-sheet, 21% turn and 30% remainder (Krell *et al.*, 1998).
A possible reason for the discrepancy between these estimates and those obtained from X-ray crystallography (50% α-helix and 13% β-sheet) could be that the analysis was carried over a restricted range of wavelengths. By analysing CD data (Figure 3.2) acquired over a more extended range of wavelengths (260nm to 178nm) at the SRS CD facility, using the SELCON procedure (Sreerama and Woody, 1993) the secondary structure content was estimated as 41% α-helix, 15% β-sheet, 17% turn and 27% remainder (section 1.3.1.2). These values are in closer accord with the crystallographic data.

The chloride-free buffer MOPS (50 mM 3-[N-Morpholino] propanesulfonic acid, pH 7.6, containing 2.5 mM K_2SO_4, 2.5 mM $MgSO_4$ and 0.4mM dithiothreitol - section 2.7) was used to assess the effect of the relatively low chloride concentration in buffer D on the structure and kinetic parameters of the enzyme. CD spectra in the far and near-UV region were acquired to check that no conformational changes were due to the change of buffer (Fig. 3.1a,b). No major differences were observed in the fluorescence spectra as is shown from the comparison between the normalised fluorescence spectra (Fig. 3.3). The normalisation (F_n/F_{350}) was necessary in order to compare results obtained on different days from SK solutions at slightly different concentrations. These data indicate that there are no differences in the overall secondary and tertiary structure in the chloride-free buffer.

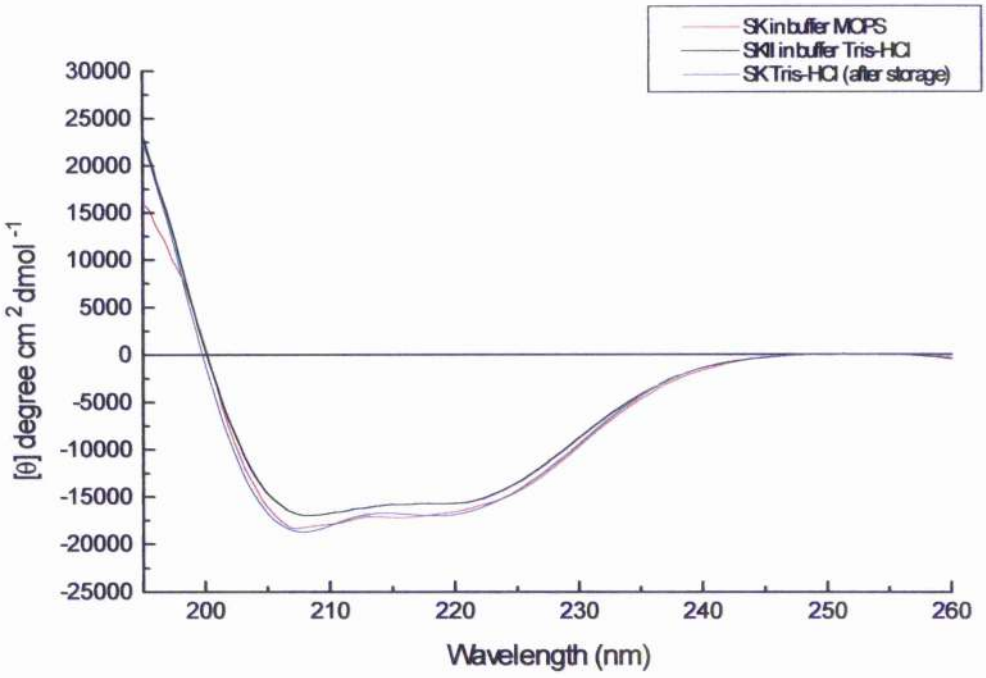

a)

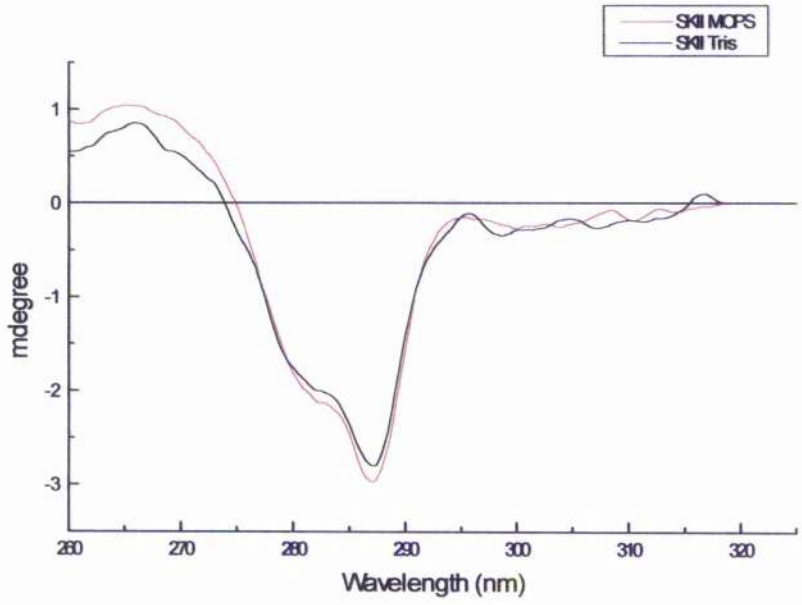

b)

Figure 3.1: Comparison of the far- (a) and near- (b) UV CD spectra in Tris and MOPS

Spectra were recorded at 20°C using samples dissolved in buffer D (35 mM Tris-HCl, pH 7.6, containing 5 mM KCl, 2.5 mM $MgCl_2$ and 0.4mM dithiothreitol) or in buffer MOPS (50 mM 3-[N-Morpholino] propanesulfonic acid, pH 7.6, containing 2.5 mM K_2SO_4, 2.5 mM $MgSO_4$ and 0.4mM dithiothreitol). (a) Far-UV CD spectra. The protein concentration was 0.15mg/ml and the cell pathlength 0.05cm; (b) Near-UV CD spectra. The protein concentration was 0.5mg/ml and the cell pathlength 0.5cm. Black line: SK in Tris buffer; Red line: SK in MOPS buffer; Blue line ((a) only): SK in Tris after storage.

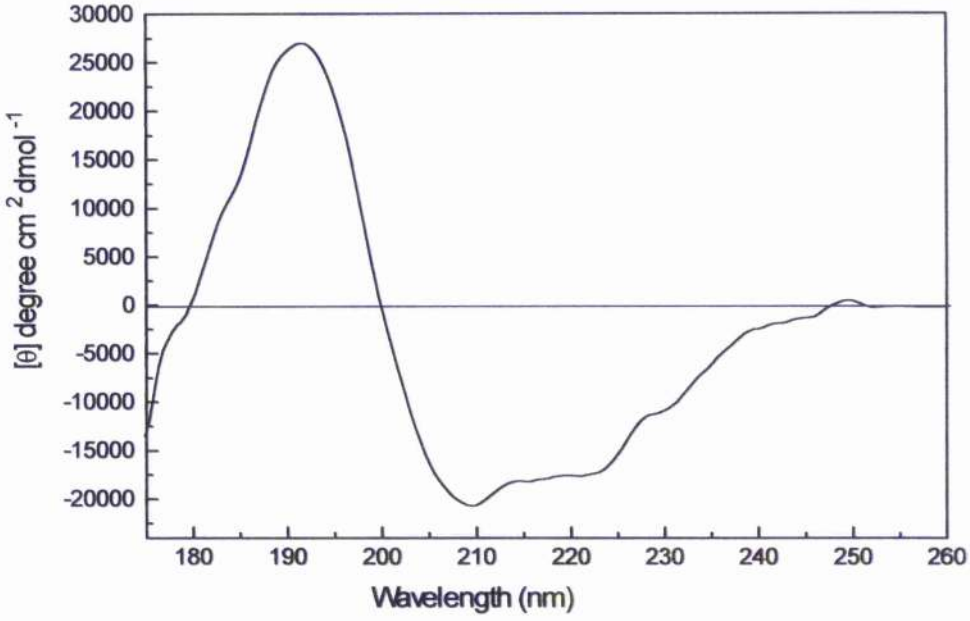

Figure 3.2: The far UV CD spectrum of SK.

The spectrum was recorded in buffer D (35 mM Tris-HCl, pH 7.6, containing 5 mM KCl, 2.5 mM $MgCl_2$ and 0.4mM dithiothreitol) using the Daresbury SRS CD facility at a protein concentration of 2mg/ml and a cell of path length 0.01mm.

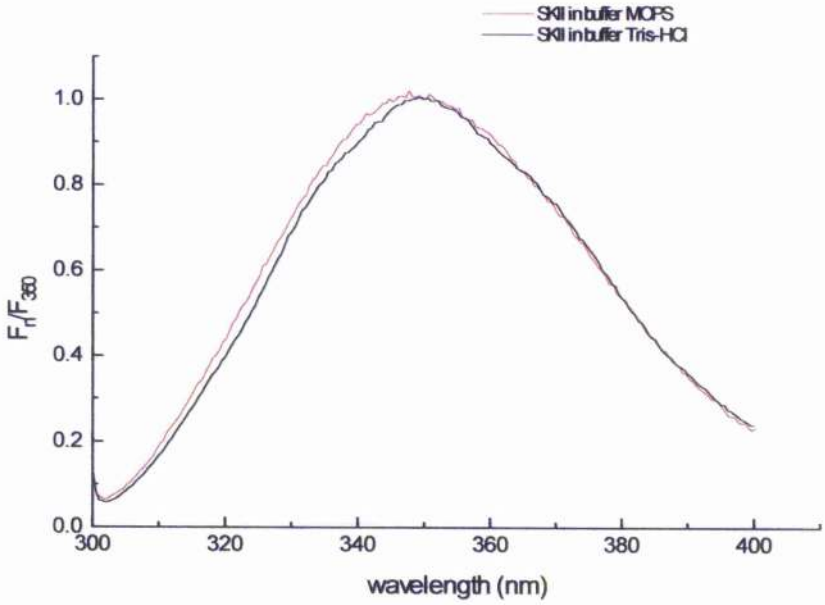

Figure 3.3: Normalised fluorescence spectra (F_n/F_{350}) in Tris-HCl and MOPS

Spectra were recorded at 20°C using samples dissolved in buffer D (35 mM Tris-HCl, pH 7.6, containing 5 mM KCl, 2.5 mM $MgCl_2$ and 0.4mM dithiothreitol) or in buffer MOPS (50 mM 3-[N-Morpholino] propanesulfonic acid, pH 7.6, containing 2.5 mM K_2SO_4, 2.5 mM $MgSO_4$ and 0.4mM dithiothreitol) and protein concentration 0.15mg/ml.

3.3.1.2 Specific activity and kinetic parameters.

The specific activity in buffer D was determined as 350μmol/min/mg (average of 5 assays). The activity of SK measured in MOPS buffer was within 10% of the activity of enzyme stored under the same conditions in Tris-HCl buffer.

The K_d for shikimate (in the absence and in the presence of 2mM ADP), for ADP and ATP, were determined by titration (section 2.3); the reported values are the averages of at least 6 experiments (Table 3.1- Figure 3.4). The apparent K_m values for shikimate and ATP (Table 3.1) were determined as described in section 2.2.

A substantial difference between Tris-HCl and MOPS is observed in the binding of shikimate (Fig. 3.4a) that seems to be stronger in MOPS than in Tris-HCl with the value of K_d being reduced from 0.6mM (Tris-HCl) to 0.22mM (MOPS) (Table 3.1). This seems to be due to the presence of chloride ions. In fact the value of K_d is restored to the value found in Tris-HCl if the chloride concentration present in the Tris buffer is restored by adding 45mM NaCl to the MOPS buffer (Fig. 3.4a). Moreover, this effect is dependent on the chloride concentration, as is demonstrated by the higher values of the K_d obtained in the presence of 100mM NaCl (Table 3.1). The binding of shikimate in Tris-HCl buffer, is strengthened by the presence of 2mM ADP, but when similar titrations were performed in a chloride-free buffer (MOPS) this synergism was no longer observed: the K_d value is changed from 0.25mM to 0.36mM in the presence of ADP. Interestingly this effect appears to be due to the presence of chloride ions, which weaken the binding of shikimate. In chapter 4 there will be reported data that demonstrate that this effect of NaCl is reversed, to some extent, by the presence of ADP giving a decrease of the K_d.

The binding of ADP does not appear to be influenced by the change of buffer the K_d values being 1.71mM and 2.16mM in Tris-HCl and MOPS respectively (Fig. 3.4b; Table 3.1).

The ATP binding is affected to a certain extent with the K_d value changing from 2.58mM (Tris-HCl) to 1.41mM (MOPS) and this difference is not dependent on the chloride ion concentration (Fig. 3.6; Table 3.1). An initial analysis of the data indicated that the binding of ATP was affected by the presence of both sulphate and chloride ions. In figure 3.4c the ATP binding curves, both in Tris-HCl and in MOPS buffer, are fitted with a hyperbolic function though the best fit in the both cases is obtained with a sigmoidal curve. The curve in MOPS plus 45mM NaCl gives instead a good hyperbolic fitting. These findings prompted a more detailed study of the effects of salts on ATP binding which will be discussed in section 4.4.

The nucleotide binding to SK occurs with relatively low affinity, as shown by the K_m (ATP) and by direct measurement of K_d (ATP) by the fluorescence quenching technique.

This indicates, in general, that the sites are relatively "open" when binding nucleotide.

Ligand	Buffer	K_d (mM)	K_m (mM)
Shikimate	Tris-HCl	0.60 ± 0.02	0.134 ± 0.02
	Tris-HCl + 2mM ADP	0.38 ± 0.02	
	MOPS	0.25 ± 0.01	
	MOPS + 2mM ADP	0.36 ± 0.01	
	MOPS + 45 mM NaCl	0.43 ± 0.02	
	MOPS + 100mM NaCl	0.86 ± 0.03	
ATP	Tris-HCl	2.58 ± 0.51	0.266 ± 0.02
	MOPS	1.41 ± 0.19	
	MOPS + 45mM NaCl	1.47 ± 0.18	
ADP	Tris-HCl	1.71 ± 0.1	
	MOPS	2.16 ± 0.1	

Table 3.1: Kinetic and binding parameters of shikimate kinase

K_m values were calculated using a hyperbolic fitting to the Michaelis-Menten equation. The assay conditions used are described in section 2.2 and the assay mix contained 5mM ATP and 3mM shikimate for K_m (shikimate) and K_m (ATP) respectively. K_d values were determined using fluorescence quenching experiments as described in section 2.3.

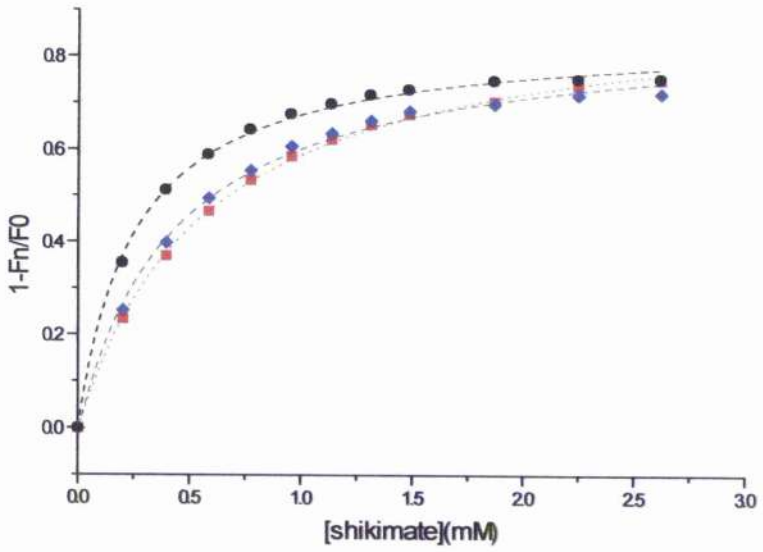

a)

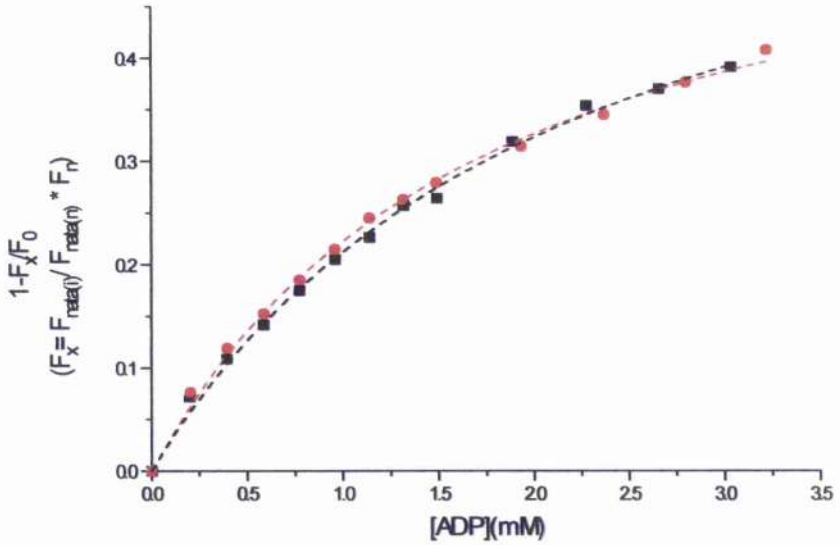

b)

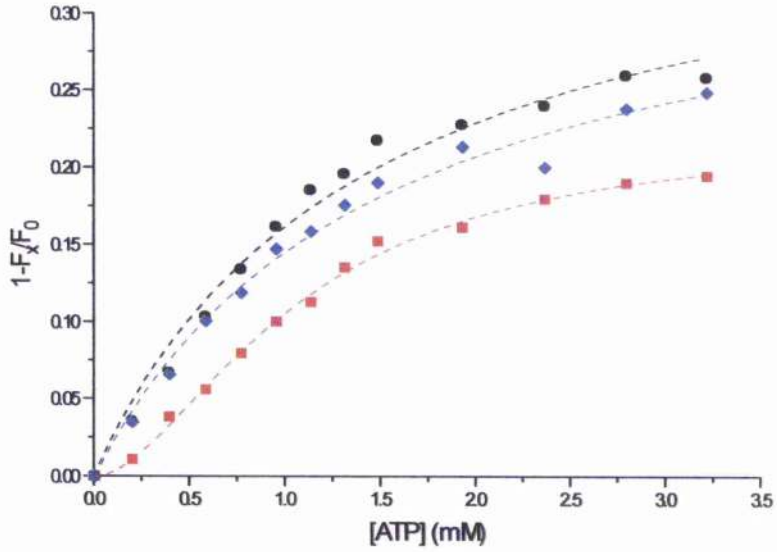

c)

Figure 3.4: Binding of substrates determined by fluorescence quenching experiments.

Aliquots of the substrate stock solution were added (10x10µl of the 10mM stock solution followed by 3x10µl of the 50mM stock solution) and the fluorescence intensity (T= 20°) at 350nm was measured after every addition after excitation at 295nm. The protein concentration was in the range 0.04-0.06mg/ml. The dissociation constants were determined by fitting the saturation curve to a hyperbolic function giving the K_d and Q_{max} values.

a) shikimate titrations: MOPS (black), Tris (red) and MOPS + 45 mM NaCl (blue).
b) ADP titrations:MOPS (black), Tris (red)
c) ATP titrations: MOPS (black), Tris (red) and MOPS + 45 mM NaCl (blue).

3.3.1.3 Protein Stability

The protein used for the experiments was generally freshly dialysed against buffer; frozen samples being used only occasionally. The stability of SK was investigated under different conditions and using a variety of measurements. For the measurements of the SK stability on storage at –20°C using activity, aliquots of an enzyme preparation were frozen and assayed after different periods of storage. Table 3.2 reports the activity values at different times of storage: further investigation should be undertaken to check for the observed increase in activity. After prolonged storage (45 days) at –20°C, there are no significant differences in the far-UV CD spectrum (Fig. 3.1a), in the fluorescence spectrum or in the binding parameters as well (the binding values acquired after storage were within 10% of the values obtained for the freshly prepared sample). The effect of incubation of protein solution at room temperature was also investigated. Spectra were acquired of a protein solution freshly dialysed and after incubation. There is a decrease in fluorescence intensity at 350nm with time of 6% after 45 min of incubation and 14% after two hours. In a further experiment, the effect of incubating a concentrated solution of SK at room temperature was investigated. After storage for 10 hours at room temperature the spectra were acquired of the protein solution at two different concentrations. Though the more concentrated solution has a lower intensity compared to the more diluted solution (Figure 3.5a), they have the same emission maxima. Comparison of these normalised spectra with that of freshly prepared SK shows that a shift of the maximum wavelength of 8nm has occurred indicative of a partial unfolding (Figure 3.5b). Increasing the concentration of the SK lead to an increase in aggregation, as shown by the A_{310} values which represent light scattering:

[SK] = 0.1mg/ml → A_{310}= 0.022

[SK] = 0.68mg/ml → A_{310}= 0.043

[SK] = 2.06mg/ml → A_{310}= 0.30

Assayed	Activity (μmol/min/mg)
Same Day	396/ 350*
After 1 day storage	375
After 4 days storage	383
After 10 day storage	328
After 11 day storage	445
After 14 day storage	489

Table 3.2: Stability measurements. Activity

The assay was carried out at 25°C in a buffer consisting of 50mM triethanolamine hydrochloride containing 50mM KCl and 5mM $MgCl_2$, titrated to pH 7.2 with KOH (assay buffer). The concentrations of the assay components were 1.6mM shikimate, 5mM ATP, 1mM PEP, 0.2mM NADH, 1 unit of each of PK and LDH. The protein concentration in assay solution was 0.1μg/ml. (*) average value of 5 assays.

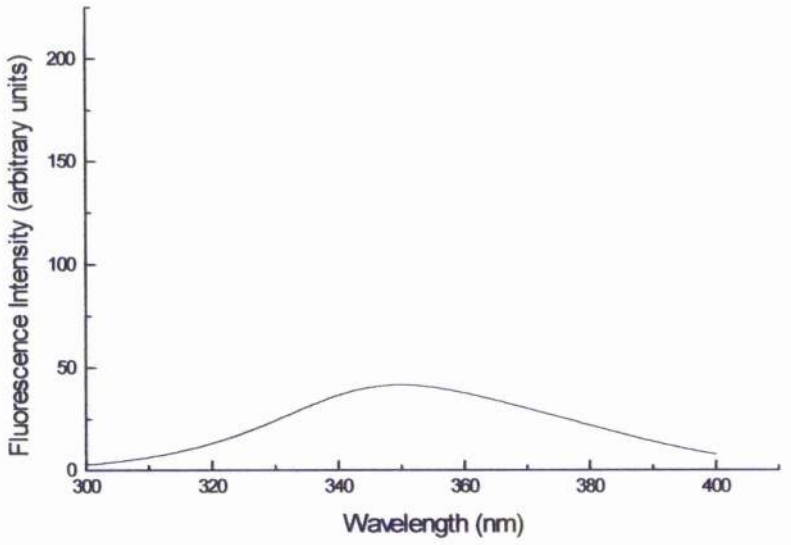

a)

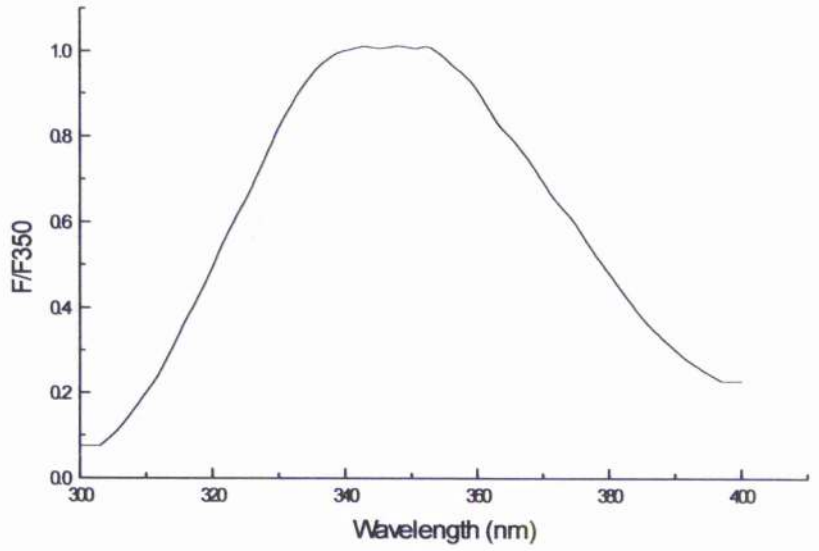

b)

Figure 3.5: Fluorescence spectra effect of storage at room temperature (20°C)

The spectra were recorded at 20°C using samples dissolved in buffer D (35 mM Tris-HCl, pH 7.6, containing 5 mM KCl, 2.5 mM $MgCl_2$ and 0.4mM dithiothreitol). The data show:

a) Fluorescence spectra after storage at room temperature (20°C); black line: 0.1mg/ml SK; grey line: 0.05mg/ml SK.
b) Normalised fluorescence spectra: effect of storage at room temperature (20°C). Protein concentration 0.1mg/ml: black line: SK fresh prepared; grey line: SK stored at 20°C.

3.3.2 Equilibrium Unfolding with GdmCl and Urea

The unfolding of SK was examined using the denaturants GdmCl and urea as described in section 2.5. Losses of secondary and tertiary structure were monitored by changes in far-UV CD at 222nm and fluorescence at 350nm (excitation at 295nm) respectively. The change in the ratio F_{355}/F_{337}, which reflects the change in emission maxima (section 3.1), is reported as well. Figure 3.6 shows the denaturation curves obtained from different sets of experiments.

The unfolding data for SK could be analysed satisfactorily in terms of a 2-state model (Pace, 1986; section 2.5) for both denaturants used: the coincidence of different structural probes suggests that no intermediate species were populated to any significant extent. From the plot of free energy change against denaturant concentration the stability of native enzyme in the absence of denaturant could be estimated as 17±1 kJ/mol with no significant difference in stability observed between the two denaturants employed (Figure 3.7).

The value of the stability is towards the lower end of those observed for a range of globular proteins (Pace, 1990), but is similar to the value estimated for the structurally similar enzyme adenylate kinase (19.6 kJ/mol) from studies of its unfolding by urea (Zhang *et al.*, 1998).

The unfolding was carried out in the chloride free buffer MOPS as well (50 mM 3-[N-Morpholino] propanesulfonic acid, pH 7.6, containing 2.5 mM K_2SO_4, 2.5 mM $MgSO_4$ and 0.4mM dithiothreitol). In this buffer system there is a small stabilisation against urea denaturation, as shown in figures 3.8a and b, probably due to the presence of sulphate anions as buffer constituents. In fact, as will be described in section 4.8, the sulphate stabilise more than chloride anions toward urea denaturation.

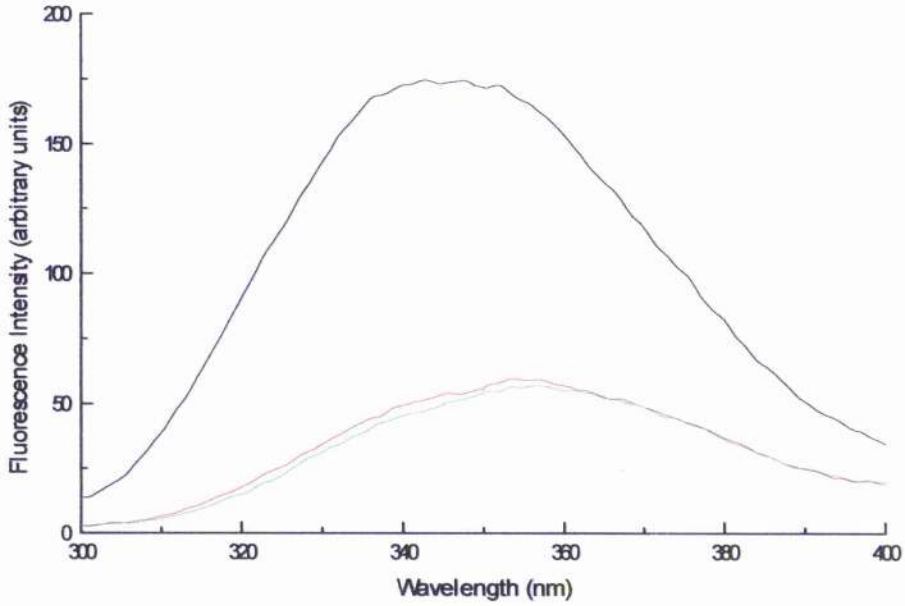
Fluorescence Intensity (arbitrary units)
200
150
100
50
0
300
320
340
360
380
400
Wavelength (nm)

a)

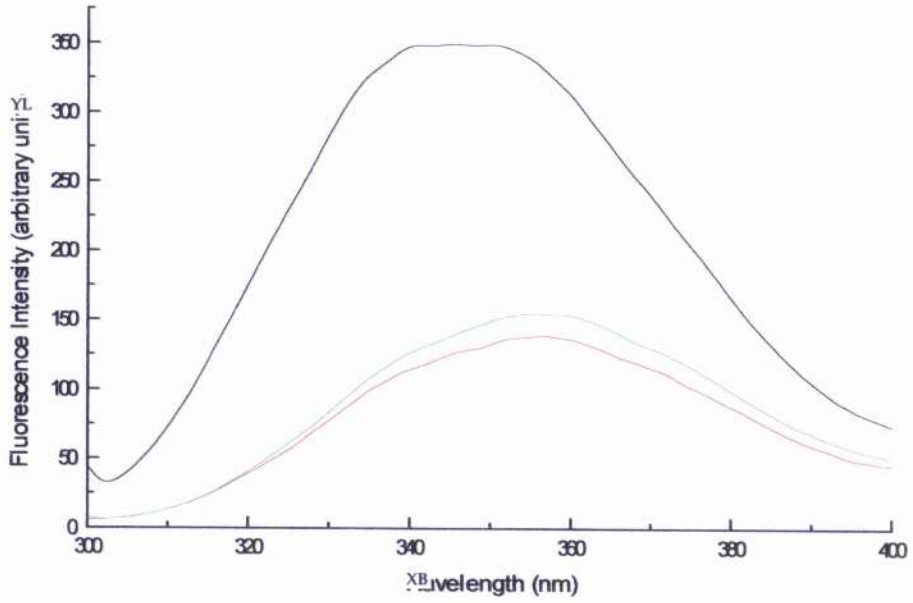
Fluorescence Intensity (arbitrary uni
350
300
250
200
150
100
50
0
300
320
340
360
380
400
velength (nm)

b)

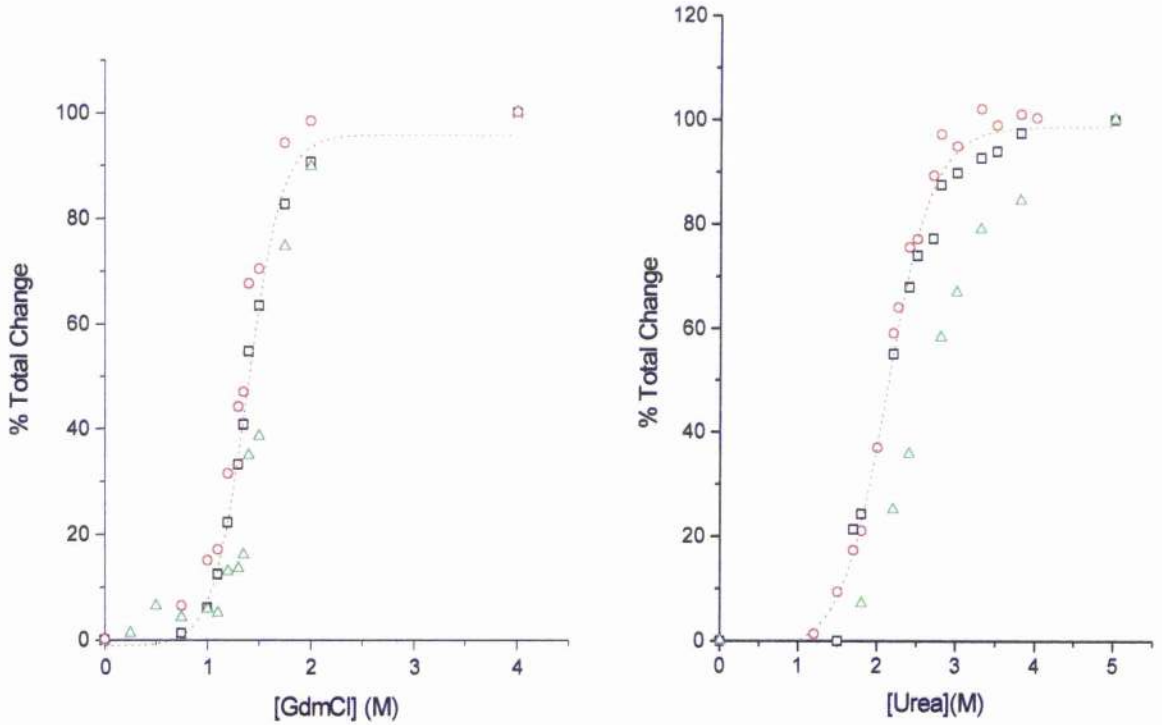

c)

Figure 3.6: Denaturation curves of SK using GdmCl and urea and spectra of native and denatured protein.

To study the unfolding process, SK (0.15mg/ml) was incubated in the appropriate buffer and in the stated concentration of denaturant for 1h at 20°C, before the CD and fluorescence data were recorded (section 2.5). The data shown: native (black in a and b) and denatured SK (a: green, 2.5M and red, 4M GdmCl; b: green, 4M and red, 8M urea). In c are shown the changes in the CD signal at 222nm (squares), changes in the fluorescence intensity at 350nm (circles) and the change in the ratio F_{355}/F_{337} (triangles) (these reflect the shift in the emission maximum of the fluorescence spectra).

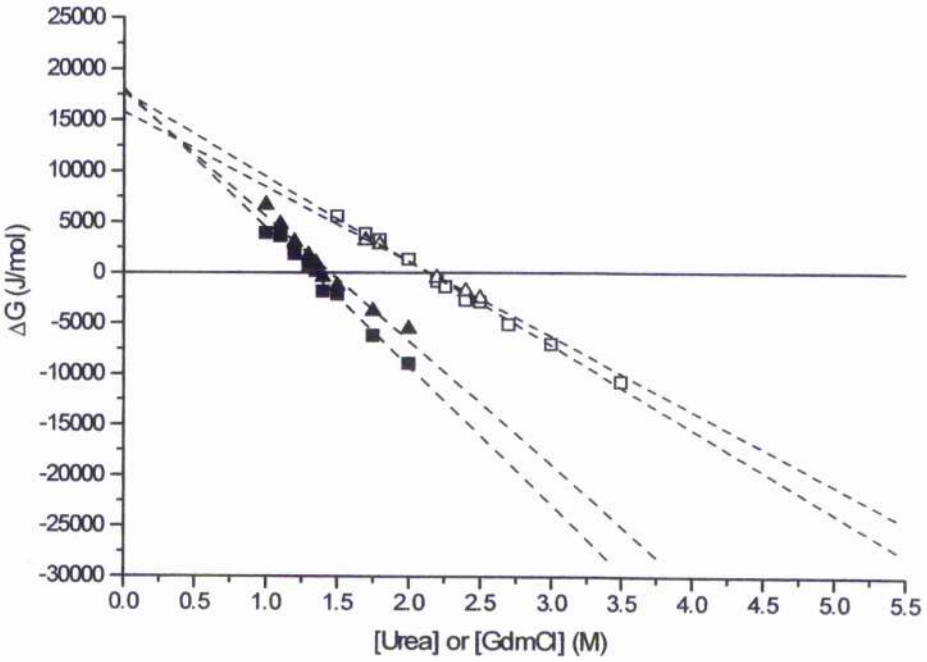

Figure 3.7: The unfolding of SK in the presence of urea and GdmCl.

The structural changes were monitored by changes in ellipticity at 222nm (triangles) and protein fluorescence at 350nm (squares) as described in the text.The open and filled symbols refer to urea and GdmCl respectively. The estimation of $\Delta G_D^{H_2O}$ was done assuming the linear dependence of ΔG_D on denaturant concentration ($\Delta G_D = \Delta G_D^{H_2O} - m$ (denaturant) = -RT ln K_{unf}) as described in section 2.5. The average m values for urea and GdmCl are respectively 7830 and 1294 j/mol^2.

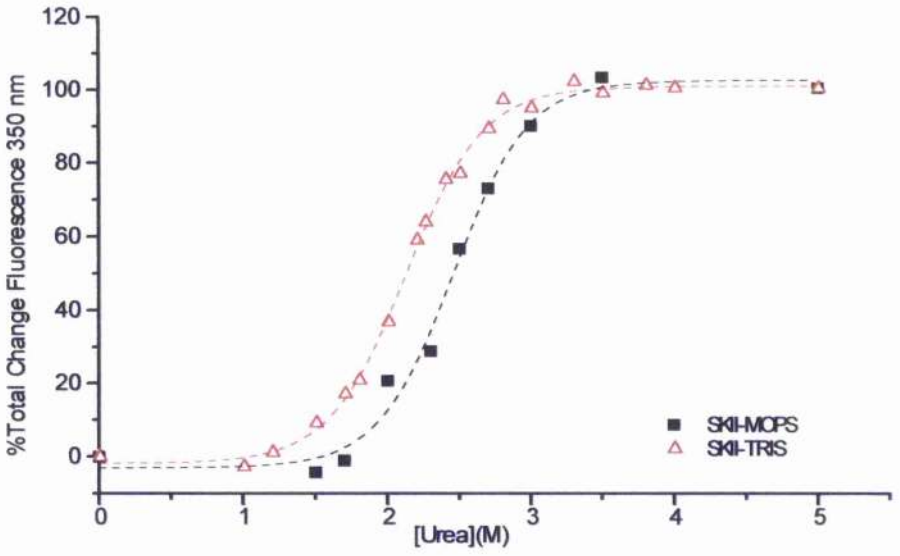

a)

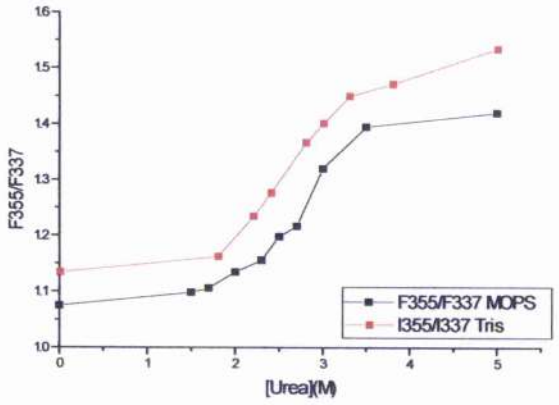

b)

Figure 3.8: Urea denaturation in MOPS buffer.

SK (0.15mg/ml) was incubated in the appropriate buffer and in the stated concentration of denaturant for 1h at 20°C fluorescence data were recorded (section 2.5). The data show:

a) The unfolding curves in MOPS (black) and Tris (red) respectively.
b) The change in the ratio F_{355}/F_{337} (triangles) (these reflect the shift in the emission maximum of the fluorescence spectra).

3.3.3 Denaturation of SK in the presence of substrates

The binding of a ligand can influence the fluorescence of Trp by different mechanisms (Eftink, 1997). The ligand can act as a quencher (by collisional or energy transfer mechanism), it can physically interact with the fluorophore changing the polarity of its environment and/or its accessibility to the solvent or it can bind at a site that is remote from the Trp residue and may induce a change in conformation that alters the Trp microenvironment. It has been previously reported that the addition of shikimate leads to quenching of SK fluorescence (Idziak *et al.*, 1997) (Fig. 3.9). To make a comparison between the spectra in the presence and in the absence of substrate the spectra were normalised (F_n/F_{350}). Because after normalisation (F_n/F_{350}) no shift in the λ_{max} of the fluorescence spectra is observed, it is possible that shikimate acts merely as a quencher without altering the Trp environment. This is also suggested by the CD near-UV spectrum in the presence of shikimate that shows no major differences from the spectrum in the absence of substrate (Fig.3.10).

When the enzyme was incubated with increasing concentrations of denaturants in the presence of shikimate (2mM), although no stabilization against chemical denaturation was observed, the changes in fluorescence showed an unusual pattern (Fig. 3.11). GdmCl at concentrations below 1M leads to a marked increase in fluorescence; under these conditions there are only very small effects on the overall secondary structure of the enzyme as judged by far-UV CD. The changes observed in the presence of urea are by contrast much less marked.

Other studies on different enzymes have shown that during denaturation inactivation occurs before noticeable conformational changes can be detected (Ribas de Pouplana *et al.*, 1991; Wang *et al.*, 2000) suggesting that the enzyme active site is situated in a more flexible region than the enzyme molecule as a whole. In order to check if the observed effects were due to a local unfolding of the shikimate binding site or to the effects of ionic strength on the binding, spectra were acquired at different concentrations of NaCl in the presence of shikimate. NaCl was chosen because it is a neutral salt in the Hofmeister series (section 4.2) and it should not have any effect on protein conformation, as was experimentally confirmed (section 4.3). Although there is a relief of quenching (an enhancement of fluorescence) at low concentrations of both denaturants, the magnitude of this effect is different for GdmCl and urea. Moreover the shape of the first part of the denaturation curve obtained with GdmCl resembles that obtained in the presence of different concentrations of NaCl suggesting that the main effect on the shikimate binding is due to the ionic strength (Figure 3.11). To complete the study of the unfolding process and of the effect of denaturant on protein structure, the changes in activity and dissociation constants have been studied in the presence of different concentrations of denaturants (section 3.3.4 and 3.3.5).

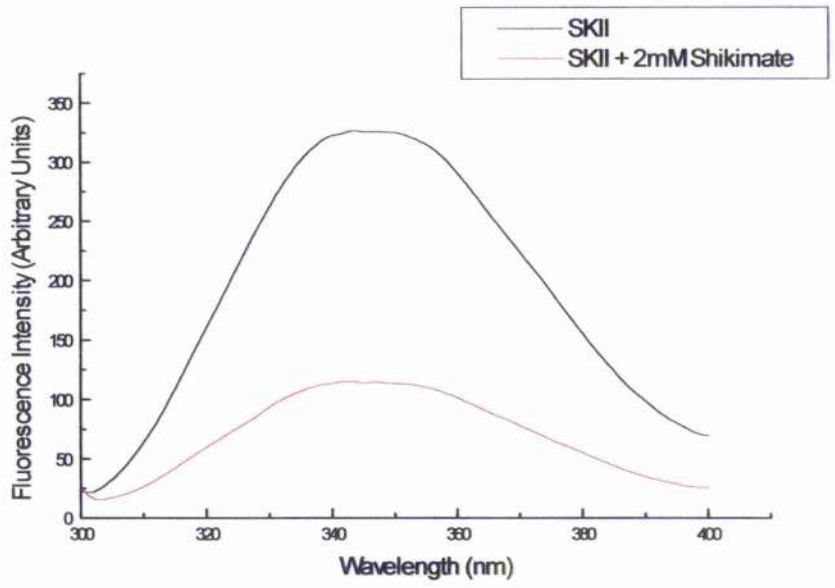

Figure 3.9: Quenching of the fluorescence due to the presence of shikimate

Spectra of SK (0.15mg/ml) were recorded at 20°C using samples dissolved in buffer D (35 mM Tris-HCl, pH 7.6, containing 5 mM KCl, 2.5 mM $MgCl_2$ and 0.4mM dithiothreitol) or in buffer D + 2mM shikimate. The data reports in black SK and in red SK in the presence of shikimate.

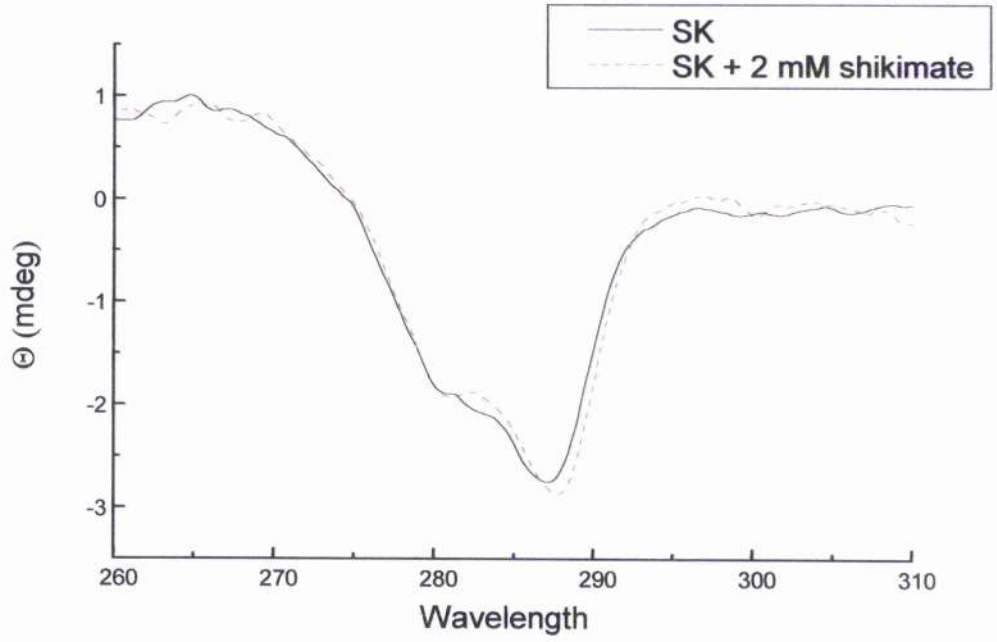

Figure 3.10: Effect of shikimate on the near-UV CD spectrum of SK.. Near UV spectra, protein concentration 0.5mg/ml, cell pathlength 0.5cm. The black and the red lines refer to enzyme in the absence of shikimate and in the presence of 2mM shikimate.

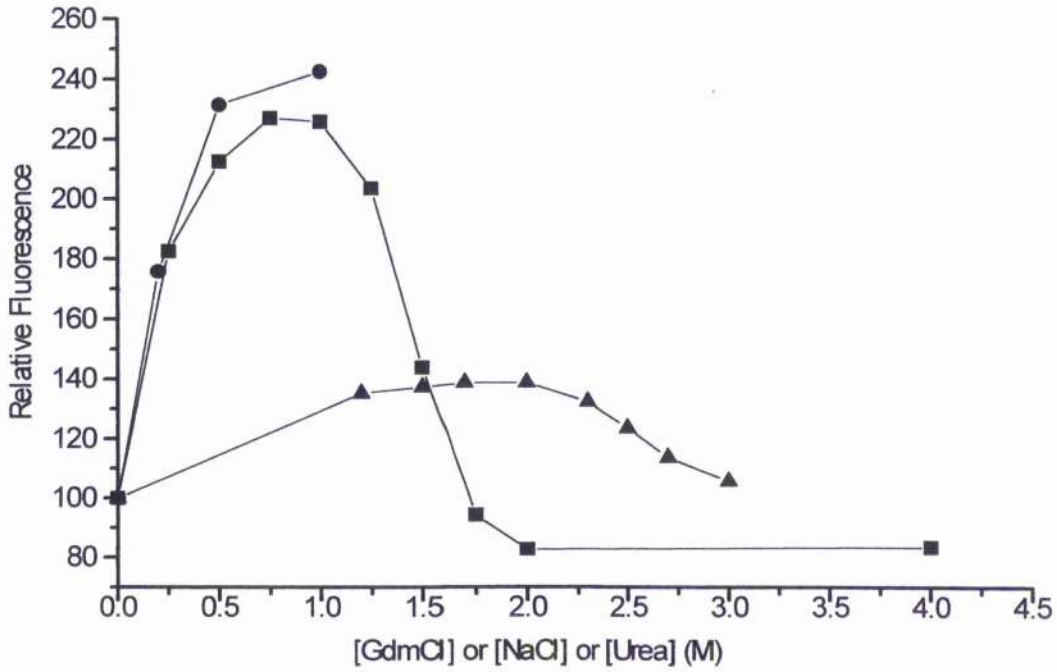

Figure 3.11: Unfolding of SK in the presence of shikimate.

SK (0.15mg/ml) was incubated in the appropriate buffer containing 2mM shikimate and in the stated concentration of denaturant or NaCl for 1h at 20°C, before the fluorescence data were recorded (section 2.5). The data shows: changes in the fluorescence intensity at 350nm in the presence respectively of GdmCl (squares), urea (triangles) and NaCl (circles).

3.3.4 Changes in K_d of substrates in the presence of denaturants

The decrease in fluorescence intensity accompanying the binding of ligands can be used to measure the dissociation constant of the binding (K_d) and the limiting degree of quenching. This is carried out by performing a titration of the protein solution with substrates and correcting the data for the volume changes during the titration (section 2.3).

By performing titrations with shikimate in the presence of fixed concentrations of GdmCl and urea, after 1-hour incubation, the variation in K_d for the substrate could be assessed. The results are shown in Fig. 3.12a and confirm the smaller effect of urea on the binding of shikimate. Control experiments performed at different concentrations of NaCl shows that an increase in the ionic strength weakens the binding of shikimate in a similar manner to low concentrations of GdmCl. This could indicate that the change in ionic strength has the largest effect on shikimate binding. To check this hypothesis titrations with different salts were performed (section 4.4).

The same type of titrations were carried out to study the binding of ADP correcting the intensity values for the inner filter effect using a reference compound (NATA). The results indicate that whereas there is a small increase in the K_d for ADP in the presence of 1M urea, the effects of GdmCl and NaCl are to decrease the K_d to a limited extent (Fig. 3.12b). However, it should be noted that the accuracy of the estimates of K_d at concentrations of GdmCl or NaCl above 0.25M was seriously affected by the marked reduction in the degree of quenching by the nucleotide under these conditions (from 55% quenching in the absence of GdmCl or NaCl to less than 25% quenching in the presence of 0.5M GdmCl or NaCl). The effects of urea appear to be more marked in the case of the ADP binding than for the shikimate. In fact there is a drastic increase of the K_d at low urea concentrations (from 1.71 to 4.52mM in 1.5M urea). The discrepancy between the effects of the two denaturants on the K_d of the substrates can suggest that, while in shikimate binding electrostatic interactions play a major role, in nucleotide binding the main factor is hydrophobic interactions, accounting for the larger effect of urea on the ADP binding.

The data obtained in this section together with the later study on the effect of salts on the binding of ligands (section 4.4) and a re-analysis of the crystallographic data using the final model (1SHK), that has led to the identification of specific chloride binding sites on the enzyme, could explain why in the crystallographic structure there is only a weak intensity for shikimate though both shikimate and ADP were present in the crystallization medium. At the NaCl concentration in question no binding of shikimate would be expected but, as explained in chapter 4, the simultaneous presence of ADP leads to a partial reversal of the effect of chloride that could explain the weak binding of shikimate observed in the X-ray studies. This will be discussed in more detail in Chapter 4.

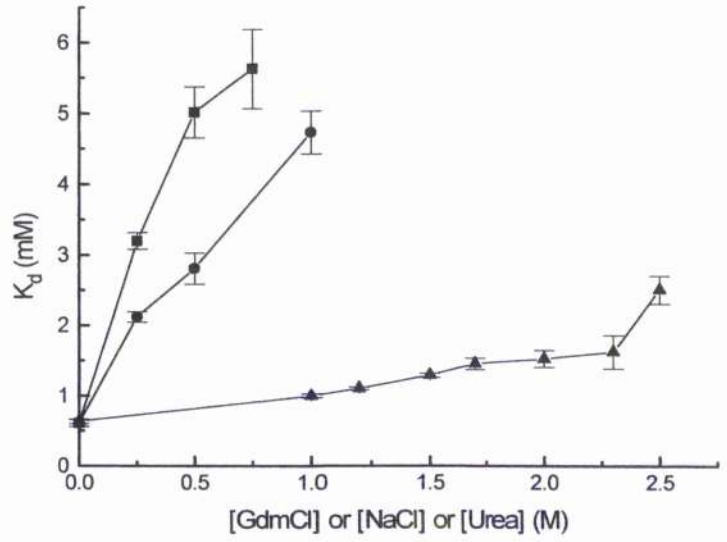

a)

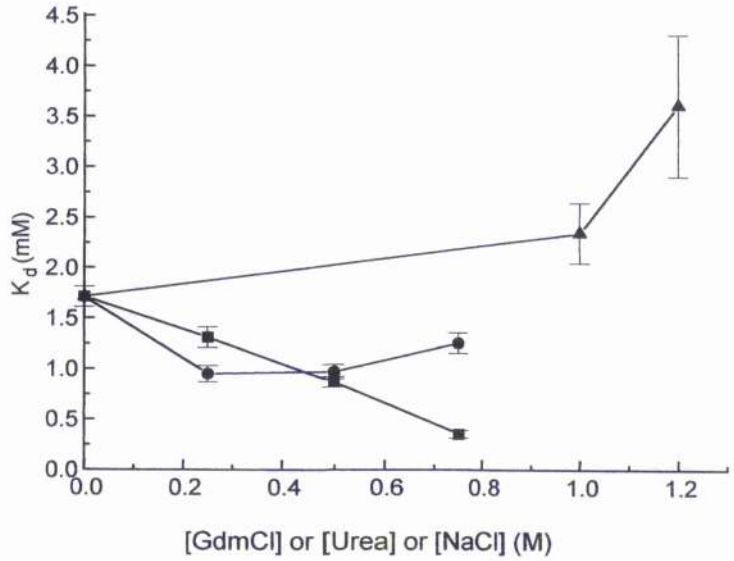

b)

Figure 3.12: The effect of denaturants and NaCl on the binding of substrates to SK.

Binding data were obtained and analysed as described in section 2.3. Changes in the K_d for shikimate (a) and ADP (b) are shown in the presence of GdmCl (squares), urea (triangles) and NaCl (circles).

3.3.5 Changes of activity in the presence of denaturants

Incubation with GdmCl leads to a marked loss of activity of SK. In the presence of 0.5M GdmCl over 75% activity is lost and less than 5% activity remains in the presence of 1M GdmCl. These changes occur at concentrations of denaturant at which the change is less than 20% of the total observed for fluorescence and less than 10% of the total observed for CD. Incubation with urea leads to much less marked losses in activity which run roughly in parallel with the structural changes, with approximately 85% and 40% activity retained in the presence of 1M and 2M urea respectively. In the presence of 4M urea, shikimate kinase retains no detectable activity (<0.1% of the control value). A significant part of the effect of GdmCl appears to be due to the chloride ions, since incubation in the presence of 0.5M and 1M NaCl leads to losses of 45% and 65% activity respectively (Fig. 3.13).

The effect of NaCl on the activity and binding resembles that of GdmCl suggesting that the ionic strength has a major contribution to the inactivation and in the weakening of binding of substrates. Since NaCl at these concentrations has little effect on the far-UV CD, or on the fluorescence of SK, as is shown in chapter 4, the ionic strength effects must be localised to the area of the shikimate binding site. The effect of NaCl and other salts on the stability and activity of SK will be discussed in detail in Chapter 4.

In summary, the loss of enzyme activity and the weakening of shikimate binding occur at much lower concentrations of GdmCl than do the overall losses of secondary and tertiary structure of the enzyme. This appears to be due to local effects of ionic strength in the area of the shikimate binding site. By contrast the loss of activity in the presence of urea occurs in the range of denaturant concentrations over which the major structural changes take place.

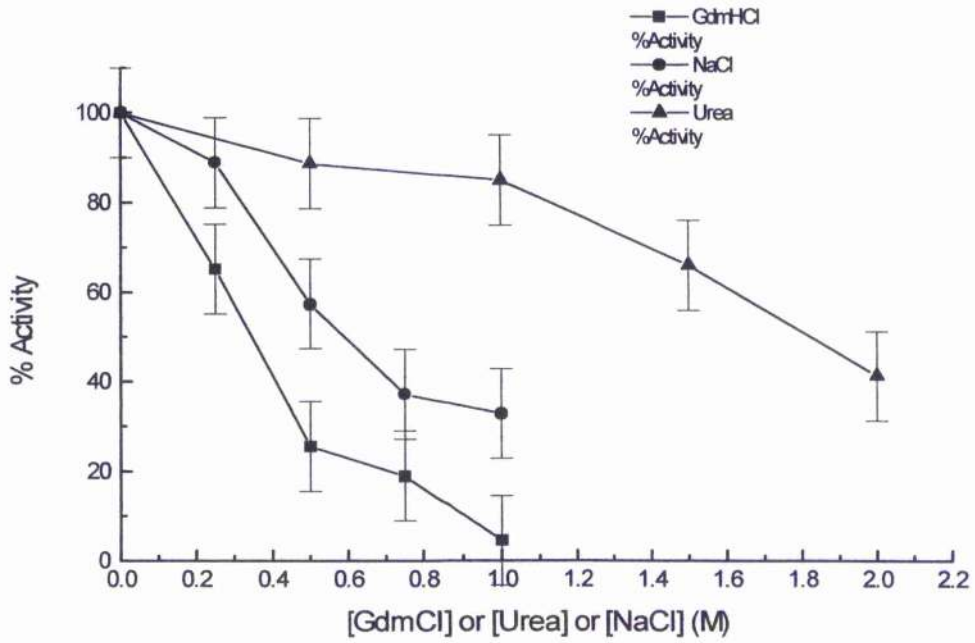

Figure 3.13: Effect on the activity of denaturants and NaCl.

A quenched assay was used in order to measure the activity of SK in the presence of denaturants as described in section 2.2.The data shows the effects on activity of GdmCl (squares), urea (triangles) and NaCl (circles).

3.3.6 Effect of denaturants on quenching of Trp fluorescence

From the position of the emission maximum in the fluorescence spectra (346nm) it is evident that the Trp side chain is substantially exposed to the solvent. Another method to obtain this type of information is to study the Trp quenching by different agents.

In fact the quenching of the fluorescence of Trp residues by addition of particular low molecular weight agents (O_2, succinimide, acrylamide, I^-, NO_3^-, etc.) can be used to probe for the exposure of the indole ring. These quenchers act by physically interacting with the excited indole ring and this interaction will be more pronounced for exposed residues.

So the quenching of the Trp fluorescence, quantified by the Stern-Volmer constants, gives information on the environment and mobility of the Trp side chain (section 2.4). In order to take into account the influence of the solution conditions, the values of K_{sv} in the presence of denaturants were obtained correcting the observed values by reference to the values obtained for the model compound NATA under the same conditions as described in section 2.4. The use of different quenchers can extend the information available: for example charged quenchers such as iodide could be used to examine the nature of the charged environment of fluorophores (section 1.3.2.4).

In the case of SK, the iodide ion is a very effective quencher as shown by its high K_{sv} (20.05 M^{-1}) when compared with the one obtained for the model compound, N-acetyltryptophan amide (10.1M^{-1}). It is likely that the high degree of quenching of SK is due to the positively charged environment provided by the three arginine side chains (Arg11, Arg58 and Arg139 ; Fig. 1.11) in the neighbourhood of Trp54 (Krell *et al.*, 1998) that create a positively charged environment increasing the effectiveness of the quenching by the negatively charged iodide ion. This is confirmed by the observation that in the presence of 4M urea the K_{sv} values for SK is reduced dramatically to 4.0 M^{-1}; by contrast the addition of 4M urea has only a very small effect on the K_{sv} of the model compound (9.5 M^{-1}). The values of K_{sv} for NaI in 50 mM MOPS, pH 7.6, containing 2.5 mM K_2SO_4, 2.5 mM $MgSO_4$ and 0.4mM dithiothreitol is similar (20.9 ± 0.21 M^{-1}) to that obtained in Tris buffer.

Using a neutral quencher as succinimide a high value of K_{sv} has been obtained both for the native and the denatured (4M urea) protein, 5.56 ± 0.11M^{-1} and 5.19 ± 0.045 M^{-1} respectively. This confirms the high degree of solvent exposure of the Trp.

3.4 Refolding of the enzyme

3.4.1 Refolding after unfolding in GdmCl

3.4.1.1 Regain of activity

The regain of activity during the refolding was measured following the procedure described in section 2.5. SK was denatured in 2.8M GdmCl and then diluted 11-fold to lower the GdmCl concentration to 0.25M to initiate refolding. At this residual concentration of GdmCl the protein is in its native conformation (section 3.3.2). The control sample was a solution of SK in 0.25M GdmCl. The activity value of this solution is 233μmol/min/mg, which is lower than the activity in the absence of denaturant (350μmol/min/mg). This is in agreement with the observed decrease in activity measured by quenched assay at different GdmCl concentrations (in 0.25M GdmCl, 65% of the activity of the enzyme in buffer was observed-section 3.3.5). Under these conditions, approximately 75% of the activity of a control sample could be regained in a first order process with rate constant of $0.0043s^{-1}$ (Figure 3.14).
The regain in activity was also followed in the presence of 40μM ANS because this probe was used in other refolding experiments and its influence on the refolding process had to be checked. The regain of activity in the presence of ANS is 15% less than in the absence of ANS (Figure 3.14).

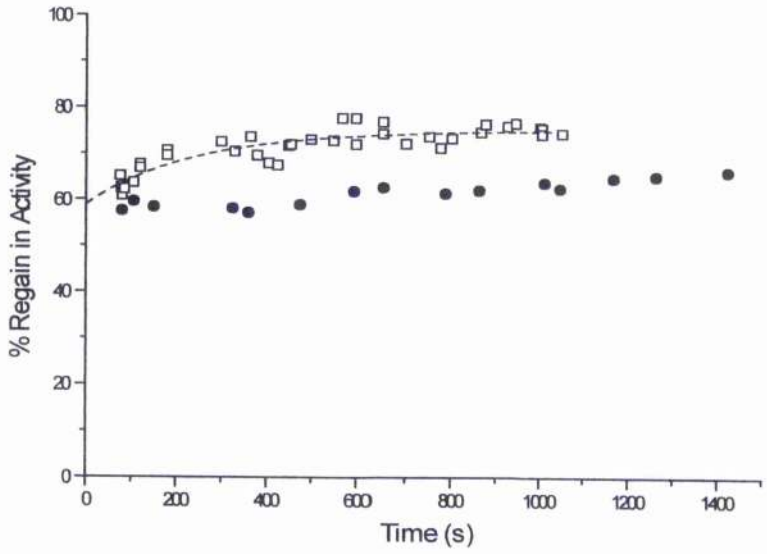

Figure 3.14: The kinetics of regain of activity of SK after denaturation in 2.8M GdmCl.

Squares: regain in activity ; closed circles: regain in activity in the presence of ANS. Activity values are expressed relative to a control sample incubated in the presence of the final concentration of GdmCl, i.e. 0.25M and 0.25M GdmCl + 40μM ANS. The dashed line shows a fit to a first order process with a rate constant of $0.0043s^{-1}$.

3.4.1.2 Regain of fluorescence intensity

The refolding was started by dilution as already described. Figure 3.15 shows an average of 10 curves obtained in manual mixing mode following the regain in fluorescence intensity at 350nm, after excitation at 295nm. Presumably 55% of the control fluorescence is regained in the dead time, 10.5 % with a rate constant of $0.0113s^{-1}$ and 17.9 % with a rate constant of $0.0024s^{-1}$ (these constants are only indicative because they refer to a manual mixing experiment). Performing light scattering experiments (section 2.4) the refolded solution presented a light scattering signal greater than the upper experimental detection limit (1000 units), indicating that some aggregation has occurred during the refolding process (section 3.4.1.5). The stopped flow experiments that followed were unsatisfactory, because of the lack of agreement with results previously obtained (Boam, 1999) probably due to aggregation. It has to be pointed out that, though the intensity of the refolded solution is not the same as that of the control solution, the normalised spectra coincide, indicating that after refolding the environment of the Trp is native-like (Fig. 3.16).

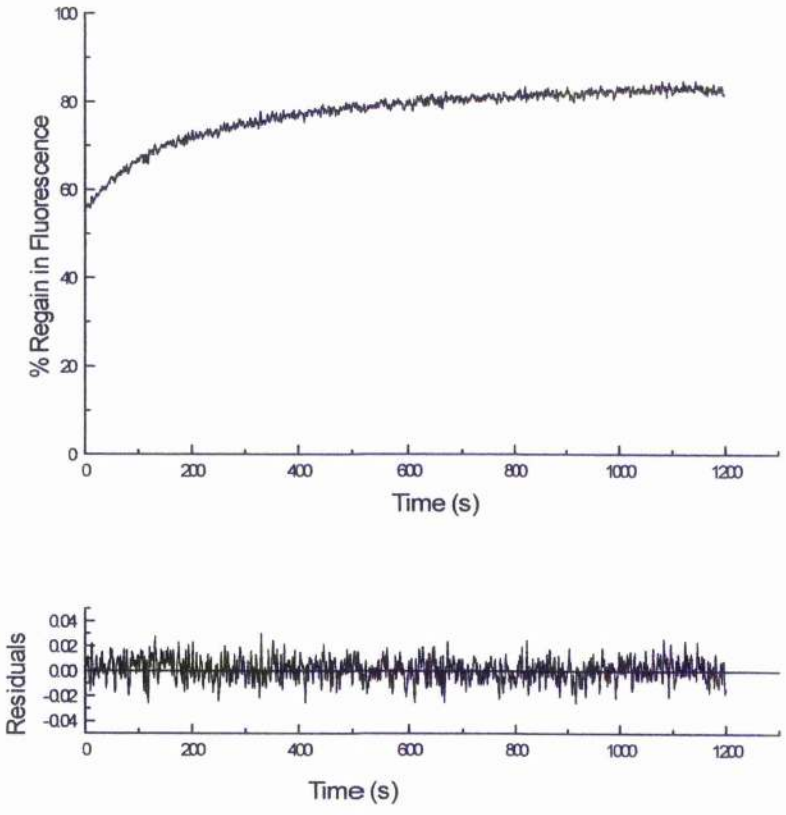

Figure 3.15: The kinetics of changes in protein fluorescence

The regain in fluorescence intensity at 350nm was followed after denaturation in 2.8M GdmCl. Refolding was initiated by manual mixing. The pattern of residuals to the curve fitting is shown.

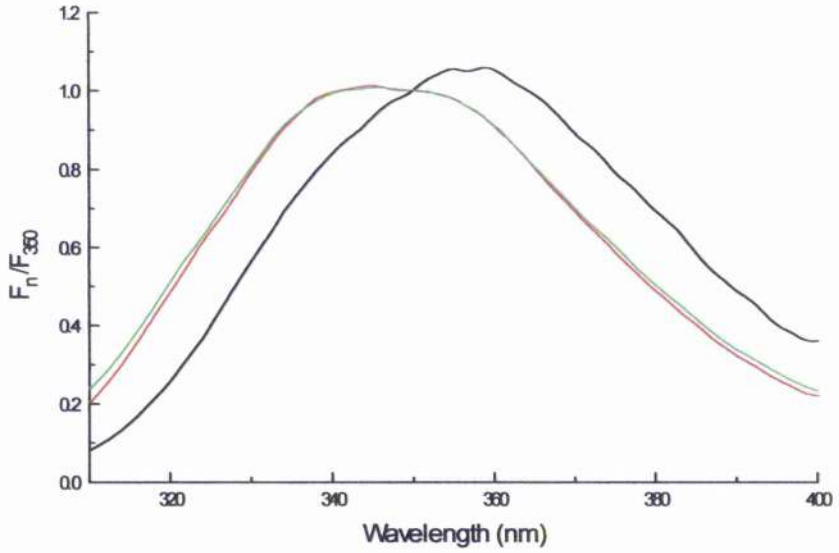

Figure 3.16: Normalised spectra of the solutions of the refolding experiment in GdmCl.

Spectra were recorded at 20°C using samples dissolved in buffer D (35mM Tris-HCl, pH 7.6, containing 5mM KCl, 2.5mM $MgCl_2$ and 0.4mM dithiothreitol) in the 300-400nm range after excitation at 295nm, T= 20°C. Black: SK + 2.8M GdmCl; Green: SK + 0.25M GdmCl (refolded); Red: SK + 0.25M GdmCl (end solution).

3.4.1.3 Refolding in the presence of shikimate

Because the shikimate binding was weakened at the final GdmCl concentration used in the refolding experiment (0.25M), it was not possible to check the formation of the shikimate-binding site during the refolding reaction.

3.4.1.4 Refolding in the presence of NaI

From the kinetic profile obtained in the presence of NaI (Fig. 3.17), it could be seen that the formation of the charged Trp environment is complete after the first 30s (considering a dead time in the manual mixing experiment of 20s). No further stopped flow experiments were undertaken because of the aggregation indicated by the refolding experiment undertaken in the presence of ANS (section 3.4.1.5).

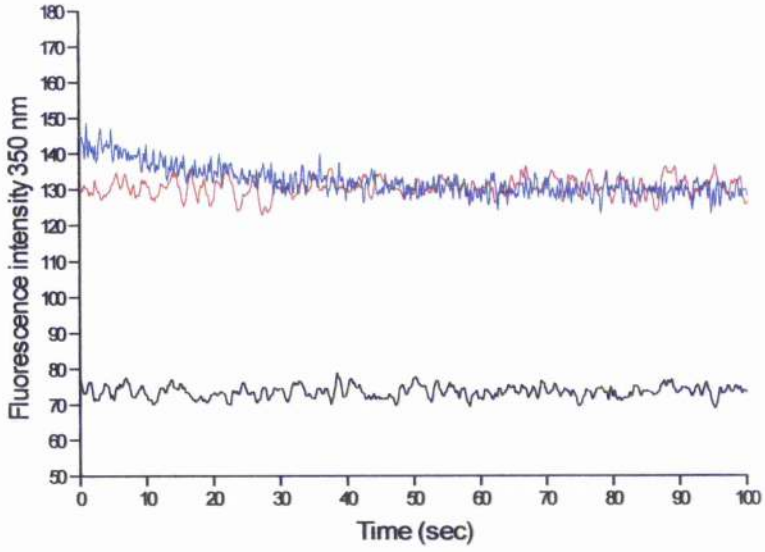

Figure 3.17: The kinetics of changes in quenching of fluorescence by iodide

The regain in fluorescence intensity at 350nm was followed after denaturation in 2.8M GdmCl. Refolding was initiated by manual mixing with an 11-fold dilution in a buffer containing 0.11M NaI. The start and end solution contained 0.1M NaI as well. Black : start solution (SK + 2.8M GdmCl); Red: end solution (SK+ 0.25M GdmCl); Blue: refolding in the presence of 0.1M NaI.

3.4.1.5 Light scattering measurements and refolding in the presence of ANS

To check if aggregation had occurred during refolding, a light scattering experiment was carried out ($\lambda_{ex} = \lambda_{em}$ = 320nm) (section 2.4). Both the control (0.25M GdmCl, equilibrium solution) and the refolded solutions give saturation of the detector (>1000 units), while the start solution (unfolded in 2.8M GdmCl) does not. This could indicate the possible formation of aggregates during the refolding process. To check if the observed saturation of the detector was due to the residual ionic strength, the light scattering was checked in the presence of 0.25M NaCl. Although no saturation of the detector was observed in 0.25M NaCl, when an ionic strength jump from 2.8M NaCl to 0.25M NaCl was carried out, it led to saturation of the detector. These control experiments using NaCl showed that the increase in light scattering resulted both from the rapid decrease in ionic strength and from the specific effects of the final concentration of GdmCl (0.25M). The observed aggregation can provide an explanation of the irreversible binding of the hydrophobic probe 1-anilino-8-naphthalene sulphonate (ANS) during the refolding after unfolding in GdmCl. This probe is commonly used to study the early stages of protein folding giving information on possible compact intermediates on the refolding pathway (a more detailed discussion on the use of this probe will be given in the sections 3.4.2.8 and 3.4.2.9).

During the refolding experiment a large increase in the binding of ANS (15-fold compared with the enzyme in 2.8M GdmCl) was observed and the dye was not subsequently released from the enzyme (Fig. 3.18). This is not due to the residual ionic strength in solution, because the equilibrium solutions in 2.8M GdmCl and 0.25M GdmCl do not give the same intensity and spectra of the refolded solution, but could be due to formation of aggregates: kinetic intermediates of folding are sometimes sensitive to aggregation because they still have significant amount of exposed hydrophobic surface (section 1.1.1.3).

In view of these difficulties, subsequent experiments on the refolding of SK were performed using urea as a denaturing agent; the procedure involved unfolding in 4M urea for unfolding and 11-fold dilution (to 0.36M urea) to initiate refolding. During this process, there was no significant increase in light scattering at 320nm during refolding showing that aggregation occurred to a negligible extent.

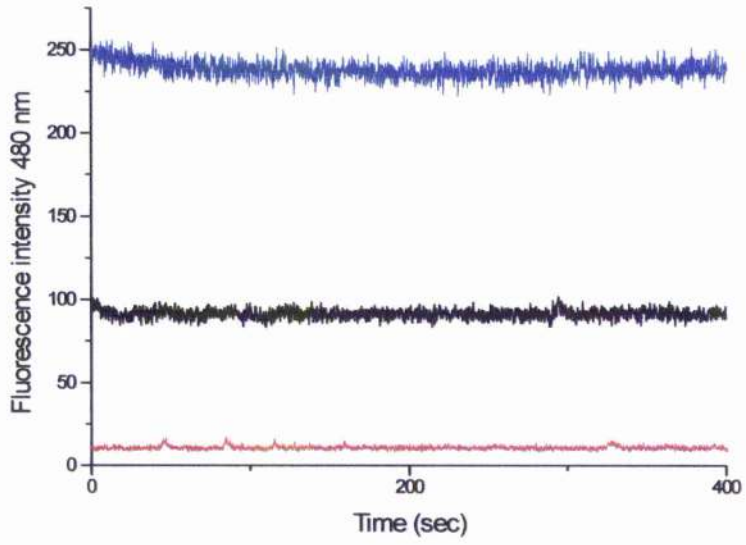

Figure 3.18: The kinetics of changes in ANS fluorescence at 480nm

Refolding of SK after denaturation in 2.8M GdmCl (manual mixing). The red, black, and blue curves refer to enzyme in the presence of 2.8M GdmCl, enzyme in the presence of 0.25M GdmCl, and enzyme during refolding respectively.

3.4.2 Refolding after unfolding in urea

3.4.2.1 Regain of activity.

The refolding was performed as described in section 2.5. The first time point at which activity can be accurately assessed was estimated to be about 80s after the start of refolding, taking into account the time taken for appropriate dilution into the assay solution and for the double-coupled assay system to achieve a constant rate. By this time between 35 and 40% of the activity of the control sample (in the presence of 0.36M urea) had been regained. Over the next 15 min, a further 50% activity was regained in a first order process with a rate constant $0.0067s^{-1}$. Thus overall approximately 90% of the activity of the control was regained. If dithiothreitol was omitted from the unfolding and refolding buffers, the extent of regain of activity was reduced to approximately 60%, showing that some damage had occurred to either or both of the 2 Cys side chains (Cys 13 and Cys 162) in the enzyme (Fig. 3.19).

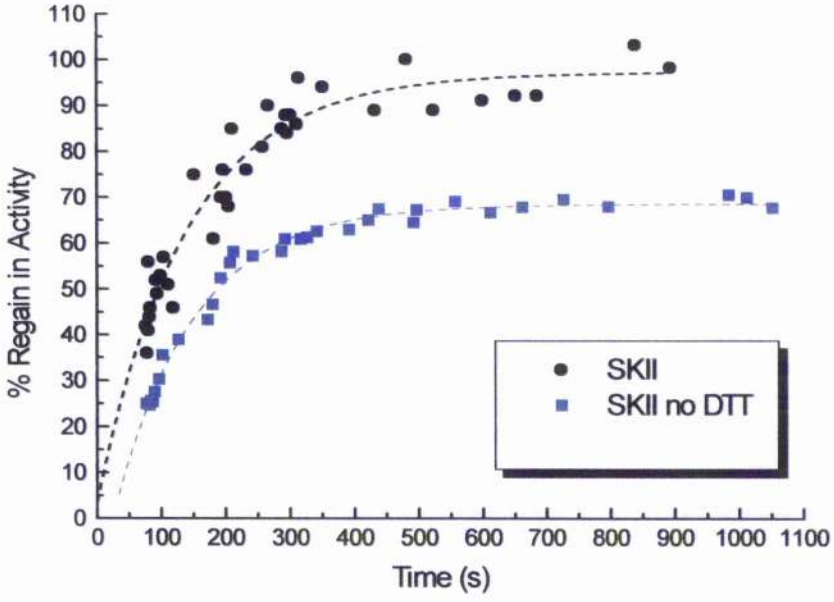

Figure 3.19: The kinetics of regain of activity of SK after denaturation in 4M urea.

Activity values are expressed relative to a control sample incubated in the presence of the final concentration of urea, i.e. 0.36M. The dashed line shows a fit to a first order process with a rate constant of $0.007s^{-1}$. The blue curve shows the regain of activity when DTT was not present in the unfolding and refolding buffers.

3.4.2.2 Regain of secondary structure on refolding

When the enzyme was unfolded in 4M urea and refolded by an 11-fold dilution to a final concentration of urea of 0.36M (section 2.5), approximately 75% of the recovery of ellipticity at 225nm was complete within the dead time (20s) of the start of the manual mixing experiment (Fig. 3.20). A further 15% of the signal was regained over the subsequent 500s with a rate constant of $0.009s^{-1}$. At the end of this period the far-UV CD spectrum of the refolded enzyme was very similar to that of native enzyme (Fig. 3.21). Using stopped flow mixing to initiate refolding it was shown that the regain of ellipticity at 225nm occurred in a number of phases. From data obtained over the first 20s of refolding, it was shown that, within 20ms, 15% of the total signal corresponding to the folded enzyme (i.e. the difference between denatured and folded enzyme) had been regained. A further 20% of the signal was regained in a first order process with a rate constant of $8s^{-1}$; in the third phase a further 40% was regained with a rate constant $0.08s^{-1}$. Finally from data over the time range 20-200s, a fourth phase was observed accounting for an additional 10% change with a rate constant $0.008s^{-1}$. Taken together, the four phases account for a regain of 85% of the native secondary structure (Fig. 3.22).

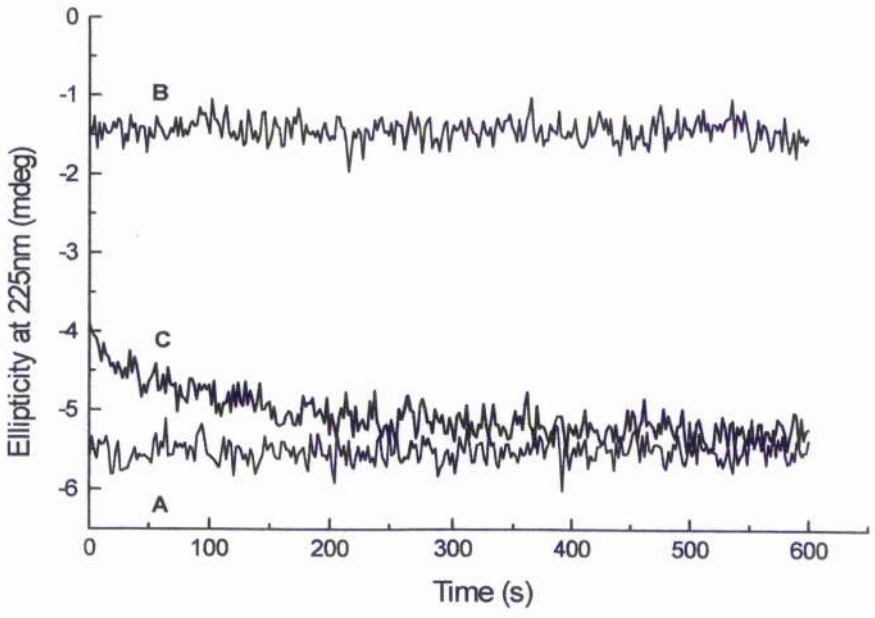

Figure 3.20: The kinetics of changes in ellipticity at 225nm

Refolding of SK after denaturation in 4M urea. The refolding was initiated by manual mixing. A: SK + 0.36M urea (end solution); B: SK + 4M urea (start solution); C: refolding solution

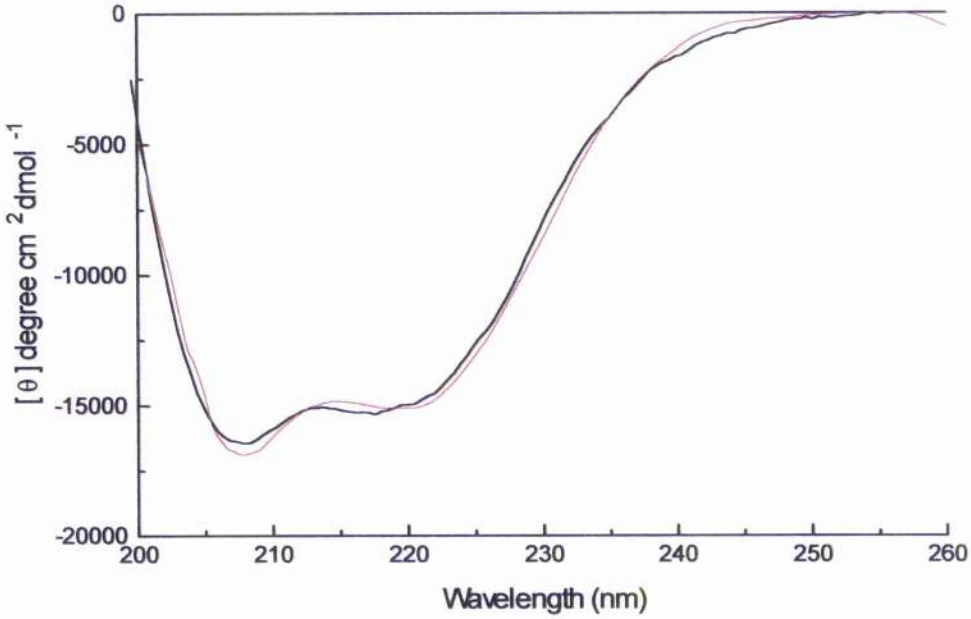

Figure 3.21: CD spetra of the refolded solution after denaturation in 4M urea

Far-UV CD spectra (protein concentration 0.15mg/ml, cell pathlength 0.05cm) were recorded at 20°C using samples dissolved in buffer D (35mM Tris-HCl, pH 7.6, containing 5mM KCl, 2.5mM $MgCl_2$ and 0.4mM dithiothreitol) as described in section 2.4. The data shows: SK in buffer Tris-HCl and 0.36M Urea (black, end point; equilibrium solution) and SK in the same conditions after the refolding by dilution (red).

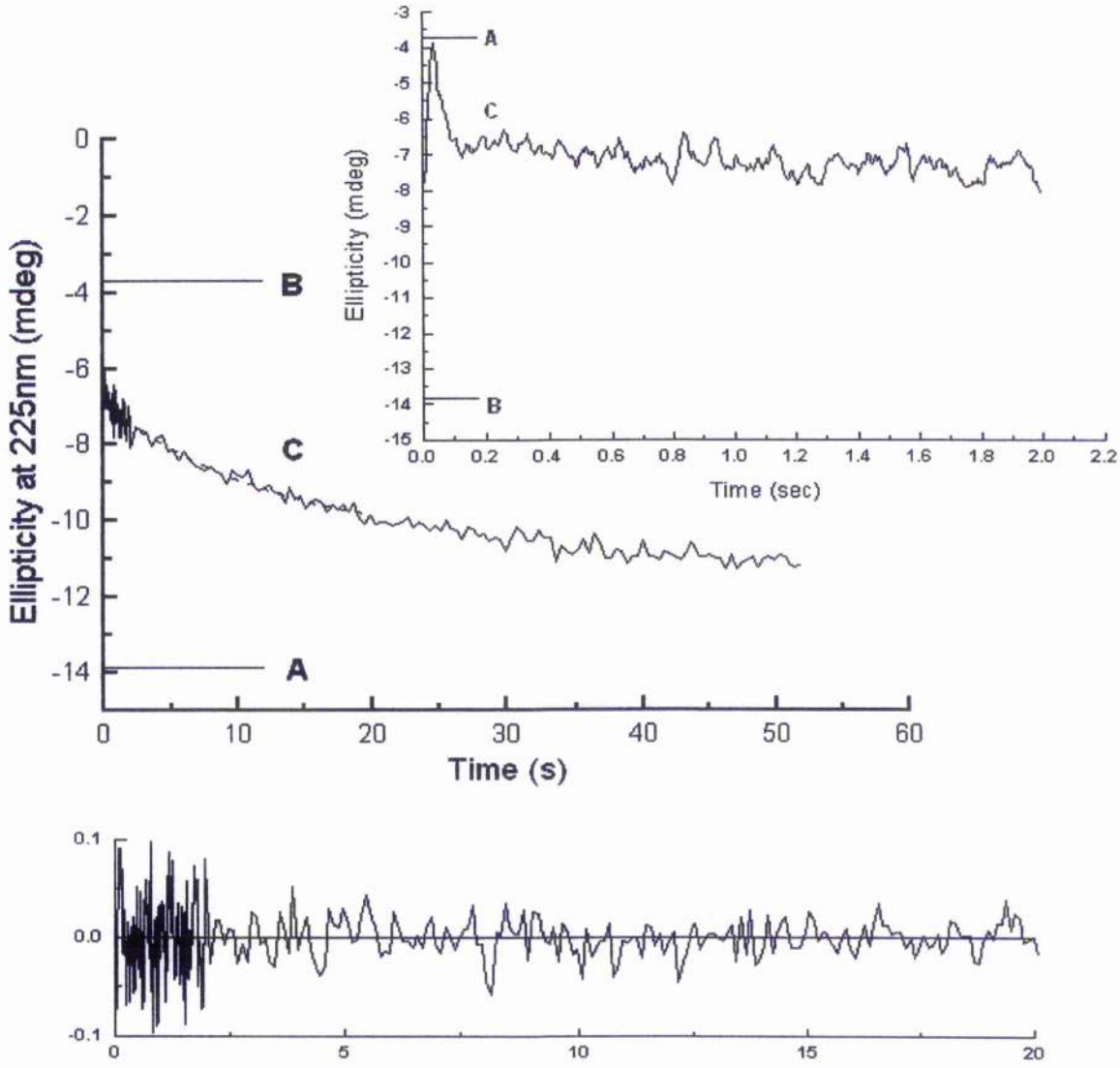

Figure 3.22: The kinetics of changes in ellipticity at 225nm

Refolding of SK after denaturation in 4M urea.The refolding was initiated by stopped flow mixing; the inset shows data in the first 2s of the reaction. Traces A, B and C refer to enzyme in the presence of 4M urea, enzyme in the presence of 0.36M urea, and enzyme during refolding respectively. The pattern of residuals to the curve fitting is shown.

3.4.2.3 Unfolding kinetics and effect of incubation time on the refolding kinetics

A set of experiments on the unfolding kinetics were performed mixing the native protein with a buffer containing urea in such a way that after dilution the concentration of urea was 4M, and the protein concentration 0.1mg/ml. After 5min the protein has a fluorescence intensity that corresponds to the unfolded protein (Fig. 3.23). The kinetic constant of the process, obtained with a first order fitting, is: $k = 0.02831 \pm 0.0001 s^{-1}$.

The effect of the incubation time on the refolding kinetics was investigated as well (manual mixing). The unfolding in 4M urea for periods ranging from 5min to 3h had no effect on either the spectroscopic properties of the unfolded enzyme, or the kinetics of refolding (table 3.3) as monitored by changes in protein fluorescence (Fig. 3.24).

Incubation time	A_1	k_1 (s^{-1})	A_2	k_2 (s^{-1})	B
5 min	32.91 ± 0.28	0.060 ± 0.001	29.03 ± 0.23	$0.0075 \pm 8\ 10^{-5}$	169.62 ± 0.042
30 min	27.37 ± 0.31	0.075 ± 0.0017	34.05 ± 0.23	$0.0083 \pm 1.1\ 10^{-4}$	169.64 ± 0.092
3 hours	27.80 ± 0.29	0.071 ± 0.0015	33.41 ± 0.23	$0.0085 \pm 9\ 10^{-5}$	167.95 ± 0.051

Table 3.3: Effect on the incubation time on the kinetic parameters.

Refolding of SK after denaturation in urea by manual mixing. A_1, A_2 are the amplitudes of the first and second phase with rate constants k_1 and k_2 respectively; B is the final fluorescence value. The dead time amplitude can be calculated by difference: B - (A_1 +A_2).

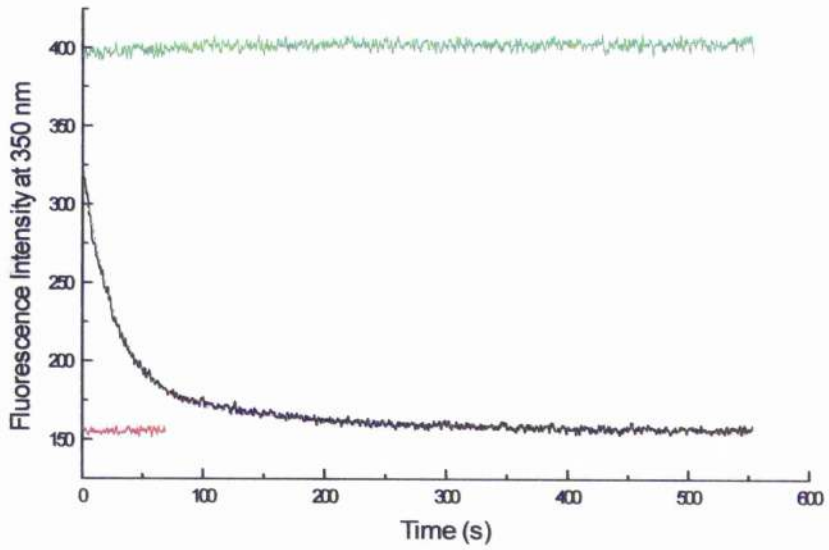

Figure 3.23: The kinetics of changes in protein fluorescence during unfolding

Unfolding was initiated by manual mixing by dilution in Tris buffer containing 4M urea (black curve). Fluorescence was monitored at 350nm. The red and green traces are referred to the unfolded (4M Urea) and native (0.36M Urea) SK respectively.

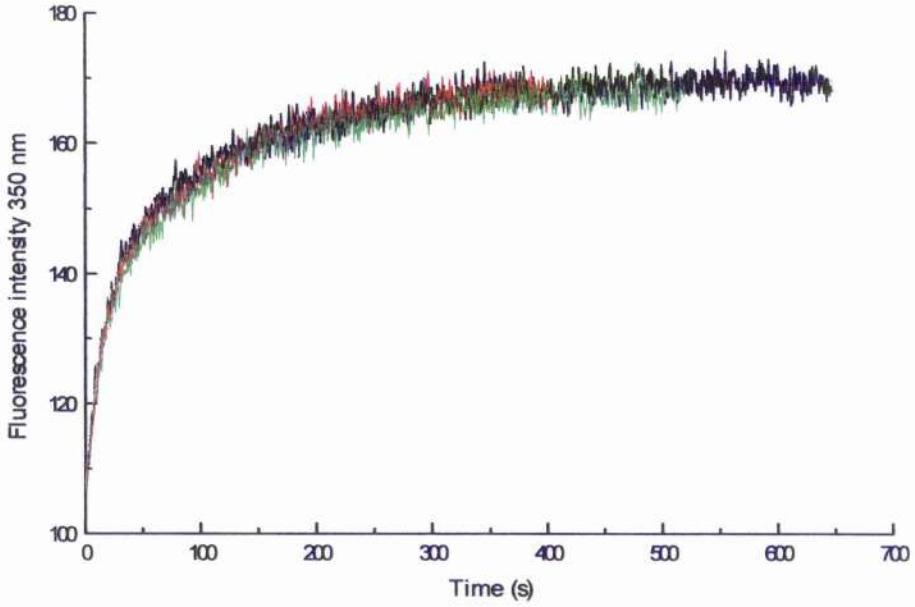

Figure 3.24: Effect of the incubation time on the refolding kinetics as monitored by fluorescence.

Refolding of SK after denaturation in 4M urea. Refolding was initiated by manual mixing and the fluorescence was monitored at 350nm. The unfolded solution was incubated for different times before starting the refolding by dilution. The data show the traces obtained when the refolding was carried out with the SK solution incubated, respectively, 5min (black), 30min (red), 3 hours (green).

3.4.2.4 Regain of fluorescence intensity on refolding

The regain of tertiary structure was monitored by changes in protein fluorescence at 350nm after dilution of the denaturant from 4M to 0.36M urea. In the manual mixing mode, the first time point at which reliable data could be obtained was approximately 20s after refolding had been initiated. Within this dead time, 35 % of the fluorescence of native enzyme (in the presence of 0.36M urea) had been regained. Over the course of 20min, a further 55 % of the fluorescence was regained in a first order process with a rate constant of $0.009s^{-1}$. Thus overall 90% of the signal of native SK was regained (Fig.3.25).

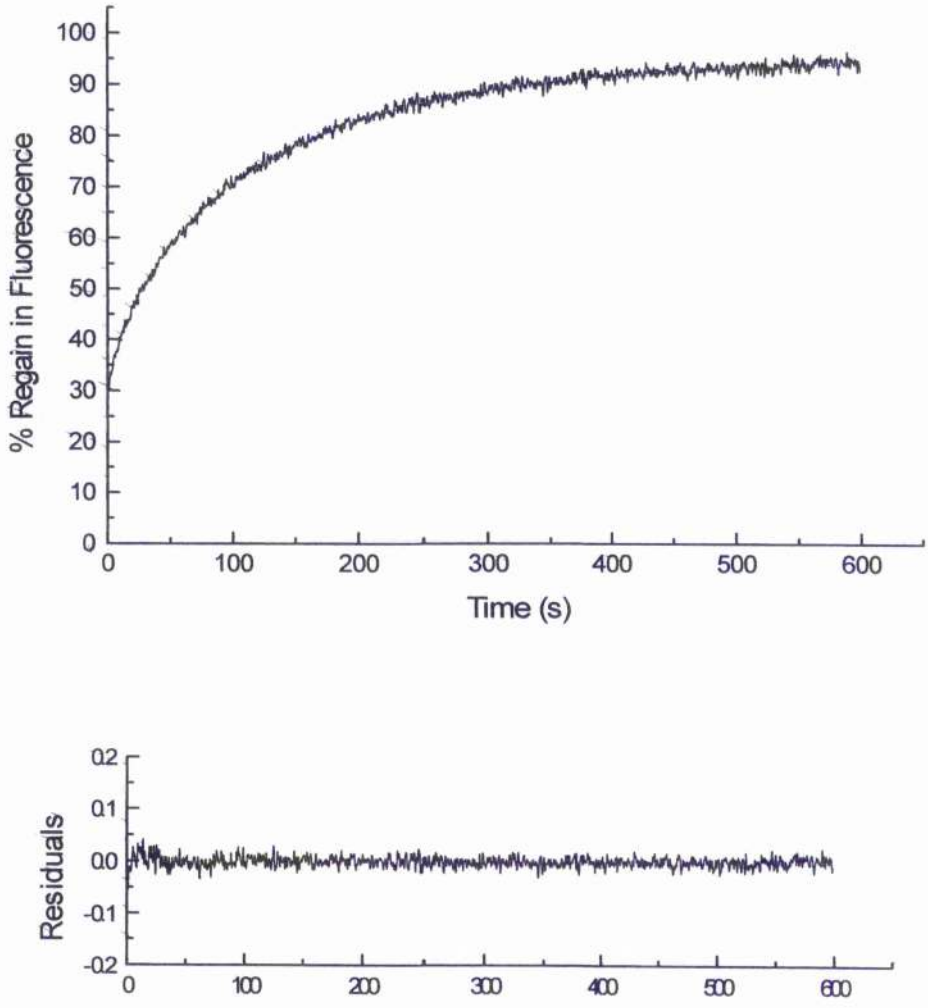

Figure 3.25: The kinetics of changes in protein fluorescence at 350nm using manual mixing Refolding of SK after denaturation in 4M urea. Refolding was initiated by manual mixing. Fluorescence was monitored at 350nm. The pattern of residuals to the curve fitting is shown.

Using stopped flow mixing techniques, it was found that less than 5% of the total change occurred within 5ms and that the subsequent changes in fluorescence occurred in two phases with amplitudes 42% and 45% of the total change with first order rate constants of $0.08s^{-1}$ and $0.009s^{-1}$ respectively. The rate of the slower process corresponds to that observed using manual mixing techniques (Fig.3.26). Using urea there is good agreement between the stopped flow and manual mixing experiments.

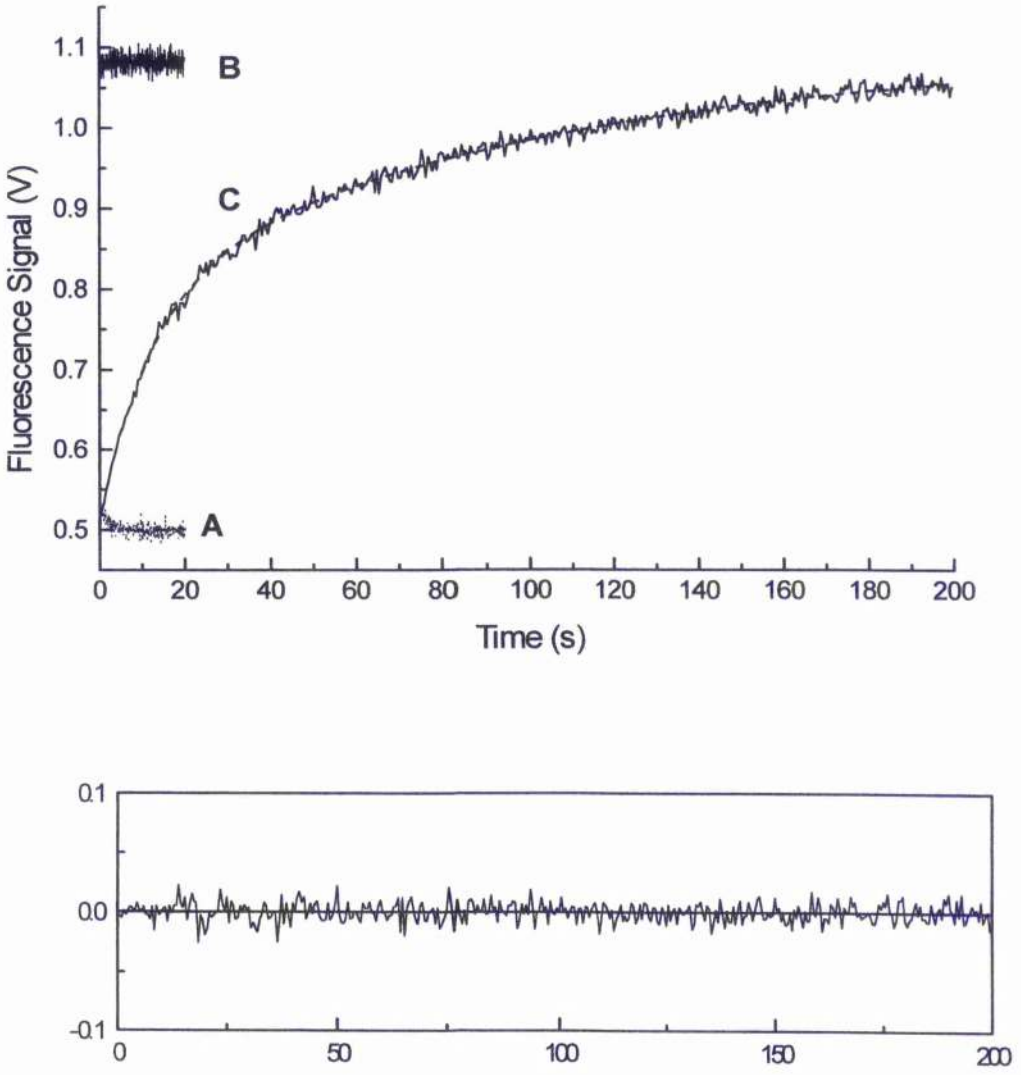

Figure 3.26:The kinetics of changes in protein fluorescence at 350nm using stopped flow mixing.

Refolding of SK after denaturation in 4M urea. Refolding was initiated by stopped flow mixing. The fluorescence signals have been corrected for the buffer signal. Curves A, B and C refer to enzyme in the presence of 4M urea, enzyme in the presence of 0.36M urea, and enzyme during refolding respectively. Fluorescence was monitored at 350nm. The pattern of residuals to the curve fitting is shown.

3.4.2.5 Refolding in the presence of shikimate

Refolding of shikimate kinase in the presence of shikimate was carried out in order to assess the stage in the process at which the shikimate binding site is formed, using the quenching of the protein fluorescence by the ligand as index of binding. This was possible using urea as denaturant, as the effects on the shikimate binding at 0.36M urea are negligible. In a preliminary experiment the binding of shikimate to the enzyme in the presence of 0.36M urea was shown to be very rapid. When 2mM shikimate was added to the enzyme (0.09mg/ml), over 95% of the fluorescence change occurred within the dead time of the stopped-flow instrument (1.8ms), implying a rate constant for the association reaction >7 x 10^5 $M^{-1}s^{-1}$.

For the refolding experiments it was necessary to monitor the refolding by changes in fluorescence at a different wavelength from 350nm. At the latter wavelength, the quenching caused by the binding of shikimate to the folded enzyme was nearly equal to the enhancement of protein fluorescence which occurred on refolding, leading to a very small overall change (Fig. 3.27). To choose the optimum wavelength different control experiments were undertaken and 330nm was chosen to follow the process.

A control refolding, performed at this wavelenth in the absence of shikimate, showed little difference in kinetics from the curve acquired at 350nm giving, when fitted with single exponential function, a rate constant of 0.06s^{-1} (Fig. 3.28).

When the refolding was carried out in the presence of 2mM shikimate, however, a markedly different pattern was observed (Fig. 3.29a, b). From the manual mixing trace it is evident that there is not a complete quenching even after 800 seconds. In the stopped flow trace after a rapid increase in fluorescence, essentially complete within 15s, there was a slow small decrease over the next 185s (Fig. 3.29 b). The rate constant for this decline (0.025s^{-1}) was rather higher than that of the slow increase in the absence of shikimate (0.009s^{-1}), which could indicate that the presence of ligand has a nucleating effect on folding of this area of the enzyme (Jaenicke, 1987). The folding of the protein (which would be expected to lead to an increase in protein fluorescence) leads to binding of shikimate and the consequent quenching results in the overall small decrease in fluorescence in this phase of the process. The simplest interpretation of these results is that only the slowest phase of folding leads to the formation of a shikimate binding site.

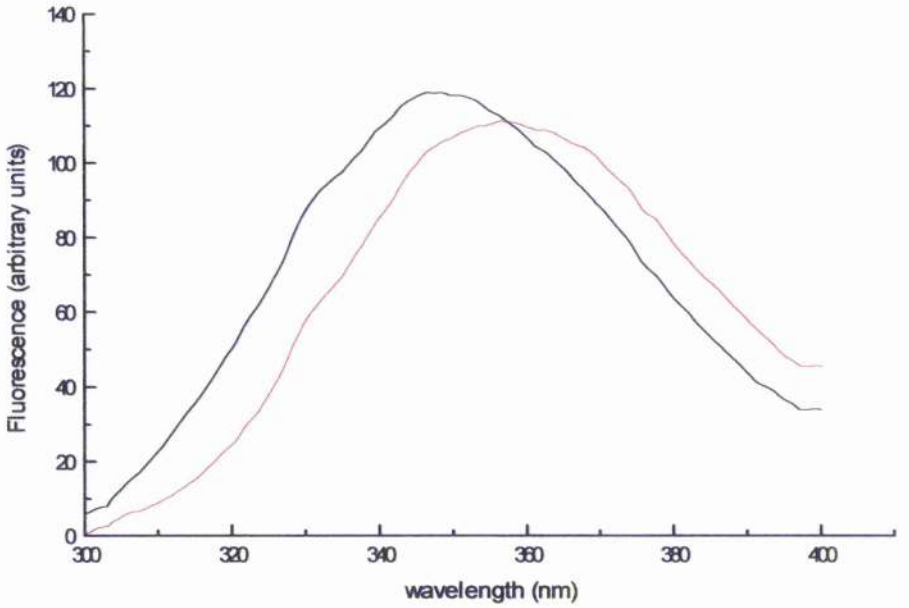

Figure 3.27: Fluorescence spectra before and after refolding in the presence of shikimate

Spectra were recorded at 20°C in the 300-400nm range after excitation at 295nm, T= 20°C. The samples were prepared in buffer D (35 mM Tris-HCl, pH 7.6, containing 5 mM KCl, 2.5 mM $MgCl_2$ and 0.4mM dithiothreitol) + 2mM shikimate and containing, respectively, 0.36M urea (black- end solution) and 4M urea (red- start solution).

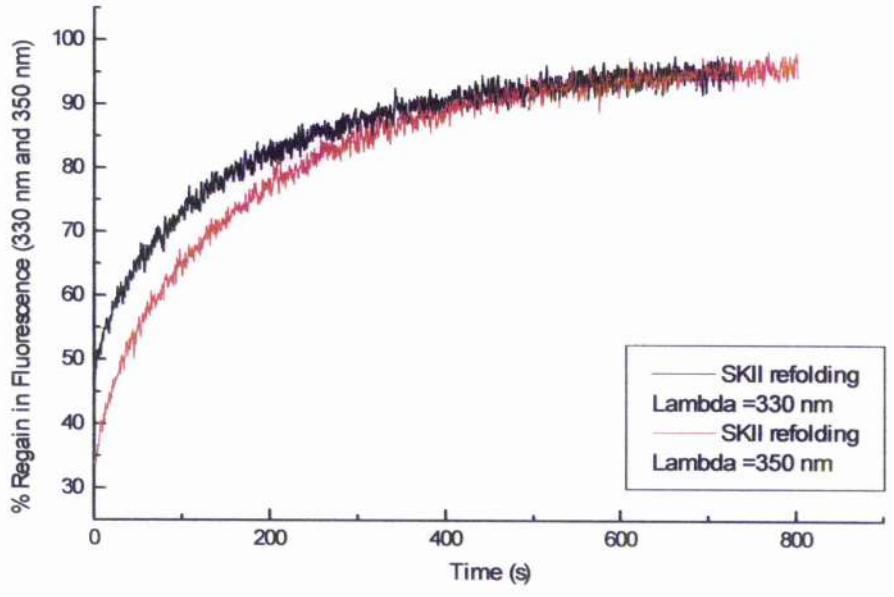

Figure 3.28:The kinetics of changes in protein fluorescence at two different wavelegths

Refolding of SK after denaturation in 4M monitored at two different wavelegths: 330nm (black); 350nm (red).

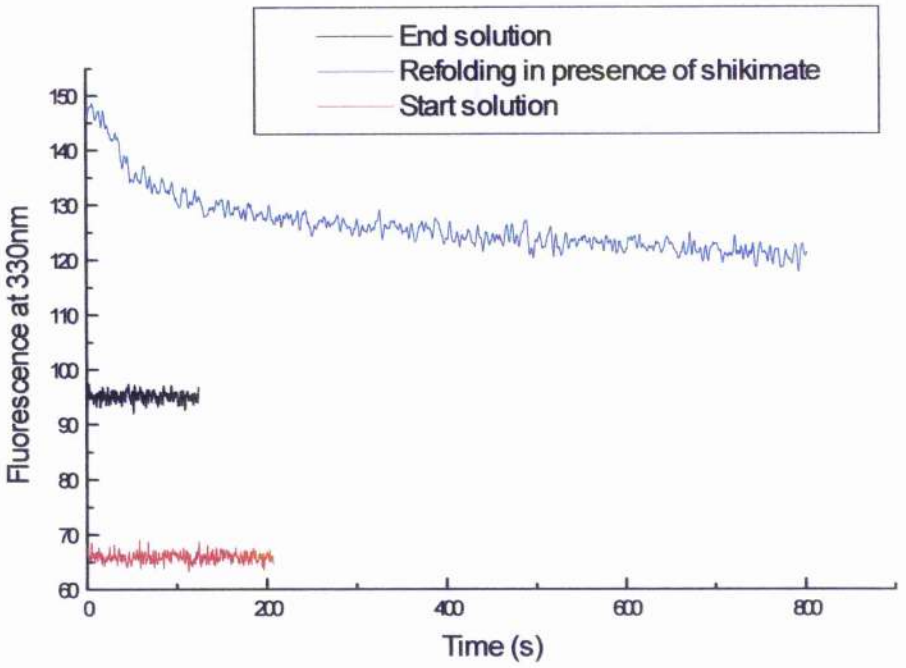

a)

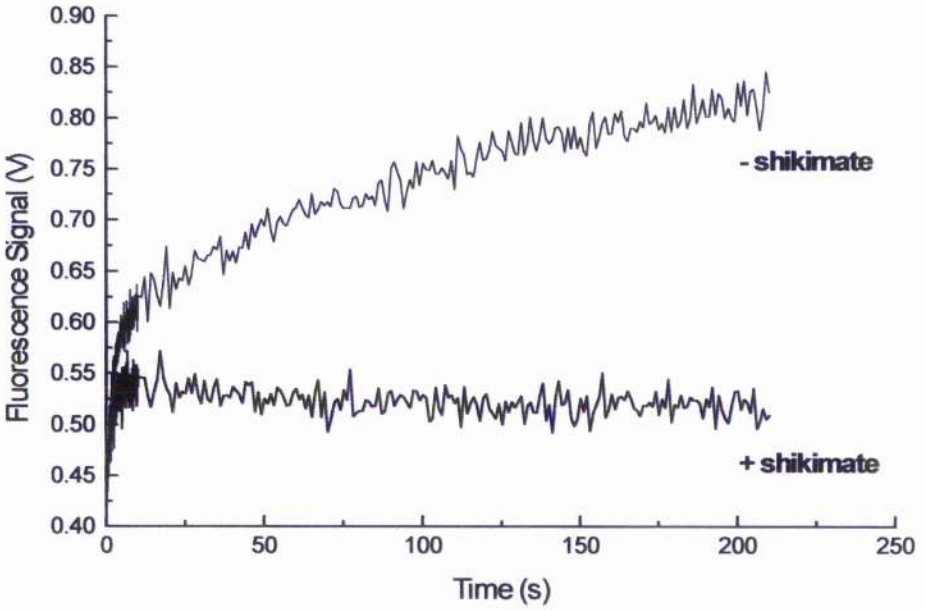

b)

Figure 3.29:The kinetics of changes in protein fluorescence in the presence of shikimate.

The refolding of SK in the presence of 2mM shikimate, monitored at 330nm, after denaturation in 4M urea, was initiated by a) manual mixing and b) stopped flow mixing (the fluorescence signals have been corrected for the buffer signal).

3.4.2.6 Refolding in the presence of ADP and ATP

The refolding experiments in the presence of 2mM ATP and 2mM ADP were performed only with manual mixing (Fig. 3.30). It seems that ATP gives a small increment in the refolding rate, while ADP gives a small decrease. For drawing any valid conclusion it would be necessary to repeat these experiments with the stopped flow apparatus.

For this reason these results are reported as a possible starting point for further investigations and will not be considered in the discussion.

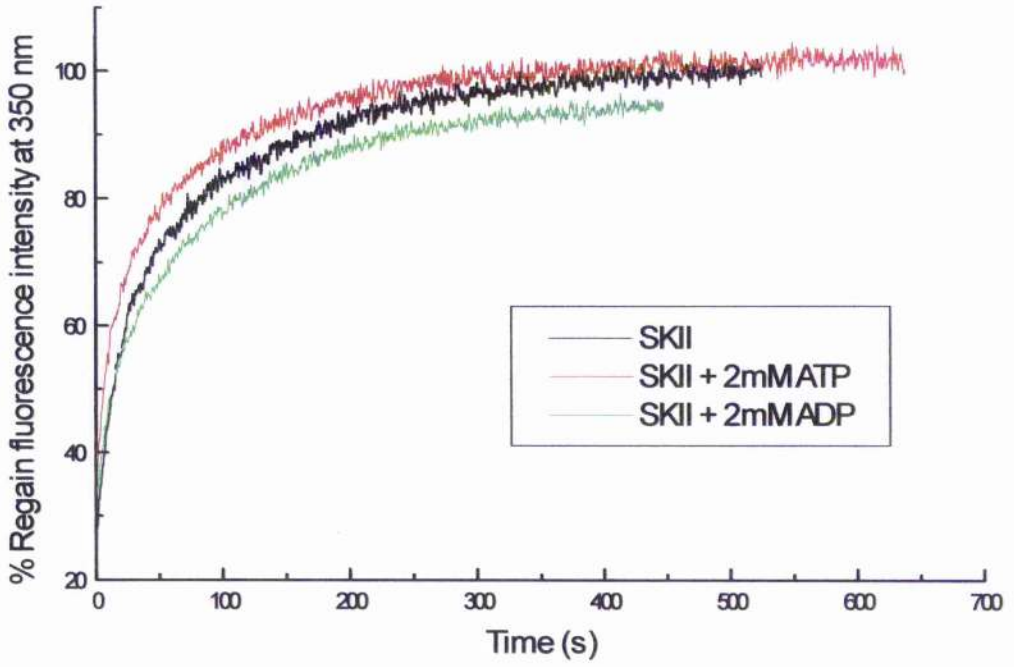

Figure 3.30: Kinetics of changes in protein fluorescence in the presence of nucleotides

Refolding of SK after denaturation in 4M urea. Fluorescence was monitored at 350nm. Refolding was initiated by manual mixing in buffer (black), and in buffer containing 2mM ATP (red), and 2mM ADP(green).

3.4.2.7 Refolding in the presence of sodium iodide

In these experiments the iodide ion was used as a probe to monitor the reconstitution of the charged environment of Trp54 during refolding. The value of the Stern-Volmer constant (K_{sv}) in 0.36M urea was determined as a preliminary control for the refolding experiments. In the presence of 0.36M urea the K_{sv} for SK ($19.0M^{-1}$) is very similar to that of native enzyme (Fig. 3.31), demonstrating the integrity of the Trp environment at this urea concentration. The values obtained with the other quencher used (succinimide), which is neutral, are reported for comparison (Table 3.4). The changes in protein fluorescence during refolding of SK in the presence of 0.1M NaI were investigated to assess at what stage in the folding process the positively charged environment of Trp 54 in native enzyme is formed.

From the data obtained using manual mixing techniques to initiate refolding (Fig. 3.32a), it was found that after 600s, the degree of quenching caused by 0.1M NaI corresponded to a K_{sv} of $17.8M^{-1}$ (i.e. very similar to that of enzyme in the presence of 0.36M urea). After 20s, the degree of quenching corresponded to a K_{sv} of $12.0M^{-1}$. The changes in fluorescence over the period from 20s to 600s could be fitted to a first order process with a rate constant $0.008s^{-1}$, which is very similar to that observed in the absence of NaI ($0.009s^{-1}$). Using stopped flow mixing to initiate refolding (Fig. 3.32b), the degree of quenching after 20s was found to correspond to a K_{sv} of $12.0M^{-1}$, identical to that observed by manual mixing. After 2s, the quenching corresponded to a K_{sv} of $6.4M^{-1}$, which is similar to the value for denatured enzyme. From these results, it is clear that the high degree of quenching and hence the positively charged environment of the Trp is formed progressively during the two (relatively slow) processes during which the changes in the Trp fluorescence itself occur.

Solution	K_{sv} (NaI)	K_{sv} (succinimide)
SK	20.05 ± 0.30	5.56 ± 0.11
SK + 0.36M Urea	20.71 ± 0.29	5.52 ± 0.20
SK + 4M Urea	4.67 ± 0.1	5.19 ± 0.045

Table 3.4: K_{sv} values for SK under different conditions
The values quoted are the means of at least 4 experiments.

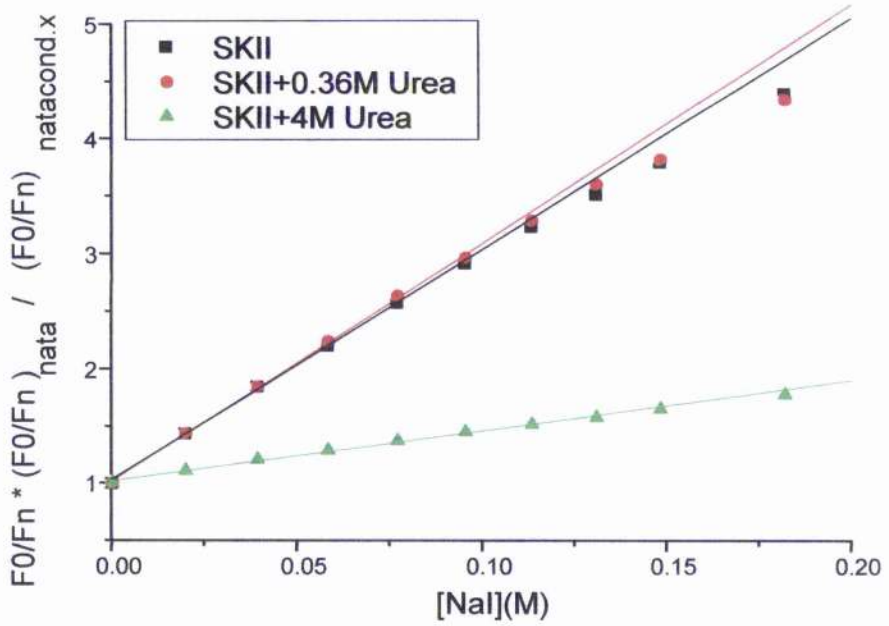

Figure 3.31: Stern-Volmer plots of SK in different conditions.

The fitting was performed by linear regression in the range 0 - 0.095M of quencher (NaI). The quenching was corrected for the effect of solvent on the fluorescence of NATA.

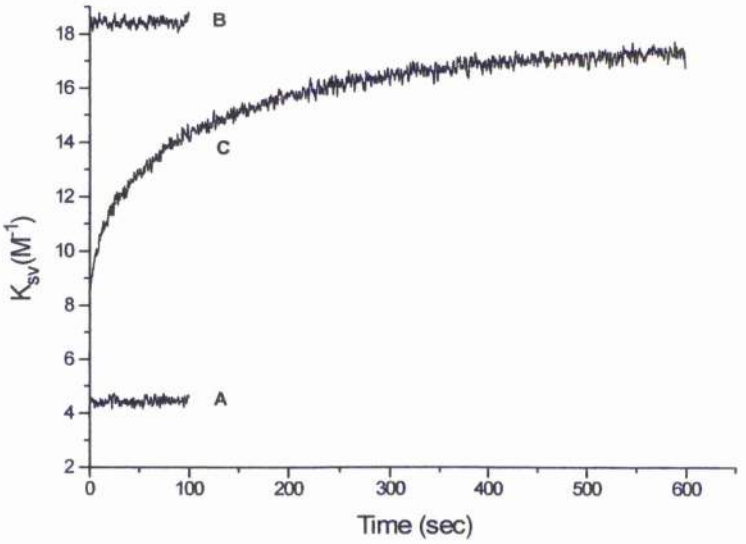

a)

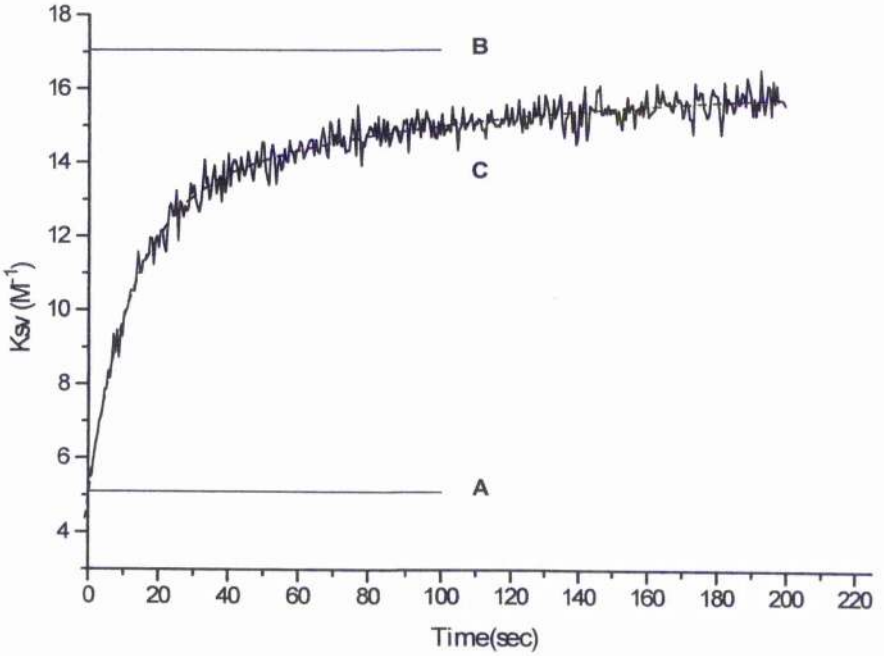

b)

Figure 3.32: The kinetics of changes in quenching of fluorescence by iodide.

Refolding of SK after denaturation in 4M urea. (a) Changes observed using manual mixing to initiate refolding. b) Changes observed using stopped flow mixing to initiate refolding.The concentration of NaI present during refolding was 0.1M, and the K_{sv} value at any given time was calculated by comparing the fluorescence intensities in the absence (F_0) and presence (F) of iodide, using the equation $K_{sv} = ((F_0/F) - 1)/(0.1)\ M^{-1}$. Curves A, B and C refer to enzyme in the presence of 4M urea, enzyme in the presence of 0.36M urea, and enzyme during refolding respectively.

3.4.2.8 ANS as a probe for the formation of early intermediates. Preliminary experiments

8-Anilino-1-naphthalene-sulphonate (ANS) is one of the most frequently used fluorescent probes for the investigations of structural properties of protein molecules.

The ANS fluorophore is virtually non-fluorescent in aqueous solution but becomes fluorescent in organic solvents or when bound to the interior of certain proteins. The probe, which is thought to bind to clusters of hydrophobic side chains of proteins (Goldberg *et al.*, 1990), was extensively used in the identification of early compact intermediates (Christensen and Pain, 1991; 1994; Ptitsyn, 1995a).

It has been found that during the folding of a number of proteins, there is rapid rise in ANS fluorescence (within about 1s) followed by a slower decline in the fluorescence (lasting up to about 10s) (Goldberg *et al.*, 1990). This has been interpreted as reflecting the formation of an intermediate state during the folding process. Such intermediates are frequently observed for proteins with a low overall stability (Fischer and Schmid, 1990).

This intermediate state has been termed "molten globule": in this state the protein is compact, but the amino acid side chains are reasonably fluid, i.e. the precise interactions stabilising the native tertiary structure have not been formed. This state is thought to bind ANS preferentially; the probe is then "squeezed out" when the final tertiary structure interactions are formed. However, there have been concerns raised that the presence of ANS may perturb the folding process (Engelhard and Evans, 1995). From other studies it has been proposed that the ANS binding could be dictated by the concentration of the chaotropic agent used for denaturation, which displaces the dye by sheer competition (Kumar *et al.*, 1996), but the existence of an increase of ANS fluorescence observed upon pressure-induced denaturation (Uversky *et al.*, 1996) confirms the validity of the use of this probe as indicator of the involvement of compact intermediates in the refolding process.

Before using ANS in the refolding buffer, a number of control experiments were carried out to check if this probe had any effect on the structure and activity of SK.

The far-UV CD spectrum of SK (Fig. 3.33) in the presence of ANS shows small changes compared to the spectrum in the absence of this probe. The measure of the regain of the activity when the refolding is carried out in the presence of ANS is another test to check if the dye perturbs the refolding process. When the refolding was performed in the presence of 40μM ANS, the regain of activity was 95% that of the control (with ANS); this activity was regained in a first order process with a rate constant $0.008s^{-1}$ (Fig.3.34). From these data, it is clear that ANS has only relatively minor effects on the catalytic site of the enzyme and its ability to refold after denaturation.

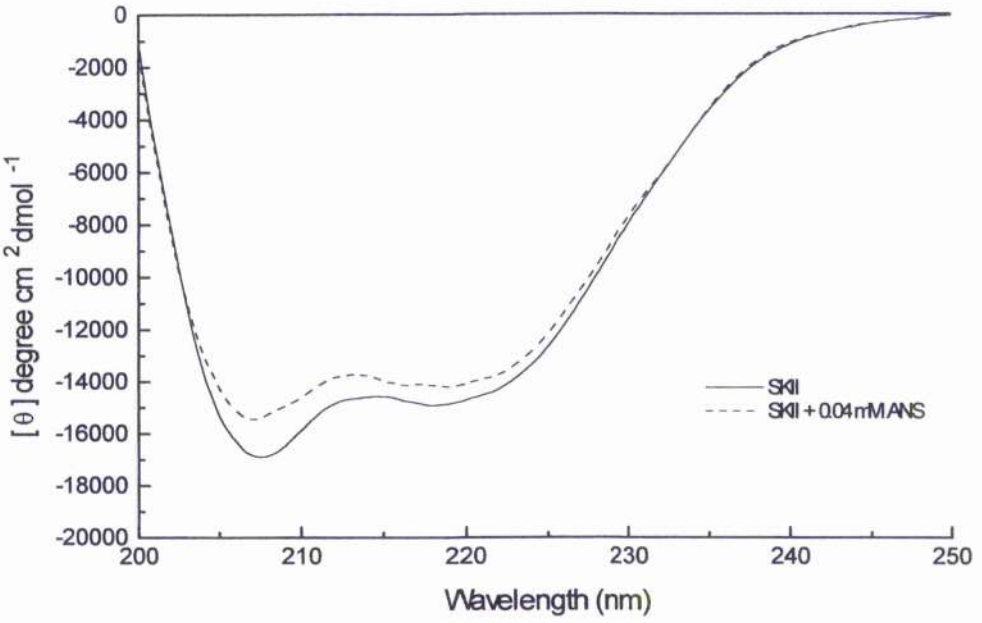

Figure 3.33: Effect of ANS on the secondary structure of SK.

The far-UV CD was acquired as described in section 2.4. The protein concentration was 0.15mg/ml. The data shows the spectra of SK in the absence (solid line) and in the presence (dashed line) of 40μM ANS.

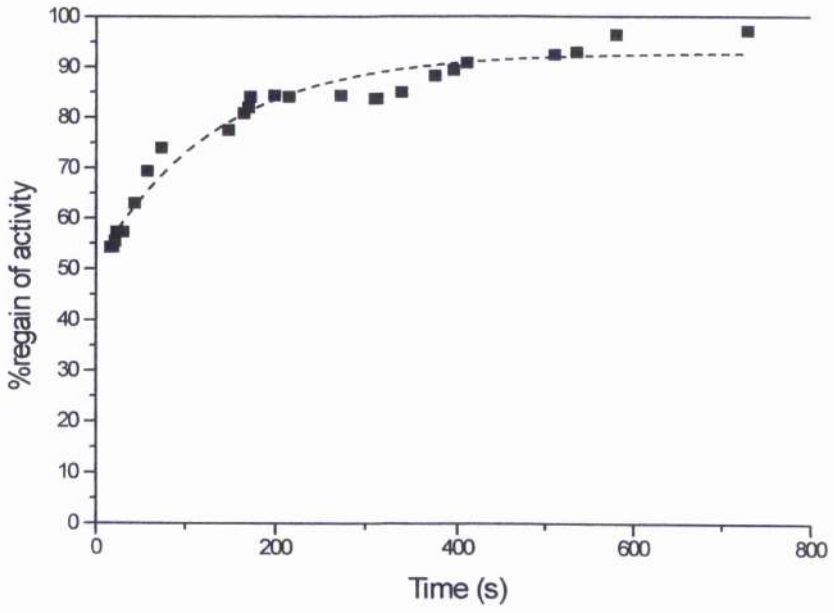

Figure 3.34: The kinetics of regain of activity of SK in the presence of 40μM ANS.

Denaturation in 4M urea. Activity values are expressed relative to a control sample incubated in the presence of the final concentration of urea, i.e. 0.36M+ 40μM ANS. The dashed line shows a fit to a first order process with a rate constant of $0.008s^{-1}$.

The effects of different medium conditions on both ANS florescence and on the fluorescence of the ANS bound to SK were investigated, since it has been reported that for some other proteins there is a change in these characteristics with an alteration of the solvent composition (Nerli and Pico, 1994). Fluorescence spectra of ANS (40μM) in buffer, in the presence of 4M urea and in the presence of 0.36M urea, both in the absence (Fig. 3.35a) and in the presence of protein (Fig. 3.35b) have been acquired and the difference spectra, to check the bound-ANS fluorescence, have been calculated (Fig. 3.35c).

From these data it seems that the presence of urea leads to an increase of the free ANS fluorescence, with this effect being more pronounced in 4M urea than in 0.36M urea. The intensity of ANS in the presence of SK in 4M urea is lower, as expected, than in buffer, while there is an increase of fluorescence intensity in 0.36M urea when compared to the sample in buffer (Fig.3.35b). This situation has already been observed for bovine serum albumin and it was deduced that low concentrations of urea induced binding of the probe (Nerli and Pico, 1994). Making the assumption that the free ANS and bound ANS are both present in solution and contribute to the fluorescence intensity, the difference spectra in each condition have been acquired:

$$(SK.ANS)_{(cond.\ X)} - (ANS)_{(cond.\ X)}$$

this "approximation" should give information on the spectra of bound ANS. The fact that this approximation is reasonable is given by the difference spectrum of the solutions in 4M urea, which is practically zero (Fig. 3.35c). From these difference spectra it appears that there is no significant increase in the binding of ANS in 0.36M urea, but that the observed increased intensity is mainly due to an increase in the fluorescence intensity of the free ANS in solution brought about by the presence of 0.36M urea (Fig. 3.35a).

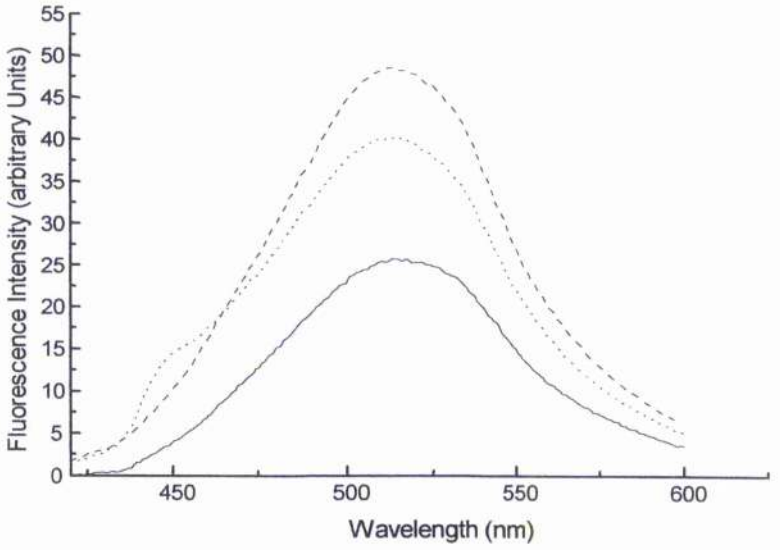

a)

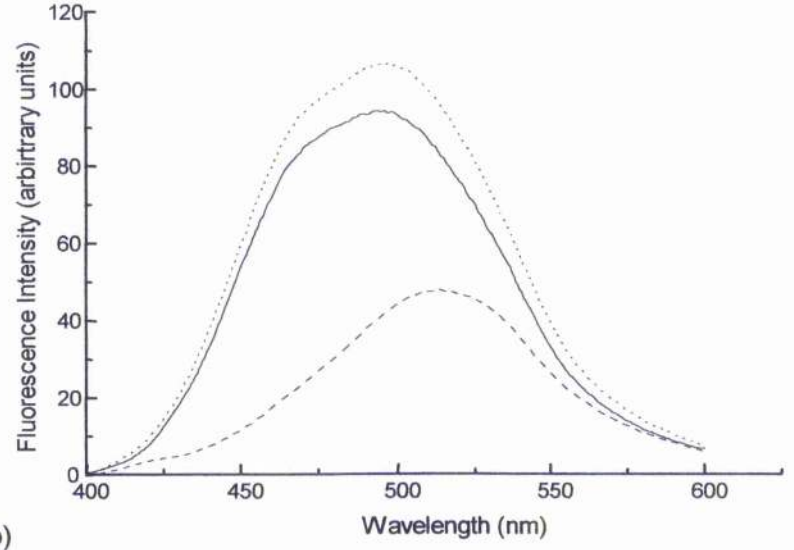

b)

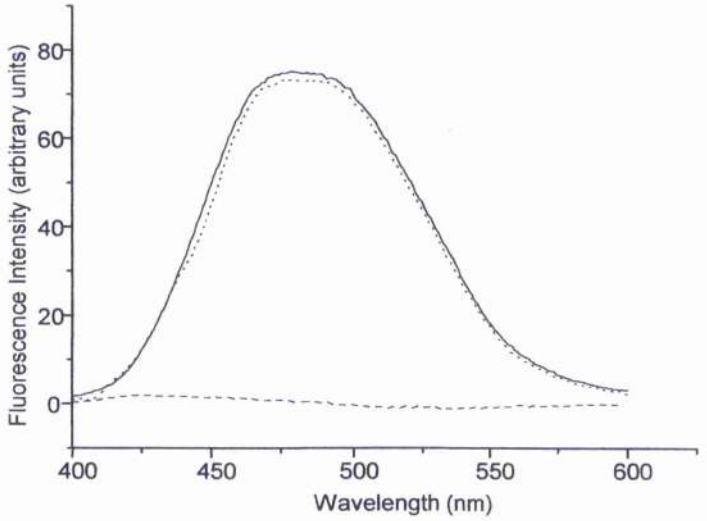

c)

Figure 3.35: ANS spectra (40μM) in buffer, in 4M urea and in 0.36M urea.

Solid line : ANS and buffer; dotted line: ANS in the presence of 0.36M Urea; dashed line: ANS in the presence of 4M Urea respectively in the absence (a) and in the presence of protein (b). (c): difference spectra: $(SK.ANS)_{(cond.\ X)} - (ANS)_{(cond.\ X)}$

Spectra were recorded in the presence of substrate (Fig. 3.36) and binding titrations were also performed (Fig. 3.37) to validate the use of ANS as a probe during refolding in the presence of substrate. The influences of ANS on SK activity was also studied.

The presence of 40μM ANS caused less than 10% change in the K_d for shikimate giving a value of 0.69mM (using the fluorescence quenching titration), and an 18% decrease in the activity of enzyme (when assayed under the standard conditions).

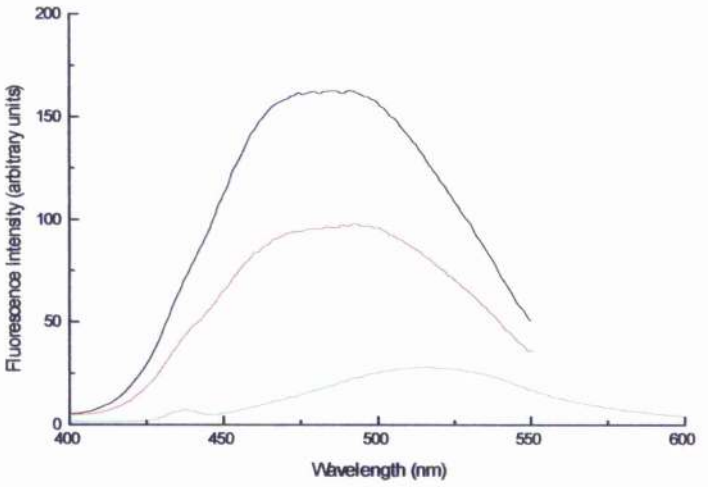

Figure 3.36: SK.ANS spectra (40 μM) in in the presence of 2mM shikimate.

The emission spectra were acquired after excitation at 380nm. The protein concentration was 0.15mg/ml. The data shows: SK + ANS (black line); SKII + ANS+shikimate (red line) and ANS (green line).

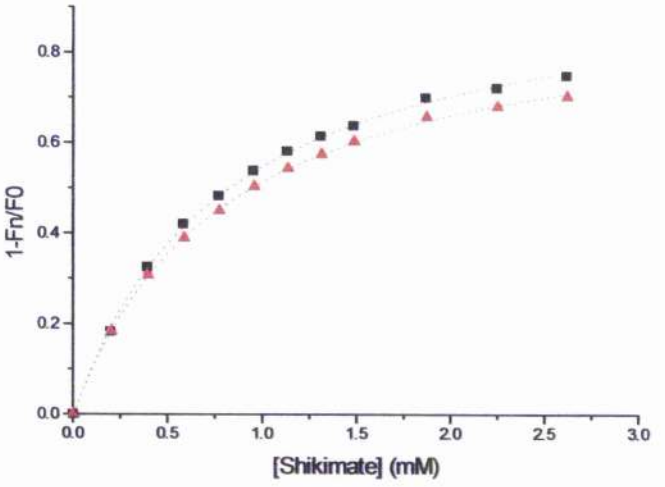

Figure 3.37: Shikimate titration in the presence of ANS.

The titrations were performed as described in section 2.3. The data show the titration curves obtained for SK alone (black) and in the presence of 40μM ANS (red).

3.4.2.9 ANS as a probe during refolding

Using urea as a denaturing agent, a characteristic pattern of changes in ANS fluorescence during refolding was observed. When refolding was initiated by manual mixing techniques, there was a rapid increase in fluorescence within the dead time of observation (20s) corresponding to approximately 10 times the fluorescence of the starting solution (enzyme in 4M urea) and 2.5 times the value of the end solution (enzyme in 0.36M urea).

This increase was followed by a decrease over the subsequent 600s to reach a value similar to that observed for the enzyme in the final concentration of urea (0.36M) (Fig. 3.38); the rate constant for this decrease was $0.009s^{-1}$.

Using stopped flow mixing techniques (Fig. 3.39 a and b) to initiate refolding, the initial rapid increase in ANS fluorescence was found to be at least 50% complete within 5ms. Further analysis of the changes in fluorescence over the first 200ms after mixing suggested that the increase occurred in two phases of approximately equal amplitude, one very fast ($k > 100s^{-1}$) and the other with a rate constant $11s^{-1}$(It should be noted that the magnitude of the faster rate constant could not be estimated accurately; the value quoted is based on the half time being less than or equal to 5ms). The subsequent decrease in ANS fluorescence (to reach a value similar to that of the enzyme in the presence of the final concentration of urea) occurred in two first order processes with rate constants $0.08s^{-1}$ and $0.012s^{-1}$; the amplitude of the faster of these two phases corresponded to 25% of the total decrease observed.

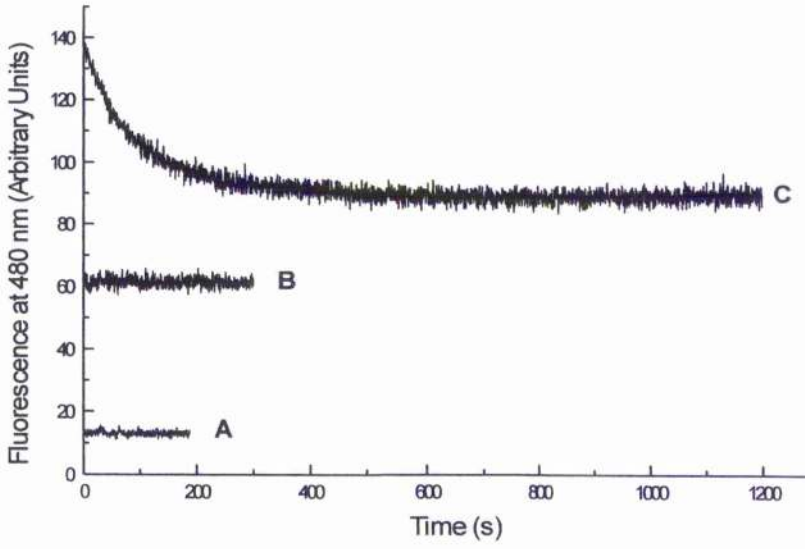

Fig. 3.38: The kinetics of changes in ANS fluorescence at 480nm

Refolding of SK (manual mixing) after denaturation in 4M urea. Curves A,B, and C refer to enzyme in the presence of 4M urea, enzyme in the presence of 0.36M Urea, and enzyme during refolding respectively.

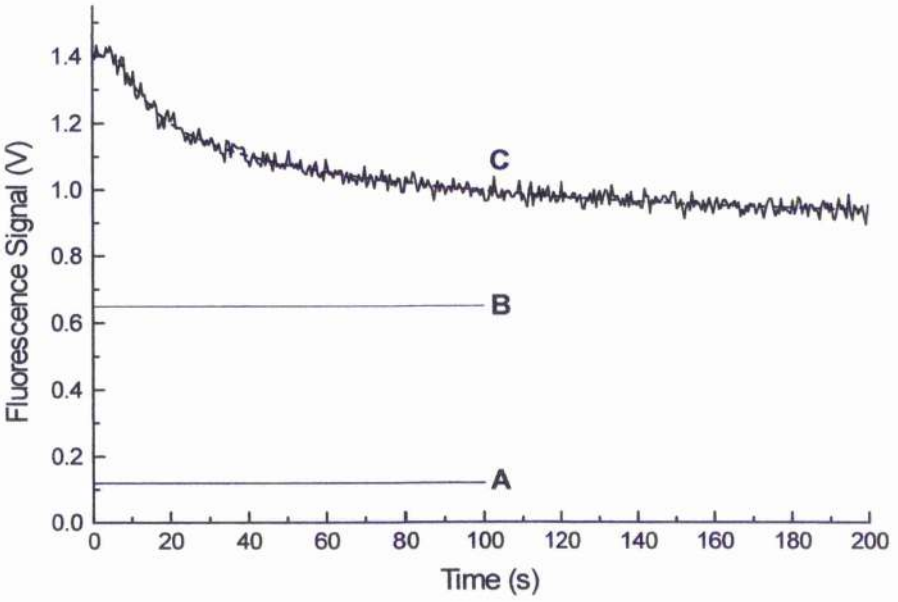

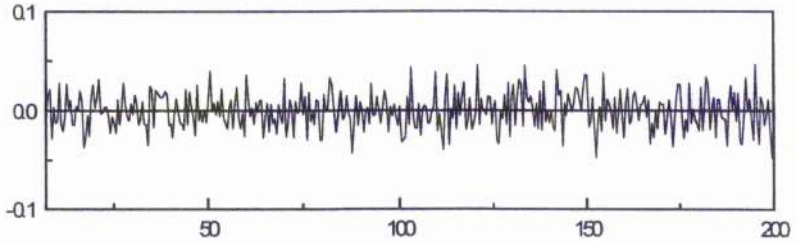

a)

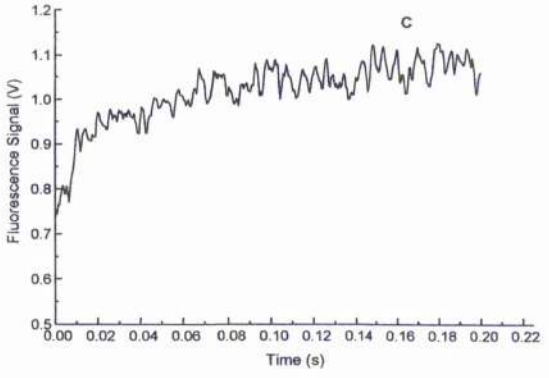

b)

Figure 3.39: The kinetics of changes in ANS fluorescence at 480nm

Refolding of SK after denaturation in 4M Urea (stopped flow mixing).
a) Curves A,B, and C refer to enzyme in the presence of 4M urea, enzyme in the presence of 0.36M Urea, and enzyme during refolding respectively.
b) The kinetics of changes in ANS fluorescence at 480nm during refolding of SK after denaturation in 4M urea. The first 20ms of the refolding curve are shown.

Preliminary refolding experiments in the presence of shikimate and ANS were performed using stopped flow mixing (Fig. 3.40a, b). In Figure 3.40 a there is the comparison between the first part of the refolding curves in the presence and absence of shikimate (ANS region) (the two curves were obtained using different slit widths). It should be noted that the presence of shikimate in solution leads to a decrease of the intensity of the spectrum (Fig.3.36) so differences observed in the kinetics of the different phases could give useful indications of the effect of substrate on the refolding process. These data should be repeated to draw any valid conclusions and could serve as a basis for further investigation.

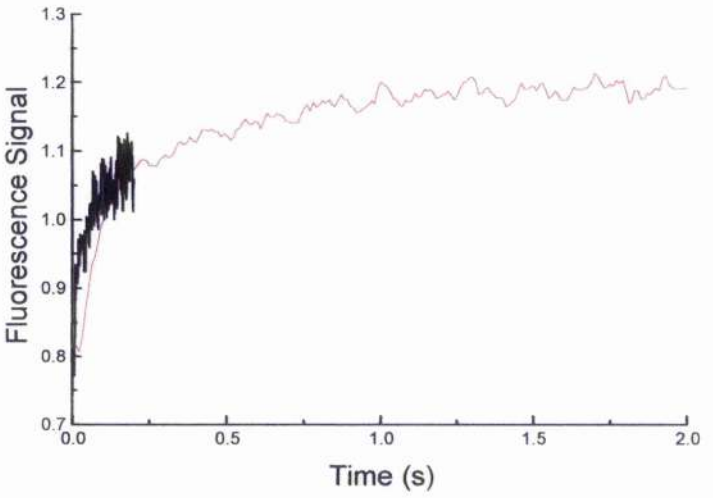

a)

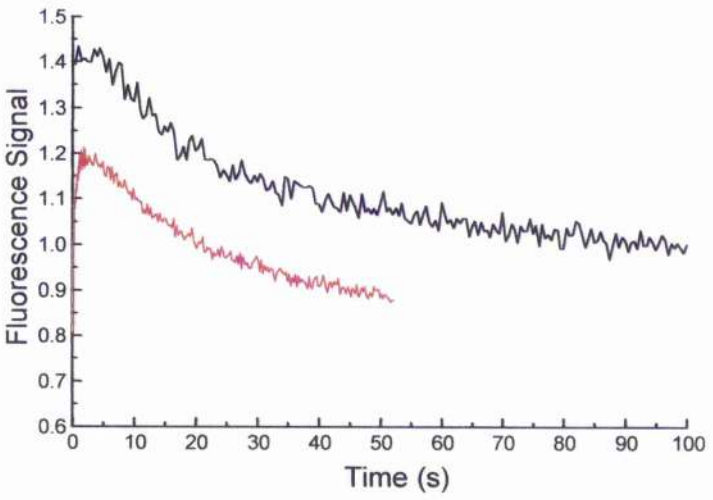

b)

Figure 3.40: The kinetics of changes in ANS fluorescence in the presence of shikimate.

Refolding of SK after denaturation in 4M Urea (stopped flow mixing). The ANS fluorescence was measured at 480nm after excitation at 380nm. The protein concentration was 0.1mg/ml during the refolding. The data shows the refolding curves obtained in the absence (black curve) and in the presence (red curve) of 2mM shikimate.

3.4.3 Model of folding pathway and properties of intermediates

For many proteins a burst (millisecond) phase was observed which is characterized by partial formation of the secondary structure and partial condensation, typical of the "pre-molten" globule (Ptitsyn, 1995; Eaton *et al.*, 2000). The next intermediate usually resembles the molten globule state: it has a degree of native-like, protected secondary structure, and even some native tertiary contacts (Ptitsyn 1995; Roder *et al.*, 1988). The further formation of native state can take from a fraction of a second to hours, expecially if there is a slow rearrangement of packing of non-native proline isomers or non-native disulphide bonds (Galzitskaya *et al.*, 2001).

Approximately 95% enzyme activity could be recovered on dilution of the urea from 4M to 0.36M. The results of spectroscopic studies indicated that refolding occurred in at least 4 kinetic phases, the slowest of which ($k = 0.009s^{-1}$) corresponded with the regain of shikimate binding and of enzyme activity. The two most rapid phases were associated with a substantial increase in the binding of 8-anilino-1-naphthalenesulphonate with only modest changes in the far-UV CD, indicating that a collapsed intermediate with only partial native secondary structure was formed rapidly.

Detailed studies of the refolding of a number of proteins after denaturation have led to the development of the nucleation-condensation model; this seeks to draw together ideas from earlier proposals which focussed attention on aspects such as formation of secondary structure or hydrophobic collapse (Fersht, 1999). In energy terms, the transition from denatured to native state is viewed in terms of a "folding landscape" in which kinetic flow can occur through a series of states of progressively lower energy in a "folding funnel" (Fersht, 1999; Brockwell *et al.*, 2000).

Although there are some differences in detail between the results of the various techniques employed in the present work to monitor the refolding of SK after denaturation in urea, when taken together the data indicate that there are probably four kinetic phases contributing to the folding process. The average rate constants for these phases are $>100s^{-1}$ (half life <7ms), $10s^{-1}$ (half life 70ms), $0.08s^{-1}$ (half life 9s) and $0.009s^{-1}$ (half life 80s). A simple outline model could thus be proposed which involves 3 intermediates (I_1, I_2 and I_3) between the unfolded state (U) and the native state (N).

$$\mathbf{U} \xrightarrow{>100\ s^{-1}} I_1 \xrightarrow{10\ s^{-1}} I_2 \xrightarrow{0.08\ s^{-1}} I_3 \xrightarrow{0.009\ s^{-1}} \mathbf{N}$$

The properties of these are indicated in Table 3.5, in which the various properties of the unfolded and final states have been normalised to 0 and 100 respectively in order to facilitate comparison.

The increase in ANS fluorescence occurs very rapidly implying that the formation of a collapsed intermediate precedes substantial regain of secondary structure. This type of result is analogous to that previously observed for the refolding of the 89 amino acid protein barstar (Agashe *et al.*, 1995) and for the small all β-sheet protein CTX(III) (Sivaraman *et al.*, 1998). It might be informative to explore the nature of the early formed intermediate(s) by using CD over a wider range of wavelengths in the far-UV. The regain of the majority, if not all, of the activity occurs during the final slow phase which is associated with the completion of regain of native fluorescence and its quenching by I^-, the further extrusion of ANS, together with small changes in secondary structure.

Property	U	k_1 (s^{-1})	I_1	k_2 (s^{-1})	I_2	k_3 (s^{-1})	I_3	k_4 (s^{-1})	N
ANS fluorescence (480nm)	0	>100	180	11	360	0.085	300	0.012	100
CD at 225nm	0		20	8	40	0.08	90	0.008	100
Protein fluorescence (350nm)	0		0		5	0.08	50	0.009	100
Fluorescence quenching (I^-)	0		0		10	0.09	50	0.008	100
Activity	0		0		0		<10	0.007	100

Table 3.5: Properties of intermediates in the refolding of shikimate kinase

U and N represent the unfolded and refolded states of the enzyme and I_1, I_2 and I_3 the intermediates inferred from the kinetic analysis of changes in activity and spectroscopic parameters during refolding. In order to facilitate comparisons, the values of U and N have been normalised to 0 and 100 respectively. In each case, more than 85% of the property of native enzyme was regained after refolding.

3.4.4 Comparison with studies on the refolding of adenylate kinase

The refolding of SK to generate active enzyme occurs considerably more slowly than for many proteins of a similar size (Jaenicke, 1987; Grantcharova *et al.*, 2001; Gunasekaran *et al.*, 2001). It has been suggested that the low rate might be a feature of a number of α/β domain proteins, where the formation of the β-sheet is expected to be a slow process requiring the formation of a large number of specific long-range contacts in the proper orientation (Houry *et al.*, 1999; Plaxco *et al.*, 1998; Sivaraman *et al.*,1998). By contrast, formation of α-helices is much more rapid, since short-range interactions are involved.The final steps in formation of the native structure of α/β domain proteins can involve slow rearrangement of domains, as observed in the case of the $p21^{rss}$ protein (Zhang and Matthews,1998).

In the refolding of a number of proteins, the *cis/trans* isomerisation of Xaa-Pro imide bonds appears to account for some or all of the slow steps involved (Schmid *et al.*,1993; Nall, 1994). On unfolding the protein, a slow isomerisation (with a time constant of the order of 100 - 1000s (Schmid *et al.*,1993)) of the Xaa-Pro imide bonds occurs to give a mixture containing typically 10-20% *cis* species at equilibrium. Upon refolding, proteins in which the Xaa-Pro bonds are in their native state can refold rapidly. Slow refolding species represents proteins in which a Xaa-Pro imide bond is trapped in the non-native conformation; productive folding can only occur after isomerisation has occurred. In many (but by no means all) such cases, the slow step(s) can be accelerated by addition of peptidyl prolyl isomerase.
While it is possible that the slowest phase of the folding of shikimate kinase could reflect Xaa-Pro isomerisation, there are good grounds for believing that this is not the case. Firstly, none of the 7 proline residues in the native enzyme contains a *cis* imide bond. Secondly no difference in the rates or amplitudes of the slow phases of the refolding process using unfolding times ranging from 5min to 3h has been found (section 3.4.2.3). Thirdly, the amplitudes of those slow phases which require *cis* $\rightarrow$ *trans* isomerisation are typically 10-20%, reflecting the proportion of *cis* Xaa-Pro imide bonds at equilibrium in the unfolded state. In the case of shikimate kinase the slowest phase in the refolding has an amplitude of 55% of the total fluorescence change, and greater than 55% of the total changes in ANS desorption, shikimate binding and catalytic activity (Table 3.5). Further detailed studies of the refolding of mutants of SK in which the proline residues had been systematically substituted and of the refolding after very short periods of unfolding (the "double jump" technique (Nall, 1994)) would help to establish the role (if any) played by isomerisation of Xaa-Pro bonds in the refolding of the enzyme.

The results obtained can be compared with those reported (Zhang *et al.*, 1998) on the refolding of the structurally similar adenylate kinase after unfolding in urea. Because Zhang *et al.* (1998) used only manual mixing techniques to initiate refolding, the early steps in the

refolding pathway were not examined. Zhang *et al.* (1998) observed that most of the ellipticity at 225nm of adenylate kinase was regained within 18s of the start of refolding and estimated the rate constant for the regain of secondary structure as >0.16s^{-1} at 25°C. The data on shikimate kinase show that 75-80% regain of ellipticity at 225nm occurs within 20s, but that this occurs in three stages. The last stage during which most of the remaining ellipticity is regained occurs with a rate constant of approximately 0.009s^{-1} at 20°C. The rate constant for the regain of activity of adenylate kinase reported by Zhang *et al.* (1998) was 0.025s^{-1} at 25°C, which is of a comparable magnitude to the value obtained for SK (0.009s^{-1} at 20°C) in the present work. In agreement with the observations reported in this thesis, Zhang *et al.* (1998) reported that there was a rapid increase in ANS fluorescence upon initiation of the refolding process, followed by a decline as the probe was released from the protein. The desorption step in the case of adenylate kinase occurred with a single rate constant (0.004s^{-1}), which is of a similar magnitude to that of the slowest step observed, associated with regain of the activity of shikimate kinase. The results extend the less complete data available for the refolding of adenylate kinase (Zhang *et al.*, 1998) indicating that the pathway described for SK should act as a model for many other members of this subclass of α/β proteins.

Appendix 3.1: Chemical modification of SK by pyridoxal-5'-phosphate.

Chemical modification techniques can be used to investigate the mechanism of an enzyme or the role of a specific residue in the catalysis. In this case pyridoxal-5'-phosphate (PLP) was chosen as a modifier because it react specifically with lysine residues forming a Schiff base. A series of controls have been performed as described in section 2.6 to validate the method. Chemical modification with PLP can be performed measuring the activity of a reduced or of a non-reduced Schiff base (section 2.6). Initially the modified enzyme was assayed without prior reduction with $NaBH_4$. Because in the case of SK a double coupled assay is used, the dilution affects the reversibility of the PLP reaction when the Schiff base is not reduced, as is evident from the comparison of the results reported in Fig. A3.1a and Fig. A3.1b of non-reduced and reduced samples respectively. In both cases there is only a partial loss of activity. A control is also reported which shows the effect of the incubation at room temperature and stirring on the SK activity. For this reason it was decided to measure the activity only of the reduced samples.

From site directed mutagenesis studies it was demonstrated (Krell *et al.*, 2001) that K15 is an essential residue for catalysis; indeed the K15M mutant did not possess detectable activity (Krell *et al.*, 2001). The residual activity found in the protection experiments even at high concentrations of PLP could be due to the existence of a non-covalent complex enzyme-PLP that is not modified by reduction with $NaBH_4$. For glutamate dehydrogenase it has been found that modification by PLP leads to only partial loss of activity (Chen and Engel, 1974). The failure to achieve complete inactivation after prolonged incubation could be due both to the fact that the covalently modified enzyme is still active, though to a lesser extent than the native one, or that the enzyme is not all covalently modified. To check between these two possibilities studies on the K_m of the modified enzyme should be performed: if the K_m of the modified enzyme is the same as that of the unmodified one, the decrease in activity is entirely attributable to a decrease in V_{max} , that is to say the amount of the active enzyme has decreased and so the partial inactivation hypothesis is excluded. (Chen and Engel, 1974).

From a pseudo-first order analysis of the results (Fig. A3.2) it is evident that there is a deviation from linearity after the first minute. It is not possible to obtain reliable values of k_{obs} even when the fitting is restricted to the first part of the curve: in fact the values of k_{obs} do not give a linear dependence on PLP concentration. It is difficult to draw any conclusions from this non-linear behaviour, because of the numerous difficulties inherent in this kind of assay (section 2.6). Although the results are not completely satisfactory, and cannot be quantified in terms of inactivation constants they nonetheless gives some useful qualitative indications, and could be the basis for protection experiments.

These protection experiments were carried out using the different substrates (shikimate, ATP and ADP) and combination of substrates (ADP and shikimate). Because from studies of the myosin-ADP-MgF_n ternary complex it was suggested that the overall conformation of the complex was quite similar to that in the presence of ATP (Park *et al.*, 1999), a preliminary protection experiment has been attemped in the presence of ADP and NaF (the Mg^{2+} ion is present as a buffer constituent). The following experiments were used as controls for protection experiments: a) the inactivation curves obtained in the absence of ligand using PLP at 1.4mM, and b) the curve obtained in the absence of PLP (effect of the incubation at room temperature and of stirring on activity).

The presence of shikimate, either alone or with ADP, does not seem to give any protection against chemical modification (Fig. A3.3). The failure of shikimate to protect the enzyme is consistent with the fact that Lys15 is not involved in shikimate binding.

While ATP gives substantial protection, with the inactivation curve practically coincident with the SK control, ADP seems to give no protection (Fig. A3.5). The differences in the protection achieved in the presence of ADP and ATP confirm the role of K15 in the coordination of the γ-phosphate and that this kind of interaction is necessary to achieve the conformational change required for catalysis, as demonstrated by the lack of protection even in the presence of shikimate and ADP. The fact that shikimate does not give any appreciable protection against PLP inactivation in the presence of ADP could support the hypothesis that the observed synergism in Tris-HCl is an artefact due to the presence of chloride ions. Probably the presence of the γ-phosphate is a key factor in determining the conformational change in the presence of ATP *plus* shikimate.

The results, reported in Fig. A3.6, seem to indicate an increased protection by ADP in the presence of NaF. Because this experiment was performed only once it could be reproduced before making any conclusion. Moreover it would be necessary to perform a control with NaF and NaCl alone to check if the protection observed is due to an ionic strength effect.

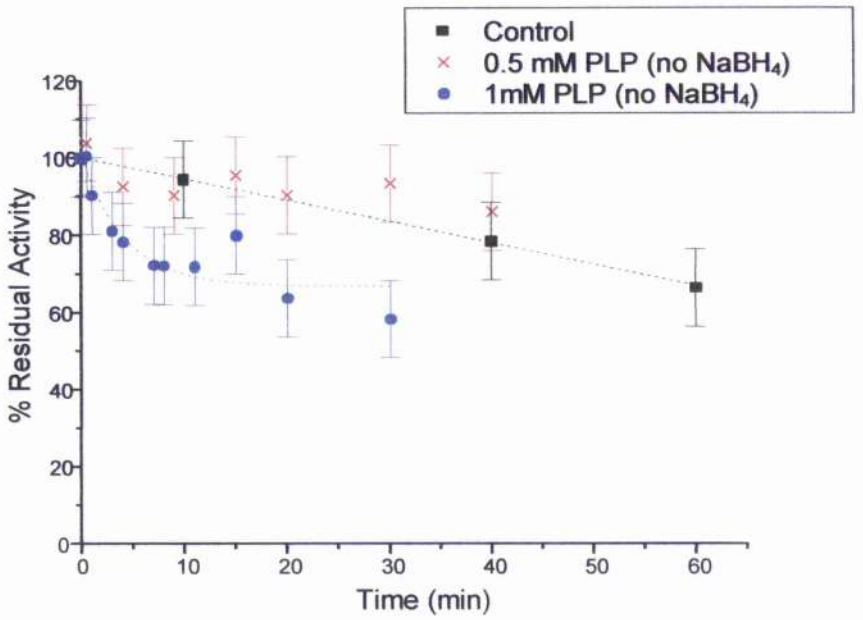

a)

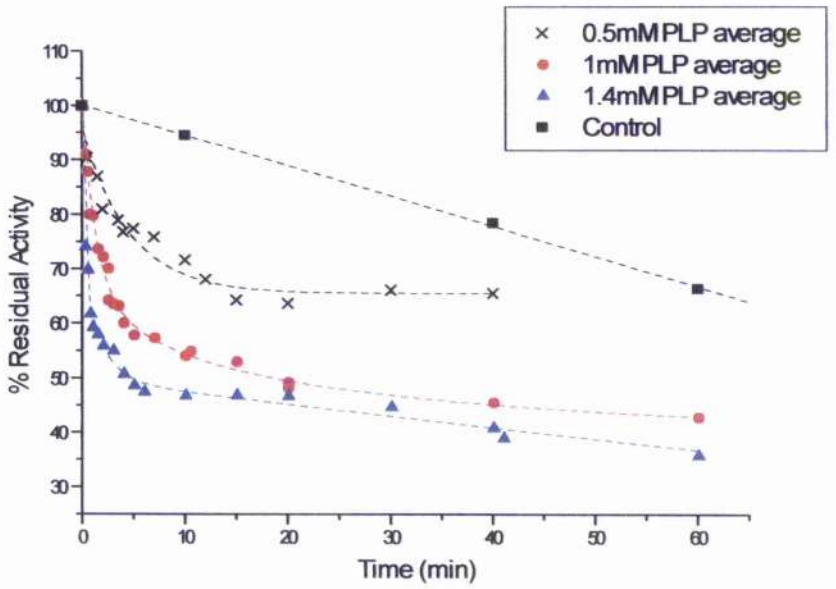

b)

Figure A3.1: Time-courses of inactivation of SK by PLP.

SK (0.046mg/ml) was incubated at room temperature (20°C) while stirring in test tubes as described in section 2.6. Reactions were carried out in assay buffer containing the stated concentrations of PLP. Zero time activity was determined by sampling prior to PLP addition. At chosen time intervals, samples (10μl) were added to 30μl of a) water (non reduced samples) or b) to a solution of 5mg/ml of $NaBH_4$ in water (reduced samples), mixed, and immediately assayed.

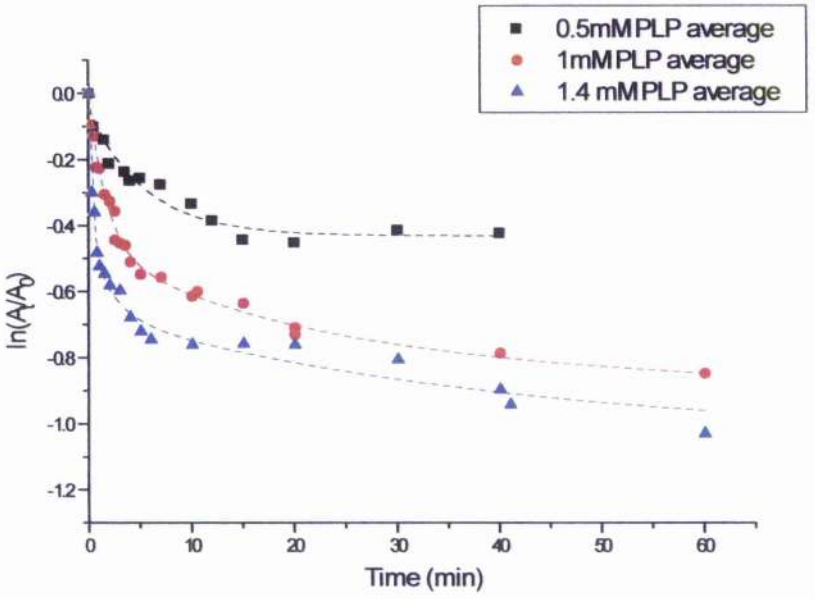

Figure A3.2: Pseudo-first-order plots of inactivation of SK at various PLP concentrations. The data were analysed as described in section 2.6.

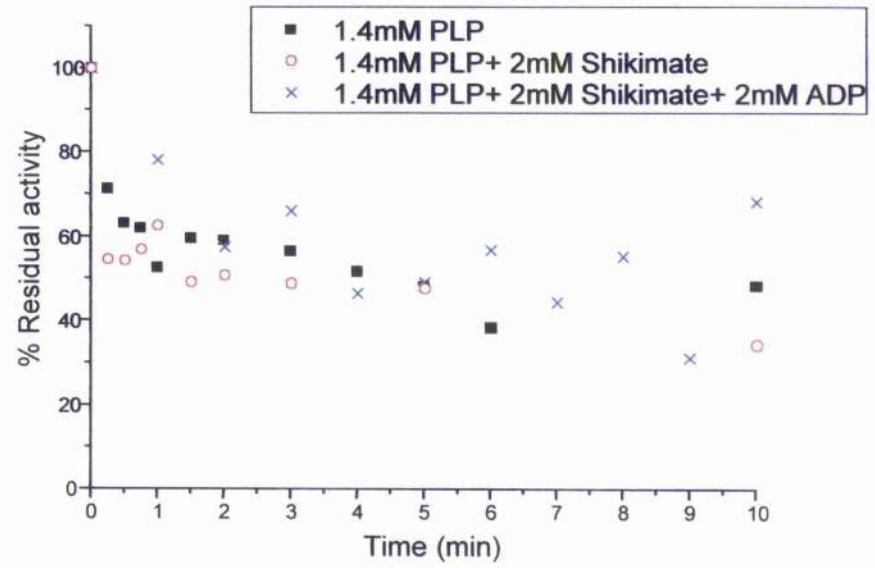

Figure A3.3: PLP inactivation:effect of shikimate, alone and with ADP.

The effect of shikimate on inactivation of SK by PLP was investigated by incubating the enzyme with PLP (1.4mM) in the absence (black) and in the presence of 2mM shikimate (red) or 2mM shikimate + 2mM ADP (blue). The zero-time activity was measured on the sample, containing the ligand, before the addition of PLP.

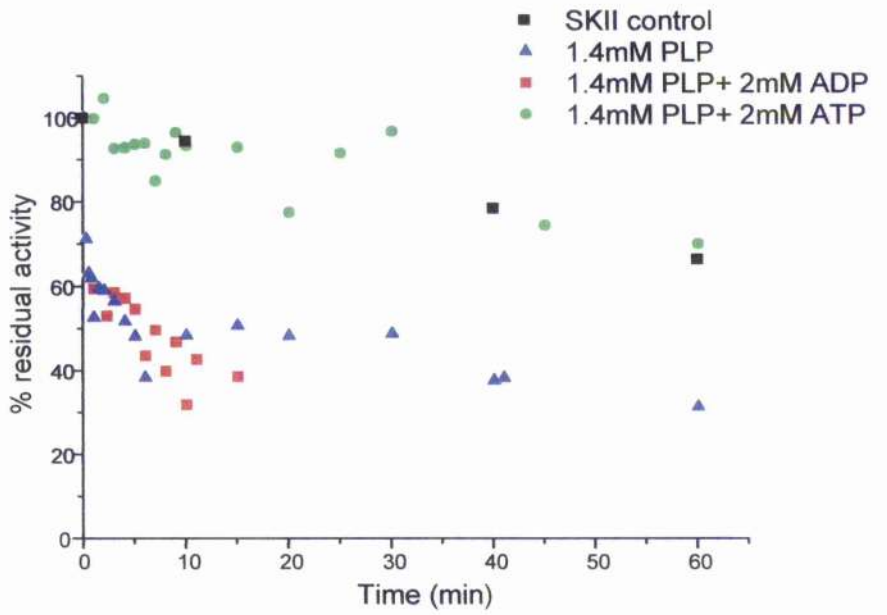

Figure A3.4: PLP inactivation: effect of nucleotide substrates.

The effect of nucleotide substrates on inactivation of SK by PLP was investigated by incubating the enzyme with PLP (1.4mM) in the absence (blue) or presence of 2mM ADP (red) and 2mM ATP (green). The inactivation due to sample stirring and incubation is reported as well (black). The zero-time activity was measured on the sample, containing the ligand, before the addition of PLP.

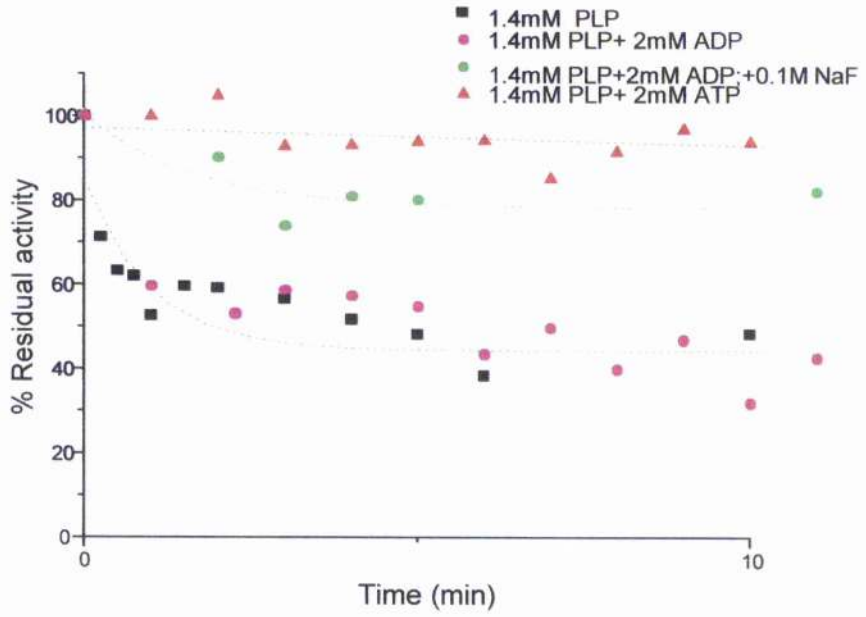

Figure A3.5: Effect of NaF and ADP on the time-course of inactivation of SK by PLP

The effect of NaF in the presence of ADP on inactivation of SK by PLP was investigated by incubating the enzyme with PLP (1.4mM) in the presence of 0.1M NaF+ 2mM ADP(green).

Chapter 4: Effects of salts on the function, conformational stability and refolding kinetics of shikimate kinase

4.1 Abstract

Comparison of the effects of urea on the enzyme with those of guanidinium chloride and NaCl indicated that both chemicals significantly weakened the binding of shikimate (section 3.3.4). To check if the observed effect was due to a general ionic strength effect or was dependent on the ionic species in solution, the effects of different salts (KCl, $CaCl_2$, $MgCl_2$, NaF, NaBr, $NaNO_3$) on the structure, activity, binding, and stability of SK have been investigated (sections 4.3 to 4.9).

The chosen salts have only small effects on the secondary structure as judged by far-UV CD. Though no effects are observed on the fluorescence spectra, NaCl and Na_2SO_4 give a tightening of the structure as shown by the effect on the near-UV CD (section 4.3).

All the salts studied have an effect on catalytic activity that seems to depend on the ionic strength and not on the particular salt used, with the exception of NaF which gives a higher degree of inactivation at lower concentration when compared with other salts (section 4.4). Moreover inclusion of salts leads to a marked stabilisation against unfolding of the enzyme by urea (section 4.8).

Differences between the salts are revealed by binding studies: by contrast with NaCl, Na_2SO_4 affects the binding of shikimate to only a small degree. Using other chloride salts and other halide salts it seems that the shikimate binding is primarily affected by the presence of chloride ions, as previously suggested by the results obtained using the chloride-free buffer MOPS (section 3.3.1.2). NaCl, Na_2SO_4 and NaF were tested for their effects on nucleotide binding, the last one chosen for its different behaviour in the activity measurements.

Both NaCl and Na_2SO_4 do not have a major effect on the binding of nucleotides leading to a decrease of the Q_{max} (limiting quenching) and an increase in the K_d. NaF, on the other side, at low concentrations (0.1M) gives a decrease of the K_d for ADP and, at higher concentrations to an increase of this parameter with no effect on the Q_{max} (section 4.6.1).

The same trend is observed for the ATP binding with fluoride again having a different effect. NaF at low concentrations determine a marked decrease of the K_d for ATP (section 4.6.2).

On the basis of their effects on the catalytic activity, binding of substrates, and conformational stability of SK, NaCl and Na_2SO_4 were selected as representative salts for a more detailed study.

When the enzyme is unfolded by incubation in 4M urea, addition of 1M NaCl or 0.33M Na_2SO_4 leads to a relatively slow refolding of the enzyme as judged by the regain of native-like CD and fluorescence (section 4.10.1). In addition the refolded enzyme can bind

shikimate weakly while no binding of nucleotide could be directly observed (sections 4.5 and 4.6). Some evidence for synergism in substrate binding has been observed that leads to the hypothesis that nucleotide binds at least to some extent. The degree of fluorescence quenching by I^- suggests that the single Trp has partially regained the positively charged environment provided by neighbouring Arg side chains in the native enzyme (section 4.10.1.4). However, the refolded enzyme does not possess detectable catalytic activity. The refolding process brought about by addition of salt in the presence of 4M urea is not associated with any change in the fluorescence of the probe ANS (section 4.10.1.3), indicating that either an intermediate formed by hydrophobic collapse is unlikely to be significantly populated or that the concentration of the chaotropic agent used for denaturation displaces the dye by sheer competition (Kumar *et al.*, 1996). The results point to both specific and general effects of salts on SK. These are discussed in the light of the structural information available on the enzyme (sections 4.10.3 and 4.10.4).

From the refolding experiments using GdmCl as denaturant (Boam, 1999 - section 3.4.1) it seems that the refolding reaction was taking place faster than when urea was used to unfold the protein. To check for an effect of the residual ionic strength on the refolding of SK different concentrations of salts were included in the refolding buffer (urea was chosen as denaturant in these experiments because of the non-ionic nature of this chemical). In general the presence of NaCl and Na_2SO_4 lead to an increase in the refolding rate, while NaF seems to impair the efficiency of refolding (Appendix 4.1).

4.2 Introduction

Salts can affect a wide range of properties of proteins, as described in section 1.1.3.2, and for this reason they are widely used both for practical applications, and for research purposes. For most proteins, solubility at first increases with ionic strength (salting in), but then decreases at high ionic strength (salting out). The first studies on the effect of ionic strength on the stability and solubility proteins were performed by Hofmeister (1888). He ranked the effectiveness of anions and cations in precipitating proteins in a series now called the Hofmeister series, in which the most stabilising ions are those that promote hydrophobic associations. In this case the folded protein is stabilised with respect to the unfolded form largely by the unfavourable free energy of transfer of the non-polar side chains from the interior of the folded protein to the surrounding water (Jelesarov *et al.*, 1998).

Salts affect the stability of proteins depending on the ways they interact with them. Their effect is defined by the balance between their preferential interactions with the native and unfolded states (Arakawa *et al.*, 1990). At high concentrations they can cause preferential hydration or preferential binding to the protein depending on the type of salt and solvent conditions (Arakawa and Timasheff, 1982) or, at low concentrations, the stabilisation could be due to a Debye-Hückel charge screening effect (Moore, 1962; Giancola *et al.*, 1997). If protein solvation is the predominant factor, the effectiveness of anions and cations in stabilizing proteins can be ranked in the Hofmeister series (von Hippel and Schleich, 1969; Goto *et al.*, 1990; Baldwin, 1996).

sulphate > phosphate > fluoride > chloride > bromide > iodide > perchlorate > thiocyanate

If discrete ion binding plays a role in the stabilization, the effect should follow the electroselectivity series of anion binding to ion-exchange resins (Washabaugh and Collins, 1986; Muzammil *et al.*, 2000). The electroselectivity series of anions towards anion exchange resins, which assumes that the net charge of anions is more important that their hydration, is as follows:

perchlorate > iodide > trichloroacetate > thiocyanate > nitrate > bromide >trifluoroacetate >chloride > acetate > fluoride

Finally, salts can weaken electrostatic interactions through Debye-Hückel screening. If this is the predominant factor for the stabilisation, this should roughly follow the ionic strength, should be observed at low concentration of salts (below 0.1M) and should be primarily associated with the cation (KCl stabilizes more than an equimolar concentration of NaCl)(Arakawa *et al.*, 1990).

The anions to the left of chloride in the Hofmeister series are called "kosmotropic" anions (water structure makers). They are small ions of high charge density that bind water molecules tightly and increase the surface tension of aqueous solutions. They are believed to stabilize the native structure of the protein molecule by causing preferential hydration of the protein, i.e. preferential exclusion of kosmotropes from the protein surface. Kosmotropes stabilise proteins and decrease their solubility (salting-out): the only change in the system during precipitation is a reduction of the protein surface exposed to the solvent due to the formation of protein-protein contacts (Timasheff and Arakawa, 1997).
The chaotropic anions (anions on the right of chloride in the Hofmeister series) are large ions of low charge density that do not bind water tightly, but rather increase the mobility of nearby water molecules. They generally destabilize the protein structure by preferentially interacting with the protein and increase their solubility (salting-in). The binding is dependent on the chemical nature of the surface of the protein in contact with the solvent and can vary strongly with the state of the system, such as pH, co-solvent concentration, and state of folding of the protein (Pace and Grimsley, 1988). The preferential binding will led to stabilization if the binding with the native state is more favourable than the binding to the unfolded state (Arakawa, 1989; Arakawa *et al.*, 1990). Hence every system needs to be studied individually in detail.

In section 1.1.3.2 the importance of the ionic strength of the solution on enzyme activity has been discussed. In the case of SK, hinge-bending motions are determinants in the enzyme activity. Since hinge-bending motions have low energy barrier height, the populations of the closed *versus* the open conformations are function of their relative stabilities. A shift in the equilibrium between the closed and open conformations may be observed in response to external factors, such as pH, temperature or ionic strength (Sinha *et al.*, 2001).

The salts can be used for studying the role that electrostatic interactions and ion binding play in the refolding of proteins, as has been discussed in section 1.1.3.2. and using different salts it can be determined which factor plays a predominant role. Some kinetic data indicate that co-solvents can influence the refolding rates by increasing the stability of the intermediates that lead to the native form. These intermediates may go undetected but can be induced to accumulate transiently at sufficiently high salt concentrations (Eder *et al.*, 1993; Ferguson *et al.*, 1999; Krantz and Sosnick, 2000). On the role of these intermediates in the refolding pathway there are contrasting opinions (Bieri *et al.*, 1999; Otzen and Oliveberg, 1999). It is still a matter of debate whether these states represent key stepping stones in the folding process, or are circumstantial pitfalls in the energy landscape. In some cases it has been demonstrated that these kinds of intermediates are off pathway: they cause a prematurely collapsed state and slow down folding by several orders of magnitude (Otzen and Oliveberg,

1999). In other cases the presence of salts has increased the rate of folding by enhancing the population of productive intermediates (Low *et al.*, 2000).

Clearly a better understanding of the ways in which salts can interact with proteins could have important applications (section 1.1.2.2) and could give valuable insights into designing experiments and to understanding phenomena such as adsorption, aggregation and stabilization which underlie many biological events (section 1.1.1.3). In this study was chosen the range of concentrations where the Hofmeister effects become important (0.1-1M): under these conditions anions play the major role (Cacace *et al.*, 1997).

4.3 Fluorescence and CD spectra: the effect of salts

4.3.1 UV and Fluorescence Spectra

Before using NaCl in the experiments described in sections 3.3.3-3.3.5 some preliminary controls were performed. In these UV, fluorescence and of CD spectra (near- and far-UV) were acquired to verify if the presence of salts had any effect on the overall enzyme conformation. The presence of NaCl in a SK solution (0.1mg/ml) increases the contribution to the light scattering at 280nm by 20.6% (calculated with the linear regression on the graph log λ vs log A) indicating an increase in the aggregation in the presence of this salt (Figure 4.1). Light scattering experiments (as described in section 2.4) in the presence of NaCl were performed during the refolding studies and as well.

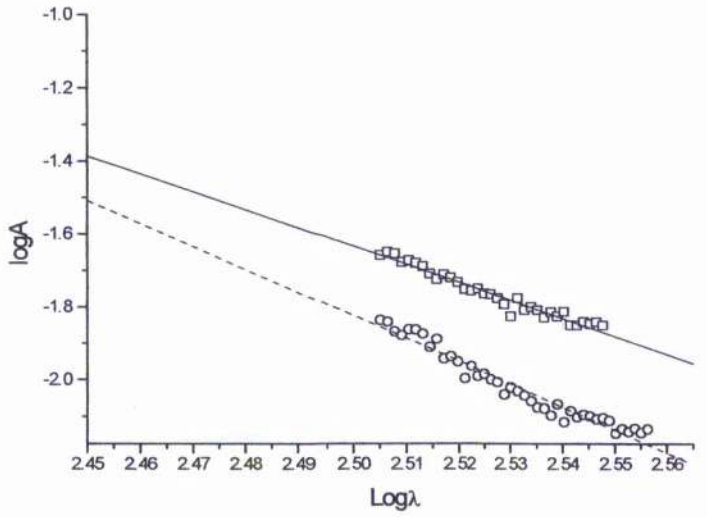

Figure 4.1: Calculation of the light scattering contribution at 280nm.

The absorption spectra of protein solutions 0.1mg/ml SK in buffer (circles) and in the presence of 1M NaCl (squares) were recorded in the range 240-400nm. The contribution of the light scattering to the absorbance at 280nm was calculated plotting the logarithm of absorbance *vs* logarithm of wavelength between 320nm and 360nm and making a linear extrapolation to the 276-282 region (Pace and Schmid, 1997).

Fluorescence spectra of protein solutions (0.15mg/ml) in the presence of NaCl were prepared by dilution from stock solutions (section 2.7) and the fluorescence spectra were recorded as described in section 2.4. The spectra were acquired immediately after preparation and after 30 minutes and 1 hour incubations at 20°C. This was done to check if the increase in aggregation observed in the presence of NaCl was accelerating the decrease of fluorescence intensity observed for SK in buffer after incubation at room temperature (section 3.3.1.3). In figure 4.2 the data are reported for NaCl: it seems that

NaCl has no effect on the time course, and the observed decrease in fluorescence seems to be due only to the incubation time.

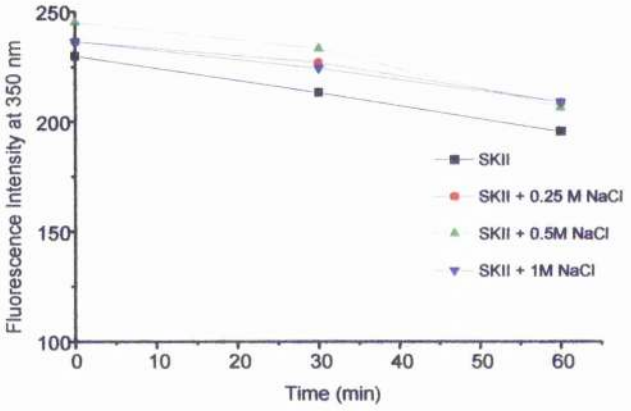

Figure 4.2: Effect of added NaCl on the decrease in fluorescence intensity at 20°C.

Fluorescence spectra were acquired after excitation at 295nm in the range 300-400nm. The protein solutions (0.15mg/ml) were incubated at room temperature (20°C) and the spectra acquired again after different incubation times. The data shows the time courses of the fluorescence intensity at 350nm: SK (black); SK + 0.25M NaCl (red); SK + 0.5M NaCl (green); SK + 1M NaCl (blue).

All the comparisons that follow are made between fluorescence spectra acquired immediately after preparation. NaCl seems to have a small effect on the intensity of the fluorescence (Figure 4.3a), and no effect on the emission maximum. A control experiment performed with the model compound NATA has demonstrated that the observed small increase was due to a non-specific effect on the Trp fluorescence (Fig. 4.3b). The fluorescence spectra in the presence of other salts were also measured. The concentrations of salts were chosen to have the same ionic strength of a 1M NaCl solution, calculated as follows:

$$\mu = \frac{1}{2} \sum_i C_i z_i^2$$

where μ is the ionic strength of the solution, C_i is the concentration of the ion, z_i is the charge of this ion, and the sum is extended to all the ions present in solution. The salts chosen were: Na_2SO_4 (0.33M and 0.17M) because sulphate is a known stabiliser; KCl (1M), $CaCl_2$ and $MgCl_2$ (0.33M) to change the cation respect to NaCl; NaF (1M) and NaBr (1M) to check the other halide salts. These salts do not give any change in the fluorescence emission maximum, indicating that the polarity of the Trp environment is unchanged (Fig. 4.4a and 4.5), and they have only a small effect on the intensity of the fluorescence spectra, with the exception of NaBr. Control experiments performed using NATA, in the presence of those salts which had a bigger effect on the SK spectra (Fig. 4.4b), demonstrated that the

effect on Trp fluorescence was due to a non-specific effect of salts, as in the case of NaCl. It should be noted that in other studies the effects of salts on NATA fluorescence were found to be opposite (a decrease in fluorescence) but in this study higher concentrations of salts were tested than those used in this study (Nishimura *et al.*, 2001).

NaBr leads to a decrease of the intrinsic Trp fluorescence both for the proteins and for NATA. An UV-spectrum of a 1M NaBr solution was acquired to assess if the observed decrease of intensity was due to inner filter effect or to the quenching of the Trp fluorescence. Because this salt absorbs around 200nm, the inner filter effect hypothesis can be excluded.

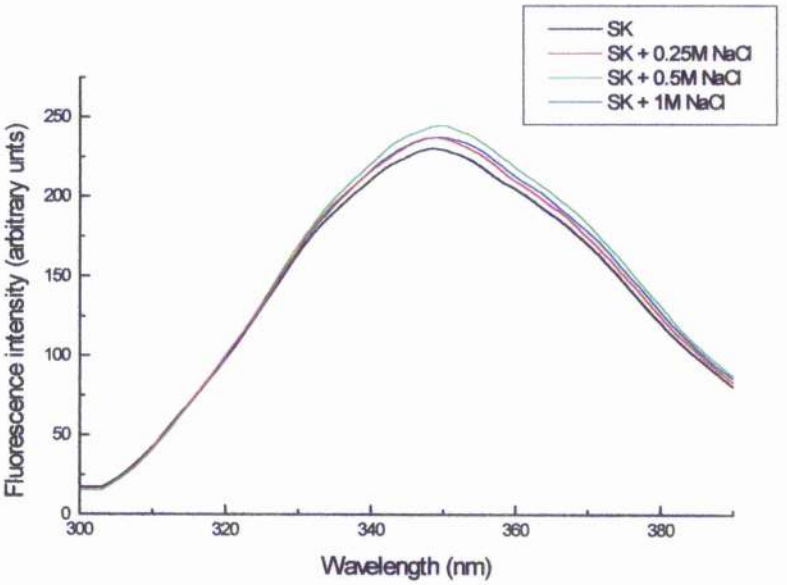

a)

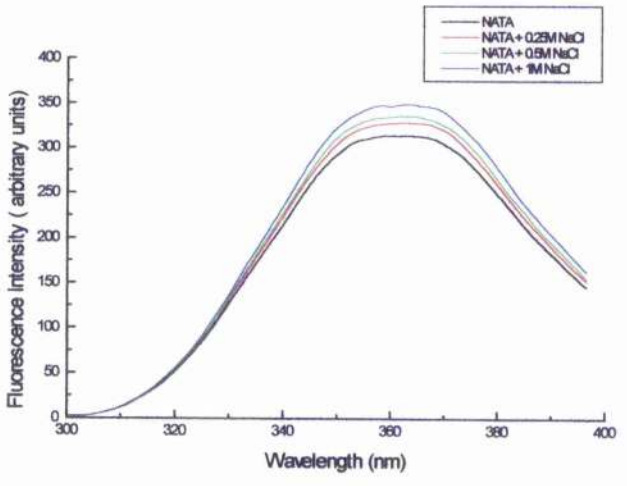

b)

Figure 4.3: Effect of NaCl on Trp fluorescence.

Fluorescence spectra were acquired in the 300-400nm range after excitation at 295nm, T= 20°C. The data shows: a) SK 0.15mg /ml in the presence of different concentrations of NaCl. b) NATA 10μM in the presence of different concentrations of NaCl.

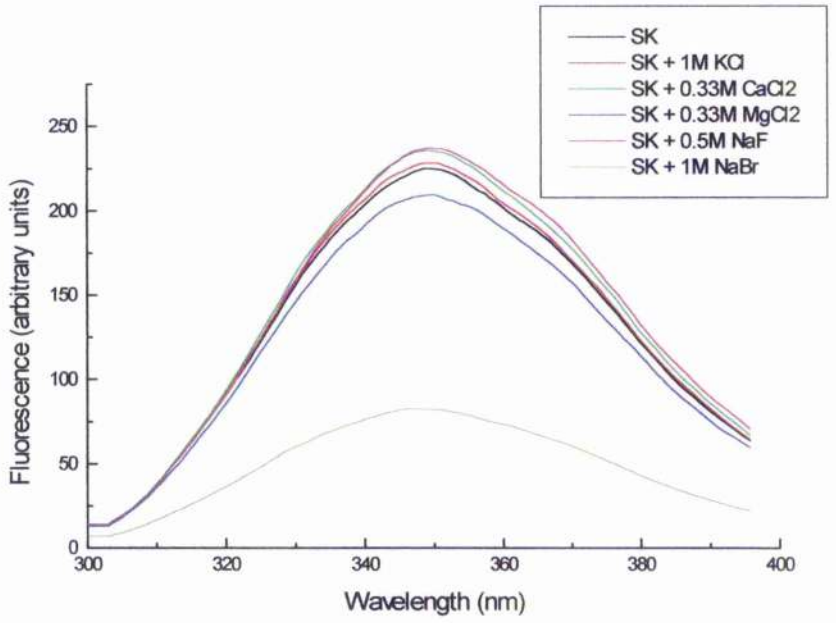

a)

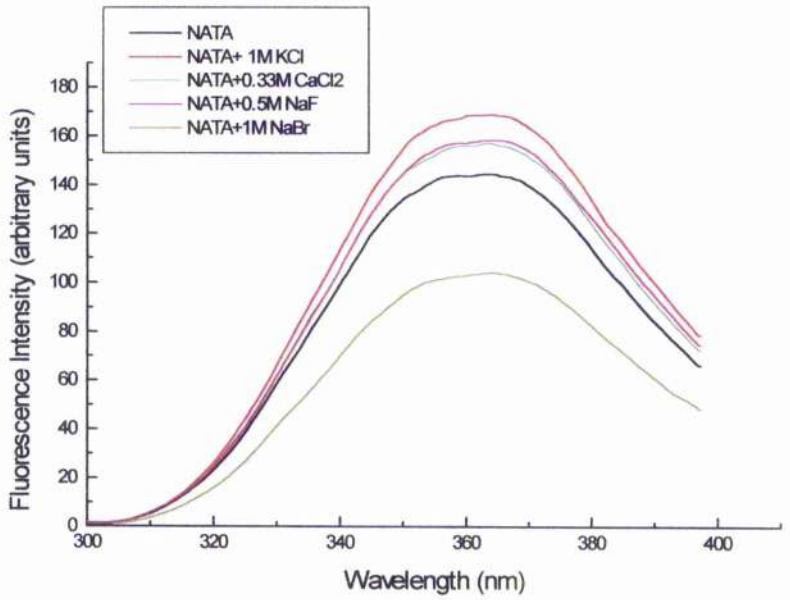

b)

Figure 4.4: Effect of KCl, $CaCl_2$, NaF and NaBr on Trp fluorescence.

Fluorescence spectra were acquired in the 300-400nm range after excitation at 295nm, T= 20°C. The data shows: a) SK 0.15mg /ml in the presence of different concentrations of salts. b) NATA 10μM in the presence of different concentrations of salts

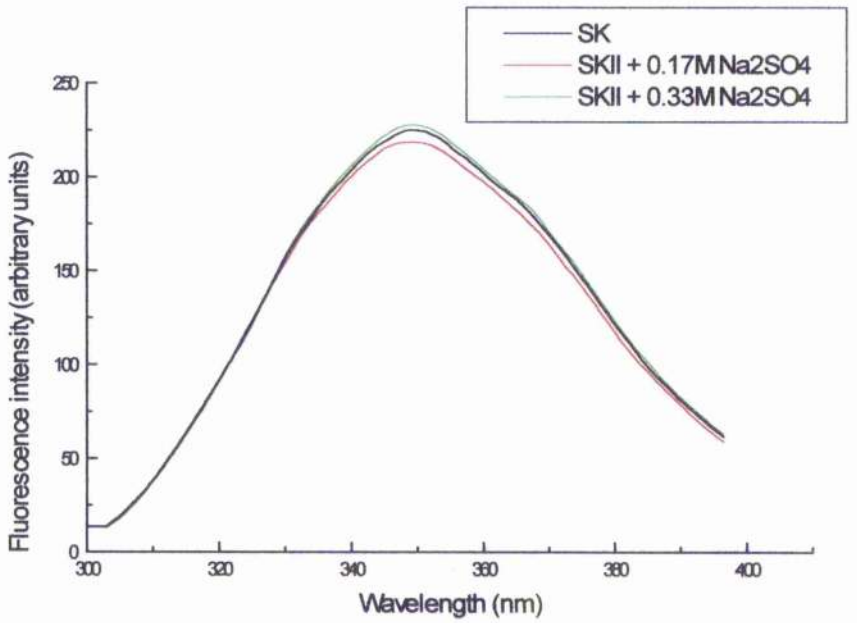

Figure 4.5: Effect of Na_2SO_4 on intrinsic Trp fluorescence.

Fluorescence spectra were acquired in the 300-400nm range after excitation at 295nm, T= 20°C. The data shows: SK 0.15mg /ml in the presence of different concentration of Na_2SO_4.

4.3.2 Circular dichroism spectra

The far-UV CD spectrum in the presence of different salts was analysed to check if the presence of salt had an effect on the secondary structure of the protein (section 1.3.1.2). The solutions were prepared at the same protein concentration (0.15mg/ml) and in the same way as the solutions for the fluorescence experiments. In Fig. 4.6 are reported the far-UV CD spectra at different NaCl concentration. At these concentrations of salt there is a slight increase in the intensity of the CD spectrum, the biggest effect being observed at 1M NaCl. The observed effect does not seem to be due to the nature of the cation, as shown by the fact that the CD spectrum in the presence of 1M KCl is very similar to that in 1M NaCl (Fig. 4.7a). NaF has the same effect, on the far-UV CD, as NaCl at a similar concentration (0.5M) (Fig. 4.7b). In general while salts as NaCl, Na_2SO_4 (Fig. 4.8) and, to a lesser extent NaF, lead to an increase of the secondary structure content of SK, salts such as $MgCl_2$ and $CaCl_2$ lead to a decrease in the CD signal in the far-UV region. It is possible that the Mg^{2+} and Ca^{2+} cations have an effect on the protein secondary structure because these two cations are known to bind to proteins (Arakawa and Timasheff, 1984) and, in this particular case, Mg^{2+} is essential for catalysis by SK.

The near-UV CD spectrum was acquired for protein solutions in the presence of 1M NaCl and 0.33M Na_2SO_4. These two salts have a limited but significant effect on the near-UV CD

spectrum with a 20-25% increase in ellipticity at 288nm (Figure 4.9). Although the strength of near-UV CD signals of proteins can arise from a number of causes (Kelly and Price, 1997), it is likely that this enhancement of the ellipticity observed for SK in the presence of these two salts reflects decreased mobility of the aromatic amino acid side chains.

This tightening of the enzyme structure probably reflects a salt-induced increase in hydrophobic interactions. A slight tightening of a protein structure may not result in any change in solvent accessibility to aromatic residues and therefore will not change the maximum fluorescence of Trp side chain. This seems to be the case of SK because, as have reported in the previous section, the presence of salts does not cause any change in the fluorescence emission maximum.

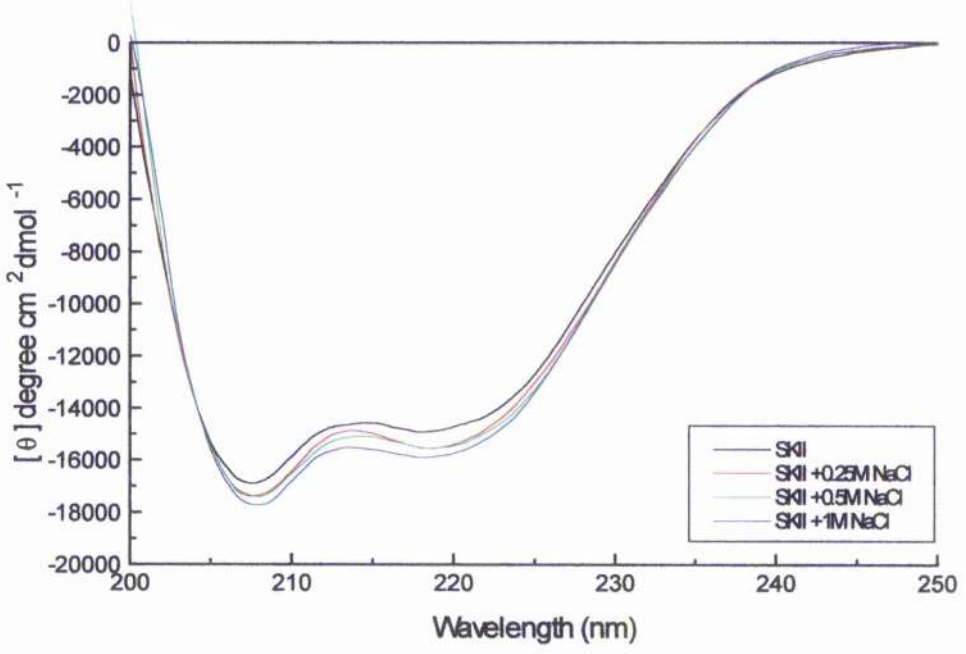

Figure 4.6: Circular dichroism spectra of SK in the presence of NaCl.

Far-UV CD spectra were recorded at 20°C using samples dissolved in buffer D (35mM Tris-HCl, pH 7.6, containing 5mM KCl, 2.5mM $MgCl_2$ and 0.4mM dithiothreitol), protein concentration 0.15mg/ml and cell pathlength 0.05cm. The data shows the spectra of SK in buffer (black), and in the presence of 0.25M NaCl (red), 0.5M NaCl (green) and 1M NaCl (blue).

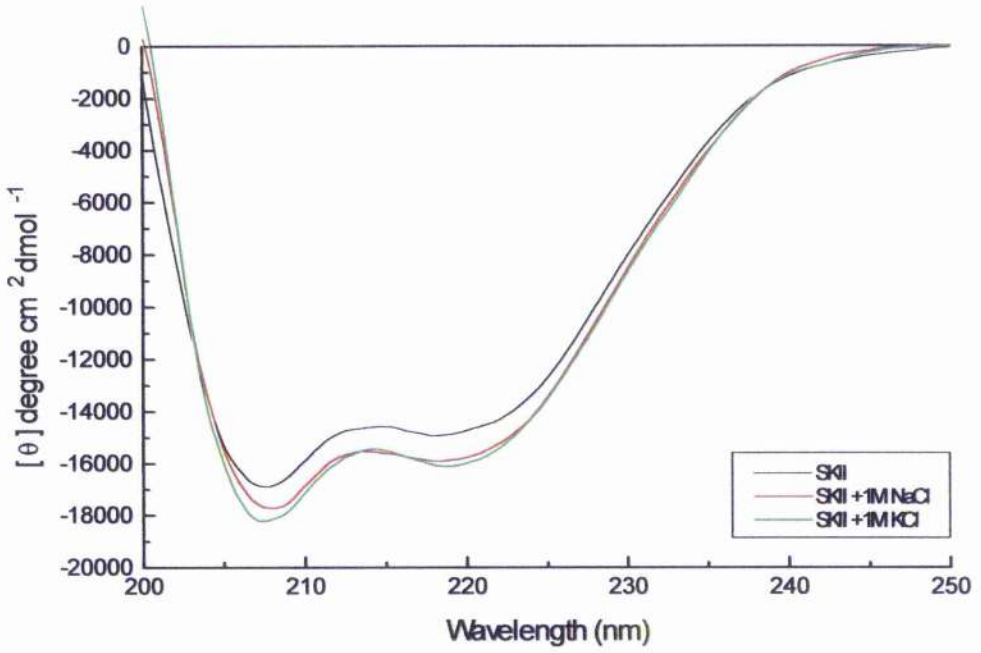

a)

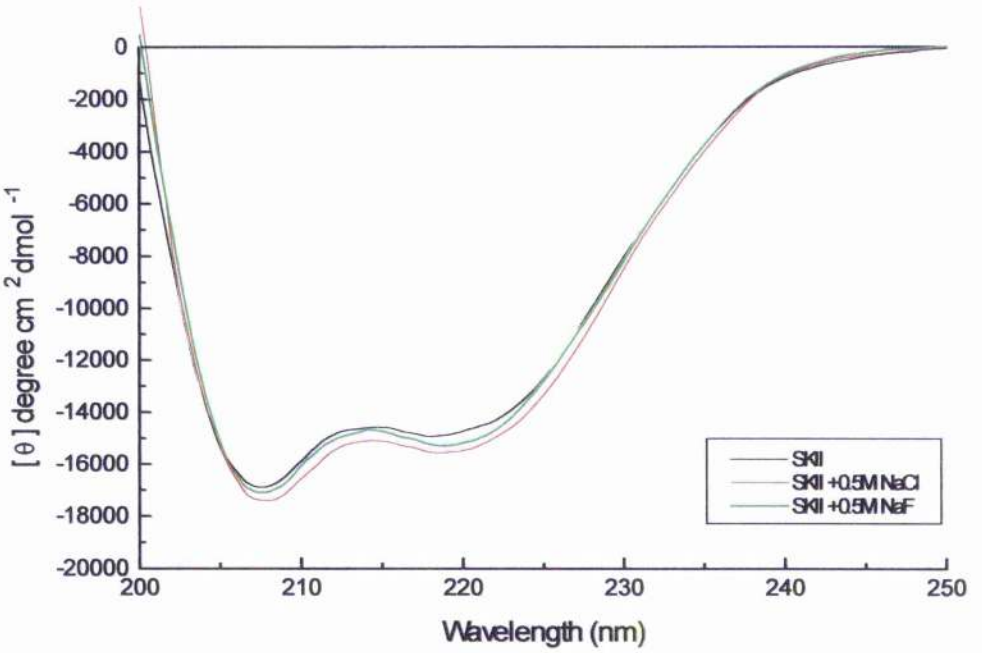

b)

Figure 4.7: Circular dichroism spectra of SK in the presence of NaCl , KCl and NaF.

Far-UV CD spectra were recorded at 20°C using samples dissolved in buffer D (35mM Tris-HCl, pH 7.6, containing 5mM KCl, 2.5mM $MgCl_2$ and 0.4mM dithiothreitol), protein concentration 0.15mg/ml and cell pathlength 0.05cm. The data shows:

a) SK in buffer (black), in the presence of 1M NaCl (red) and 1M KCl (green).
b) SK in buffer (black), in the presence of 0.5M NaCl (red) and 0.5M NaF (green).

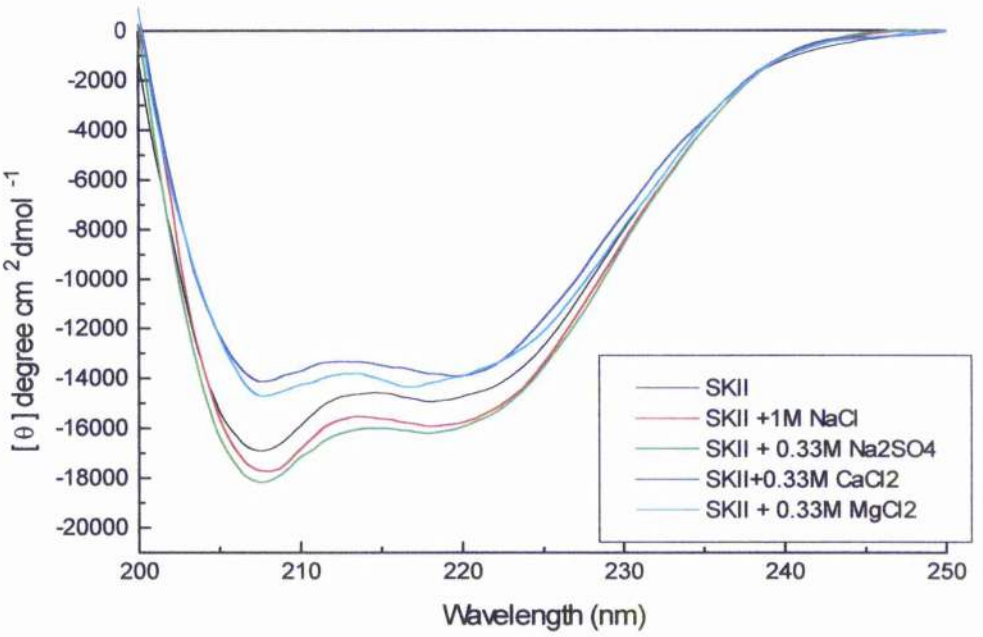

Figure 4.8: Effects of other salts on the CD spectra of shikimate kinase.

Far-UV CD spectra were recorded at 20°C using samples dissolved in buffer D (35mM Tris-HCl, pH 7.6, containing 5mM KCl, 2.5mM $MgCl_2$ and 0.4mM dithiothreitol), protein concentration 0.15mg/ml and cell pathlength 0.05cm. The data shows: SK in buffer (balck) and in the presence of 1M NaCl (red), 0.33M Na_2SO_4 (green), 0.33M $CaCl_2$ (blue) and 0.33M $MgCl_2$ (cyan).

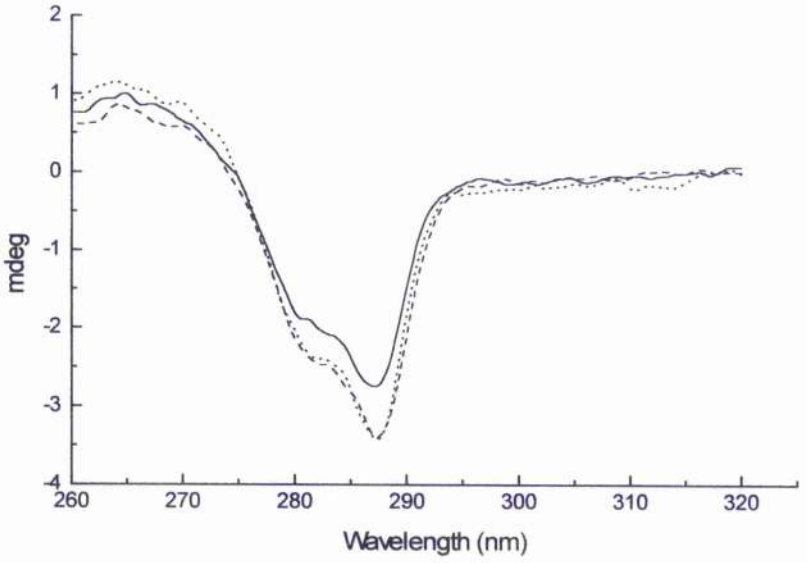

Figure 4.9: Near-UV CD spectra of SK in the presence of 1M NaCl and 0.33M Na_2SO_4 .

Near-UV spectra were recorded at a protein concentration of 0.5mg/ml in buffer D in a cell of pathlength 0.5cm. The solid, dashed and dotted lines refer to enzyme in the absence of salts, in the presence of 1M NaCl and in the presence of 0.33M Na_2SO_4 respectively.

4.4 Effect of salts on the activity and the kinetic parameters

As previously reported, incubation of SK with urea leads to a loss of activity, with 85% and 40% activity retained in the presence of 1M and 2M urea respectively. The incubation of SK with low concentrations of GdmCl leads to more marked losses of activity; thus in the presence of 0.5M and 1M GdmCl 75% and 95% activity is lost respectively. A significant part of the effect of GdmCl appears to be due to the ionic strength of the solution, since incubation in the presence of 0.5M and 1M NaCl leads to losses of 45% and 65% activity respectively (section 3.3.5).

The quenched assay procedure (section 2.2) was used to assess the effects of a number of salts (NaCl, KCl, NaBr, $NaNO_3$, $MgCl_2$, $MgSO_4$ and Na_2SO_4) on the activity of SK.
Controls were performed to check the feasibility of this assay in order to check that the salts (even after dilution into the "capture system") had no significant effect on the efficiency of the coupling enzymes (pyruvate kinase and lactate dehydrogenase): known concentrations of ADP were added to the capture system and the rapid decrease in the concentration of NADH was found to correspond to the concentration of ADP added, confirming that the quenched assay method was valid. The obtained theoretical and experimental values are reported in table 4.1. From these data it seems that calcium ions and nitrate ions have an effect on the coupling enzymes, this effect being more pronounced for the former kind of ions. Because calcium ions are reported as inhibitors of pyruvate kinase, one of the coupling enzymes used in the SK assay (Mildvan and Cohn, 1965; Betts and Evans, 1968), it was not possible to further study the effects of calcium ions on the SK activity.
The results (shown in Table 4.2) indicate that for these salts the activity declines in a manner that is approximately related to the ionic strength of the solution (Fig. 4.10).
The exceptions are NaF and $NaNO_3$; however for $NaNO_3$ the effect on the coupling enzymes has to be taken into account (Table 4.1). From the data of Table 4.1 and 4.2 it seems that $NaNO_3$ has an effect on both SK and the coupling enzymes, giving 78% of residual activity in the control experiment but 5% of residual activity under the same conditions in the assay.
NaF has the biggest effect on the enzyme activity, and no effect on the coupling enzymes. Fluoride is a known inhibitor of some proteins, among them enolase (Nowak and Maurer, 1981; Bunick and Kashket, 1982; Lebioda *et al.*, 1993), urease (Todd and Hausinger, 2000) and the ATPase activity and transport. In this last case, usually fluoride ion has been reported to be an inhibitor of proteins like myosin (Maruta *et al.* 1993; Park *et al.*, 1999) and G-proteins (Bigay *et al.*, 1987) in the presence of traces of AlF_3 or BF_3. There is evidence that fluoride ion can form a ternary complex with Mg^{2+} and ADP in the absence of Al^{3+} that mimics the transition state of the ATPase reaction (Antonny *et al.*, 1990; 1993; Maruta *et al.*, 2000). In the case of shikimate kinase the inhibition is observed at higher concentrations of

NaF than those reported in the above mentioned studies so, if binding exists, it is very weak. It has to be pointed out that the protection experiments performed on the PLP inactivation of SK (appendix 3.2) lead to the suggestion that fluoride ions have some effect on SK but this should be further investigated before drawing any firm conclusions.

NaCl and Na_2SO_4 were selected as representative salts for more detailed study on the effect on the kinetic parameters. Using the continuous (double-coupled assay) the effects of NaCl and Na_2SO_4 on the kinetic parameters of SK were determined with the results shown in Table 4.3. Although the results show that salts have multiple effects on the kinetic parameters, some trends emerge. The inclusion of 0.5M NaCl leads to an approximately 2-fold increase in the apparent K_m values for both substrates; in addition there is a decrease of about 40% in the value of V_{max}. The inclusion of 0.17M Na_2SO_4 (which has the same ionic strength as 0.5M NaCl) causes a substantial (8-fold) increase in the apparent K_m for ATP and a small (1.3-fold) increase in the apparent K_m for shikimate. These changes are accompanied by a 50-60% decrease in V_{max}. The effect of salts on enzyme activity can be due to different factors: the salts can bind to particular sites on the protein, they can increase the hydration of protein surface, or salts can increase the hydrophobic interaction giving an increase in the rigidity of the enzyme with the elimination of the dynamic motion that is required for efficient catalysis.

In order to gain further insights into the origins of the changes in kinetic parameters, the effects of salts, in particular NaCl and Na_2SO_4 on the binding of substrates have been explored.

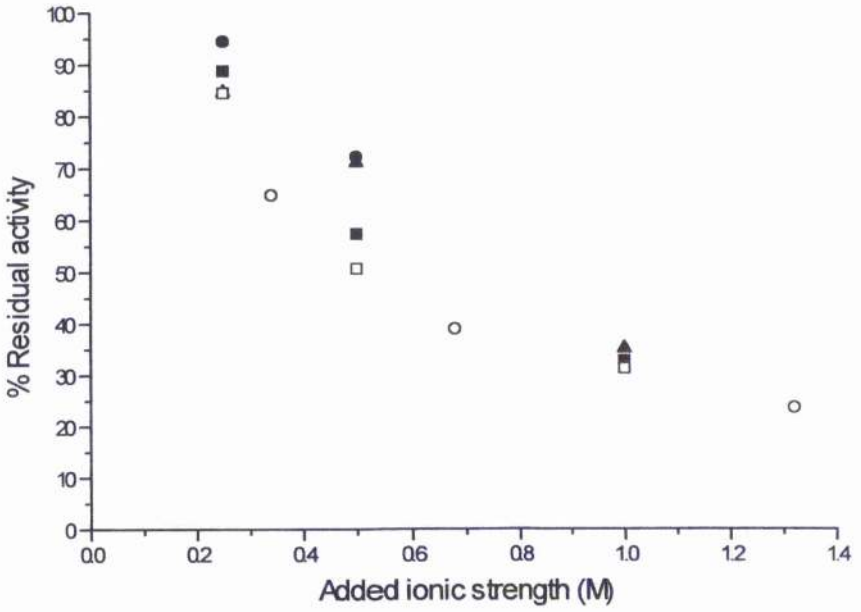

Figure 4.10: Effects of salts on the activity of shikimate kinase.

Quenched assay procedure.The reaction was carried out as described in section 2.2. The data are shown in terms of the added ionic strength for NaCl (filled squares), KCl (filled circles), $MgCl_2$ (filled triangles), Na_2SO_4 (open squares) and $MgSO_4$ (open circles).

Conditions in SK assay	**Conditions in assay after quenching**	**[ADP] (μM) Theoretical**	**[ADP] (μM) Experimental**
0.33M Na_2SO_4	0.016M Na_2SO_4	30.7	33.1
0.5M NaF	0.024M NaF	30.7	31.7
1M NaBr	0.048M NaBr	30.7	31.8
0.33M $MgCl_2$	0.016M $MgCl_2$	30.7	31.7
0.33M $CaCl_2$	0.016M $CaCl_2$	30.7	0
0.33M $Ca(NO_3)_2$	0.016M $Ca(NO_3)_2$	30.7	0
1M $NaNO_3$	0.048M $NaNO_3$	30.7	24.08
4M Urea	0.2M Urea	58.6	56.2
4M Urea + 1M NaCl	0.2M Urea + 0.048M NaCl	29.2	29.2

Table 4.1: Controls of the quenched assay procedure

The concentration of an ADP stock solution was determined as described in section 2.3 This stock solution was diluted in the appropriate conditions in an "incubation solution" and then assayed as described in section 2.2.

Salt added	[Salt] (M)	% Activity
NaCl	0.1M	94.2
	0.25M	88.8
	0.5M	57.4
	1M	32.8
Na_2SO_4	0.085M	84.5
	0.17M	50.7
	0.33M	31.3
NaF	0.1M	82.8
	0.25M	6.1
	0.5M	0
NaBr	0.1M	116.1
	0.25M	85.6
	0.5M	71.5
	1M	14.74
NaI	0.1M	85.3
	0.25M	61.5
	0.5M	6.1
KCl	0.1M	94.5
	0.25M	94.5
	0.5M	72.2
$MgCl_2$	0.085M	84.7
	0.17M	71.1
	0.33M	35.1
$MgSO_4$	0.085M	64.9
	0.17M	39.0
	0.33M	23.7
$NaNO_3$	0.1M	100.9
	0.25M	61.0
	0.5M	35.1
	1M	4.8

Table 4.2: Effects of salts on the activity of shikimate kinase

The activities were determined using the quenched assay method as described in the text. The values are referred to the activity in buffer D as 100%.

Solution	K_m (ATP) (mM)	V_{max} (ATP) (μmol/min/mg)	K_m (shikimate) (mM)	V_{max} (shikimate) (μmol/min/mg)
SK	0.27 ± 0.02	348 ± 10	0.13 ± 0.02	301 ± 11
SK + 0.25M NaCl	0.59 ± 0.07	367 ± 15	0.20 ± 0.01	220 ± 4
SK + 0.5M NaCl	0.67 ± 0.11	211 ± 13	0.25 ± 0.04	175 ± 6
SK + 0.083M Na_2SO_4	1.95 ± 0.27	262 ± 15	0.11 ± 0.02	198 ± 7
SK + 0.17M Na_2SO_4	2.13 ± 0.52	177 ± 18	0.18 ± 0.04	124 ± 6

Table 4.3: Effects of salts on the kinetic parameters of SK

The kinetic parameters were determined by using the double-coupled assay as described in section 2.2.

4.5 Effects of salts on binding of shikimate

Addition of low concentrations (up to 1M) of GdmCl to the enzyme-shikimate complex led to an increase in fluorescence indicating that binding of the substrate had been weakened causing a relief of substrate-induced quenching (section 3.3.3). The weakening of shikimate binding (as demonstrated by an increase in protein fluorescence) was also observed in the presence of NaCl at concentrations up to 1M, indicating that the decrease in affinity for the substrate largely arose from the effect of increased ionic strength (section 3.3.4). To check the effect of salts on shikimate binding two different kinds of experiments have been performed as described in section 2.3: in one set of experiments a protein solution containing stated concentration of salts was titrated with shikimate, while in another set of experiments a solution of protein and substrate (2mM shikimate) was titrated with a stock solution of salt.

By performing titrations of the enzyme with shikimate in the presence of various concentrations of salts, it has been possible to demonstrate that all the salts tested have an effect on shikimate binding leading to an increase of the K_d. At comparable ionic strengths, chloride ions have a much greater effect on the stability of the enzyme-substrate complex than the other anions tested (Table 4.4). This effect is markedly concentration-dependent for chloride ions and does not depend on the cation as demonstrated by the values obtained for 0.33M $CaCl_2$ and 0.33M $MgCl_2$ (0.66M chloride concentration) being similar to the NaCl solution closest in chloride ion concentration (0.5M). Fluoride ions (0.5M) seem to have no major effect on the shikimate binding.

The second set of titrations was performed by titrating a solution of SK and shikimate with stock solutions of salts prepared as described in section 2.7. The interesting feature of these kinds of experiments is that it is possible to examine the effects on the binding of shikimate at low concentrations of salts. Table 4.5 reports the values of the K_d calculated when plotting the titration curves as a function of the anion concentration. NaCl and $CaCl_2$ give very similar values of K_i, while KCl gives a slightly higher value though the titration curve seems to be similar to the one obtained with NaCl (Fig. 4.11). Because also KCl has a different effect on the activity, it is not possible to say, with the available data, if the observed difference is due to an artefact in the fitting process or to a real effect. NaF does not have any effect on shikimate binding, results that confirm the previous results obtained with the shikimate titration. In the case of NaCl the effects on the K_d (Table 4.4) indicated that the salt competed with the shikimate, with a K_i value estimated as 0.12M (Table 4.5).

These results point to the possibility that there is a specific effect of the chloride ion on the shikimate-binding site of SK. As previously reported (section 3.3.1.2) the binding of shikimate, in Tris-HCl buffer, is strengthened in the presence of ADP, indicating that a degree of synergism occurs in substrate binding. This synergism is also observed in the

presence of NaCl or Na_2SO_4, that were chosen as representative salts, but is considerably more pronounced in the former case (Table 4.6 and Fig. 4.12).

Solution	Q_{max}	K_d (mM)
SKII (TRIS)	0.89 ± 0.008	0.60 ± 0.017
+ 0.25M NaCl	0.84 ± 0.015	2.12 ± 0.075
+ 0.5M NaCl	0.79 ± 0.025	2.81 ± 0.172
+ 1M NaCl	0.88 ± 0.036	4.73 ± 0.30
+ 0.085M Na_2SO_4	0.88 ± 0.018	1.07 ± 0.05
+ 0.17M Na_2SO_4	0.87 ± 0.016	1.36 ± 0.053
+ 0.33M Na_2SO_4	0.89 ± 0.014	1.39 ± 0.046
+ 0.5M NaF	0.99 ± 0.03	1.08 ± 0.07
+ 0.33M $MgCl_2$	0.77 ± 0.045	2.8 ± 0.263
+ 0.33M $CaCl_2$	0.67 ± 0.046	1.96 ± 0.24

Table 4.4: Binding of shikimate in the presence of different salts.

The titration was performed as described in section 2.3 The protein concentration used was in the range 0.04-0.06mg/ml, the volume of the SK solution was 1ml. The results were expressed as K_d (dissociation constant) and Q_{max} (limiting quenching of fluorescence).

Salt	Q_{max}	K_i (mM)
NaCl	0.80 ± 0.032	0.12 ± 0.016
KCl	0.95 ± 0.044	0.24 ± 0.025
$CaCl_2$	0.97 ± 0.038	0.11 ± 0.014
Na_2SO_4	0.41 ± 0.057	0.096 ± 0.035

Table 4.5: Titration with salts in the presence of shikimate.

Aliquots of salts stock solution were added (11x10µl) and the fluorescence intensity at 350nm was recorded (excitation wavelength 295nm; T= 20°C). The protein concentration used was in the range 0.04-0.06mg/ml; the volume of the SK solution was 1ml, the shikimate concentration 2mM. The results were expressed as K_i and Q_{max}.

Solution	K_d (mM)	K_d (mM) (+ 2mM ADP)
SKII (Tris)	0.60 ± 0.02	0.38 ± 0.02
SKII + 1M NaCl	4.73 ± 0.30	1.74 ± 0.07
SKII + 0.33M Na_2SO_4	1.39 ± 0.05	1.25 ± 0.06

Table 4.6: Binding of shikimate in the absence and presence of ADP.
The titrations were performed as described in section 2.3 in buffer Tris-HCl and and in buffer Tris-HCl containing 2mM ADP.

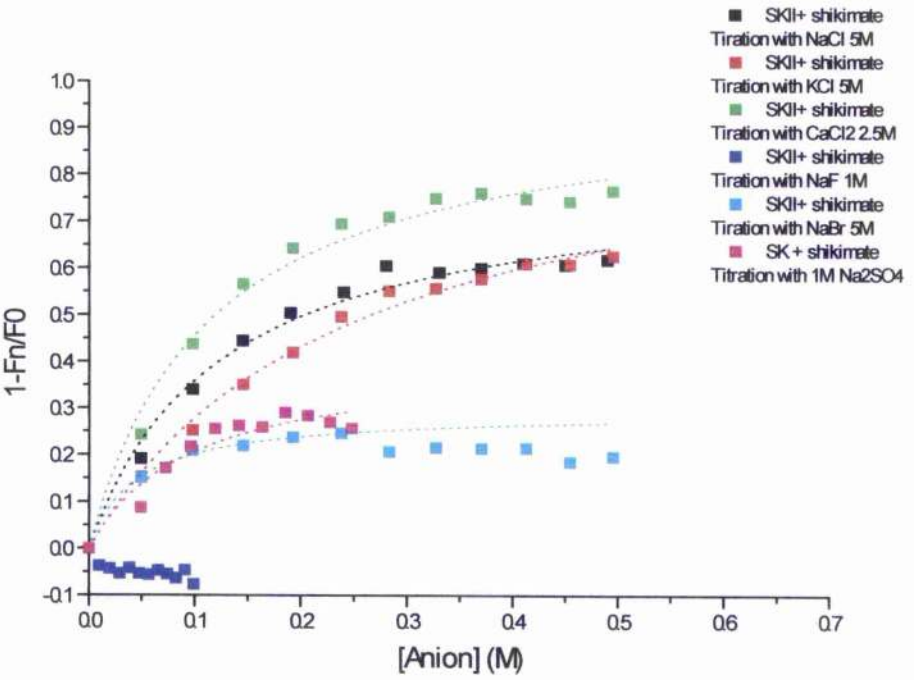

Figure 4.11: Titration with salts: effect on the shikimate binding.

A protein solution (0.04-0.06mg/ml) in the presence of shikimate (2mM) was titrated with stock solutions of salts and the fluorescence change recorded. The data were fitted by hyperbolic function to give an estimation of the K_i as reported in Table 4.5.

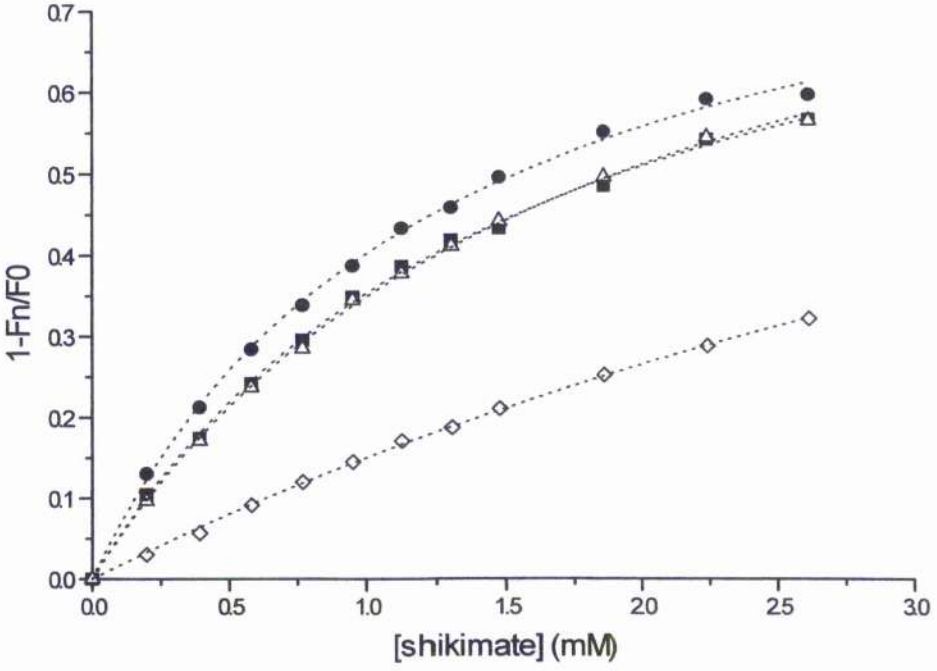

Figure 4.12: Binding of shikimate in the presence of salts; effect of the presence of ADP.

The titration was performed as described in section 2.3. The protein concentration used was in the range 0.04-0.06mg/ml, the ADP concentration was 2mM; the volume of the SK solution was 1ml. The data were analysed by fitting to a hyperbolic curve to give the values of K_d reported in Table 4.6. The data show the shikimate titration curves in the presence of shikimate and respectively:1M NaCl (open diamonds), 1M NaCl+2mM ADP (open triangles), 0.33M Na_2SO_4 (squares), 0.33M Na_2SO_4+2mM ADP (circles).

4.6 Effects of salts on the binding of nucleotides

NaCl, Na_2SO_4 and NaF were chosen to study the effects of salts on the binding of nucleotides because of their different effects on activity and shikimate binding.

The fluorescence quenching curves were corrected for the inner filter effect as described in section 2.3 (for each condition a corresponding titration was performed in duplicate with NATA). In some cases the low value of Q_{max} made detailed analysis of the data difficult.

4.6.1 ADP binding

The binding of ADP was tightened to a moderate extent in the presence of NaCl and Na_2SO_4 (Fig. 4.13a, b and Table 4.7). The effect, in general, does not seems to be salt concentration-dependent: from data obtained at lower concentrations of these salts it was not possible to discern any obvious trend in terms of the effect of ionic strength on binding of ADP. NaF, at low concentrations (0.1M), gives an increase in the Q_{max} and a decrease of K_d though to a smaller extent when compared with the other two salts tested. Moreover it leads to an increase of K_d at higher concentrations with no effect on the Q_{max} (Fig. 4.13c).

Solution	Q_{max}	K_d (mM)
SKII (TRIS)	0.6 ± 0.017	1.71 ± 0.1
+ 0.25M NaCl	0.38 ± 0.013	0.92 ± 0.08
+ 0.5 M NaCl	0.38 ± 0.011	0.97 ± 0.07
+ 1 M NaCl	0.35 ± 0.014	1.07 ± 0.10
+ 0.085M Na_2SO_4	0.37 ± 0.013	0.96 ± 0.09
+ 0.17 M Na_2SO_4	0.39 ± 0.02	1.75 ± 0.18
+ 0.33 M Na_2SO_4	0.38 ± 0.021	0.78 ± 0.11
+ 0.1 M NaF	0.69 ± 0.024	1.38 ± 0.10
+ 0.25 M NaF	0.62 ± 0.020	1.94 ± 0.12
+ 0.5 M NaF	0.63 ± 0.045	2.49 ± 0.31

Table 4.7: ADP binding
Aliquots of ADP stock solution were added (10x10µl of the 10mM stock solution followed by 5x10µl of the 50mM stock solution) and the fluorescence intensity at 350nm was recorded (excitation wavelength 295nm - T= 20°C). The protein concentration used was in the range 0.04-0.06mg/ml, the volume of the SK solution was 1ml. The data were analysed by fitting to a hyperbolic curve to give the values of K_d (dissociation constant) and Q_{max} (limiting quenching of fluorescence).

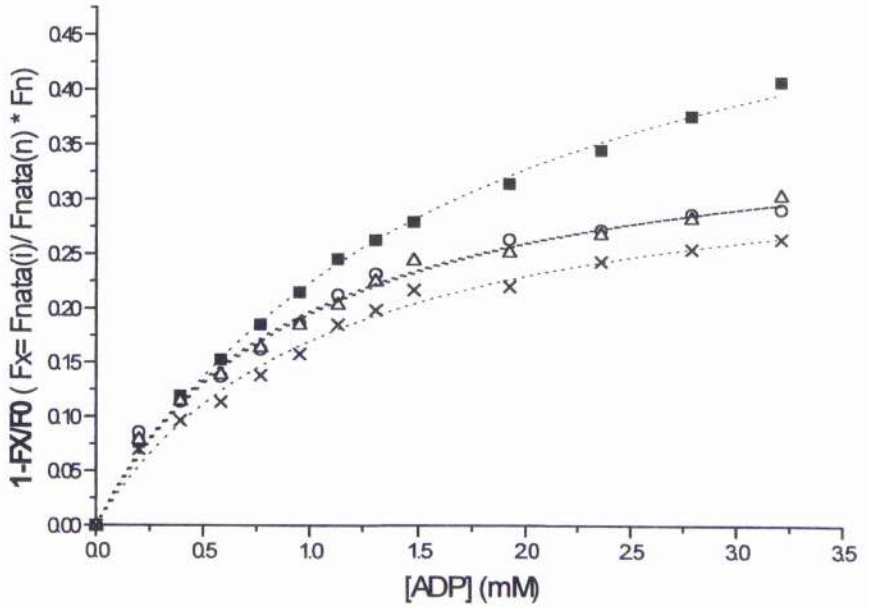
1-FX/F0 (Fx= Fnata(i)/ Fnata(n) * Fn)
0.00
0.05
0.10
0.15
0.20
0.25
0.30
0.35
0.40
0.45
0.0
0.5
1.0
1.5
2.0
2.5
3.0
3.5
[ADP] (mM)

a)

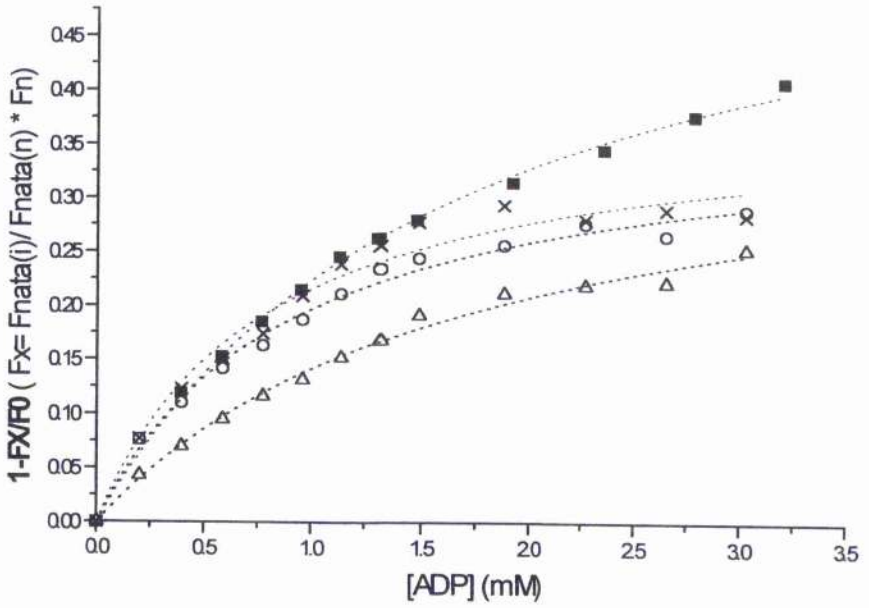
1-FX/F0 (Fx= Fnata(i)/ Fnata(n) * Fn)
0.00
0.05
0.10
0.15
0.20
0.25
0.30
0.35
0.40
0.45
0.0
0.5
1.0
1.5
2.0
2.5
3.0
3.5
[ADP] (mM)

b)

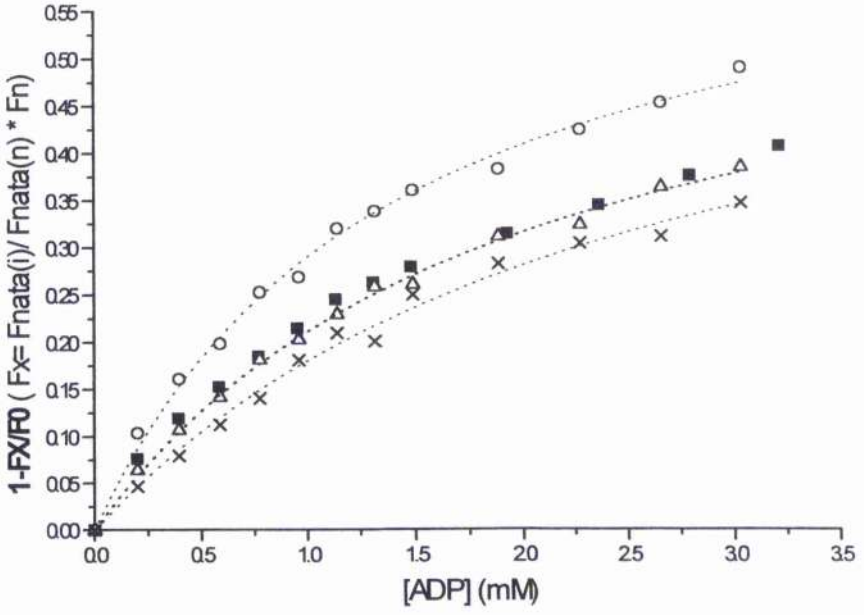

c)

Figure 4.13: ADP binding in the presence of salts
The titrations were performed as described previously and in section 2.3.
a) Squares: SK; open circles: 0.25M NaCl; open triangles: 0.5M NaCl; crosses: 1M NaCl
b) Squares: SK; open circles: 0.085M Na_2SO_4; open triangles: 0.17M Na_2SO_4; crosses: 0.33M Na_2SO_4
c) Squares: SK; open circles: 0.1M NaF; open triangles: 0.25M NaF; crosses: 0.5M NaF

4.6.2 ATP binding and comparison with ADP titration curves

As reported previously (Krell *et al.*, 2001), when the ATP binding constant was measured by fluorescence quenching, ATP was found to bind rather weakly to the enzyme with a K_d (2.6 mM) some 10-fold higher than the apparent K_m for this substrate. Changing the buffer Tris-HCl to MOPS has an effect only on the binding of ATP while no effect was detected for ADP binding (section 3.3.1.2). The titration curves obtained for ATP in Tris-HCl and MOPS are reported in figure 4.14. Though the given values of K_d reported in Table 3.1 are obtained with a hyperbolic fitting, it seems that the best fitting is obtained with the Hill equation ($y= A^* X^h/ K+X^h$) (Fig. 4.14). This had been noted previously (Boam, 1999) but the origins of this behaviour remain unclear. ATP titrations were performed in the presence of NaCl, Na_2SO_4 and NaF as for ADP. The binding parameters were determined by monitoring the quenching of protein fluorescence as described for ADP and in section 2.3. The presence of salts "removes" the sigmoidal trend and the best fitting is obtained with a hyperbolic function. Moreover the presence of salts leads to a modest increase in the affinity for this substrate, with the K_d values reduced by approximately 2-fold (Fig. 4.15 a, b, c and table 4.8), with NaF

having the biggest effect (Fig. 4.15 c), though at a lower concentration when compared with other salts.

Solution	K_d (mM)
SK (Tris-HCl)	2.58 ± 0.51*
SK + 0.25M NaCl	1.19 ± 0.11
SK + 0.5M NaCl	1.02 ± 0.06
SK + 0.085M Na_2SO_4	1.14 ± 0.08
SK + 0.17M Na_2SO_4	1.38 ± 0.12
SK +0.1M NaF	0.98 ± 0.08

Table 4.8: ATP binding in the presence of salts.

*Value obtained by fitting to a hyperbolic function.The titration was performed as described in section 2.3

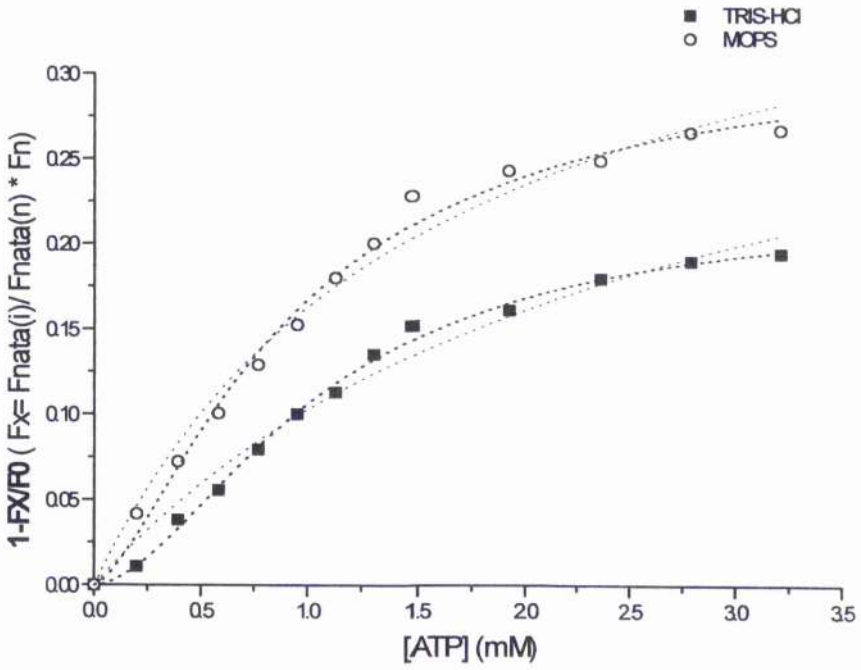

Figure 4.14: Titration curves for ATP obtained in buffers Tris and MOPS.

Red fitting: hyperbolic function fitting (data: table 3.1); Black fitting: Hill equation: MOPS: K= 0.89mM; h= 1.47; Q_{max}= 0.32;Tris-HCl: K= 1.10mM; h= 1.76; Q_{max} = 0.22.

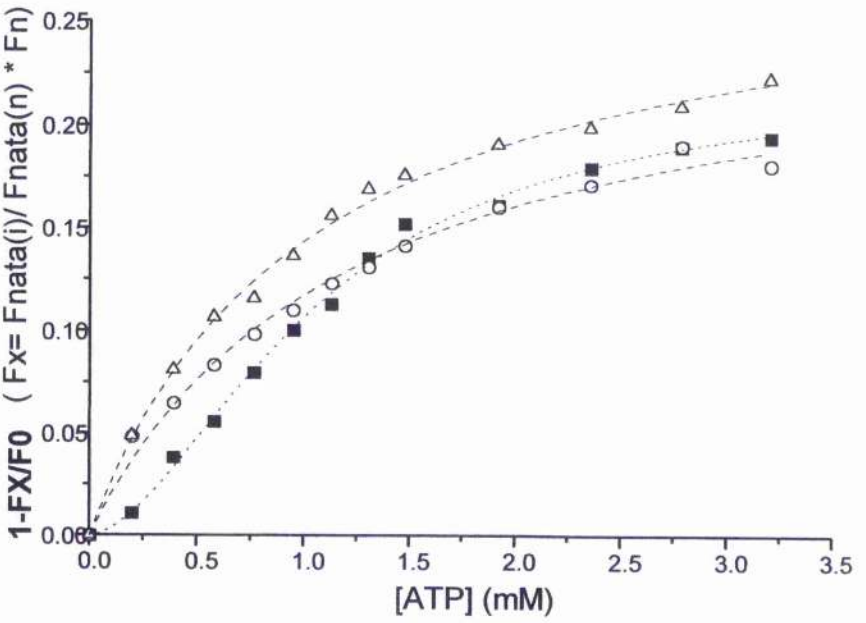

a) SK (filled squares); 0.25M NaCl (open circles); 0.25M NaCl (open triangles)

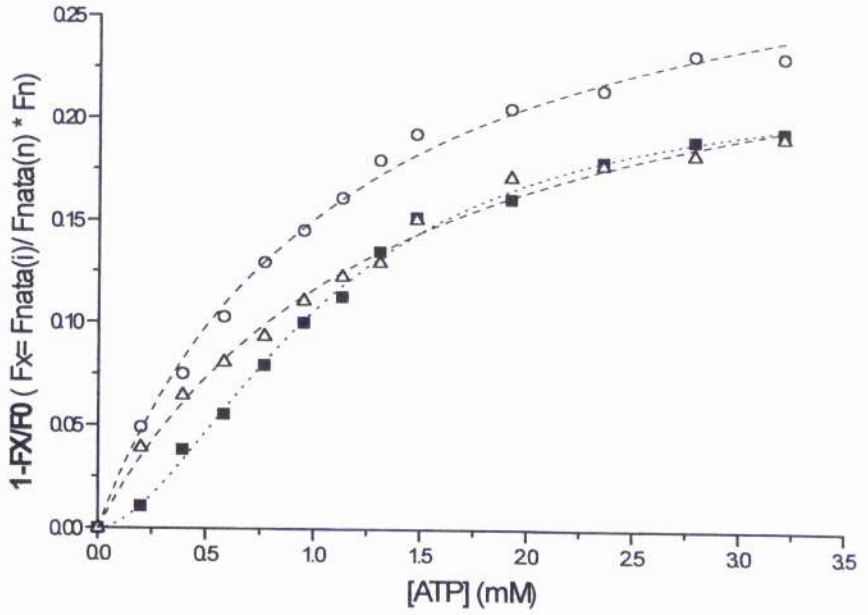

b) SK (filled squares); 0.085M Na_2SO_4 (open circles); 0.17M Na_2SO_4 (open triangles)

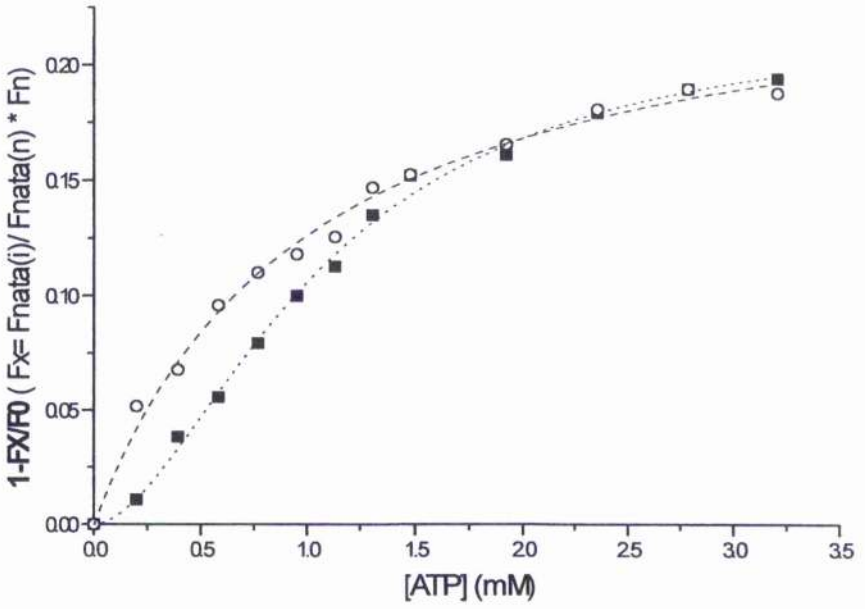

c) SK (filled squares); 0.1M NaF (open circles), (only one experiment was performed)

Figure 4.15: ATP titrations in the presence of salts.

The data show titrations performed in the presence of different concentrations respectively of a) NaCl; b) Na_2SO_4; c) NaF 0.1M

4.7 Effects of salts on the quenching of fluorescence by NaI

Quenching of the fluorescence of SK by NaI can be used as an index to check the integrity of the electrostatic environment of the single Trp (Trp54) in the enzyme (section 1.3.2.4).
Enzyme solutions containing salts were titrated with NaI and the data were analysed according to the general form of the Stern-Volmer equation (section 2.4).
Control experiments were performed to correct for any small effects of these salts on the quenching of the fluorescence of N-acetyltryptophan amide (NATA). The data (summarised in Table 4.9) show that the effects are correlated principally with the ionic strength of the solution and the nature of the anion added: the observed decrease in K_{sv} probably reflects a screening of the charge of the Arg side chains in the proximity of the side chain of Trp54. In fact an ion like fluoride, which is highly hydrated in solution due to its high charge density, has the lower screening effect (Collins, 1995). The NaBr has a larger effect but probably this is due to the fact that the bromide ion can act as a quencher of the Trp fluorescence (section 4.3.1).

Conditions	K_{sv} (M^{-1})	$K_{sv\ NATA}$ (M^{-1})	$K_{sv(SK+x)} * K_{sv\ (nata)}/K_{sv(nata+x)}$ (M^{-1})
Tris-HCl	20.0	10.1	**20.0**
+1M KCl	14.5	10.2	**14.4**
+0.5M NaF	22.2	11.2	**20.0**
+1M NaBr (*)	6.12	6.64	**9.31**
+0.33M $CaCl_2$	17.1	10.5	**16.5**
0.33M Na_2SO_4	17.2	11.7	**14.9**

Table 4.9: Stern-Volmer constants for the quenching of Trp54 fluorescence by NaI
The Stern-Volmer constants were determined from plots of F/F_0 *vs* $[I^-]$ as described in section 2.4.

4.8 Equilibrium unfolding in the presence of different salts

The order of effectiveness by which different salts stabilise protein molecules generally follows the Hofmeister series, which is believed to occur through the modification of water structure. If anion-binding plays a role, the order of stabilisation will follows the electroselectivity series (section 4.2).

The effect of salts on the stability of SK was studied using a range of different salts and at different concentrations for NaCl and Na_2SO_4. The salts were chosen to test both the effects of cations and anions on the stability of the enzyme. Among the cations tested were: K^+, Na^+, Ca^{2+} and Mg^{2+} which have a decreasing order of stabilisation according to the Hofmeister series for cations. Among the anions were chosen, in order of effectiveness: SO_4^{2-}, F^-, Cl^-, Br^- where chloride is neither a typical kosmotrope nor a chaotrope. The unfolding curves obtained in the presence of three different concentration of NaCl are shown in Fig. 4.16.

The presence of NaCl gives a marked stabilisation against denaturation by urea, and this stabilisation is concentration dependent. The stabilising effect does not depend on the cation used, as demonstrated by the unfolding curve obtained in the presence of KCl which shows a similar stabilisation to that obtained in 1M NaCl (Figure 4.16).
Na_2SO_4 is a well-known stabiliser and salting out agent and has the biggest effect at the same ionic strength, as it is shown in figure 4.17. Finally the effects of NaBr, $MgCl_2$, $CaCl_2$ and NaF were investigated, though a limited number of points were acquired (Figure 4.18).

Estimated values for $[Urea]_{1/2}$ (concentration of urea required to give 50% unfolding) are shown in Table 4.10, though it should be noted that in some cases only a rough estimate was possible due to the small number of data-points. In all cases, the salts stabilised the enzyme against unfolding by urea. For example, the addition of 1M NaCl increased the $[urea]_{1/2}$ from 2.1M to 4.6M. From the data it appears that the anion dominates, as demonstrated by the equivalence of the unfolding curves obtained using KCl and NaCl, and by the fact that 0.33M $MgCl_2$ give a stabilisation similar to 0.5M NaCl. The larger degree of stabilisation observed with $MgCl_2$ compared with $CaCl_2$ probably reflects specific coordination of Mg^{2+} with protein side chains (Thr16 and Asp32). Instead the higher degree of stabilisation given by anions such as sulphate or fluoride can be explained with their position in the Hofmeister series.
The strong stabilising effect of the chloride ion does not correlate with its position in the Hofmeister series but, as suggested by the shikimate binding data (section 4.5) and demonstrated by crystallographic evidence (section 4.10.3 and 4.10.4), ion binding can play a role. This effect could reflect general effects of the ionic strength as well as specific binding to, and hence stabilisation of, the folded state.

In summary, the effects of the salts reflect a stabilisation of the folded conformation either by favourable screening interactions with surface charges on the enzyme (as is likely to be the case with sulphate ions) or by binding to specific sites (as is likely to be the case with chloride ions) (section 4.2). The net effect of these mechanisms is rather similar so that 0.33M Na_2SO_4 has a similar but slightly larger effect on $[urea]_{1/2}$ compared with that of 1M NaCl.

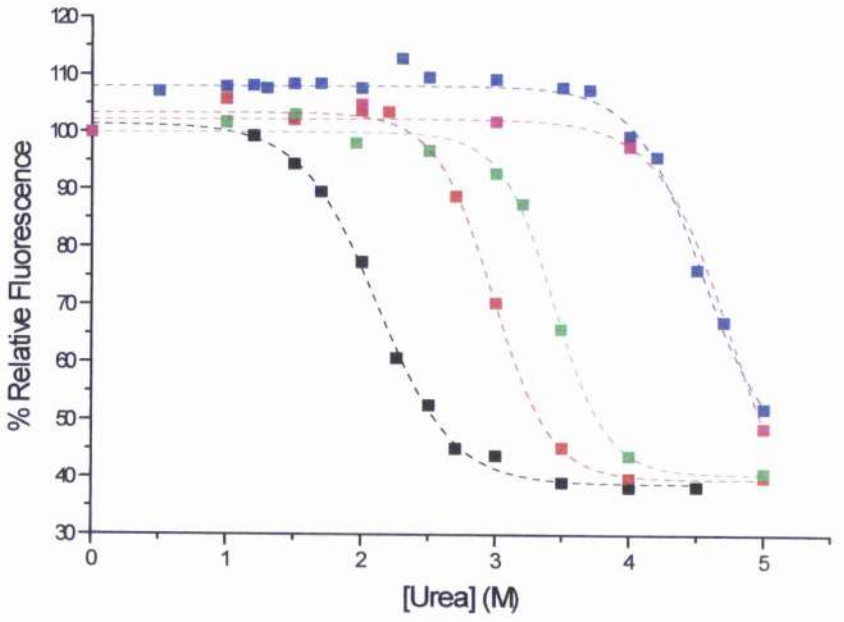

Figure 4.16: Urea-induced unfolding in the presence of NaCl and KCl.

To study the unfolding process, SK (0.15mg/ml) was incubated in the appropriate buffer, in the stated concentration of urea and the chosen concentration of salt for 1h at 20°C, before fluorescence data were recorded (section 2.5). The data shown are the changes in the fluorescence intensity at 350nm in the presence, respectively of: Tris-HCl (Black); SK + 0.25M NaCl (red); SK + 0.5M NaCl (green); SK + 1M NaCl (blue); SK + 1M KCl (magenta).

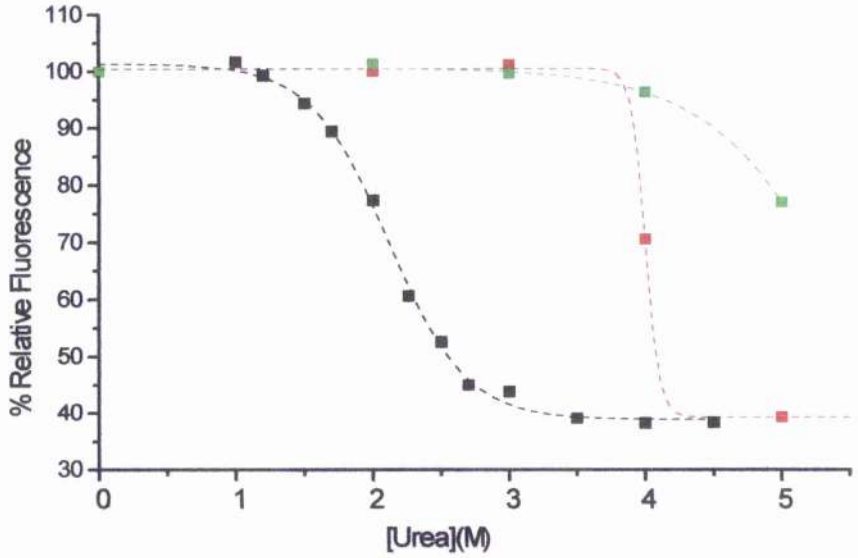

Figure 4.17: Urea-induced unfolding in the presence of Na_2SO_4

SK (0.15mg/ml) was incubated previously described before fluorescence data were recorded (section 2.5). The data shown are the changes in the fluorescence intensity at 350nm in the presence, respectively of: buffer (Black); 0.17M Na_2SO_4 (red) and 0.33M Na_2SO_4 (green).

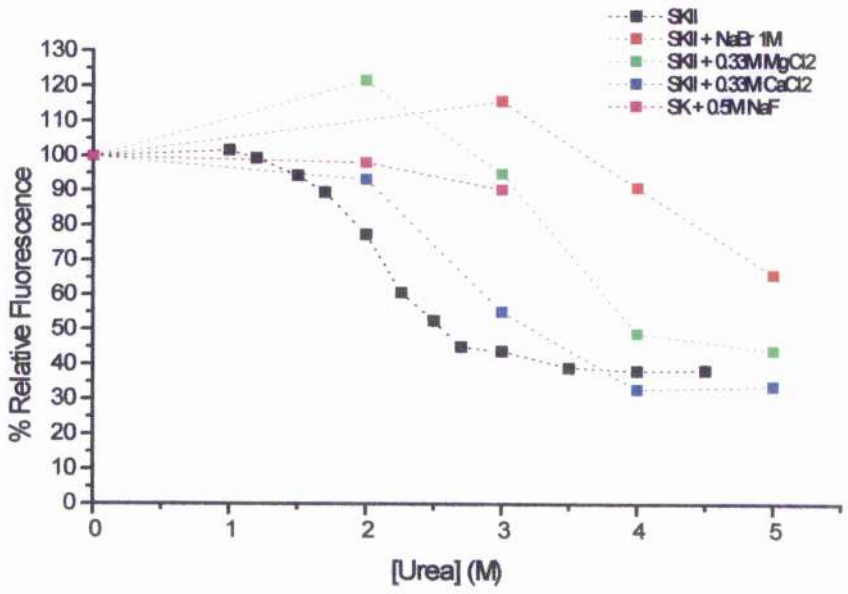

Figure 4.18: Urea-induced unfolding in the presence of NaBr, $MgCl_2$ $CaCl_2$, and NaF

SK (0.15mg/ml) was incubated previously described before fluorescence data were recorded (section 2.5). The data shown are the changes in the fluorescence intensity at 350nm in the presence, respectively of: buffer (Black); 1M NaBr (red) and 0.33M $MgCl_2$ (green), 0.33M $CaCl_2$ (blue), 0.5M NaF (magenta).

Solution	$[Urea]_{1/2}$ (M)
SK (Tris-HCl)	2.1
SK (MOPS)	2.4
SK + 0.25M NaCl	3.0
SK + 0.5M NaCl	3.4
SK + 1M NaCl	4.6
SK + 0.17M Na_2SO_4	4.0
SK + 0.33M Na_2SO_4	5.3
SK + 1M KCl	4.6
SK + 1M NaBr	4.8
SK + 0.33M $CaCl_2$	2.8
SK + 0.33M $MgCl_2$	3.3

Table 4.10: Values of $[Urea]_{1/2}$ for unfolding of SK

The unfolding of SK by urea was monitored by changes in protein fluorescence at 350nm as described in section 3.3.2.

4.9 Conclusions

Salts are known to have a variety of effects on the structure and function of proteins (sections 1.1.2.2 and 4.2). Anions and cations can be ranked in the Hofmeister series (Scopes 1994) which was originally drawn up on the basis of their ability to precipitate mixtures of proteins. The order of ions in the series can be understood in terms of the degree of hydration of the ions; this will alter the stability of a protein by influencing the extent of its hydration. Strongly hydrated anions such as sulphate and weakly hydrated cations such as ammonium provide the greatest degrees of stabilisation. In addition to these general effects, specific effects can arise if there are appropriate ion binding sites in proteins (Pace et al., 1998) as for example calcium binding sites in ribonuclease T_1 (Deswarte *et al.*, 2001) and zinc binding sites in alcohol dehydrogenase (Plapp *et al.*, 1978).

The studies on SK reported show that both general and specific effects of ions can be observed. When the effects of salts on the substrate binding and catalytic properties of the enzyme are analysed, a complex pattern emerges. In terms of shikimate binding, it is clear that chloride ions markedly weaken the interactions (Table 4.4) and this can be described in terms of a competitive binding model. The X-ray data (to be discussed in section 4.11.3; Fig. 4.32) show that chloride ions bind at sites (C3, C4 and C5) which are thought to play a role in the binding of shikimate. In the earlier X-ray studies of SK, residual electron density in this region was interpreted as bound shikimate. In re-analysed X-ray data this electron density is still seen, but it can be concluded that if indeed shikimate is bound it is not in a catalytically meaningful orientation. Due to the competitive nature of chloride binding it is therefore more likely that the chloride ions give a better indication of the correct position of the shikimate.
It is of interest that the X-ray structure of SK from *Mycobacterium tuberculosis* in complex with ADP shows a total of 6 chloride ions in the molecule (Gu *et al.*, 2002). The only one of these bound in the active site cavity, namely to the P-loop lysine, has no equivalent in the *E. chrysanthemi* SK structure. The chloride C3 found in *E. chrysanthemi* SK and the K15M mutant SK is not present in the *M. tuberculosis* SK structure, due to the replacement of Arg11 by a Pro in the latter enzyme, thereby blocking the main chain amide nitrogen.

There is no direct evidence for the location(s) of bound sulphate ion(s) in the *E. chrysanthemi* SK structure; however it is likely that one or more could be bound near Arg58, thereby accounting for the smaller effects of sulphate on shikimate binding. Analysis of the effects of salts on the kinetic parameters of SK (Table 4.3) indicates that the K_m for shikimate is increased in the presence of chloride, although to a smaller extent than the K_d. The effects of sulphate on the K_m for shikimate are less pronounced than those of chloride (Table 4.3).

The effects of salts on the binding of nucleotide substrates are more difficult to relate to the kinetic parameters. Both chloride and sulphate lead to a strengthening of the binding of both

ADP and ATP, which at first sight would be unexpected in terms of the proposed binding sites for these anions. A possible explanation for the effects of salts on K_d for ADP and ATP is that the dominant contribution to the relatively low affinity of the substrates for SK and other kinases (Price, 1972) is in fact made by the hydrophobic interactions between the adenine base and the enzyme; these would be enhanced by increasing ionic strength. The polar interactions between the phosphate groups of ADP and ATP and the enzyme may contribute relatively little to the energetics of interaction, but are of course crucial for the correct alignment of substrates for the phosphotransfer reaction. By contrast, both chloride and sulphate lead to an increase in the K_m for ATP, which is particularly marked in the case of sulphate (Table 4.3). This would be consistent with the proposal that these anions occupy sites crucial for the binding of the nucleotide substrate in the correct orientation for catalysis.

Both salts lead to a marked reduction in the catalytic efficiency (as reflected by V_{max}) of the reaction. The magnitude of V_{max} presumably reflects the ability of the domains of the enzyme to move so as to ensure the correct alignment of substrates, as well as to undergo conformational changes required for product release. In this context, it may be significant that, on the basis of the near-UV CD data (Fig. 4.9), both salts appear to bring about a decrease in the mobility of the enzyme, and this can be accounted for by the X-ray results. However, further work using methods such as NMR would be required to characterise the changes in mobility in more detail. The relative movements of the domains would also affect the extent of synergism in substrate binding, and it is clear from Table 4.6 that this depends on the type of salt being studied. The locations of the binding sites for chloride ions both at substrate binding sites but also between the domains of SK (Fig. 4.32) provide an explanation for the range of effects of the salts on the kinetic properties of the enzyme (Table 4.3).

4.10 Refolding of enzyme in 4M Urea by addition of salts

Since an increase in ionic strength leads to a marked degree of stabilisation against unfolding by urea, it was reasoned that addition of salt to a previously unfolded solution of enzyme (in 4M urea) might promote refolding of the denatured enzyme. By carrying out this ionic strength jump (with the urea concentration maintained at 4M) as outlined in section 2.5, it was found that this was indeed the case. It should be noted that when refolding was carried out in this fashion, there was no evidence for formation of aggregates as determined by light scattering experiments. The refolding process and the properties of the product formed were investigated as outlined below.

4.10.1 Spectroscopic studies

4.10.1.1 Regain of secondary structure

In the presence of 4M urea, the far UV CD spectrum of shikimate kinase indicates that the secondary structure has been essentially completely lost. After the ionic strength jump, the enzyme was found to regain native-like secondary structure as judged by the far-UV CD spectrum. Fig. 4.19 shows the spectra of the native and denatured enzyme and the enzyme refolded in 4M Urea plus 1M NaCl or in 4M Urea plus 0.33M Na_2SO_4.

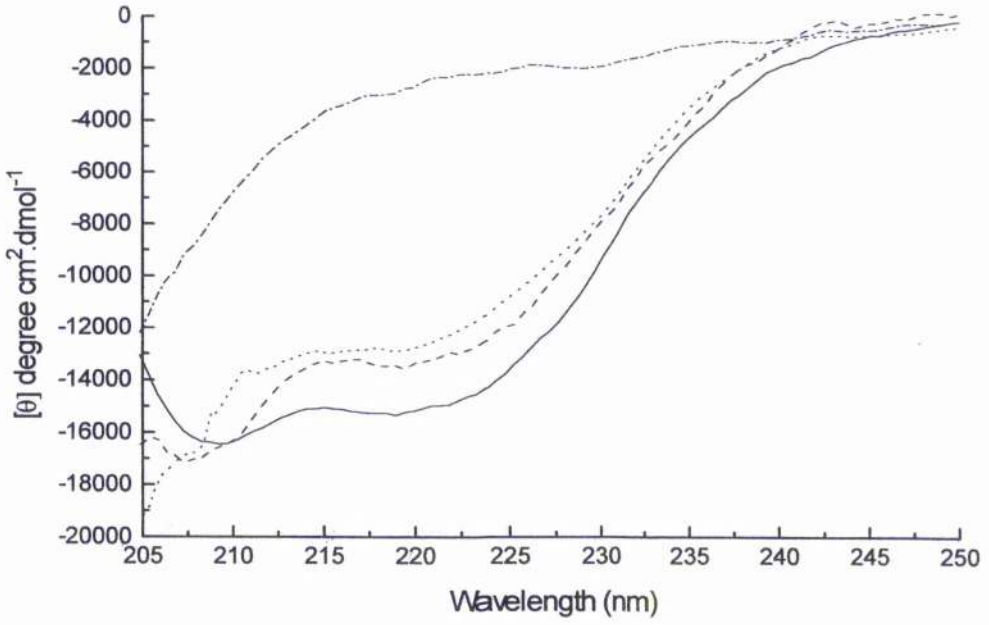

Figure 4.19: Refolding of denatured SK by addition of salts monitored by CD.

Far-UV CD spectra of SK in buffer D (solid line), SK in buffer D plus 4M urea (dashed and dotted line), SK denatured in 4M urea and refolded by addition of 1M NaCl (dashed line), SK denatured in 4M urea and refolded by addition of 0.33M Na_2SO_4 (dotted line). The concentration of SK was 0.072mg/ml and the cell pathlength was 0.05cm.

The kinetics of the regain of secondary structure in this process are markedly different from those previously observed in denaturant jump experiments, i.e. dilution from 4M urea to 0.36M urea (section 3.4.2). In the latter experiment, three kinetic phases could be discerned using a combination of manual mixing and stopped flow mixing to initiate refolding with rate constants $8s^{-1}$, $0.08s^{-1}$ and $0.009s^{-1}$; 75% of the signal was regained within the dead time of manual mixing (20s). In the ionic strength jump experiments, using a final concentration of 1M NaCl, however, the changes in the CD signal at 225nm were much slower. Only 20% of the total change was observed in the dead time of manual mixing and the remaining signal was regained with a rate constant of $0.0024s^{-1}$ (Fig. 4.20). In the presence of 0.33M Na_2SO_4, the changes in CD were somewhat more rapid than in the presence of NaCl, with 35% of the total change observed in the dead time of the manual mixing and the remaining signal regained with a rate constant of $0.0083s^{-1}$ (Fig. 4.21).

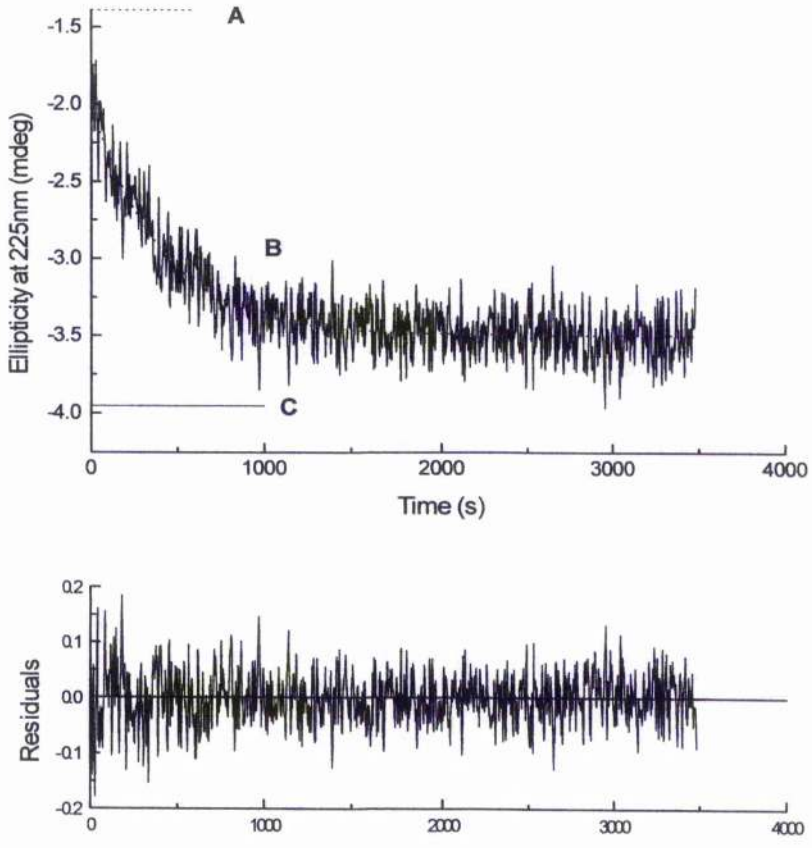

Figure 4.20: Kinetics of changes in ellipticity at 225nm on addition of 1M NaCl to SK.

Protein denatured by incubation in 4M urea. Curves A, B and C represent SK plus 4M urea, SK during refolding on addition of salt, and refolded SK respectively. The SK concentration was 0.072mg/ml and the cell pathlength was 0.05cm. The lower panel shows the pattern of residuals from the fit to a single exponential process.

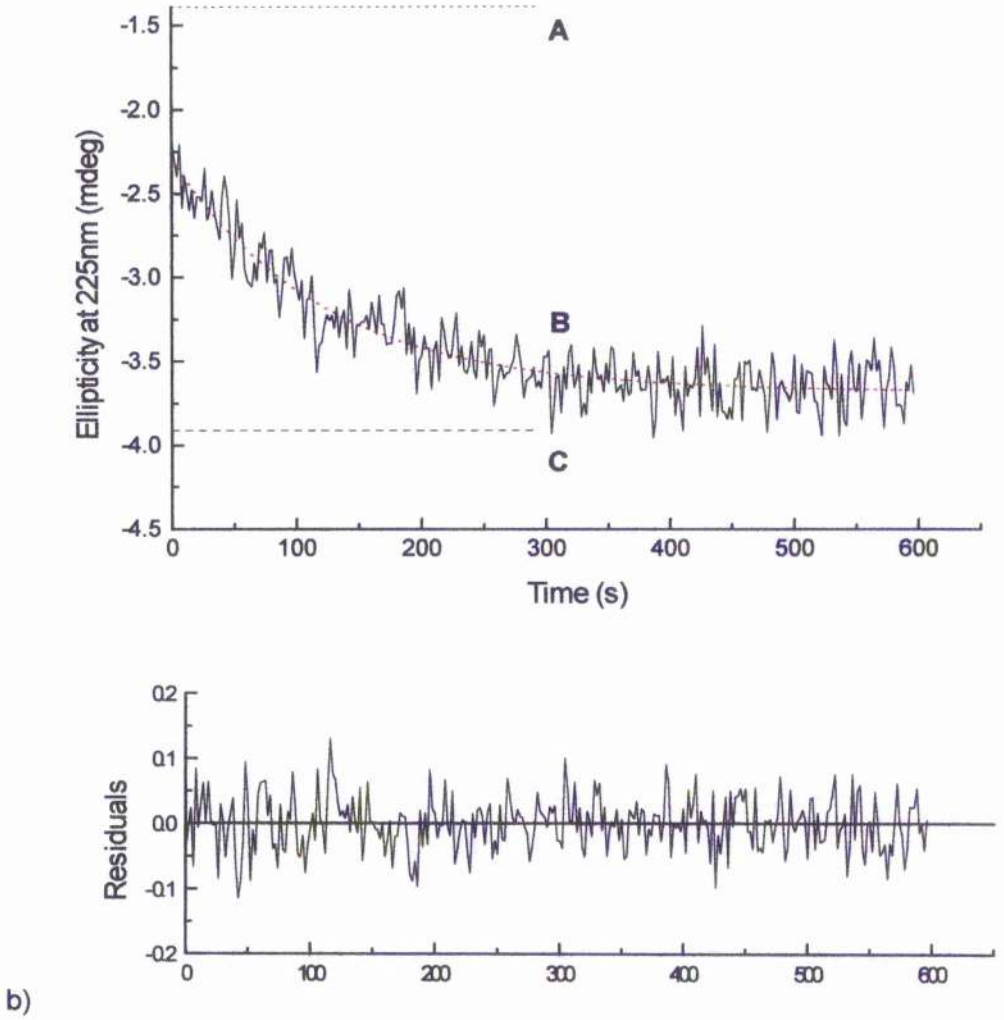

b)

Figure 4.21: Kinetics of changes in ellipticity at 225nm on addition of 0.33M Na_2SO_4.

Protein denatured by incubation in 4M urea. Curves A, B and C represent SK plus 4M urea, SK during refolding on addition of salt, and refolded SK respectively. The SK concentration was 0.072mg/ml and the cell pathlength was 0.05cm. The lower panel shows the pattern of residuals from the fit to a single exponential process.

4.10.1.2 Regain of fluorescence intensity

In the presence of 4M urea, the emission maximum of shikimate kinase is 356nm, characteristic of a Trp side chain fully exposed to solvent. After an ionic strength jump, the fluorescence spectrum becomes native-like with an emission maximum at 348nm (Fig. 4.22). The kinetics of the changes in fluorescence at 350nm after initiating refolding by an ionic strength jump are shown in figure 4.23. After addition of NaCl to a final concentration of 1M, very little change (<5% of the total) occurs within the dead time of manual mixing (20s); the observed change occurs in two phases with rate constants $0.005s^{-1}$ (14% amplitude) and $0.002s^{-1}$ (78% amplitude). Using 0.33M Na_2SO_4 to initiate refolding, the changes are more rapid; the kinetic parameters for the two phases are $0.019s^{-1}$ (43% amplitude) and $0.005s^{-1}$ (50% amplitude) (Fig. 4.23). In both cases the rate of the slower phase of the change in fluorescence corresponds approximately with the rate of the change monitored by CD.

The fluorescence results contrast with those obtained when refolding is initiated by a denaturant jump (also shown in Fig. 4.23) where two phases are observed with rate constants $0.08s^{-1}$ (42% of total change and largely complete in the dead time of manual mixing) and $0.009s^{-1}$ (45% of the total change) (section 3.4.2).

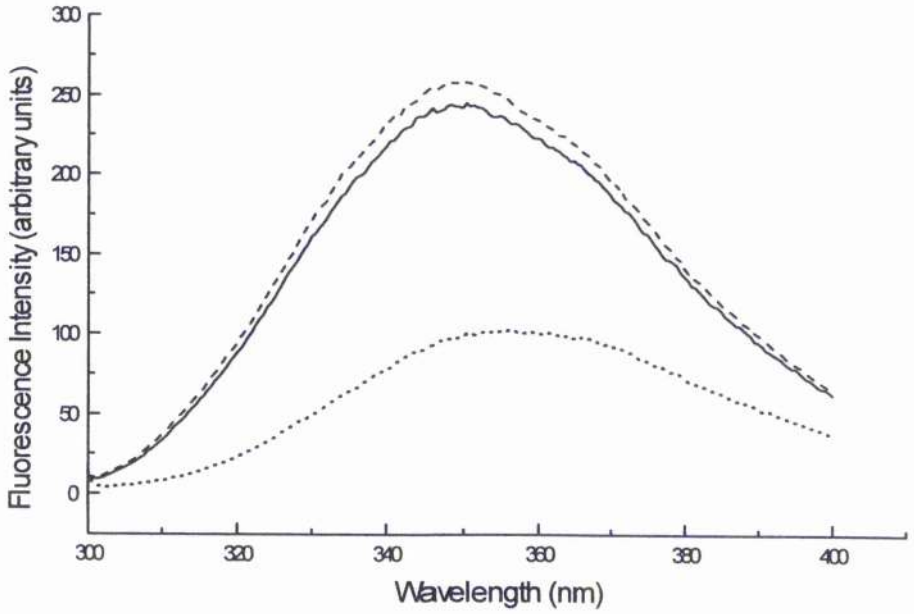

Figure 4.22: Refolding of denatured SK by addition of salts monitored by fluorescence.

Fluorescence spectra of unfolded SK (dotted line) and SK refolded by addition of 1M NaCl (solid line) or 0.33M Na_2SO_4 (dashed line).

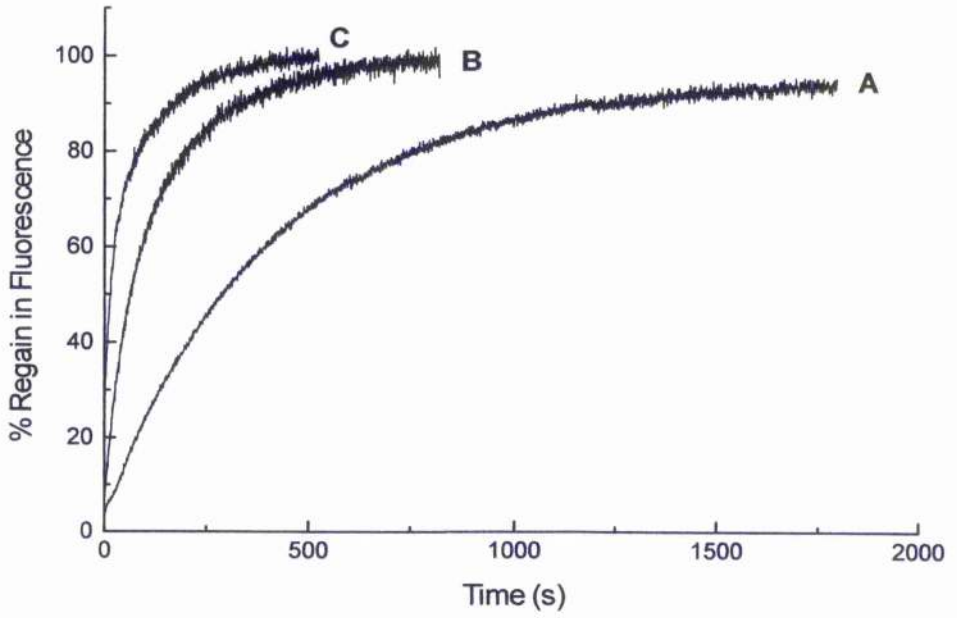

Figure 4.23: Refolding of denatured SK by addition of salts monitored by fluorescence.

Kinetics of changes in fluorescence at 350nm. Curves A and B represent refolding of SK brought about by addition of 1M NaCl and 0.33M Na_2SO_4 respectively. Curve C represents refolding of SK brought about by a denaturant jump.

4.10.1.3 Refolding in the presence of ANS

When refolding of shikimate kinase is initiated by a denaturant jump using urea, there is a marked and rapid increase in the fluorescence of ANS, followed by a slow release of the probe. These results indicate that the refolding process may proceed via rapid formation of a "compact intermediate" structure, though unlike a classical molten globule this intermediate would appear to contain relatively little of the secondary structure of native enzyme (section 3.4.2.8). By contrast, when the ionic strength jump was used to initiate refolding, no changes in ANS fluorescence could be detected during the refolding process although the Trp fluorescence of the refolded protein indicates a native-like structure had been formed (Fig. 4.24). While these results may indicate that the ionic strength jump-induced refolding does not involve a rapid collapse to a compact intermediate, it is possible that the presence of 4M urea may inhibit the binding of ANS to hydrophobic sites, as has been demonstrated in the case of cardiotoxin III (Kumar *et al.*,1996) and by previous ANS spectra recorded under different conditions (section 4.10.5.1).

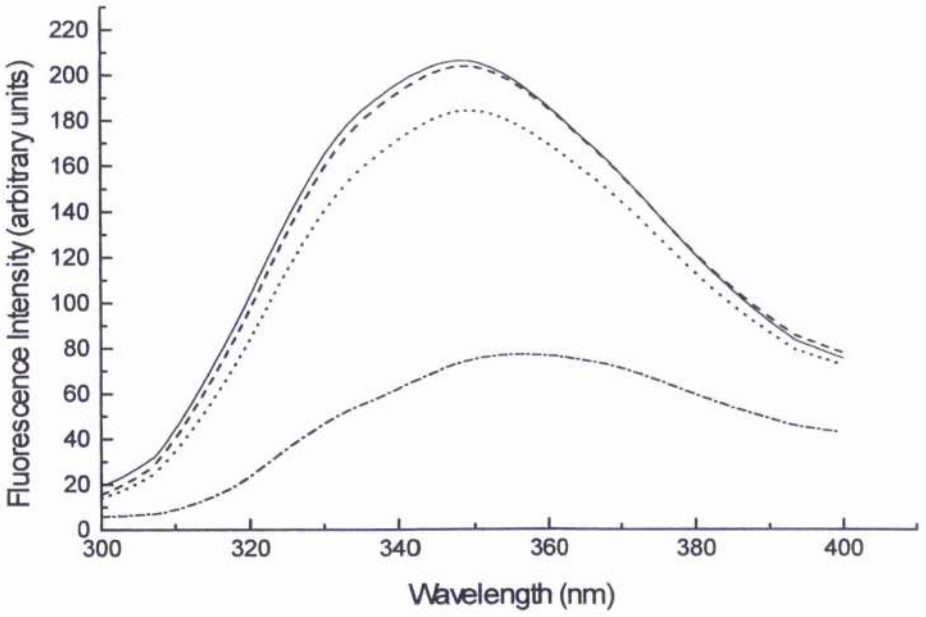

a)

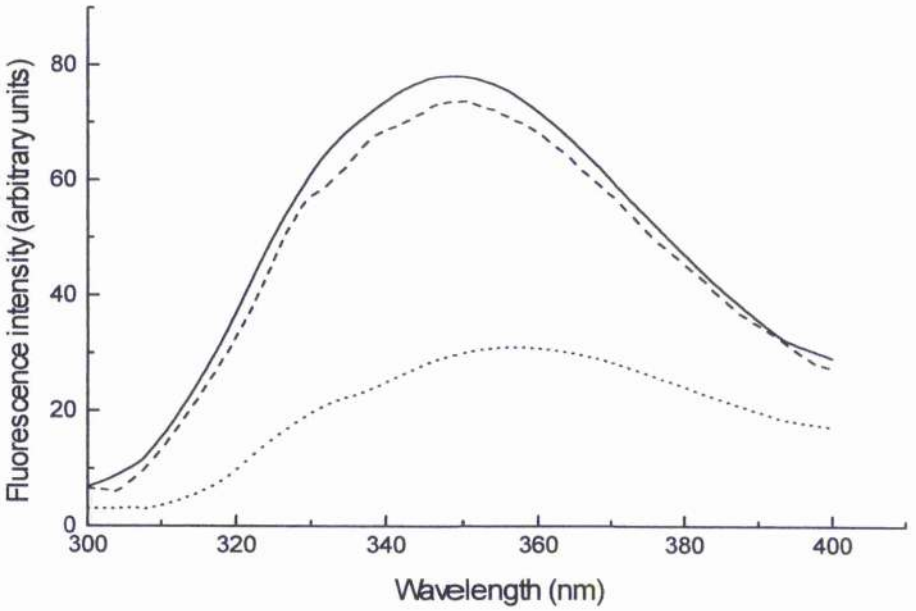

b)

Figure 4.24: Tryptophan emission spectra of SK refolded in 4M Urea and salts.

Refolding in the presence of ANS. The data show: a) line: SKII + 1M NaCl + ANS; dash: SKII + 4M Urea +1M NaCl + ANS (End); dots: SKII + 4M Urea + 1M NaCl + ANS (refolded); dash and dots: SKII + 4M Urea + ANS . b) Line: SKII + 4M Urea + 0.33M Na_2SO_4 + ANS (end); Dash: SKII + 4M Urea +0.33M Na_2SO_4 + ANS (refolded); Dots: SKII + 4M Urea + ANS

4.10.1.4 Refolding in the presence of NaI

In the presence of 4M urea the K_{sv} for quenching of the protein fluorescence by NaI is $4M^{-1}$ (Table 4.11). The dramatic reduction of the value for native enzyme ($20M^{-1}$) reflects the loss of the positively charged environment of the Trp provided by neighbouring Arg side chains. When refolding is initiated by an ionic strength jump this value is increased to $10.1M^{-1}$ and $10.8M^{-1}$ in the presence of 1M NaCl or 0.33M Na_2SO_4 respectively. While it is evident that refolding has led to a re-establishment of a positively charged environment around the Trp, the lower values of K_{sv} compared with those for native enzyme in the presence of 1M NaCl or 0.33M Na_2SO_4 ($15.2M^{-1}$ or $14.9M^{-1}$ respectively) show that the process is not complete (Table 4.11).

When the refolding initiated by an ionic strength jump was performed in the presence of 0.1M NaI, the changes in protein fluorescence were found to fit two successive first order processes (Fig. 4.25). The spectra acquired immediately after the refolding (Fig. 4.26) confirm the Stern-Volmer values: the refolded enzyme in 4M urea does not give the same degree of quenching as the native enzyme reflecting the disruption of the Trp charged environment. When refolding is initiated by 0.33M Na_2SO_4, the kinetic parameters ($0.016s^{-1}$ (amplitude 32%) and $0.004s^{-1}$ (amplitude 41%)) are similar to those observed for the changes in protein fluorescence in the absence of NaI (Fig. 4.27). However, when refolding is initiated by 1M NaCl, the changes are faster in the presence of NaI ($0.043s^{-1}$ (7% amplitude) and $0.005s^{-1}$ (85% amplitude)) (Fig. 4.28). These data point to the possibility that chloride ions play a role in enhancing the rate of formation of the positively charged environment of the Trp side chain.

Solution	K_{sv} (M^{-1})
SK (Tris-HCl)	20.0
SK + 4M Urea	4.0
SK + 4M Urea + 1M NaCl (refolded)	10.1
SK + 4M Urea + 0.33M Na_2SO_4 (refolded)	10.8

Table 4.11: Stern-Volmer constants for the quenching of Trp54 fluorescence by NaI

The Stern-Volmer constants were determined from plots of F/F_o vs. $[I^-]$ as described in section 2.4.

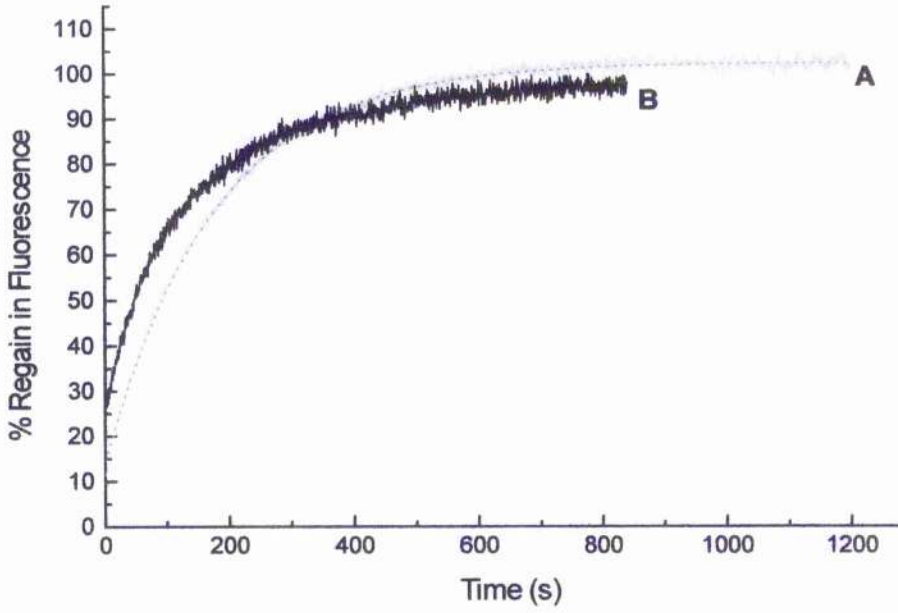

Figure 4.25: Refolding of denatured SK by addition of salts monitored by fluorescence.

Refolding in the presence of NaI 0.1M. Kinetics of changes in fluorescence at 350nm. Curves A and B represent refolding of SK brought about by addition of 1M NaCl and 0.33M Na_2SO_4 respectively in the presence of 0.1M NaI.

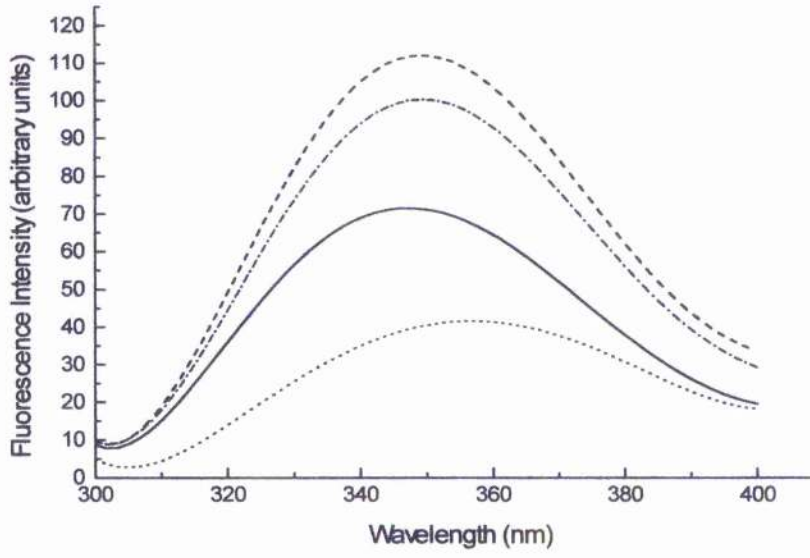

Figure 4.26:Fluorescence emission spectra of refolded SK solution in the presence of NaI

The spectra represent: SK in the presence of 0.36M Urea (line); SK + 4M Urea (dots); SK + 4M Urea + 1M NaCl (dashes); SK+ 4M Urea + 0.33M Na_2SO_4 (dashes and dots)

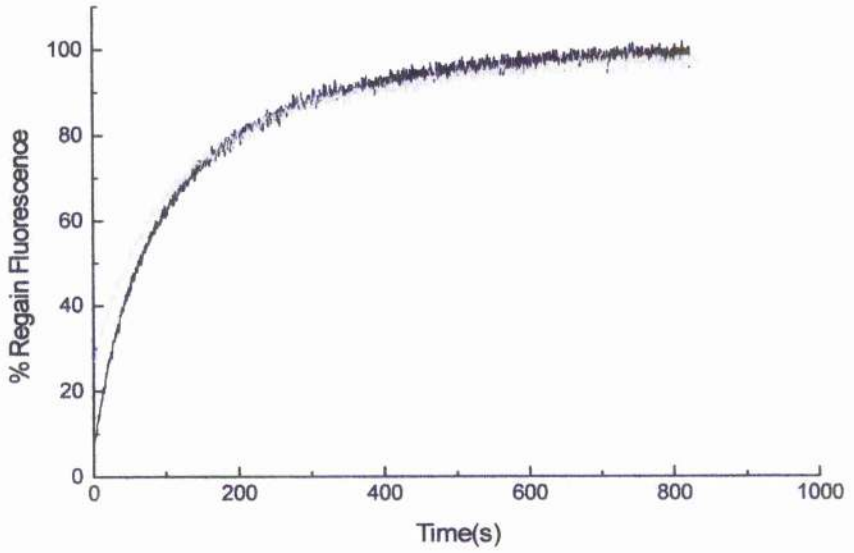

Figure 4.27: Comparison between salt-induced refolding in the absence and presence of NaI.

Kinetics of changes in fluorescence at 350nm following an ionic strength jump in Na_2SO_4. The curves represent: SK refolded in 0.33M Na_2SO_4 and 4M urea in the absence (black) and in the presence (light gray) of NaI.

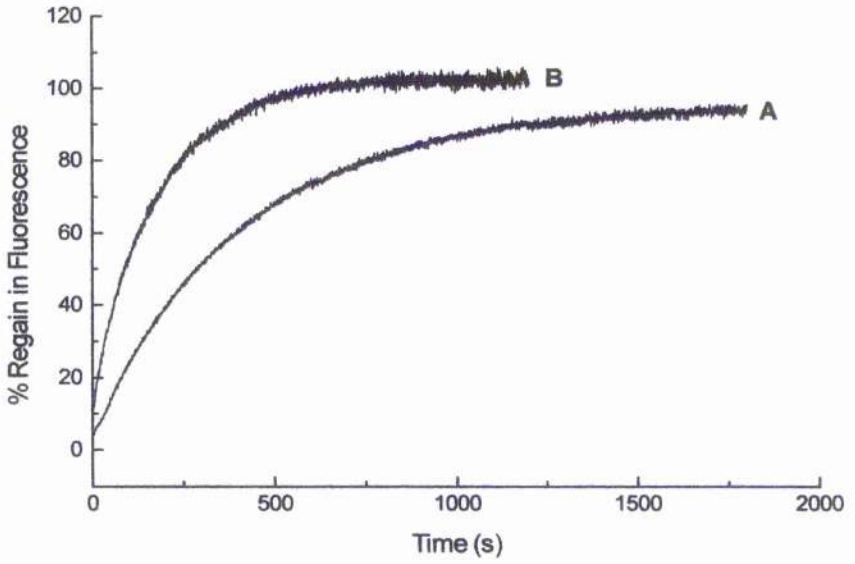

Figure 4.28: Comparison between salt-induced refolding in the absence and presence of NaI.

Kinetics of changes in fluorescence at 350nm following an ionic strength jump in NaCl. The curves represent: SK refolded in 1M NaCl and 4M Urea in the absence (A) and in the presence (B) of NaI.

4.10.1.5 Comparison between the refolding traces obtained by different techniques

From the comparison of different traces obtained monitoring different parameters different patterns emerge for the two salts used. In the case of NaCl (Fig. 4.29a) in the dead time of the manual mixing experiment a state is formed with 22% of secondary structure (see Appendix 4.2 for fitting data) but with no tertiary interactions as far as the Trp environment is concerned. But when the trace obtained following the regain in fluorescence in the presence of NaI (a quencher sensitive to the charged Trp environment due to the presence of three arginines) is considered, 10.5% of the signal is regained in the dead time of the manual mixing mode (20s).

Chloride ions were found to interact with SK (section 4.11.3) and there are usually arginines between the residues with which they interact. In SK, from the crystallographic structure, it appears that these interactions involve Arg11, 139 and 58 which are clustered around the single Trp (Trp54) of SK. In particular one of the chloride ions (section 4.11.3) interacts, in some SK structures, with both Arg11 and 139. This could indicate that the charged arginine cluster plays a role in the NaCl-induced folding.

For example the binding of salts to a specific site could be considered as a possible "nucleating" point that could lead to the subsequent folding of the entire protein molecule. This "template" effect is known to have an influence in the synthesis of macrocyclic molecules where the ion acts as a conformational template (Consoli *et al.*, 2001).

When the refolding induced by Na_2SO_4 is considered the regain in fluorescence in the presence and absence of NaI gives the same trace with the same rate constants (k_1=0.015s^{-1} and k_2= 0.0043s^{-1}) indicating that the regain of the charged Trp environment and the regain of the tertiary environment are formed in the same type of process (Fig. 4.29b). These considerations lead to the idea that the induced refolding by the two salts may follow different mechanisms.

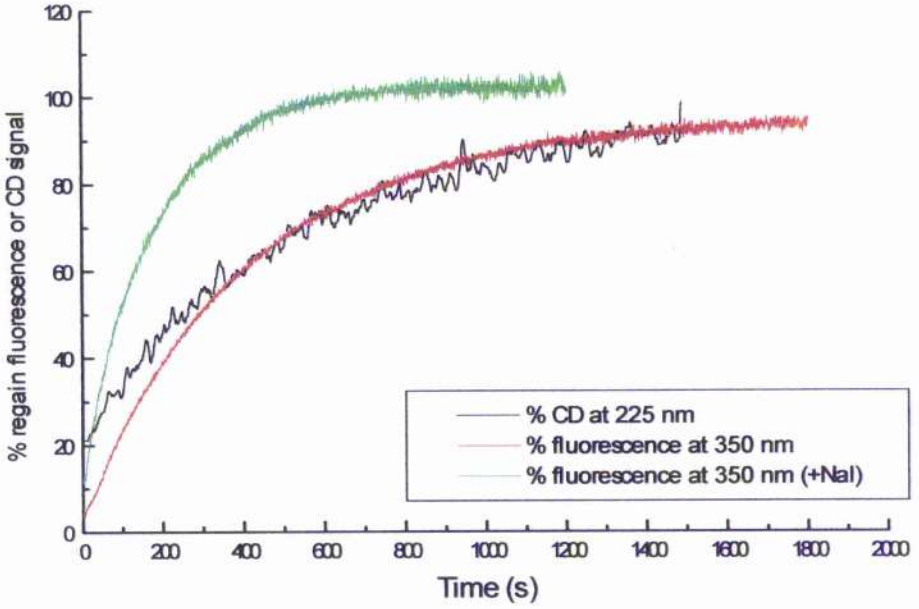

a)

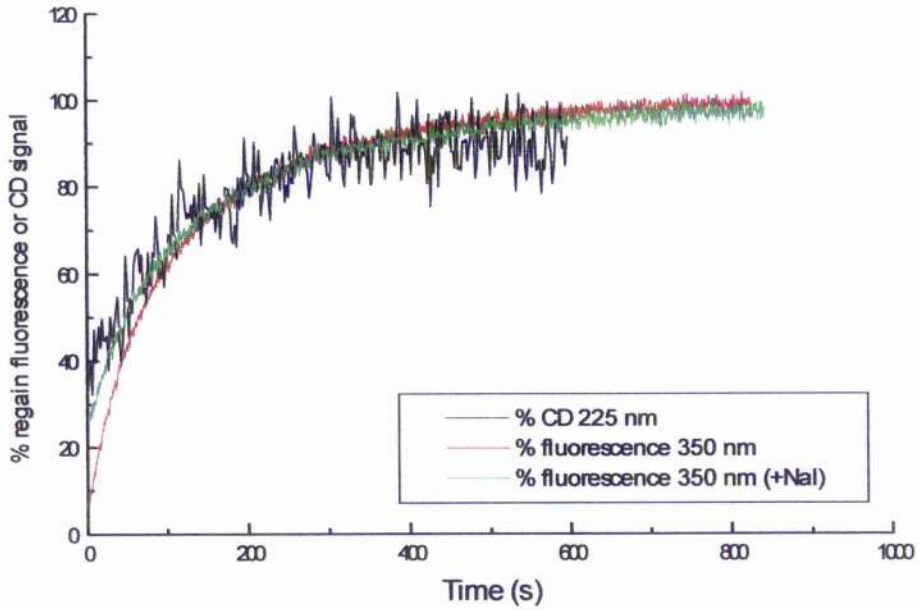

b)

Figure 4.29: Comparison of different traces obtained after the salt-induced refolding.

Kinetics of changes in CD at 225nm (black), in fluorescence at 350nm (red), in the presence of NaI (green) when SK is refolded in 4M urea and in 1M NaCl (a) and in 0.33M Na_2SO_4 (b) respectively.

4.10.2 Substrate binding and activity studies

In the presence of 4M urea, there is no detectable binding of shikimate to the enzyme as indicated by the lack of effect of the substrate on the fluorescence of the protein (Fig. 4.30). After refolding by an ionic strength jump, binding of shikimate could be demonstrated by fluorescence quenching. In the presence of 4M urea plus either 1M NaCl or 0.33M Na_2SO_4, the K_d values for shikimate were found to be 3.0mM or 3.8mM respectively (Table 4.12 and Fig. 4.30). When the titrations were performed in the presence of 2mM ADP, the binding of shikimate was tighter with the K_d values 1.4mM or 2.4mM in urea plus 1M NaCl or 0.33M Na_2SO_4 respectively (Table 4.12 and Fig. 4.31). It should be noted that for the refolded enzyme there was a significantly lower extent of fluorescence quenching on binding shikimate (25-45%) compared with native enzyme (90-95%), indicating that the refolded enzyme is capable of undergoing more limited conformational changes on binding the substrate. In separate experiments it was shown that addition of ADP to either the unfolded or the refolded enzyme led to no significant quenching of the fluorescence; a similar result was found for ATP. These results indicate that the binding site for the nucleotide substrate had not been correctly formed on refolding. It has to be pointed out that, when ADP titrations in the presence of urea were undertaken, urea was shown to have a drastic influence on the nucleotide binding. In fact, at a concentration of 1M urea, where no significant conformational changes were observed as judged by CD and fluorescence spectra, the effect on the K_d is quite marked (from 1.77 to 2.34mM - section 3.3.4). Using the quenched assay system it was not possible to demonstrate any significant regain in activity after refolding the enzyme in 4M urea by addition of 1M NaCl or 0.33M Na_2SO_4; the activity observed is less than 0.5 % of the control value. It should be noted that the presence of these salts (in the absence of urea) was found to lead to a loss of approximately 65% activity (section 4.4). Hence it can be concluded that the refolding induced by the ionic strength jump does not lead to the formation of a catalytically competent species. On the basis of the data obtained, this appears to be due to the disruption of the nucleotide binding site and the reduced conformational response on binding shikimate; thus the correct orientation of bound substrates required for catalysis is not achieved.

Solution	K_d (mM)	K_d (mM)(+ 2mM ADP)
SK (Tris-HCl)	0.60 ± 0.02	0.38 ± 0.02
SK + 4M Urea + 1M NaCl (refolded)	3.06 ± 0.33	1.36 ± 0.10
SK + 4M Urea + 0.33M Na_2SO_4 (refolded)	4.28 ± 0.37	2.40 ± 0.34

Table 4.12: Binding of shikimate to SK in the absence and in the presence of ADP

The binding of shikimate was determined by monitoring the extent of quenching of fluorescence at 350nm as described in section 2.3.

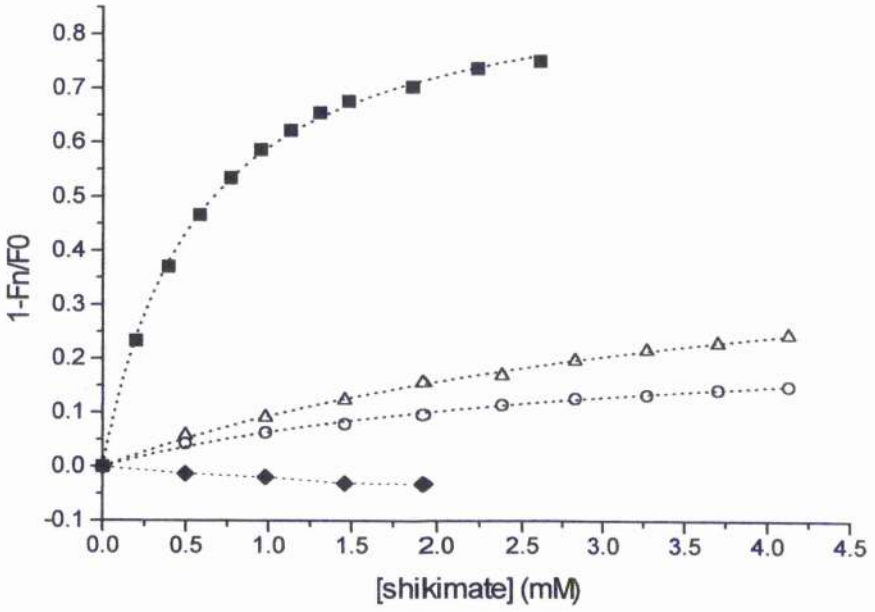

Figure 4.30: Binding of shikimate to refolded SK

Squares: SKII; diamonds: SKII + 4M Urea; Open Triangles: SKII + 4M Urea + 0.33M Na_2SO_4;Open Circles: SKII + 4M Urea + 1M NaCl

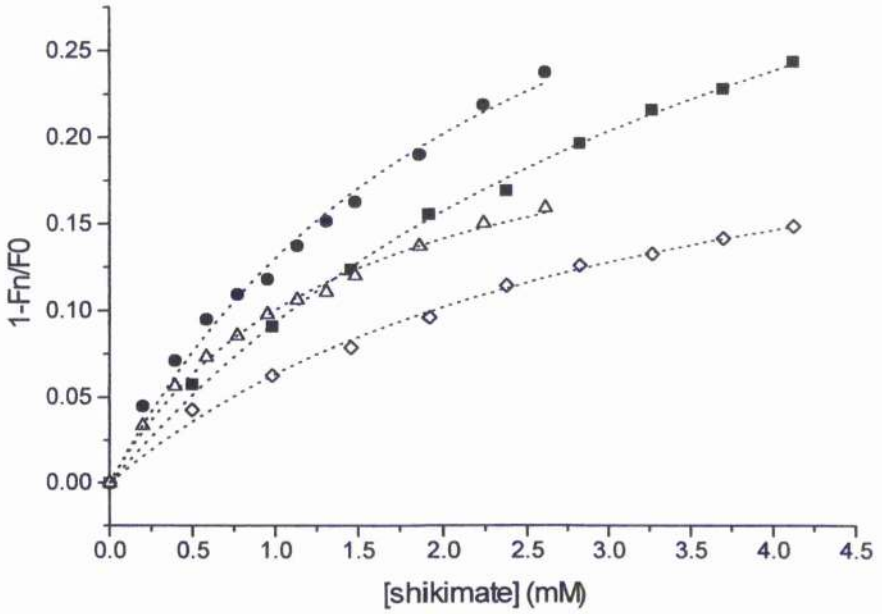

Figure 4.31: Binding of shikimate to refolded SK in the absence and presence of ADP

Filled squares – 0.33M Na_2SO_4 + 4M Urea; Filled circles – 0.33M Na2SO4 + 4M Urea + 2mM ADP; Open diamonds - 1M NaCl + 4M Urea; Open triangles – 1M NaCl + 4M Urea + 2mM ADP

4.10.3 The location of the chloride ions in shikimate kinase

The X-ray structure of SK was solved at 1.9Å resolution from crystals grown in approximately 2M NaCl (Krell *et al.*, 1998). A more detailed analysis of these data reveals a total of 21 chloride ions bound to the two molecules within the asymmetric unit of the crystal. Twelve chloride ions are bound to chain A (Fig. 4.32), nine to chain B. Of these ions, seven are common to both chains and are labelled in figure 5 and referred to here as C1-C7 (designated as 601-607 in the PDB file); these will be discussed in detail.

Two chlorides bind in the nucleotide-binding domain of SK, C1 is bound in an equivalent position to the β-phosphate of the nucleotide, C2 in a position equivalent to the α-phosphate. Both chlorides are located in the Walker A motif or P-loop region, C1 forming hydrogen bonds to the amide backbone of Gly12, Gly14 and C2 to the amide of Thr17.

Chloride C3 is of interest as it binds to the amide backbone of Arg11 and is in an equivalent position to the chloride found in the K15M SK mutant structure (Krell *et al.*, 2001), although the P-loop is shifted in this structure. The K15M SK structure was crystallised in 0.1M Tris-HCl, and only one chloride ion is present, strongly suggesting that this chloride-binding site is of higher affinity than the others found in the native high salt SK structure. Additional hydrogen bonds formed by this chloride are different between the mutant SK and the two chains of the native SK due to differences in protein conformation. In chain A additional hydrogen bonds are made with the guanidinium groups of Arg11 and Arg139; however these are not essential as the chloride in the K15M structure lacks the Arg11 interaction and the B molecule lacks both these interactions.

As previously described, molecule A and molecule B are non-equivalent in the native SK structure (Krell *et al.*,1998). In comparison with molecule A, the side chain of Arg139 in molecule B is shifted away from the active site as is the shikimate binding domain (residues 32-60). As a result the position of the chlorides C4 and C5, although comparable, are in different positions in the structure as a result of these conformational changes. Chloride C4 in molecule A hydrogen bonds to the guanidinium of Arg58, whereas in molecule B it hydrogen bonds to the side chain of Arg139. Chloride C4 in molecule A hydrogen bonds to the NE of Arg58, whereas in molecule B the hydrogen bond is to NH2 of Arg58.

Finally, away from the active site, chloride C6 hydrogen bonds to the amide nitrogen of Glu85 at the end of an α-helix and chloride C7 (which shows partially occupancy) hydrogen bonds to NH2 of Arg88. These two chlorides form the types of interactions seen for the other chlorides which are interacting with either the main chain amide at the end of an alpha helix (helix dipole) or a positively charged amino acid side chain.

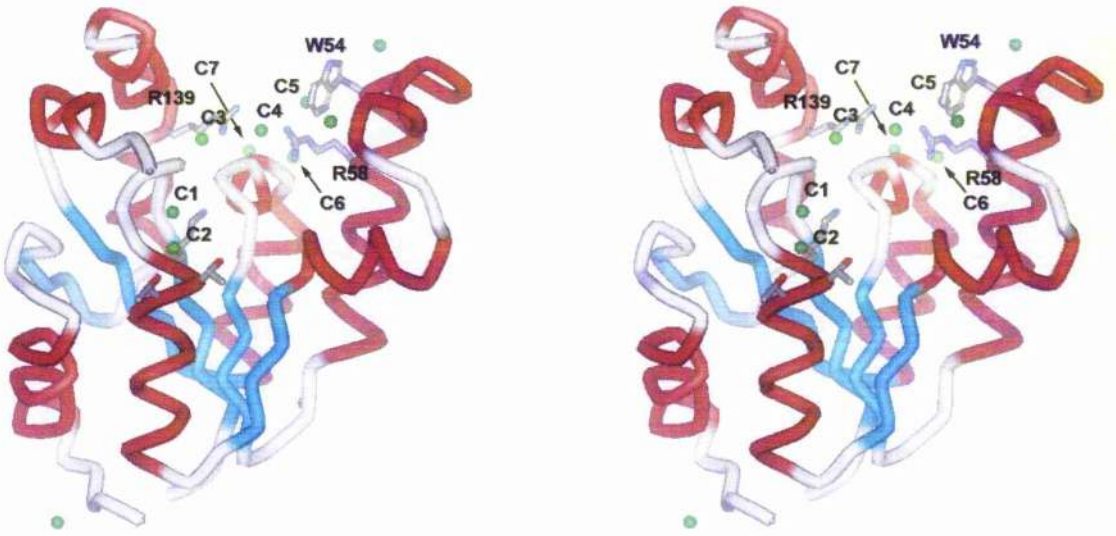

Figure 4.32: A stereoview of the native shikimate kinase structure.

Molecule A is represented in tubular form coloured according to secondary structure (α-helix red, β-sheet green). Chloride ions are shown as green spheres and are labelled C1 - C7; these are designated as 601-607 in the PDB file. Key amino acid side chains are represented as stick, coloured according to atom type, and labelled in black. The diagram was composed in WEBLAB viewer (Accelrys, Inc.)

4.10.4 Structural basis for effects of salts on shikimate kinase

The presence of discrete chloride ions within in the structure of SK permits a structural interpretation of a number of the solution studies. Discrete sulphate binding sites have not been observed directly in any crystal structure of SK but their probable positions can be deduced from the positions of inorganic phosphate in the K15M mutant of SK (Krell *et al.*, 2001) and of the phosphate groups of ADP in the SK-ADP complex.

There is compelling evidence that like other NMP kinases, SK can undergo significant conformational changes on binding substrates. The observation that chloride ions lead to a tightening of the structure of SK can be rationalised by the binding of chlorides C1 and C2 in the P-loop of the protein, thereby potentially ordering the lid domain of the structure. Chlorides C3, C4 and C5 interact directly with residues implicated in shikimate binding, namely Arg58 and Arg139. Both regions are responsible for hinged movements characteristic of NMP kinases. Tightening of the structure is a characteristic of substrate binding and therefore it is not surprising that both chloride and sulphate inhibit binding of ATP and shikimate in the catalytically competent orientation. That inhibition of enzyme activity increases in an ionic strength-dependent manner probably represents the screening of charges important for shikimate and ATP binding. The structure suggests that this could be due in part to the presence of weak binding sites for chloride and sulphate on the surface of the protein that are the same sites as the binding sites for shikimate and ATP.

The structure shows a number of chloride ions in the vicinity of Trp54. Chlorides C4 and C5 could act to screen the quenching of Trp54 by iodide and, due to their proximity to Arg58, it is probable that sulphate would bind in similar positions and perform the same function.

4.11 Conclusions

The presence of salts leads to a marked increase in stability towards unfolding by urea (section 4.8). This effect could reflect general effects of the ionic strength as well as specific binding to, and hence stabilisation of, the folded state (section 4.2). An interesting feature of this work is that it is possible to induce refolding of the enzyme in 4M urea, simply by increasing the ionic strength. This type of behaviour has been observed in a few other systems, such as the 63-residue N-terminal domain of the C1 repressor from bacteriophage 434 (Dotsch *et al.*, 1995) and the peroxidase from *Coprinus cinerus* (Tams and Welinder, 1996).

Although the refolded SK has similar secondary and tertiary structure to the native enzyme as judged by CD and fluorescence and appears able to bind shikimate, albeit more weakly than native enzyme and with a reduced conformational response as judged by the limiting extent of fluorescence quenching. However, although there is no direct evidence (from fluorescence quenching data) for binding of nucleotide substrates to the refolded enzyme, there is indirect evidence for some interaction with nucleotide from the observed tightening of shikimate binding in the presence of 2mM ADP (Table 4.12). The failure of the refolded enzyme to display catalytic activity is likely to reflect subtle perturbations both of the nucleotide binding site itself and of the ability of the enzyme to bring the substrates into the correct alignment for the phosphotransfer reaction. It remains a task for future work to characterise this "partially folded" form of SK in more detail and to examine whether conditions can be found under which it can be readily converted to an active form.

Appendix 4.1 Refolding of SK in the presence of salts

The refolding of SK in the presence of different concentrations of salts was carried out to examine the effect of residual ionic strength on the refolding reaction and to check for any specific effect. For this purpose NaCl, Na_2SO_4 and, to some extent, NaF were used.

A4.1.1 Regain of Activity

The presence of NaCl or Na_2SO_4 in solution leads to inhibition of SK as reported in section 4.5. The residual activities at concentrations of 0.25M NaCl and 0.085M Na_2SO_4 are 88.8% and 84.5% respectively. Because at higher concentrations there is a more pronounced inhibition, these two concentrations were chosen to follow the regain of activity and, as a control, a protein solution at the same salt concentration was tested. From the results obtained (Fig. A4.1) it was not possible to fit satisfactorily the data because the process is faster than in the absence of salts and the initial amplitude is higher, indicating that a large amount of activity has been regained before the first data point could be collected.

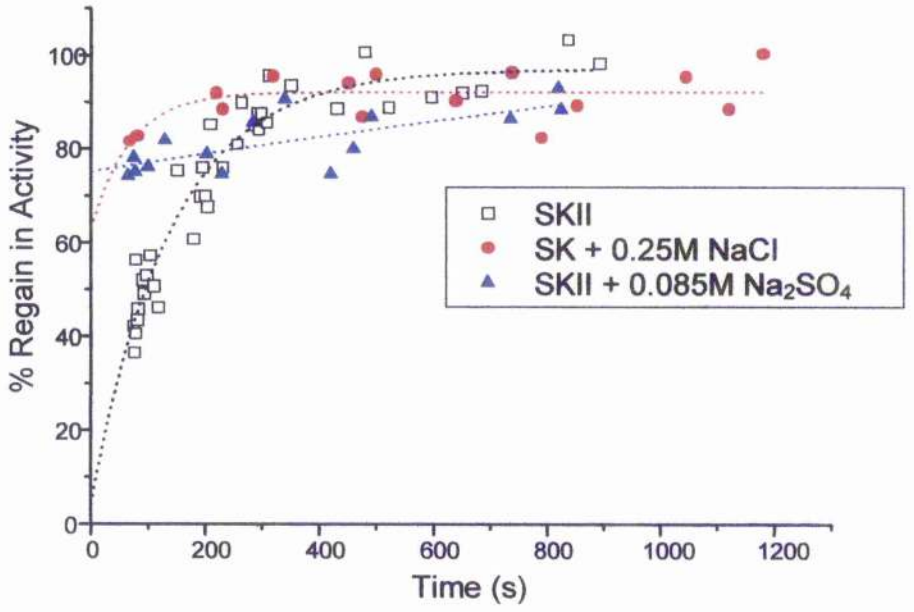

Figure A4.1: The kinetics of regain of activity: effect of added NaCl and Na_2SO_4

The data show the regain in activity in Tris buffer and in Tris buffer in the presence of salts. Activity values are expressed relative to a control sample incubated in the presence of the final concentration of urea, and salt i.e. 0.36M urea + 0.25M NaCl or 0.085M Na_2SO_4.

A4.1.2 Regain of secondary structure

The regain of CD signal at 225nm was followed when NaCl, Na_2SO_4 and NaF were present in the refolding buffer. All the controls were prepared in the presence of 0.36M urea and salt. The concentrations of salt used in the refolding buffer were: 0.25M and 1M for NaCl (Fig. A4.2a); 0.085M and 0.17M for Na_2SO_4 (Fig. A4.2b) and 0.5M for NaF (Fig. A4.2c). In general the presence of these salts seems to accelerate the rate of regain of secondary structure, though no fitting was possible because the regain was nearly complete in the dead time of the manual mixing experiment (20s). Addiction of NaF leads to the regain of only the 46% of the signal of the control solution; hence it probably interferes with the refolding process.

It has to be noted that, performing the refolding with GdmCl (2.8M → 0.25M) the regain of the CD signal was complete within the dead time of the manual mixing experiment (Boam, 1999). While NaCl leads to a complete regain of the control signal at both concentrations, Na_2SO_4 at 0.33M does not (67% of the control signal is regained), even though this salt is a better stabiliser. These data suggest that the ionic strength could play an important role in the refolding of SK. Because the process is faster than in the absence of salts it is not possible to check eventual differences in stabilising refolding intermediates between the two salts used. For this reason it would be interesting to check the regain of secondary structure using the stopped flow apparatus. Only a preliminary stopped-flow experiment with 1M NaCl in the refolding buffer was carried out (Fig. A4.3), but more experimental work would be necessary using other NaCl concentrations and Na_2SO_4 to draw any valid conclusions.

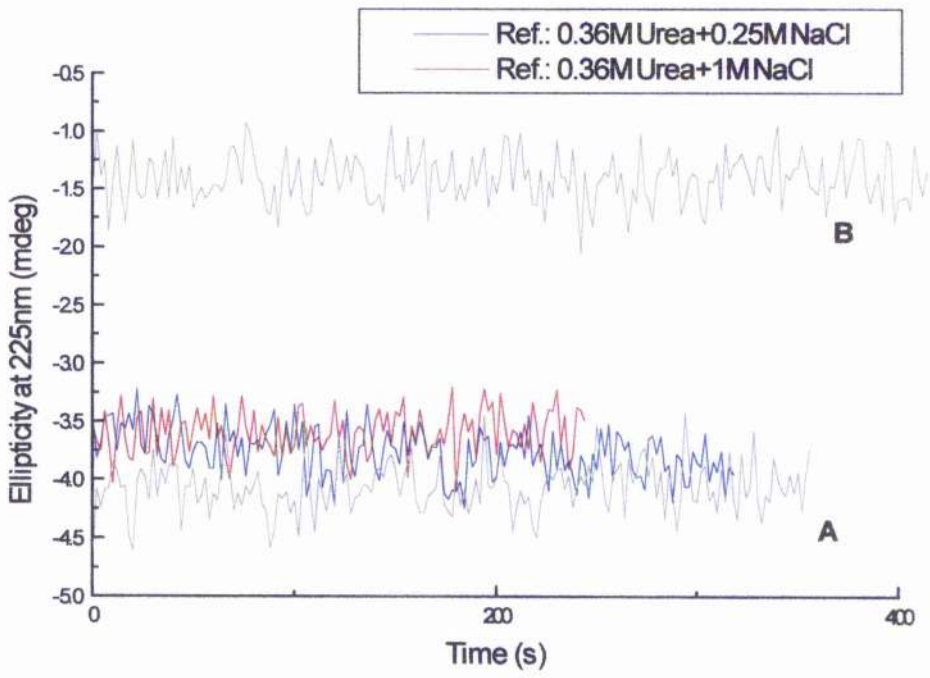

a)

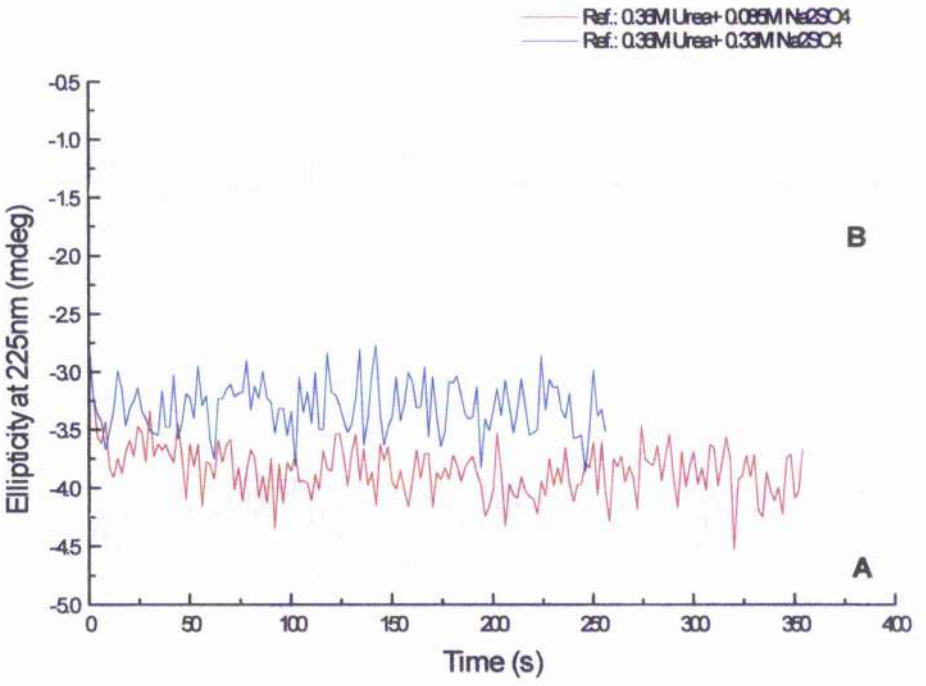

b)

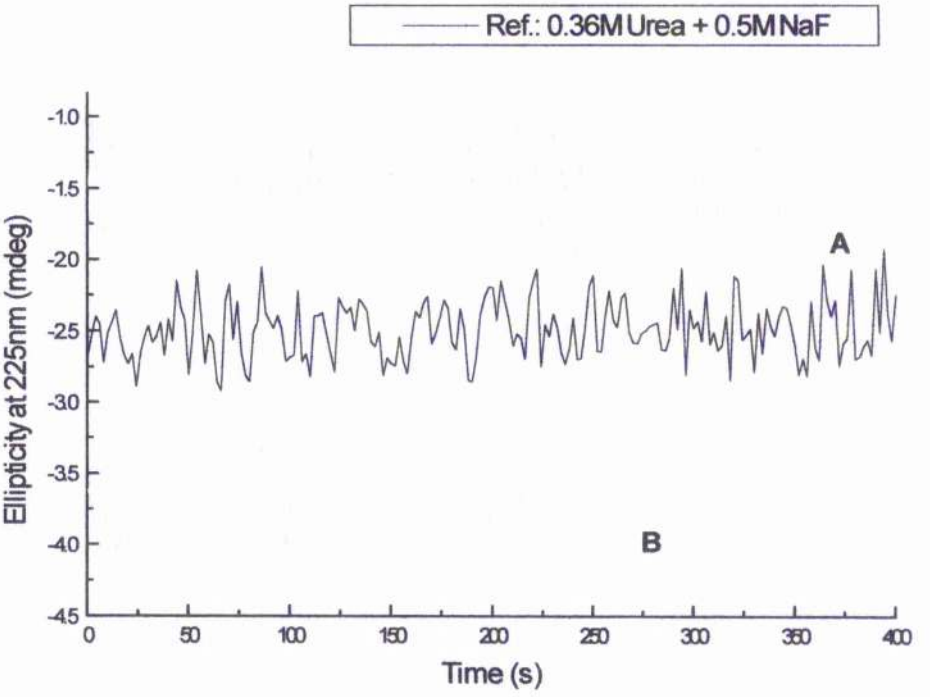

c)

Figure A4.2: Kinetics of changes in ellipticity in the presence of salts (manual mixing).

Protein denatured by incubation in 4M Urea. The SK concentration was in the range 0.08 – 0.09mg/ml and the cell pathlength was 0.05cm. A and B refers to the start (4M Urea) and end (0.36M Urea + salt) solutions.The refolding was started by dilution, lowering the urea concentration to 0.36M following the change of signal at 225nm, in buffer containing different concentration of salts: a) 0.25M and 1M NaCl; b) 0.085M and 0.33M Na_2SO_4 c) 0.5M NaF.

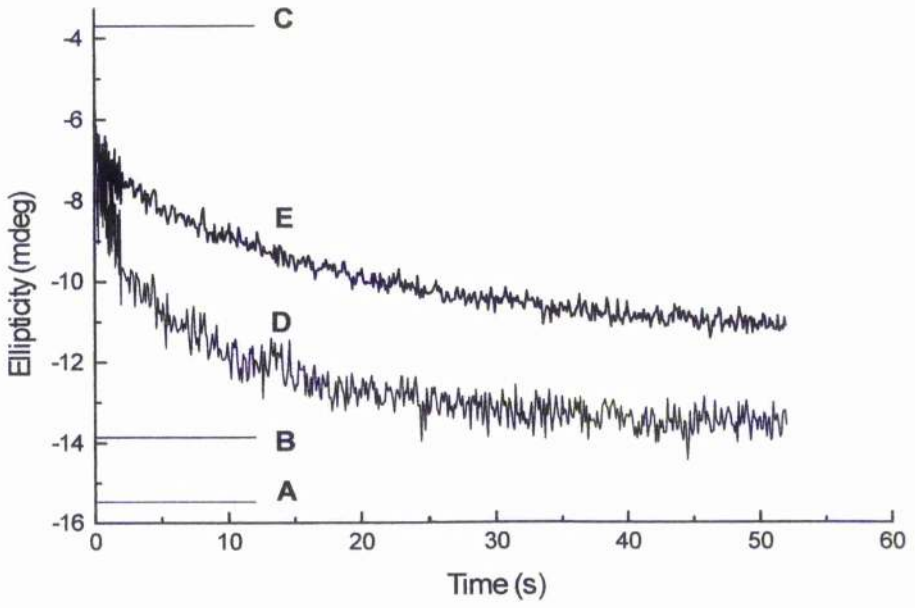

Figure A4.3: Kinetics of changes in ellipticity in the presence of 1M NaCl (stopped flow)

Refolding of SK after denaturation in 4M urea.The refolding was initiated by stopped flow mixing and monitored at 225nm; the inset shows data in the first 2s of the reaction. Curves A, B and C refer to enzyme in the presence of 0.36M urea + 1M NaCl, enzyme in the presence of 0.36M urea, and enzyme in the presence of 4M urea. Curves E and D are the refolding curves in buffer and in buffer +1M NaCl respectively.

A4.1.3 Regain of fluorescence intensity

A4.1.3.1 Preliminary Light scattering experiments

During the refolding in the presence of GdmCl the light scattering signal was greater than the upper experiment detection limit (1000 units) for both the refolded and the equilibrium solution (0.25M GdmCl). An ionic strength jump was performed (2.8M → 0.25M NaCl) to assess if the aggregate formation was influencing the fluorescence signal during the refolding (section 3.4.1.5). This experiment led to the conclusion that the observed aggregation at 0.25M GdmCl derived both from the ionic strength jump and from the induced aggregation of partially exposed hydrophobic surfaces.

Light scattering experiments were performed, as described in section 2.4, to check for formation of aggregate in the presence of higher concentrations of salts. Solutions at two different protein concentration (0.1mg/ml and 0.15mg/ml) and salt concentration (0.25M, 0.5M and 1M) were prepared and the light scattering was measured ($\lambda_{ex} = \lambda_{em}$ =320nm). Only for the solution at 1M NaCl was the light scattering signal greater than 1000 units.

A4.1.3.2 Regain of fluorescence intensity in the presence of chloride

When NaCl was included in the refolding buffer a different pattern of refolding was observed (Fig. A4.4). In general the presence of NaCl leads to an increase of the refolding rate, with the lowest concentrations of NaCl being more effective than the higher one. No important difference is observed between 0.25M and 0.5M, both giving traces that could be fitted with a double exponential function indicating the existence of at leasts two phases with rate constants, for the refolding in 0.25M NaCl, of $0.12s^{-1}$ (no salt: $0.08s^{-1}$) and $0.012s^{-1}$ (no salt: $0.009s^{-1}$). The rate constants and relative amplitude of the phases are reported in appendix 4.2. During the refolding in the presence of 1M NaCl some aggregate formation may occur: in fact the refolded solution in the presence of 1M NaCl gives light scattering signal at 320nm greater than 1000 units.

The effect of protein concentration was checked for the refolding in the presence of 0.25M NaCl where the biggest effect on the refolding rate had been observed. The refolding traces, after normalisation, for protein concentrations of 0.1mg/ml and 0.5mg/ml are coincident (Fig. A4.5). Moreover the nature of the cation had no effect on the refolding rate as demonstrated by refolding experiments performed including 0.25M KCl in the refolding buffer (Fig. A4.6). It would be interesting to perform these experiments using the stopped flow instrument because the most significant difference that is observed in the manual mixing mode is in terms of the initial amplitude from 32% in the absence of salt (considering the manual mixing trace) to 45% (value referred to the refolding trace obtained in 0.25M NaCl). Only one trial experiment was carried out with stopped flow mixing, at 1M NaCl (Fig. A4.7). The rate constants obtained fitting the curve with a double exponential function are: $0.094s^{-1}$(no salt: $0.08s^{-1}$) and $0.017s^{-1}$(no salt: $0.009s^{-1}$) so it seems that the most significant effect of the NaCl, at this concentration, is on the rate constant of the slower phase.

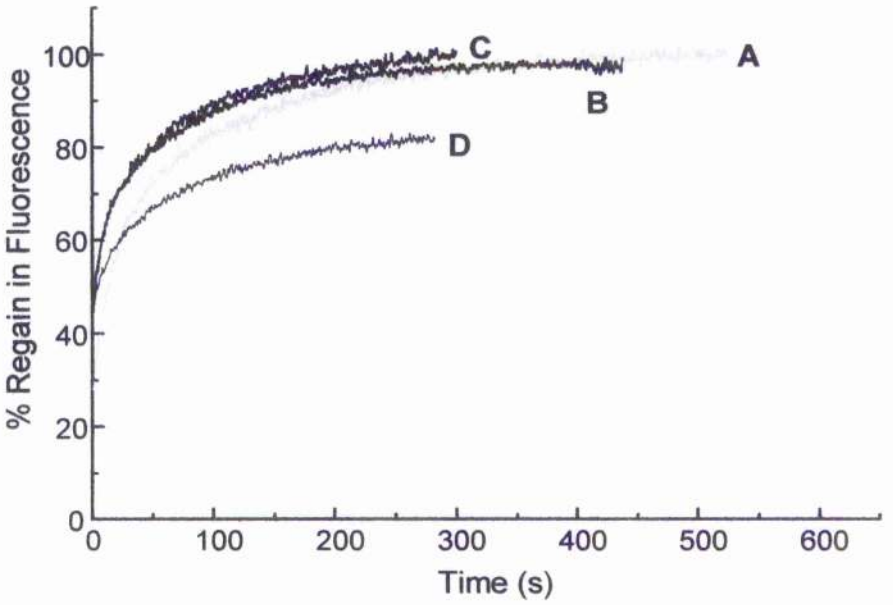

Figure A4.4: Kinetics of changes in protein fluorescence in the presence of NaCl.

Refolding of SK, initiated by manual mixing, after denaturation in 4M urea and followed at 350nm. Curves A, B and C refer to refolding of the enzyme in the refolding buffer (A) and in the presence of: 0.25M NaCl (B), 0.5M NaCl (C) and 1M NaCl (D).

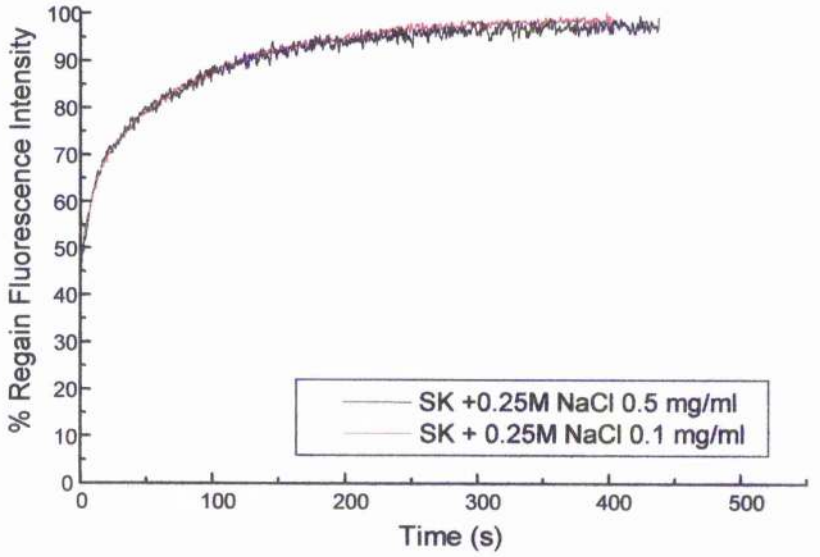

Figure A4.5: Protein concentration dependence of the kinetics of refolding.

Kinetics of changes at 350nm. Protein denatured in 4M Urea at two different concentrations and refolded by 11-fold dilution in buffer containig 0.25M NaCl

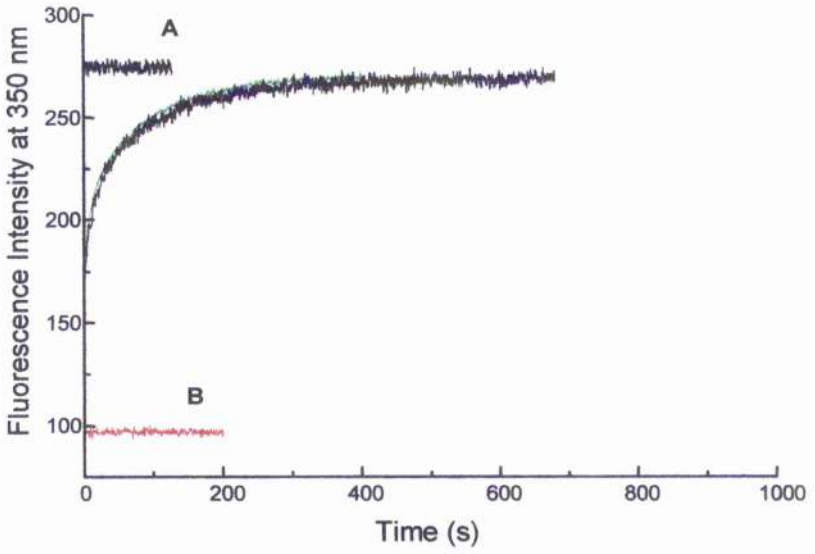

Figure A4.6: Kinetics of changes in protein fluorescence in the presence of NaCl and KCl

Refolding of SK, initiated by manual mixing, after denaturation in 4M urea and followed at 350nm. The data shows the refolding of the enzyme in the presence of: 0.25M NaCl (green) and in the presence of 0.25M KCl (black). The end (A) and start (B) point are reported.

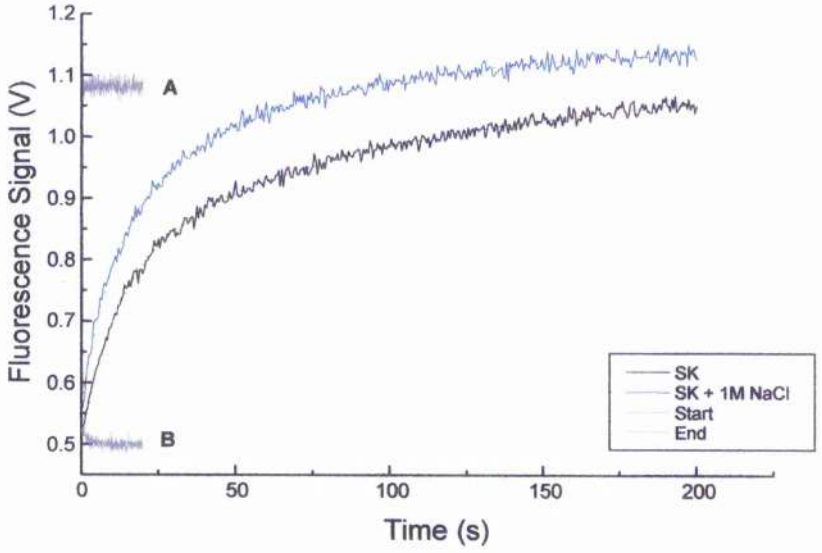

Figure A4.7: Kinetics of changes in protein fluorescence in the presence of 1M NaCl.

Refolding of SK after denaturation in 4M urea. Refolding was initiated by stopped flow mixing and followed at 350nm. The fluorescence signals have been corrected for the buffer signal. Curves A, B refer to enzyme in the presence of 0.36M urea and enzyme in the presence of 4M urea. The black curve is referred to the enzyme during refolding in buffer and the blue curve to the enzyme during refolding in buffer +1M NaCl.

A4.1.3.3 Regain of fluorescence intensity in the presence of sulphate

The effect of sulphate on the refolding of SK is different from that observed in the presence of NaCl at the same ionic strength (Fig. A4.8). At low concentration of Na_2SO_4 only a small increase of the refolding rate is observed: the k_1 is raised from $0.08s^{-1}$ in the absence of salts (manual mixing trace) to $0.1s^{-1}$ in the presence of 0.85M Na_2SO_4, while the k_2 increases from $0.009s^{-1}$ to $0.010s^{-1}$. But at higher ionic strength, the rate decreases respect to the rate of refolding in the absence of salt (k_1= $0.03s^{-1}$ and k_2= $0.005s^{-1}$ in 0.33M Na_2SO_4 - see appendix 4.2 for the rate constants and phase amplitude values). With Na_2SO_4 the light scattering was <1000 units after a jump to 0.085M but there is aggregation for the jumps to 0.17M and 0.33M. There is an increase of the starting amplitude in the presence of Na_2SO_4 (32% in the absence of salt, referred to the manual mixing trace, and 38%, 48% and 49% in the presence of 0.085M, 0.17M and 0.33M Na_2SO_4 respectively), but a concomitant decrease of the refolding yield, i.e. 94%, 83% and 71% for Na_2SO_4 concentrations of 0.085M, 0.17M and 0.33M respectively.

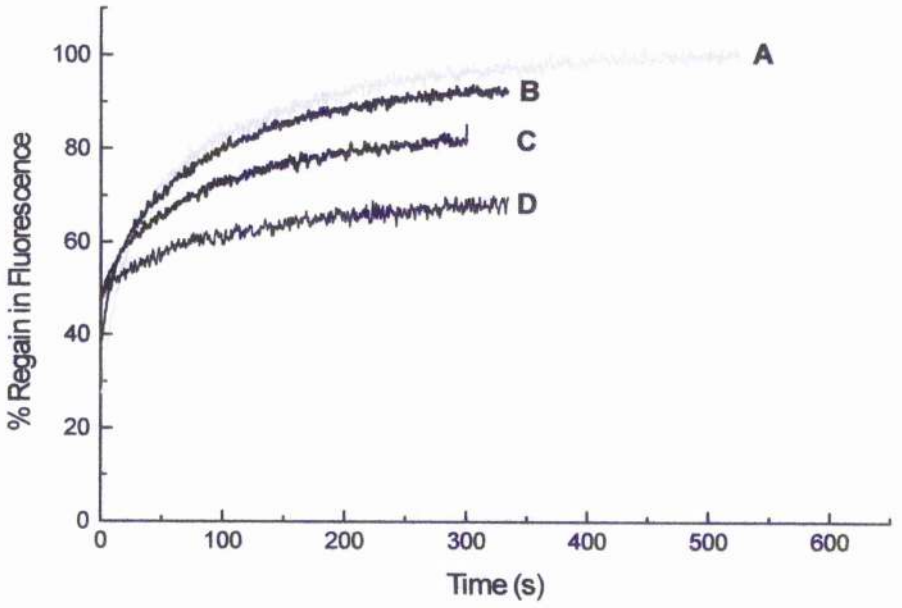

Figure A4.8: The kinetics of changes in protein fluorescence in the presence of Na_2SO_4.

Refolding of SK, initiated by manual mixing, after denaturation in 4M urea and followed at 350nm. Curves A, B and C refer to refolding of the enzyme in the refolding buffer (A) and in the presence of: 0.085M Na_2SO_4 (B), 0.17M Na_2SO_4 (C) and 0.33M Na_2SO_4 (D).

A4.1.3.4 Refolding in the presence of fluoride

The fluoride ion is another strong stabiliser of SK (section 4.8) and has no major effect on the secondary structure or fluorescence intensity of SK (section 4.3); however it inhibits the SK activity at lower concentrations when compared with the other salts tested (section 4.4). It has no effect on the shikimate binding (section 4.5) but it has an effect on the nucleotide binding leading to a decrease of the K_d for ATP at low concentration (0.1M) (section 4.6). When the refolding was carried out in the presence of 0.5M NaF there is a regain of 50% of the native fluorescence relative to the end point of the protein solution in the presence of fluoride (Fig. A4.9). The fluorescence spectrum of the refolded solution is native-like in terms of the emission maximum wavelength (Fig. A4.10).

This effect on the refolding is not common, for example it has been found that fluoride ion induced an acceleration of the oxidative folding of reduced pancreatic ribonuclease A (Low *et al.*, 2000). Further investigations would be necessary to check the reason for the observed effect.

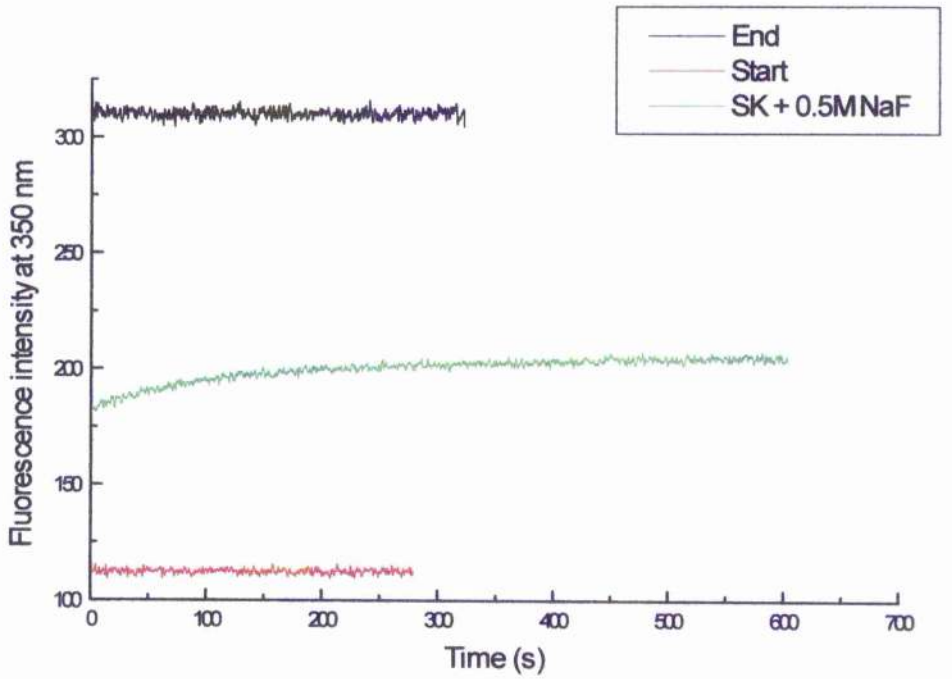

Figure A4.9: Kinetics of changes in protein fluorescence in the presence of NaF

Refolding of SK, initiated by manual mixing, after denaturation in 4M urea and followed at 350nm. Protein concentration was 0.084mg/ml.

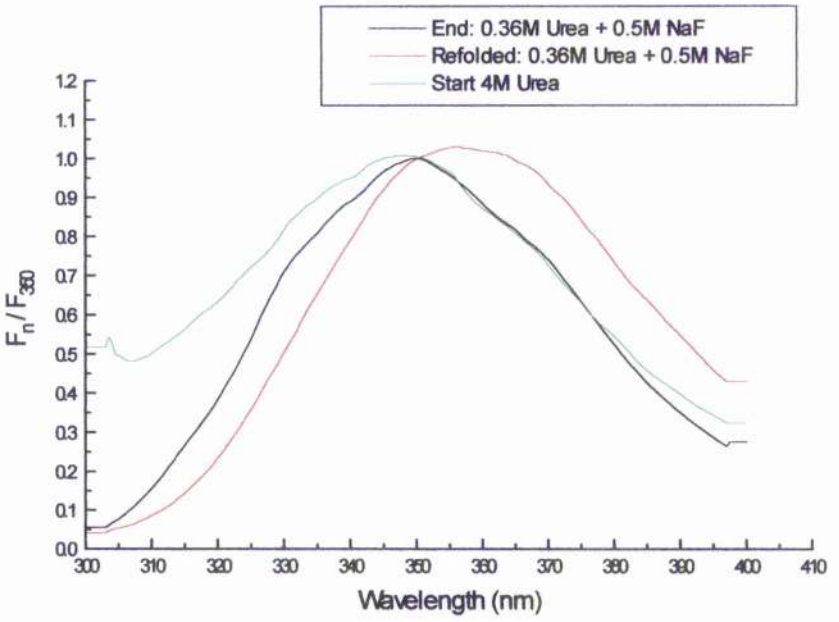

Figure A4.10: Normalised fluorescence spectra (refolded solution) in the presence of NaF

Spectra were recorded at 20°C in the 300-400nm range after excitation at 295nm, T= 20°C and normalised dividing for the intensity at 350nm (F_n/F_{350}).

A4.1.4 Refolding with salts in the presence of sodium iodide

The refolding in the presence of 0.1M NaI was performed only in the presence of 1M NaCl, (Fig. A4.11) but because of the ionic nature of the quencher, further experiments in the presence of salts were not undertaken because of difficulties of interpretation of the experiments due to the multiple effects present.

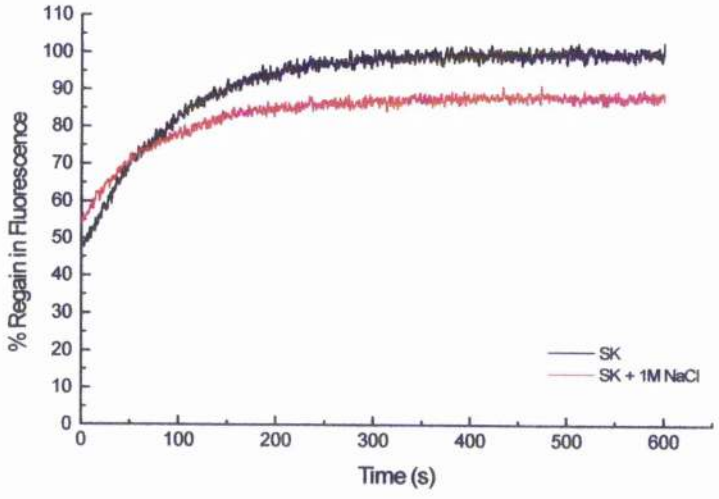

Figure A4.11: Refolding of denatured SK in the presence of 1M NaCl (NaI 0.1M)

Kinetics of changes in fluorescence at 350nm. The curves represent refolding of SK brought about by dilution in buffer (black) and buffer +1M NaCl (red) in the presence of 0.1M NaI.

A4.1.5 Refolding in the presence of ANS

A4.1.5.1 ANS spectra in the presence of NaCl

The effects of different conditions on both ANS florescence and on the fluorescence of the ANS bound to SK was investigated. Fluorescence spectra of an ANS solution (40 μM) in buffer, in the presence of 1M NaCl and 4M urea plus 1M NaCl, both in the absence than in the presence of protein were acquired. The free-ANS spectra, the SK bound ANS spectra and the difference spectra $(SK.ANS)_{(cond.\ X)} - (ANS)_{(cond.\ X)}$ are reported (Fig. A4.12 (a,b,c)). The presence of NaCl leads to an increase in the fluorescence of ANS in solution (free ANS) (Fig. A4.12a), but a decrease in the fluorescence when protein is present (Fig. A4.12b). From the difference spectra (Fig. A4.12c) it seems that the presence of urea does not allow ANS to bind to the protein. This is also observed in the presence of 1M NaCl, conditions under which SK has a native-like conformation.These results are useful to interpret the kinetics of ANS fluorescence change during refolding in the presence of salts (section 4.10.5.2) and of the refolding in 4M urea induced by salt (section 4.11). In fact, because the presence of NaCl in solution leads to a decrease of ANS fluorescence the initial increase observed in the refolding experiment when salt is present in the refolding buffer cannot be due to an artefact. Moreover, the competition of urea for ANS binding sites could explain the absence of ANS binding observed during the refolding in 4M urea induced by salts.

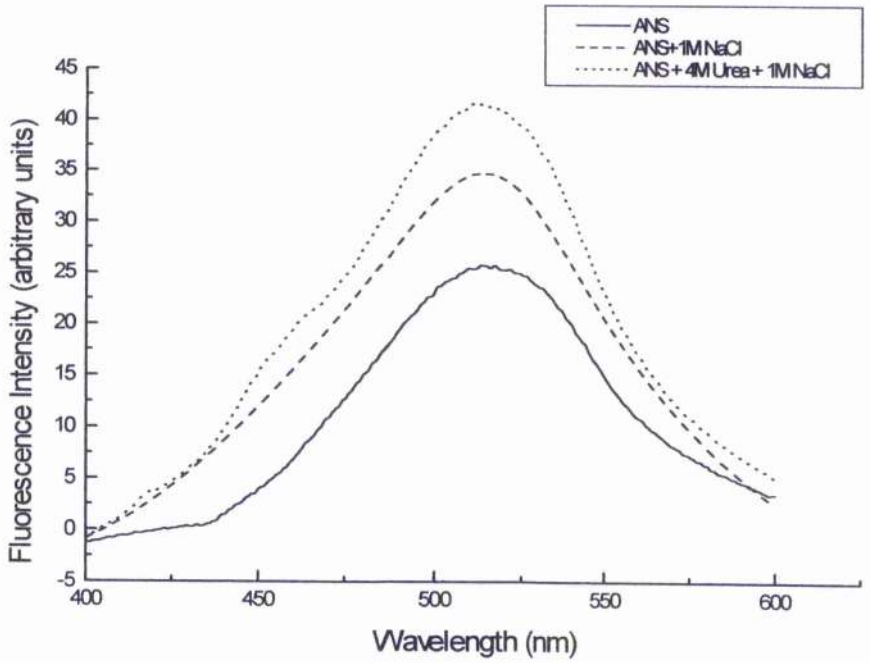

a)

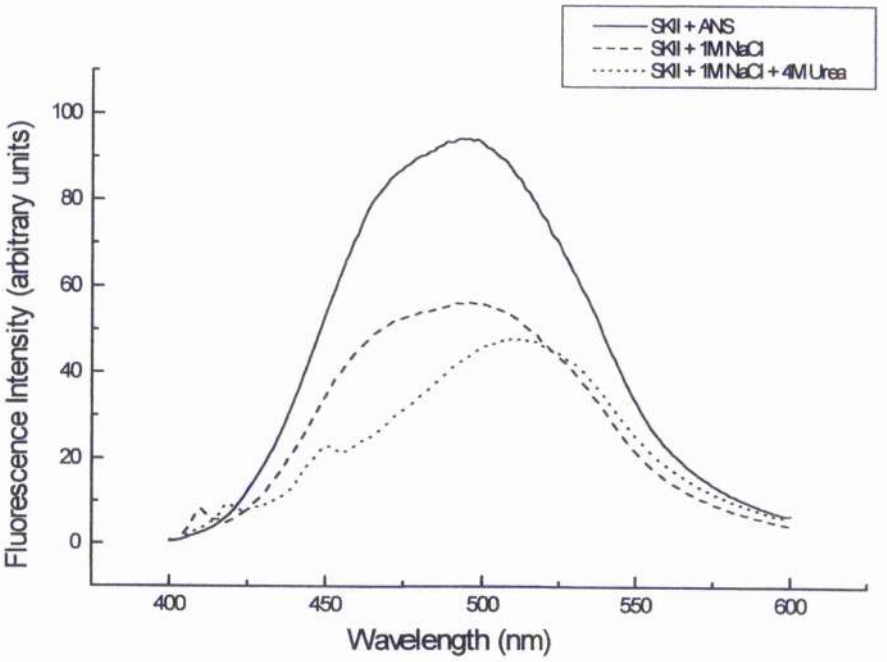

b)

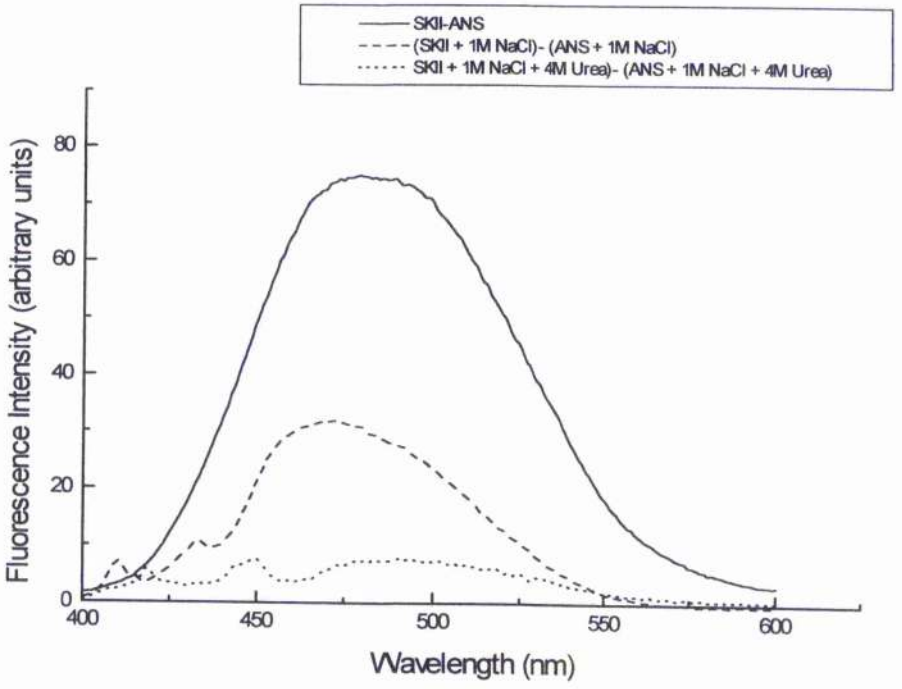

d)

Figure A4.12: ANS spectra (40 μM) in buffer and in the presence of NaCl and Urea. The emission spectra were acquired after excitation at 380nm. Solid line : ANS and buffer; dotted line: ANS in the presence of 1M NaCl + 4M Urea; dashed line: ANS in the presence of 1M NaCl respectively and in the absence (a) and in the presence of protein (b). (c): difference spectra: $(SK.ANS)_{(cond.\ X)} - (ANS)_{(cond.\ X)}$

A4.1.5.2 Refolding in the presence of ANS

The refolding experiment in the presence of ANS was carried out at only one concentration of NaCl (1M). Figure A4.13 shows a comparison between the traces obtained in the absence and presence of salt. It seems that the presence of salt increased the initial jump observed.

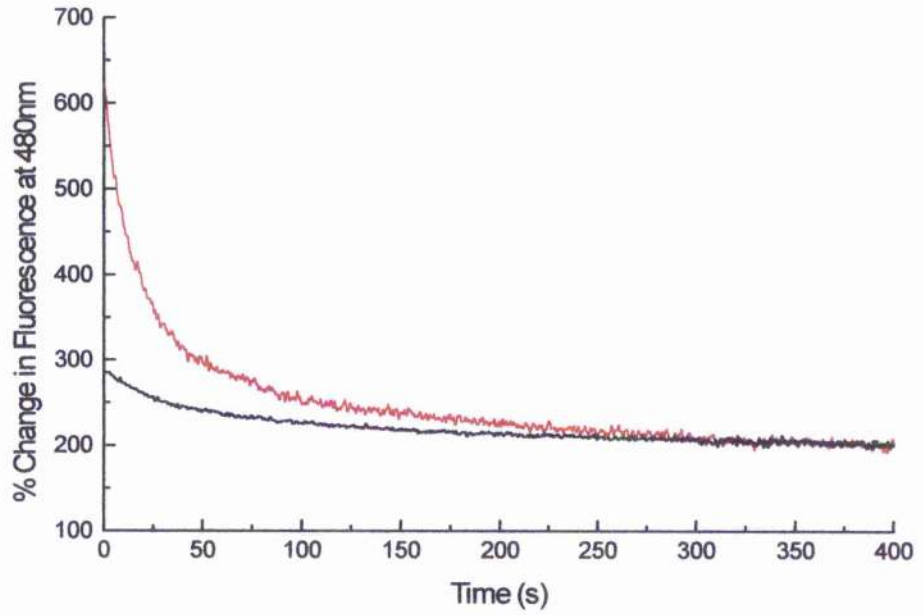

Figure A4.13: Changes in ANS fluorescence in the presence of 1M NaCl.
Refolding of SK (manual mixing) after denaturation in 4M urea. Change in ANS fluorescence during refolding in buffer Tris (black), buffer Tris+1M NaCl (red). The protein concentration was 0.1mg/ml and the ANS concentration 40μM.

A4.1.6 Conclusions

From the refolding experiments in the presence of salts after dilution of urea from 4M to 0.36M it appears that both the ionic strength and the chloride ions have an influence on the refolding process of SK . The presence of salts in the refolding buffer seems to accelerate, at low concentrations of NaCl or Na_2SO_4, the rate of regain of both structure and activity, while fluoride ion seems to impair this process. Further studies on the effect of fluoride on SK would be interesting because of the effects this salt has on binding, stability and refolding. The results obtained with NaCl or Na_2SO_4 could explain the faster refolding observed when GdmCl was used as denaturant (Boam, 1999) and underline the importance of taking into accont the residual ionic strnegth of the solution. From the observed differences between NaCl and Na_2SO_4 it seems possible that the two salts exert their effects by different mechanisms. Stopped flow experiments using these two salts would be useful to distinguish between different mechanisms because, for example in the manual mixing CD experiment, all the changes happened before the dead time of this experiment. The increase observed in ANS fluorescence in presence of salt could be an indication of the formation of a more compact intermediate, but again stopped flow experiments could be useful to investigate this in more detail.

Appendix 4.2: Refolding in the presence of salts: fitting values

	SK + 0.25M NaCl	SK + 0.5M NaCl	SK + 1M NaCl
Fluorescence (Manual Mixing)	A_1 = 19.35 ± 0.12 k_1 = 0.12 ± 0.0015 A_2 = 33.5 ± 0.08 k_2 = 0.012 ± 0.00004 B = 97.87 ± 0.017	A_1 = 22.61 ± 0.18 k_1 = 0.11 ± 0.0019 A_2 = 35.67 ± 0.12 k_2 = 0.011 ± 0.00008 B = 100.64 ± 0.053	A_1 = 10.75 ± 0.18 k_1 = 0.068 ± 0.0019 A_2 = 26.74± 0.14 k_2 = 0.098 ± 0.00012 B = 83.41 ± 0.07
	SK + 0.085M Na_2SO_4	**SK + 0.17M Na_2SO_4**	**SK + 0.33M Na_2SO_4**
Fluorescence (Manual Mixing)	A_1 = 16.70 ± 0.13 k_1 = 0.099± 0.0016 A_2 = 38.5 ± 0.09 k_2 = 0.010 ± 0.00005 B = 93.66 ± 0.038	A_1 = 7.2 ± 0.16 k_1 = 0.084± 0.0037 A_2 = 27.85 ± 0.12 k_2 = 0.0098 ± 0.0001 B = 83.1 ± 0.062	A_1 = 6.51 ± 0.57 k_1 = 0.032± 0.003 A_2 = 15.61 ± 0.31 k_2 = 0.0054 ± 0.0004 B = 70.8 ± 0.37

Table A4.1: Values of the fitting of refolding in the presence of salt (denaturant dilution)

Conditions	Fluorescence	Fluorescence +NaI	CD
SK + 4M Urea + 1M NaCl	A_1 = 13.9 ± 1.43 k_1 = 0.0046 ± 0.0002 A_2 = 78.12 ± 1.42 k_2 = 0.0022 ± 0.00002 B = 95.3 ± 0.034	A_1 = 7.24 ± 0.14 k_1 = 0.042 ± 0.0017 A_2 = 84.85 ± 0.12 k_2 = 0.0054 ± 8.56 10^{-6} B = 102.6 ± 0.014	A = 73.7 ± 0.27 k = 0.002 ± 0.00002 B = 21.9 ± 0.27
SK + 4M Urea + 0.33M Na_2SO_4	A_1 = 42.93 ± 0.45 k_1 = 0.019 ± 0.0002 A_2 = 49.66 ± 0.44 k_2 = 0.0047 ± 0.00004 B = 100.01 ± 0.0458	A_1 = 31.62 ± 0.71 k_1 = 0.016 ± 0.0003 A_2 = 40.61 v 0.695 k_2 = 0.0043 ± 0.00007 B = 98.42 ± 0.072	A = 55.1 ± 1.39 k = 0.0083 ± 0.00046 B = 35.8 ± 1.48

Table A4.2: Values of the fitting of the refolding traces (ionic strength jump experiments)

A_1, k_1, A_2, k_2 are respectively the amplitude and the rate constants of the first and second phases of the process. B is the total amplitude regained during the process. The amplitude at the beginning of the process is given by difference: B minus the amplitude of the two phases. In the last column (CD) of table 4.14: A is the amplitude of the phase with k being the rate constant, while B is the starting amplitude. The total amplitude regained during the process is given summing B and A.

Chapter 5: General Discussion

5.1 Activity and ligand binding studies

To be catalytically active an enzyme such as SK must bind the substrates in the correct position to allow the movements that lead to productive catalysis. For SK, as for other NMP kinases, during catalysis there is the closure of the active site around the bound substrates (hinge-bending motions). These motions have low energy barrier heights between the well minima so the relative equilibrium between populations of the closed and the open conformations can be shifted by external factors, such as pH, T or ionic strength (Sinha *et al.*, 2001). The comparison between the effect of different salts and denaturants on SK has highlighted differences between the effects of anions on substrate binding and catalysis.
In fact it has been found that non-ionic species, such as urea, lead to a loss of activity, with 85% and 40% activity retained in the presence of 1M and 2M urea respectively, while the incubation of SK with low concentrations of GdmCl or salts leads to more marked losses of activity. It should be pointed out that only minor differences have been observed in the far-UV CD and fluorescence spectra of SK in the presence of salts: this rules out the possibility of a major structural alteration as a possible explanation of the observed decrease in activity.
The decrease in activity has been found to be related to the ionic strength of the solution with the exceptions of NaF and $NaNO_3$, which lead to higher degrees of inactivation at the same concentration as the other salts used. Under these conditions different factors, such as specific binding to particular residues or preferential hydration of protein surfaces (leading to an increase the hydrophobic interactions) can affect enzyme activity. The two effects will lead to a decrease in activity by different mechanisms: the ions can bind to a site close to the substrate binding site establishing interactions with residues which normally interact with the substrate or, in the second case, the increase in the rigidity of the enzyme could lead to the elimination of the dynamic motion that is required for efficient catalysis.
That an increase in ionic strength leads to an increase in structural rigidity has been suggested by the increased intensity of the CD signal in the near-UV region. The study of the effects of salts and denaturants on the binding and kinetic parameters has given further insights allowing some distinction between these two mechanisms to be made. In fact it was expected that, if the first mechanism was predominant, there would be a bigger effect on the binding constant while, if the rigidity of the protein was responsible for the observed decrease of activity, there would be still binding though not productive, leading to a decrease in V_{max}.
The quenching of the fluorescence of the single Trp residue of SK (Trp54) as consequence of the binding of shikimate, and to a lesser extent of nucleotides, (Idziak *et al.*, 1997) has

been extensively used to study the effects of the solvent conditions on the binding of substrates. In particular it seem that while the change in ionic strength has the largest effect on shikimate binding and a smaller effect on nucleotide binding, the effects of urea (non-ionic) appear to be more marked in the case of the ADP binding than for the shikimate. This could indicate that different kind of interactions are predominant for the binding of these two substrates: in the case of shikimate binding electrostatic interactions play a major role, whereas in the binding of nucleotides the main factor is hydrophobic interactions, which would explain the larger effect of urea on the binding of ADP. It would be of interest to study the effects of other non-ionic co-solvents on the binding of nucleotides.

When titration experiments with shikimate were carried out in the presence of ADP the effect of medium composition on the hinge-bending movements was demonstrated. The decrease of the K_d for shikimate in the presence of ADP has been considered to be a consequence of the hinge-bending movements typical of NMP kinases. This degree of synergism has been found to be very markedly dependent on the type of salt present in the buffer system. From this it follows that it is important to consider the effects of different medium conditions on parameters such as binding and activity. In the case of SK, use of a different buffer system (MOPS) instead of the Tris normally used gave different results as far as the binding of shikimate and the substrate synergism were concerned.

Analysis of the effects of salts on the kinetic parameters of SK indicates that while the K_m for shikimate is increased in the presence of chloride, although to a smaller extent that the K_d, the effects of sulphate on the K_m for shikimate are less pronounced than those of chloride. Both salts lead to a marked reduction in the catalytic efficiency (as reflected by V_{max}) of the reaction. The magnitude of V_{max} presumably reflects the ability of the domains of the enzyme to move so as to ensure the correct alignment of substrates, as well as to undergo conformational changes required for product release.
These data were confirmed by the re-analysis of the crystallographic data using the recently refined structural model (1SHK) with the identification of specific chloride binding sites on the enzyme. The binding sites are mainly arginine side chains and, in particular, chloride ions establish interactions with two residues involved in the binding of the carboxylate group of shikimate, Arg139 and Arg58. Probably the binding of ADP affects in some way the binding of these chloride ions increasing the K_d for shikimate: this could explain the higher degree of synergism observed when chloride was present in the buffer system.

Further work using methods such as NMR or fluorescence energy transfer would be required to characterise further the changes in mobility. Moreover it would be interesting to study in more detail the effects of NaF on activity and binding by determining the K_m and V_{max} in the presence of this salt.

5.2 Stability studies: Chemical denaturation

The stability and activity of an enzyme are two parameters which do not always go in the same direction. This is especially true for enzymes, such as SK, where flexibility plays a determining role in catalysis. A flexible molecule can be depicted as having an energy funnel with a rugged bottom with low energy barriers separating the conformers. A change in solvent composition will result in a change in the height of these barriers. So a thermodynamic stabilization, influencing the distribution of conformers, could lead to a higher kinetic barrier between the stabilized conformer and the one catalytically competent (Kumar *et al.*, 2000). This seems to be the case for SK which has been found to be strongly stabilised under conditions leading to a marked degree of inactivation.

Chemical denaturation studies employed both urea and GdmCl because it has been demonstrated that the comparison of the effects of these two denaturants can give valuable insights into the understanding of the mechanism of unfolding. Differences were found between the two denaturants used, especially when comparing the changes in activity or the K_d for substrates with the degree of unfolding measured by CD and fluorescence as functions of the denaturant concentration. Unfolding by urea was used for the investigation of salt effects on the protein (Pace and Scholtz, 1997; Pace and Grimsley, 1988): for this purpose a range of different salts and different concentrations of NaCl and Na_2SO_4 have been explored. The salts at high concentrations stabilise the protein conformation mainly by two mechanisms: preferential hydration, ranked in the Hofmeister series, and preferential binding. The stabilising effect observed in the case of SK depends from the anion and the degree of stabilisation can be explained with their position in the Hofmeister series, with the exception of NaCl. Specific effects can arise if there are appropriate ion binding sites in proteins (Pace *et al.*, 1998) as for example calcium binding sites in ribonuclease T_1 (Deswarte *et al.*, 2001) and zinc binding sites in alcohol dehydrogenase (Plapp *et al.*, 1978). The strong stabilising effect of the chloride ion on SK can be explained by ion binding, as suggested by the shikimate binding data and confirmed by crystallographic evidence. In fact the X-ray data show that chloride ions bind at sites which are thought to play a role in the binding of shikimate. The net effect of these mechanisms is rather similar so that 0.33M Na_2SO_4 has a similar but slightly larger effect on $[urea]_{1/2}$ compared with that of 1M NaCl.

It would be interesting to study the effect of nucleotides, especially ATP, on chemical denaturation (ATP has been reported to stabilise the SK against thermal denaturation; Boam, 1999) using GdmCl as denaturant, because of the marked effect of urea on the binding of nucleotide.

5.3 Refolding after denaturation

When SK is refolded from the urea-denatured state the results of spectroscopic and activity studies indicated that refolding occurs in at least 4 kinetic phases: the average rate constants for these phases are >100s^{-1} (half life <7ms), 10s^{-1} (half life 70 ms), 0.08s^{-1} (half life 9s) and 0.009s^{-1} (half life 80s). The slowest phase (k = 0.009s^{-1}) corresponds to the regain of shikimate binding and of enzyme activity and the two most rapid phases are associated with a substantial increase in the binding of 8-anilino-1-naphthalenesulphonate with only modest changes in the far-UV CD. This indicates that a collapsed intermediate with only partial native secondary structure was formed rapidly, as have been found for the refolding of other proteins such as the 89 amino acid protein barstar (Agashe *et al.*, 1995) and the small all β-sheet protein CTX(III) (Sivaraman *et al.*, 1998). The refolding process is slower than for many proteins of a similar size (Jaenicke, 1987; Grantcharova *et al.*, 2001; Gunasekaran *et al.*, 2001): this might be a feature of a number of α/β domain proteins, where the formation of the β-sheet is expected to be a slower process than the formation of α-helices (Houry *et al.*, 1999; Plaxco *et al.*, 1998; Sivaraman *et al.*, 1998). The outline model proposed involves 3 intermediates (I_1, I_2 and I_3) between the unfolded state (U) and the native state (N). The results indicate that the pathway described for SK should act as a model for many other members of this subclass of α/β proteins.

A more complete understanding of the folding mechanism will be derived from further experimental investigations to explore the nature of the early formed intermediate(s) by using CD over a wider range of wavelengths in the far-UV or using a range of selected mutants. These could be used in conjunction with theoretical studies such as those reported in the case of AK, where molecular dynamics calculations were used to demonstrate the importance of the N-terminal 36 residue block of adenylate kinase from *Saccharomyces cerevisiae* in directing the folding of the protein (Kumar *et al.*, 2001). Indirect evidence suggesting that this may also be the case for the folding of SK comes from our observations that the native structure of the shikimate-binding domain is only formed at the later stages of the process. Moreover further detailed studies of the refolding of mutants of SK in which the proline residues had been systematically substituted and of the refolding after very short periods of unfolding (the "double jump" technique (Nall, 1994)) would help to establish the role (if any) played by isomerisation of Xaa-Pro bonds in the refolding of the enzyme.

The residual ionic strength in solution seems to have an effect on the outcome and the rate of the refolding process. This effect seems to depend on the ionic species present in solution. In fact it has been found that the presence of NaCl or Na_2SO_4 in the refolding buffer leads to an increase in the refolding rate of both structure and activity. These results can account for the faster refolding observed when GdmCl was used as denaturant (Boam, 1999)

and underline the importance of taking into account the residual ionic strength of the solution during the refolding studies. Differences have been observed between the effects of NaCl and Na_2SO_4 on the refolding of SK suggesting that these two salts may exert their effect by different mechanisms. A more detailed study using stopped flow mixing would be useful to check this hypothesis. Finally further studies on the effect of fluoride on SK, which seem to impair the refolding process, would be interesting because of the particular effects of this salt on binding, stability and refolding.

SK can be refolded in 4M urea simply by increasing the ionic strength: this has been observed in a few other systems, such as the 63-residue N-terminal domain of the C1 repressor from bacteriophage 434 (Dotsch *et al.*, 1995) and the peroxidase from *Coprinus cinerus* (Tams *et al.*, 1996). The refolded SK in these conditions has similar secondary and tertiary structure to the native enzyme. It appears to be able to bind shikimate weakly but with a reduced conformational response as judged by the limiting extent of fluorescence quenching. Though there is no direct evidence (from fluorescence quenching data) for binding of nucleotide substrates to the refolded enzyme, there is indirect evidence for some interaction with nucleotide from the observed tightening of shikimate binding in the presence of 2mM ADP. The refolded enzyme does not display catalytic activity: this is likely to reflect subtle perturbations both of the nucleotide binding site itself and of the ability of the enzyme to bring the substrates into the correct alignment for the phosphotransfer reaction. From the analysis of different traces obtained monitoring different parameters, characteristic patterns emerge for the two salts used. In the case of refolding induced by Na_2SO_4, the charged Trp environment and the tertiary environment are formed in the same type of process; this does not appear to be the case when NaCl is used to start the refolding. It seems that the charged arginine cluster in SK could play a role in the case of the refolding induced by chloride ions. From the re-analysis of the crystallographic structure it appears that chloride ions are involved in interactions with Arg11, 139 and 58 which are clustered around the single Trp (Trp54) of SK. In particular one of the chloride ions interacts, in some of SK structures, with both Arg11 and 139. So the binding of chloride to a specific site could be considered as a "nucleating" point that could lead to the subsequent folding of the entire protein molecule. These considerations lead to the idea that the refolding induced by the two salts may follow different mechanisms.

It would be interesting in future work to characterise this "partially folded" form of SK in more detail and to examine whether conditions can be found under which it can be readily converted to an active form. Moreover a study of the interactions present in the 4M unfolded enzyme (e.g. by NMR), in the absence and in presence of salts, would give insights into the cluster of interactions that are likely to be involved in this kind of folding process.

5.4 Future work

It would be interesting to use the SRS facility to study the early events in the folding of this protein and to undertake a more detailed study, using the SF-instruments available in the lab, of the effects of different salts on the refolding, thus extending the manual mixing data already available. Therefore, it would be possible to check for general effects (eg: ionic strength) or specific effects due to ion binding.

The role of the N-terminal segment in the refolding could be studied in more detail, both with dynamic simulations (like those already performed with adenylate kinase) and with studies of mutants (eg: studying the refolding of the K15M mutant).

Because mobility plays an important role in enzyme activity, it would be interesting to perform studies using methods such as NMR to characterise the changes in mobility, in different medium conditions, in more detail.

More protection experiments could be carried out in the prescence of different salts and particularly in the prescence of NaF because some of the results obtained in this work seem to indicate an increased protection by ADP in the prescence of NaF. Moreover the effects of this particular salts on the refolding, activity and binding of substrates could be studied in more detail.

Finally it would be interesting to further characterise the "partially folded" form of SK obtained in 4M urea and to examine whether conditions can be found under which it can be readily converted to an active form.

References

Adams R.D., Babin J.E., Tasi M. (1987) An unusual example of intramolecular hydrogen bonding in a metal carbonyl cluster compound -- Synthesis and crystal and molecular structure of RU6(CO)16(MU-CO)2(MU-OH)2(MU-4-S). *Inorganic Chemistry* **26**: 2561-2563

Agashe V.R., Shastry M.C.R., Udgaonkar J.B. (1995) Initial hydrophobic collapse in the folding of barstar. *Nature* **377**: 754-757

Aguzzi A., Weismann C. (1997) Prion research: the next frontier. *Nature* **389**: 795-798

Akiyama S.,Takahashi S., Ishimori K., Morishima I. (2000) Stepwise formation of α-helices during cytochrome c folding. *Natl. Struct. Biol.* **7**: 514-520

Altamirano M.M., Golbik R., Buckle A.M., Fersht A.R. (1997) Refolding chromatography with immobilized mini-chaperones. *Proc. Natl. Acad. Sci. USA* **94**: 3576-3578

Anderson K.S., Johnson K.A. (1990) Kinetic and structural analysis of enzyme intermediates: lessons from EPSP synthase. *Chem. Rev.* **90**: 1131-1149

Anfinsen C.B. (1983) Principles that govern the folding of protein chains. *Science* **181**: 223-230

Antonny B., Bigay J., Chabre M. (1990) A novel magnesium-dependent mechanism for the activation of transducin by fluoride. *FEBS Lett.* **268**: 277-280

Antonny B., Sukumar M., Bigay J., Chabre M., Higashijma T. (1993) The mechanism of aluminium-independent G-protein activation by fluoride and magnesium.^{31}P-NMR spectroscopy and fluorescence kinetics studies. *J. Biol. Chem.* **268**: 2393-2402

Arai M., Ikura T., Semisotnov G.V., Kihara H., Amemiya Y., Kuwajima K. (1998) Kinetic refolding of beta-lactoglobulin. Studies by synchrotron X-ray scattering, and circular dichroism, absorption and fluorescence spectroscopy. *J.Mol. Biol.* **275**: 149-162

Arakawa T. (1986) Thermodynamic analysis of the effect of concentrated salts on protein interaction with hydrophobic and polysaccaride columns. *Arch. Biochem. Biophys.* **248**: 101-105

Arakawa T. (1989) The stabilization of beta-lactoglobulin by glycine and NaCl. *Biopolymers* **28**: 1397-1401

Arakawa T., Bhat R., Timasheff S.N. (1990) Why preferential hydration does not always

stabilize the native structure of globular protein. *Biochemistry* **29**: 1924-1931

Arakawa T., Timasheff S.N. (1982) Preferential interactions of proteins with salts in concentrated solutions. *Biochemistry* **21**: 6545-6552

Arakawa T.A., Timasheff S.N. (1984) Mechanism of protein salting in and salting out by divalent cation salts: balance between hydration and salt binding. *Biochemistry* **23**: 5912-5923

Aronson B.D., Somerville R.L., Epperly B.R., Dekker E.E. (1989) The structure of *Escherichia coli* L-threonine dehydrogenase. *J. Biol. Chem.* **264**: 5226-5232

Asea A., Rehli M., Kabingu E., Boch J.A., Bare O., Auron P.E., Stevenson M.A., Calderwood S.K. (2002) Novel signal transduction pathway utilized by extracellular HSP70: role of toll-like receptor (TLR) 2 and TLR4. *J. Biol. Chem.* **277**: 15028-15034

Bai Y., Englander S.W. (1996) Future direction in folding: the multi-state nature of protein structure. *Proteins* **24**: 145-151

Baker D., Sohl J.L., Agard D.A. (1992) A protein-folding reaction under kinetic control. *Nature* **356**: 263-265

Balasubramanian S., Abell C., Coggins J.R. (1990) Observation of an isotope effect in the chorismate synthase reaction. *J. Amer. Chem. Soc.* **112**: 8581-8583

Baldwin R.L. (1989) How does protein folding get started? *Trends Biochem. Sci.* **14**: 291-294

Baldwin R.L. (1994) Matching speed and stability. *Nature* **369**: 183-184

Baldwin R.L. (1996) How Hofmeister ion interactions affect protein stability. *Biophys. J.* **71**: 2056-2063

Baldwin R.L., Rose G.D. (1999a) Is protein folding hierarchic? I. Local structure and peptide folding. *Trends. Biochem. Sci.* **24**: 26-33

Baldwin R.L., Rose G.D. (1999b) Is protein folding hierarchic? II. Folding intermediates and transition states. *Trends. Biochem. Sci.* **24**: 77-83

Bandyopadhyay A.K., Sonawat H.M. (2000) Salt dependent stability and unfolding of [Fe2-S2] Ferrodoxin of halobacterium salinarium: spectroscopic invenstigations. *Biophysical J.* **79**: 501-510

Banerji S., Wakefield A.E., Allen A.G., Maskell D.J., Peters S.E., Hopkin J.M. (1993) The cloning and characterization of the *arom* gene of *Pneumocystis carinii*. *J. Gen.*

Mocrobiol. **139**: 2901-2914

Banuelos S., Muga A. (1995) Binding of molten globule-like conformations to lipid bilayers. *J. Biol. Chem.* **270**: 29910-29915

Barazi H.O., Zhou L., Templeton N.S., Krutzsch H.C., Roberts D.D. (2002) Identification of heat shock protein 60, as a molecular mediator of alpha 3 beta 1 integrin activation. *Cancer Res.* **62**: 1541-1548

Barteri M., Gaudiano M.C., Santucci R. (1996) Influence of glycerol on the structure and stability of ferric horse heart myoglobin: a SAXS and circular dichroism study. *Biochim. Biophys. Acta* **1295**: 51-58

Bartlett P.A., McLaren K.L., Max M.A. (1994) Divergence between the enzyme catalyzed and noncatalyzed synthesis of 3- dehydroquinate. *J. Org. Chem.* **59**: 2082-2085

Bartlett P.A., Satake K. (1988) Does dehydroquinate synthase synthesize dehydroquinate? *J. Amer. Chem. Soc.* **110**: 1628-1630

Baskakov I.V., Legname G., Baldwin M.A., Prusiner S.B., Cohen F.E. (2002) Pathway complexity of prion protein assembly into amyloid. *J. Biol Chem.* **277**: 21140-21148

Batalia M.A., Kirksey T.J., Sharma A., Jiang L., Abastado J.P., Yan S., Zhao R., Collins E.J (2000) Class I MHC is stabilized against thermal denaturation by physiological concentrations of NaCl. *Biochemistry* **39**: 9030-9038

Batas B., Schiraldi C., Chaudhuri J.B. (1999) Inclusion body purification and protein refolding using microfiltration and size exclusion chromatography. *J. Biotechnol.* **681**: 49-158

Bedell J.L., McCrary B.S., Edmondson S.P., Shriver J.W. (2000) The acid-induced folded state of Sac7d is the native state. *Protein Sci.* **9**: 1878-1888

Bender S.L., Widlanski T., Knowles J.R. (1989) Dehydroquinate synthase: the use of subtrate analogues to probe the early steps of the catalyzed reaction. *Biochemistry* **28**: 7560-7572

Bertrand L., Vertommen D., Depiereux E., Hue L., Rider M.H., Feytmans E. (1997) Modelling the 2-kinase domain of 6-phosphofructo-2-kinase/fructose-2,6-biphosphatase on adenylate kinase. *Biochem. J.* **321**: 615-621

Betts G., Evans H. (1968) The effect of cations on the electrophoretic mobility and substrate binding properties of pyruvatekKinase. *Biochim. Biophys.Acta* **167**: 190 -193

Bieri O., Wildegger G., Bachmann A., Wagner C., Kiefhaber T. (1999) A salt-induced kinetic intermediate is on a new parallel pathway of lysozyme folding. *Biochemistry* **38**: 12460-12470

Bigay J., Deterre P., Pfister C., Chabre M. (1987) Fluoride complexes of aluminium or beryllium act on G-proteins as reversibly bound analogues of the γ phosphate of GTP. *EMBO J.* **6**: 2907-2913

BioDrugs 2002 16: 72-74. Cancer Vaccine - Antigenics: Heat-shock protein cancer vaccine-antigenics, HSPPC-96, Oncophage ®

Bloemendal M., Johnson W.C. Jr. (1995) Structural information on proteins from circular dichroism spectroscopy possibilities and limitations, in: *Physical Methods to Characterize pharmaceutical proteins*, ed. By J.H.Herron et al.Plenum Press, New York

Boam D.J. Structure and stability studies of shikimate kinase. M.Sc. Thesis, University of Glasgow. October 1999

Bossemeyer D. (1995) Protein kinases - Structure and function. *FEBS Lett.* **369**: 57-61

Bradford M.M. (1976) A rapid and sensitive method for the quantitation of microgram quantities of protein utilizing the principle of protein-dye binding. *Analyt. Biochem.* **72**: 248-254

Braun P., Tommassen J. (1998) Function of bacterial propeptides. *Trends Microbiol.* **6**: 6-8

Brazin K.N., Mallis R.J., Fulton D.B., Andreotti A.H. (2002) Regulation of the tyrosine kinase Itk by the peptidyl-prolyl isomerase cyclophilin A. *Proc. Natl. Acad. Sci USA* **99**: 1899-1904

Bremers A.J, Parmiani G. (2000) Immunology and immunotherapy of human cancer: present conceps and clinical developments. *Crit. Rev. Onc. Hemat.* **34**: 1-25

Brockwell D.J., Smith, D.A., Radford, S.E. (2000) Protein folding mechanisms: new methods and emerging ideas. *Curr. Opin. Struct. Biol.* **10**: 16-25

Brooks III C. L., Gruebele M., Onuchic J. N., Wolynes P. G. (1998) Chemical physics of protein folding. *Proc. Natl. Acad. Sci. USA* **95**: 11037–11038

Bryngelson J.D., Onuchic J.N., Socci N.D., Wolynes P.G. (1995) Funnels, pathways, and the energy landscape of protein folding: a synthesis. *Proteins* **21**: 167-195

Bucciantini M., Giannoni E., Chiti F., Baroni F., Formigli L., Zurdo J., Taddei N., Ramponi G., Dobson C.M., Stefani M. (2002) Inherent toxicity of aggregates implies a

common mechanism for protein misfolding diseases. *Nature* **416**: 507-511

Bunick F.J., Kashket S. (1982) Binding of fluoride by yeast enolase. *Biochemistry* **21**: 4285-4290

Burton R.E, Huang G.S., Daugherty M.A., Calderone T.L., Oas T.G. (1997) The energy landscape of a fast-folding protein mapped by Ala →Gly substitutions. *Nat. Struct. Biol.* **4**: 305-310

Busch M.R., Ho C.E. (1990) Effects of anions on the molecular basis of the Bohr effect of hemoglobin. *Biophys. Chem.* **37**: 313-322

Bychkova V.E., Pain R.H., Ptitsyn O.B. (1988) The "molten globule" state is involved in the translocation of proteins across membranes? *FEBS Lett.* **238**: 231-234

Bychkova V.E., Ptitsyn O.B. (1995) Folding intermediates are involved in genetic diseases? *FEBS Lett.* **359**: 6-8

Cacace M.G., Landau E.M., Ramsden J.J. (1997) The Hofmeister series: salt and solvent effects on interfacial phenomena. *Q. Rev. Biophys.* **30**: 241-277

Campbell L., Gumbleton M., Ritchie K. (2001) Caveolae and caveolins in human disease. *Adv. Drug Delivery Revs.* **49**: 325-335

Cantor C.T., Schimmel P.R. (eds.) (1980) Biophysical Chemistry Vol.2, Freeman, New York, pp. 409-418

Capaldi A.P., Radford S.E. (1998) Kinetic studies of beta-sheet protein folding. *Curr.Op. Struc. Biol.* **8**: 86-92

Chan H.S., Dill K.A. (1990) Origins of structure in globular proteins. *Proc. Natl. Acad. Sci. USA* **87**: 6388-6392

Charles I.G., Keyte J.W., Brammar W.J., Smith M., Hawkins A.R. (1986) The isolation and nucleotide sequence of complex *AROM* locus of *Aspergillus nidulans*. *Nucleic Acids Res.* **14**: 2201-2213

Chen S.S., Engel P.C. (1974) Protection of glutamate dehydrogenase by nicotinamide-adenine dinucleotide against reversible inactivation by pyridoxal-5'-phosphate as a sensitive indicator of conformational change induced by substrates and substrate analogues. *Biochem. J.* **143**: 569-574

Chen S.S., Engel P.C. (1975) Equilibrium protection studies of the interaction of bovine glutamate dehydrogenase with purine nucleotide effectors. *FEBS Lett.* **58**: 202-205

Chen S.S., Engel P.C. (1975) The equilibrium position of the reaction of bovine liver glutamate dehydrogenase with pyridoxal-5'-phosphate. A demonstration that covalent modification with this reagent completely abolishes catalytic activity. *Biochem. J.* **147**: 351-358

Chiti F., Taddei N., Webster P., Hamada M., Fiaschi T., Ramponi G., Dobson C.M. (1999a) Acceleration of the folding of acylphosphatase by stabilization of local secondary structure. *Nat. Struct. Biol.* **6**: 380-387

Chiti F., Webster P., Taddei N., Clark A., Stefani M., Ramponi G., Dobson C.M. (1999b) Designing conditions for *in vitro* formation of amyloid protofilaments and fibrils. *Proc. Natl. Acad. USA* **96**: 3590-3594

Chothia C., Lesk A.M., Dodson G.G., Hodgkin D.C. (1983) Transmission of conformational change in insulin. *Nature* **302**: 500-505

Christensen H., Pain R.H. (1991) Molten globule intermediates and protein folding. *Eur. J. Biophys.* **19**: 221-229

Christensen H., Pain R.H. (1994) The contribution of the Molten Globule model, in *Mechanisms of Protein Folding* (Pain, R.H., ed.), IRL Press, Oxford, pp. 55-79

Clarke D.T., Jones G.R. (1999) Extended circular dichroism measurements using synchrotron radiation show that the assembly of clathrin coats requires no change in secondary structure. *Biochemistry* **38**: 10457-10462

Cleland J.L., Wang D.I. (1990) Cosolvent assisted protein refolding. *Biotechnology* (NY) **8**:1274-1278

Clementi C., Jennings P.A., Onuchic J.N. (2000) How native-state topology affects the folding of dihydrofolate reductase and interleukin-1 beta. *Proc.Natl.Acad. USA* **97**: 5871-5876

Coggins J.R. (1989) The shikimate pathway as target for herbicides. In "Herbicides and Plant Metabolism" (ed. Dodge, A.) pp.97-112. *Cambridge University Press, Cambridge*

Cohen F.E. (1999) Protein misfolding and prion diseases. *J. Mol. Biol.* **293**: 313-320

Coligan J.E., Dunnl B.M., Ploegh H.L., Speicher D.W. Wingfield P.T. In *Current Protocols in Protein Science* Chap. 7: Characterization of recombinant proteins; unit 7.6: Determining the CD spectrum of proteins. 1997- John Wiley & Son, Inc.

Collins K.D. (1995) Sticky ions in biological systems. *Proc. Natl. Acad. Sci. USA* **92**: 5553-5557

Consoli G.M., Cunsolo F., Geraci C., Neri P. (2001) Remarkable alkali cation template effect in 1,5-bridged calix [8] arenes. *Organic Lett.* **3**: 1605-1608

Cornish-Bowden A.C. (1995) *Analysis of enzyme kinetic data*. Oxford University Press, Oxford

Creighton T.E. (1990) Protein Folding . *Biochem.J.* **270**: 1-16

Creighton T.E.. (1994) The Protein Folding Problem, in *Mechanisms of Protein Folding* (Pain, R.H., ed.), IRL Press, Oxford, pp. 1-25

Cronet P., Bellsolell L., Sander C., Coll M., Serrano L. (1995) Investigating the structural determinants of the p21-like triphosphate and Mg^{2+} binding site. *J. Mol. Biol.* **249**: 654-664

Dagget V. (1998) Structure-function aspects of prion proteins. *Curr.Op. Biotech.* **9**: 359-365

Damaschun G., Damaschun H., Gast K., Zirwer D. (1999) Proteins can adopt totally different folded conformations. *J.Mol. Biol.* **29**: 1715-1725

Davies G.M., Barrett-Bee K.J., Jude D.A., Lehan M., Nichols W.W., Pinder P.E., Thain J.L., Watkins W.J., Wilson R.G. (1994) (6S)-6-fluoroshikimic acid an antibacterial agent acting on the aromatic biosynthetic pathway. *Antimmicrob. Agents Chemother.* **38**: 403-406

De Bernardez Clark E. (1998) Refolding of recombinant proteins. *Curr. Op. Biotech.* **9**: 157-163

De Bernardez Clark E. (2001) Protein Refolding for industrial processes. *Curr. Op. Biotech.* **12**: 202-207

De Feyter R.C., Davidson B.E., Pittard J. (1986) Nucleotide sequences of the transcription unit containing the *aroL* and *aroM* genes from *Escherichia coli* K-12. *J. Bacteriol.* **165**: 233-239

De Feyter R.C., Pittard J. (1986a) Genetic and molecular analysis of *aroL*, the gene encoding shikimate kinase II in *Escherichia coli* K-12. *J. Bacteriol.* **165**: 226-232

De Feyter R.C., Pittard J. (1986b) Purification and properties of shikimate kinase II from *Escherichia coli* K-12. *J. Bacteriol.* **165**: 331-333

Deka R.K., Kleanthous C., Coggins J.R. (1992) Identification of the essential histidine residue at the active site of *Escherichia coli* dehydroquinase. *J. Biol. Chem.* **267**: 22237-22242

Deng Y., Smith D.L. (1999) Rate and Equilibrium constants for protein unfolding and refolding determined by hydrogen exchange-mass spectrometry. *Analyt. Biochem.* **276**: 150-160

Deswarte J., De Vos S., Langhorst U., Steyaert J., Loris R. (2001) The contribution of metal ions to the conformational stability of ribonuclease T1-Crystal versus solution. *Eur. J. Biochem.* **268**: 3993-4000

Dever T.E., Glynias M.J., Merrick C. (1987) GTP-binding domain: three consensus sequence elements with distinct spacing. *Proc. Natl. Acad. Sci. USA* **84**: 1814-1818

Diederichs K., Schulz G.E. (1990) Three-dimensional structure of the complex between mitochondrial matrix adenylate kinase and its substrate AMP. *Biochemistry* **29**: 8138-8144

Dill K.A. (1985) Theory for the folding and stability of globular proteins. *Biochemistry* **24**: 1501-1509

Dill K.A. (1990) Dominat forces in protein folding. *Biochemistry* **29**: 7133-7155

Dill K.A. (1999) Polymer principles and protein folding. *Protein Sci.* **8**: 1166-1180

Dill K.A., Chan H.S. (1997) From Levinthal to pathways to funnels. *Nature Struct. Biol.* **4**: 10-9

Dinner A., Sali A., Karplus M. (1996) The folding mechanism of larger proteins. *Proc. Natl. Acad. Sci. USA* **93**: 8356-8361

Dobson C.M., Karplus M. (1999) The fundamentals of protein folding: bringing together theory and experiment. *Curr.Op. Struc.Biol.* **9**: 92-101

Dodd G.H., Radda G.K. (1968) 1-anilinonaphthalene-8-sulphonate, a fluorescent conformational probe for glutamate dehydrogenase. *Biochem. J.* **114**: 407-417

Dorin *et al.* (1998) Process for recovering refractile bodies containing heterologous proteins from microbial hosts. U.S. patent 4, 748, 234. Issued May31

Dotsch V., Wider G., Siegal G., Wuthrich K. (1995) Salt-stabilized globular protein structure in 7M aqueous urea solution. *FEBS Lett.* **372**: 288-290

Dreusicke D., Karlplus A., Schulz G.E. (1988) Refined structure of porcine cytosolic adenylate kinase at 2.1 Å resolution. *J. Mol. Biol.* **199**: 359-371

Dreusicke D., Schulz G.E. (1986) The glycine-rich loop of adenylate kinase forms a giant anion hole. *FEBS Lett.* **208**: 301-304

Duncan K., Edwards R.M.,Coggins J.R. (1987) The pentafunctional *arom* enzyme S. *cerevisiae* is a mosaic of monofunctional domains. *Biochem. J.* **246**: 375-386

Eaton W.A., Munoz V., Hagen S.J., Jas G.S., Lapidus L.J., Henry E.R., Hofrichter J. (2000) Fast Kinetics and mechanisms in protein folding. *Annu. Rev. Biophys. Biomol. Struct.* **29**: 327-359

Eder J., Rheinnecker M., Fersht A.R. (1993) Folding of substilin BPN': characterization of a folding intermediate. *Biochemistry* **32**: 18-26

Eftink M.R. (1991) Fluorescence techniques for studying protein structure. *Methods Biochem. Anal.* **35**: 127-205

Eftink M.R. (1997) Fluorescence methods for studying equilibrium macromolecule-ligand interactions. *Methods in Enzymol.* **278**: 221-255

Eftink M.R., Ghiron C.A. (1976) Exposure of tryptophanyl residues in proteins. Quantitative determination by fluorescence quenching studies. *Biochemistry* **15**: 672-680

Eftink M.R., Ghiron C.A. (1981) Fluorecence quenching studies with proteins. *Analyt. Biochemistry* **114**: 199-227

Eftink M.R., Ghiron C.A. (1984) Indole fluorescence quenching studies on proteins and model systems: use of the inefficent quencher succinimide. *Biochemistry* **23**: 3891-3898

Eftink M.R., Shastry M.C.R. (1997) Fluorescence methods for studying kinetics of protein-folding reactions. *Methods in Enzymol.* **278**: 258-286

Ellis R.J. (1998) Steric chaperones. *Trends. Biochem. Sci.* **23**: 43-45

Ellis R.J., Hartl F.U. (1999) Principles of protein folding in the cellular environment. *Curr. Op. Struc. Biol.* **9**: 102-110

Ellis R.J., Pinheiro T.J.T. (2002) Danger - misfolding proteins. *Nature* **416**: 483-484

Engelhard M., Evans P.A. (1995) Kinetics of interaction of partially folded proteins with a hydrophobic dye - evidence that molten globule character is maximal in early folding intermediates. *Protein Sci.* **4**: 1553-1562

Englander S.W. (2000) Protein folding intermediates and pathways studied by hydrogen exchange. *Annu. Rev. Biophys. Biomol. Struct.* **29**: 213-238

Englander S.W., Sosnick T.R., Engòander J.J., Mayne L. (1996) Mechanisms and uses of hydrogen exchange. *Curr. Op. Struc. Biol.* **6**: 18-23

Essex D.W., Li M., Miller A., Feinman R.D. (2001) Protein disulfide isomerase and sulfydryl-dependent pathways in platelet activation. *Biochemistry* **40**: 6070-6075

Essex D.W., Miller A., Swiatkowska M., Feinman R.D. (1999) Protein disulfide isomerase catalyzes the formation of disulfide-linked complexes of vitronectin with thrombin-antithrombin. *Biochemistry* **38**: 10398-10405

Essex P.W., Chen K., Swiatkowska M. (1995) Localization of protein disulfide isomerase to the external surface of the platlet plasma membrane. *Blood* **86**: 2168-2173

Eykman J.F. (1891) Uber die Shikimisaure. *Chem. Ber.* **24**: 1278-1303

Fandrich M., Fletcher M.A., Dobson C.M. (2001) Amyloids fibrils from muscle myoglobin. *Nature* **410**: 165-166

Ferguson N., Capaldi A.P., James R., Kleanthous C., Radford S.E. (1999) Rapid folding with and without populated intermediates in the homologous four-helix proteins Im7 and Im9. *J. Mol. Biol.* **286**: 1597-1608

Ferrari D.M., Soling H.D. (1999) The protein disulphide-isomerase family: unravelling a string of folds. *Biochem.J.* **339**: 1-10

Ferreira S.T., De Felice F.G. (2001) Protein dynamics, folding and misfolding: from basic physical chemistry to human conformational diseases. *FEBS Lett.* **498**: 129-134

Fersht A.R. (1993) Protein folding and stability: the pathway of folding of barnase. *FEBS Lett.* **325**: 5-16

Fersht A.R. (1995) Characterizing transition states in protein folding: an essential step in the puzzle. *Curr. Op. Struc. Biol.* **5**: 79-84

Fersht A.R. (1997) Nucleation mechanisms in protein folding. *Curr. Op. Struc. Biol.* **7**: 3-9

Fersht A.R. (1999) *Structure and mechanism in protein science: a guide to enzyme catalysis and protein folding.* Freeman, New York, pp. 540-614

Fersht A.R. (1999) Transition-state structure as a unifying basis in protein-folding mechanisms: contact order, chain topology, stability, and extended nucleus mechanism *Proc. Natl. Acad. Sci. USA* **97**: 1525-1529

Fischer G., Bang H., Mech C. (1984) Detremination of enzymatic catalysis for the *cis /trans* – isomerization of peptide bonds in proline-containing peptide. *Biomed. Biochim. Acta* **43**: 1101-1111

Fischer G., Schmid F.X. (1990) The mechanism of protein folding. Implications of in vitro refolding models for the novo protein folding and translocation in the cell. *Biochemistry* **29**: 2205-2212

Fisher T.E., Oberhauser A.F., Carrion-Vazquez M., Marszalek P.E., Fernandez J.M. (1999) The study of protein mechanics with the atomic force microscope. *Trends Biochem. Sci.* **24**: 379-384

Freedman R.B., Klappa P., Ruddock L.W. (2002) Protein disulfide isomerases exploit synergy between catalytic and specific binding domains. *EMBO Rep.* **3**: 136-140

Frost J.W., Bender J.L., Kadonaga J.T., Knowles J.R. (1984) Dehydroquinate synthase from *Escherichia coli*: purification, cloning, and construction of overproducers of the enzyme. *Biochemistry* **23**: 4470-4475

Fry D.C., Kuby S.A., Mildwan A.S. (1987) NMR studies of the AMP-binding site and mechanism of adenylate kinase. *Biochemistry* **26**: 1645-1655

Frydman J. (2001) Folding of newly translated proteins in vivo: the role of molecular chaperones. *Annu. Rev. Biochem.* **70**: 603-647

Galzitskaya O.V., Ivankov D.N., Finkelstein A.V. (2001) Folding nuclei in proteins. *FEBS Lett.* **489**: 113-118

Garbe T., Selvos S., Hawkins A., Dimitriadis G., Young D., Dougan G., Charles I. (1991) The *Mycobacterium tubercolosis* shikimate pathway genes: evolutionary relationship between biosynthetic and catabolic 3-dehydroquinases. *Mol. Gen. Genet.* **228**: 385-392

Garner C.C., Hermann K.M. (1984) Structural analysis of 3–deoxy–D-*arabino*-heptulosonate 7-phosphate by ^{1}H and natural-abundance ^{13}C NMR spectroscopy. *Carbohydr. Res.* **132**: 317-322

Garrido C., Gurbuxanni S., Ravagnan L., Kroemer G. (2001) Heat shock proteins: endogenous modulators of apoptotic cell death. *Biochem. Biophys. Res. Comm.* **286**: 433-442

Gegg C.V., Bowers K.E., Matthews C.R. (1997) Probing minimal independent folding units in dihydrofolate reductase by molecular dissection. *Protein Sci.* **6**: 1885-1892

Gerstein M., Schuls G., Chothia C. (1993) Domain closure in adenylate kinase *J.Mol.Biol.* **229**: 494-501

Gething M.J., Sambrook J. (1992) Protein folding in the cell. *Nature* **355**: 33-45

Giancola C., De Sena C., Fessas D., Graziano G., Barone G. (1997) DSC studies on

bovine serum albumin denaturation. Effects of ionic strength and SDS concentration. *Int. Journ. Biol. Macromol.* **20**: 193-204

Gianni S., Brunori M., Travaglini-Allocatelli C. (2001) Refolding kinetics of cytochrome C551 reveals a mechanistic difference between urea and guanidine. *Protein Sci.* **10**: 1685-1688

Gibson F. (1999) The elusive branch-point compound of aromatic amino acid biosynthesis. *Trends. Biochem. Sci.*. **24**: 36-38

Gilbert H.F. (1994) The formation of native disulfide bonds, in *Mechanisms of Protein Folding* (Pain, R.H., ed.), IRL Press, Oxford, pp. 104-136

Gill S.C., von Hippel P.H. (1989) Calculation of protein extinction coefficients from amino-acid sequence data. *Analyt. Biochem.* **182**: 319-326

Glenner G.G., Eanes E.D., Bladen H.A., Linke R.P., Termine J.D. (1974) Beta-pleated sheet fibrils. A comparison of native amyloid with synthetic protein fibrils. *J. Histochem. Cytochem.* **22**: 1141-1158

Goldbeck R.A., Kim-Shapiro D.B., Kliger D.S. (1997) Fast natural and magnetic circular dichroism spectroscopy. *Annu. Rev. Phys. Chem.* **48**: 453- 479

Goldbeck R.A., Thomas Y.G. , Chen E., Esquerra R.M., Kliger D.S.(1999) Multiple pathways on a protein-folding energy landscape: Kinetic evidence. *Proc. Natl. Acad. Sci. USA* **96**: 2782-2787

Goldberg E., Semisotnov G.V., Friguet B., Kuwajima K., Pitsyn O.B., Sugai S. (1990) An early immunoreactive folding intermediate of the tryptophan synthase beta 2 subunit is a 'molten globule'. *FEBS Lett.* **263**: 51-56

Goto Y., Calciano L.J., Fink A.L. (1990) Acid-induced folding of proteins. *Proc. Natl. Acad. Sci. USA* **87**: 573-577

Goto Y., Takahashi N., Fink A.L. (1990) Mechanism of acid-induced folding of proteins. *Biochemistry* **29**: 3480-3488

Grantcharova V., Alm E.J., Baker D., Horwich A.L. (2001) Mechanisms of Protein Folding. *Curr. Op. Struc. Biol.***11**: 70-82

Greenfield N.J. (1996) Methods to estimate the conformation of proteins and polypeptides from circular dichroism data. *Anal. Biochem.* **235**: 1-10

Griffin H.G., Gasson M.J. (1995) The gene (aroK) encoding shikimate kinase i from *Escherichia coli. DNA Sequence* **5**: 195-197

Gruys K.J., Marzabadi M.R., Pansegrau P.D., Sikorski J.A. (1993) Steady-state kinetic evaluation of the reverse reaction for *Escherichia coli* 5-enolpyruvylshikimate 3-phosphate synthase. *Arch. Biochem. Biophys.* **304**: 345-351

Gu Y., Reshetnikova L., Li Y., Wu Y., Yan H., Singh S., Ji X. (2002) Crystal structure of shikimate kinase from *Mycobacterium tuberculosis* reveals the dynamic role of the LID domain in catalysis. *J. Mol. Biol.* **319**: 779-789

Guerois R., Serrano L. (2001) Protein design based on folding models. *Curr. Op. Struc. Biol.* **11**: 101-106

Guijarro J.I., Sunde M., Jones J.A., Campbell J.D., Dobson C.M. (1998) Amyloid fibril formation by an SH3 domain. *Proc. Natl. Acad. Sci. USA* **95**: 4224-4228

Gunasekaran K., Eyles S.J., Hagler,A.T. , Gierasch L.M. (2001) Keeping it in the family: folding studies of related proteins. *Curr. Opin. Struct. Biol.* **11**: 83-93

Hamada D., Kidokoro S., Fukada H. , Takahashi K., Goto Y. (1994) Salt-induced formation of the molten globule state of cytochrome c studied by isothermal titration calorimetry. *Proc. Natl. Acad. Sci. USA* **91**: 10325-10329

Hamada D., Chiti F., Guijarro J.I., Kataoka M., Taddei N., Dobson C.M. (2000) Evidence concerning rate-limiting steps in protein folding from the effects of trifluoroethanol. *Nat. Struct. Biol.* **7**: 58-61

Hammarstrom P., Carlsson U. (2000) Is the unfolded state the rosetta stone of the protein folding problem? *Biochim. Biophys. Res. Comm.* **276**: 393-398

Harding M.W., Galat A., Uehling D.E., Schreiber S.L. (1989) A receptor for the immunosuppressant FK506 is a *cis-trans* peptidyl-prolyl isomerase. *Nature* **341**: 758-760

Harrar Y., Bellini C., Faure J.D. (2001) FKBPs: at the crossroads of folding and transduction. *Trends Plant Sci.* **6**: 426-431

Harris J.M., Gonzales-Bello C., Kleanthous C.K., Hawkins A.R., Coggins J.R., Abell C. (1996) Evidence from kinetic isotope studies for an enolate intermediate in the mechanism of type II dehydroquinases. *Biochem J.* **319**: 333-336

Harrison S.C., Durbin R. (1985) Is there a single pathway for the folding of a polypeptide chain? *Proc. Natl. Acad. Sci. USA* **82**: 4028-4030

Hartl F.U. (1996) Molecular chaperones in cellular protein folding. *Nature* **381**: 571-580

Hasemann C.A., Istvan E.S., Uyedak K., Deisenhofer J. (1996) The crystal structure of the bifunctional enzyme 6-phosphofructo-2-kinase/fructose-2,6-bisphosphatase reveals distinct domain homologies. *Structure* **4**: 1017-1029

Haslam E. (1993) Shikimic acid: Metabolism and Metabolites. Chichester: John Wiley & Sons

Hawkes T.R., Lewis T., Coggins J.R., Mousdale D.M., Lowe D.J., Thorneley R.N.F. (1990) Chorismate synthase, pre-steady-state kinetics of phosphate release from 5-enolpyruvylshikimate 3-phosphate. *Biochem.J.* **265**: 899-902

Hawkins A.R., Smith M. (1991) Domain structure and interaction within the pentafunctional arom polypeptide. *Eur. J. Biochem.* **196**: 717-724

Heidary D.K., O'Neill J.C., Roy M., Jennings A. (2000) An essential intermediate in the folding of dihydropholate reductase. *Proc. Natl. Acad. Sci. USA* **97**: 5866-5870

Hendrick J.P., Hartl F.U. (1993) Molecular chaperone functions of heat-shock proteins. *Annu. Rev. Biochem.* **62**: 349-384

Hermann K.M. (1995a) The common aromatic biosynthetic pathway. In *Amino Acids: Biosynthesis and Genetic Regulation*, ed. K.M. Hermann, R.L. Somerville, 17: 301-322. London: Addison-Wesley. 453 pp.

Hermann K.M. (1995b) The shikimate pathway as an entry to aromatic secondary metabolism. *Plant Physiol.* **107**: 7-12

Hermann K.M., Weaver L.M. (1999) The shikimate pathway. *Annu. Rev. Plant Physiol. Plant Mol. Biol.* **50**: 473-503

Hlodan R., Hartl F.U. (1994) How the protein folds in the cell, in *Mechanisms of Protein Folding* (Pain, R.H., ed.), IRL Press, Oxford, pp. 194-228

Hofmeister F. (1888) Zur lehre von der wirkung der salze. II. *Arch. Exp. Pathol. Parmakol. (Leipzig)* **24**: 247-260

Honig B. (1999) Protein Folding: from the Levinthal paradox to structure prediction. *J.Mol.Biol.* **293**: 283-293

Hope J., Shearman M.S., Baxter H.C., Chong A., Kelly S.M., Price N.C. (1996) Cytotoxicity of prion protein peptide ($PrP^{106-126}$) differs in mechanism from the cytotoxic activity of the Altzheimer's disease amyloid peptide Aβ25-35. *Neurodegeneration* **5**: 1-11

Hornby D.P., Whitmarsh A., Pinabarsi H., Kelly S.M., Price N.C., Shore P., Baldwin

G.S., Waltho J. (1994) The DNA recognition subunit of a DNA methyltransferase is predominantly a molten globule in the absence of DNA. *FEBS Lett.* **355**: 57-60

Horovitz A. (1998) Structural aspects of GroEL function. *Curr. Op. Struc. Biol.* **8**: 93-100

Horwich A.L., Weber-Ban E.U., Finley D. (1999) Chaperone rings in protein folding and degradation. *Proc. Natl. Acad. Sci. USA* **96**: 11033-11040

Houry W.A., Frishman D., Eckerskorn C., Lottspeich F., Hartl F.U. (1999) Identification of in vivo substrates of the chaperonin GroEL. *Nature* **402**: 147-154

Hung H.C., Chang G.G. (2001) Multiple unfolding intermediates of human placental alkaline phosphatase in equilibrium urea denaturation. *Biophysical J.* **81**: 3456-3471

Huth J.R., Perini F., Lockridge O., Bedows E., Ruddon R.W. (1993) Protein folding and assembly in vitro parallel intracellular folding assembly. *J. Biol. Chem.* **268**: 16472-16482

Hutter M.C., Helms V. (2000) Phosphoryl transfer by a concerted reaction mechanism in UMP/CMP-kinase. *Protein Sci.* **9**: 2225-2231

Idziak C., Price N.C., Kelly S.M., Krell T., Boam D.J., Lapthorn A.J., Coggins, J.R. (1997) The interaction of shikimate kinase from *Erwinia chrysanthemi* with substrates. *Biochem. Soc. Trans.* **25**: S627

Itzhaki L.S., Otzen D.E., Fersht, A.R. (1995) The structure of the transition state for folding of chymotrypsin inhibitor 2 analysed by protein engineering methods: evidence for a nucleation-condensation mechanism for protein folding. *J. Mol. Biol.* **254**: 260-288

Jaattela M. (1999) Escaping cell death: survival proteins in cancer. *Exp. Cell Res.* **248**: 30-43

Jaenicke R. (1987) Folding and association of proteins. *Prog. Biophys. Mol. Biol.* **49**: 117-137

Jaenicke R. (1991) Protein folding: local structures, domains, subunits, and assemblies. *Biochemistry* **30**: 3147-3161

Jaenicke R. (2000) Stability and stabilization of globular proteins in solution. *J. Biothechnol.* **79**: 193-203

Jaspard E. (2000) Role of protein solvent interactions in refolding: Effects of cosolvent additives on the renaturation of porcine pancreatic elastase at various pHs. *Arch. Biochem. Biophys.* **375**: 220-228

Jelesarov I., Durr E.,Thomas R.M., Bosshard H.R. (1998) Salt effect on hydrophobic interaction and charge screening in the folding of a negatively charged peptide to a coiled coil (leucine zipper). *Biochemistry* **37**: 7539-7550

Johnson C.M., Price N.C. (1987) Denaturation and renaturation of the monomeric phosphoglycerate mutase from *Schizosaccharomyces pombe*. *Biochem. J.* **245**: 525-530

Johnson W.C.Jr (1988) Secondary structure of proteins through circular dichroism spectroscopy. *Ann. Rev. Biophys. Biophys. Chem.* **17**: 145-166

Karplus M., Weaver D.L. (1979) Diffusion-collision model for protein folding. *Biopolymers* **18**: 1421-1437

Karplus M., Weaver D.L. (1994) Protein folding dynamics. The diffiusion-collision model and experimental data. *Protein Sci.* **3**: 650-668

Kaytor M.D., Warren S.T. (1999) Aberrant protein deposition and neurological disease. *J. Biol. Chem.* **274**: 37507-37510

Kelly J.W. (1998) The environmental dependency of protein folding best explains prion and amyloid diseases. *Proc. Natl. Acad. Sci. USA* **95**: 930-932

Kelly S.M., Price N.C. (1997) The application of circular dichroism to studies of protein folding and unfolding. *Biochim. Biophys. Acta* **1338**: 161-185

Kelly S.M., Price N.C. (2000) The Use of circular dichroism in the investigation of protein structure and function. *Curr. Protein and Peptide Science* **1**: 349-384

Kinoshita K., Sadanami K., Kidera A., Go N. (1999) Structural motif of phosphate-binding site common to various protein superfamilies: all-against-all structural comparison of protein-mononucleotide complexes. *Protein Engineering* **12**: 11-14

Kirkitadze M.D., Barlow P.N., Price N.C., Kelly S.M., Boutell C., Rixon F.J., McClelland D.A. (1998) The herpes simplex virus triplex protein, VP23, exists as a molten globule. *J. Virology* **72**: 10066-10072.

Kishore G.M., Shah D.M. (1988) Amino acid biosynthesis inhibitors as herbicides. *Annu. Rev. Biochem.* **57**: 627-663

Kleanthous C., Reilly M., Cooper A., Kelly S.M., Price N.C., Coggins J.R. (1991) Stabilisation of the shikimate pathway enzyme dehydroquinase by covalently bound ligand. *J. Biol. Chem.* **266**: 10893-10898

Kleanthous C.K., Deka R., Davis K., Kelly S.M., Cooper A., Harding S.E., Price N.C.,

Hawkins A.R., Coggins J.R. (1992)A comparison of the enzymological and biophysical properties of two distinct classes of dehydroquimase enzymes. *Biochem. J.* **282**: 687-695

Kleppe R., Uhlemann K., Knappskog P.M., Haavik J. (1999) Urea induced denaturation of human phenylalanine hydroxylase. *J. Biol. Chem.* **274**: 33251-33258

Koshland D.E. (1958) Application of a theory of enzyme specificity to protein synthesis. *Proc. Natl. Acad. Sci. USA* **44**: 98-104

Krantz B.A., Sosnick T.R. (2000) Distinguishing between two-state and three-state model for ubiquitin folding. *Biochemistry* **39**: 11696-11701

Krell T., Coggins J.R., Lapthorn A.J. (1998) The three-dimensional structure of shikimate kinase. *J. Mol. Biol.* **278**: 983-997

Krell T., Coyle J.E., Horsburgh M.J., Coggins J.R., Lapthorn A.J. (1997) Crystallisation and preliminary X-ray crystallographic analysis of shikimate kinase from *Erwinia chrysanthemi. Acta Crystallographica* **D53**: 612-614

Krell T., Maclean J., Boam D.J., Cooper A., Resmini M., Brocklehurst K., Kelly S.M., Price N.C., Lapthorn A.J., Coggins J.R. (2001) Biochemical and X-ray crystallographic studies on shikimate kinase: the important structural role of the P-loop lysine. *Protein Sci.* **10**: 1137-1149

Kulkarni S.K., Ashcroft A.E., Carey M., Masselos D., Robinson C.V., Radford S.E. (1999) A near-native state on the slow refolding pathway of hen lysozyme. *Protein Sci.* **8**: 35-44

Kumar S., Ma B., Tsai C., Sinha N., Nussinov R. (2000) Folding and binding cascades: Dynamic landscapes and population shifts. *Protein Sci.* **9**: 10-19

Kumar S., Sham Y.Y., Tsai C.J. , Nussinov R. (2001) Protein folding and function: the N-terminal fragment in adenylate kinase. *Biophysical J.* **80**: 2439-2454

Kumar T.K.S., Jayaraman G., Lin W.Y., Yu C. (1996) Effect of chaotropic denaturant on the binding of 1-anilino-8-naphthalene sulfonic acid to proteins. *Biochim. Biophys. Acta* **1294**: 103-105

Kurzchalia T.V., Patron R. (1999) Membrane microdomains and caveolae. *Curr. Op. Cell. Biol.* **11**: 424-431

Kuwajima K., Yamaya H., Miwa S., Sugai S., Nagamura T. (1987) Rapid formation of secondary structure framework in protein folding studied by stopped-flow circular

dichroism. *FEBS Lett.* **221**: 115-118

Labhardt A.M. (1986) Folding intermediates studied by circular dichroism. *Methods in Enzymol.* 131: 126-135

Lahav J., Gofer-Dadosh N., Luboshitz J., Hess O., Shaklai M. (2000) Protein disulfide isomerases mediates integrin-dependent adhesion. *FEBS Lett.* **475**: 89-92

Lakowicz J.R. (1983a) Introduction to Fluorescence. In: *Principles of Fluorescence Spectroscopy.* Chap. 1, pp.1-18. Plenum Press, New York

Lakowicz J.R. (1983b) Protein Fluorescence. In: *Principles of Fluorescence Spectroscopy.* Chap. 11, pp.341-379. Plenum Press, New York

Lansbury P.T. Jr. (1999) Evolution of amyloid: what normal protein folding may tell us about fibrillogenesis and disease. *Proc. Natl. Acad. Sci. USA* **96**: 3342-3344

Lascu I., Schaertl S., Wang C., Sarger C., Giartosio A., Briand G., Lacombe M.L., Konrad M. (1997) A point mutation of human nucleoside diphosphate kinase A found in aggressive neuroblastoma affects protein folding. *J. Biol. Chem.* **272**: 15599-15602

Lebioda L., Zhang E., Lewinski K., Brewer J.M. (1993) Fluoride inhibition of yeast enolase: crystal structure of the enolase-Mg^{2+}-F^--Pi complex at 2.6 Å resolution. *Proteins* **16**:219-225

Leech A.P., Boetzel R., McDonald C., Shrive A.K., Moore G.R., Coggins J.R., Sawyer L., Kleanthous C. (1998) Re-evaluating the role of His-143 in the mechanism of Type I dehydroquinase from *Escherichia coli* using two-dimensional ^{1}H, ^{13}C NMR. *J. Biol. Chem.* **273**: 9602-9607

Levinthal C. (1968) Are there pathways for protein folding? *J. Chim. Phys.* **65**: 44-45

Lilie H., Schwarz E., Rudolph R. (1998) Advances in refolding of proteins produced in *E. coli*. *Curr. Op. Biotech.* **9**: 497-501

Lindsay J.G., Glover L.A. (1992) Targeting proteins to mitochindria: a current overview. *Biochem. J.* **284**: 609-620

Lopez-Hernandez E., Serrano, L. (1996) Structure of the transition state for folding of the 129 amino acid protein CheY resembles that of a smaller protein CI-2. *Fold. Des.***1**: 43-55

Low L.K., Shin H.C., Narayan M., Wedemeyer W., Scheraga H.A. (2000) Acceleration of oxidative folding of bovine pancreatic ribonuclease A by anion-induced stabilization

and formation of structured native-like intermediates. *FEBS Lett.* **472**: 67-72

Ma B., Kumar S., Tsai C.J., Nussinov R. (1999) Folding funnels and binding mechanisms. *Protein Engineering* **12**: 713-720

Ma B., Tsai C.J., Nussinov R. (2000) Binding and folding: in search of intramolecular chaperone-like building block fragments. *Protein Engineering* **13**: 617-627

Majumder K., Selvapandiyan A., Fattah F.A., Arora N., Ahmad S., Bhatnagar R.K. (1995) 5-enolpyruvyl-shikimate 3-phosphate synthase of *Bacillus subtilis* is an allosteric enzyme. *Eur. J. Biochem.* **229**: 99-106

Mande S.C., Sobhia M.E. (2000) Structural characterization of protein-denaturant ineractions: crystal structures of hen egg-white lysozyme in complex with DMSO and guanidinium chloride. *Protein Engineeing* **13**: 133-141

Martin J., Langer T., Boteva R., Schramel A., Horwich A.L., Hartl F.U. (1991) Chaperonin-mediated protein folding at the surface of GroEL through a "molten globule"-like intermediate. *Nature* **352**: 36-42

Maruta S., Aihara T., Uyehara Y., Homma K., Sugimoto Y., Wakabayashi K. (2000) Solution structure of myosin-ADP-MgF_n ternary complex by fluorescent probes and small-angle synchrotron x-ray scattering. *J. Biochem. (Tokyo)* **128**: 687-694

Maruta S., Henry G.D., Sykes B.D., Ikebe M. (1993) Formation of the stable myosin-ADP-aluminium fluoride and stable myosin-ADP-beryllium fluoride complexes and their analysis using 19F NMR. *J. Biol. Chem.* **268**: 7093-7100

Massimino M.L., Griffoni C., Spisni E., Toni M., Tomasi V. (2002) Involvment of caveolae and caveolae-like domains in signalling cell survival and angiogeneis. *Cell. Sign.* **14**: 93-98

Matouschek A., Serrano L., Fersht A.R. (1994) Analysis of protein folding by protein engineering, in *Mechanisms of Protein Folding* (Pain R.H., ed.), IRL Press, Oxford, pp.137-159

Matsuo Y., Nishikawa K. (1994) Protein structural similarities predicted by a sequence-structure compatibility method. *Protein Sci.* **3**: 2055-2063

McCandliss R.J., Poling M.D., Hermann K.M. (1978) 3-deoxy-D-*arabino*-heptulosonate 7-phosphate synthase. Purification and molecular characterization of the phenylalanine-sensitive isoenzyme from *E. coli*. *J. Biol. Chem.* **253**: 4259-4265

McClelland D.A, Price, N.C. (1998) Stopped flow analysis of the refolding of hen egg white riboflavin binding protein in its native and dephosphorylated forms. *Biochim. Biophys. Acta* **1382**: 157-166

McClelland D.A., McLaughlin S.H., Freedman R., Price N.C. (1995) The refolding of hen egg white riboflavin-binding protein: effect of protein disulphide isomerase on the reoxidation of the reduced protein. *Biochem. J.* **311**: 133-137

McPherson A. (1982) Preparation and analysis of protein crystals. Wiley, New York, pp. 1-51 and 82-159

Mevarech M., Frolow F., Gloss L.M. (2000) Halophilic enzymes: proteins with a grain of salt. *Biophysical Chemistry* **86**: 155-164

Midvan A.S. (1997) Mechanism of signaling and related enzymes. *Proteins* **29**: 401-416

Mildvan A., Cohn M. (1965) Kinetic and magnetic resonance studies of the pyruvate kinase reaction. I. Divalent metal complexes of pyruvate kinase *J. Biol. Chem.* **240**: 238

Millar G., Hunter M., Lewendon A., Coggins J.R. (1986) The cloning and expression of the aroL gene from *Escherichia coli* K-12. *Biochem. J.* **237**: 427-437

Milner-White J.E., Coggins J.R., Anton I.A. (1991) Evidence for an ancestral core structure in nucleotide-binding proteins with the type A-motif. *J.Mol. Biol.* **221**: 751-754

Minor D.L., Kim P.S. (1996) Context-dependent secondary structure formation of a designed protein sequence. *Nature* **380**: 730-734

Minton N.P., Whitehead P.J., Atkinson T., Gilbert H.J. (1989) Nucleotide sequence of an *Erwinia chrysanthemi* gene encoding shikimate kinase. *Nucleic Acids Res.* **17**: 1769

Miranker A., Robinson C.V., Radford S.E., Aplin R.T., Dobson C.M. (1993) Detection of transient protein folding population by mass spectrometry. *Science* **262**: 896-900

Mirny L.A., Abkevich V.J., Shakhnovich E.I. (1998) How evolution makes proteins fold quickly. *Proc. Natl. Acad. Sci. USA* **95**: 4976-4981

Moore J.D., Hawkins A.R., Charles I.G., Deka R., Coggins J.R., Cooper A., Kelly S.M., Price N.C. (1993) Characterisation of the type I dehydroquinase from *Salmonella typhi*. *Biochem. J.* **295**: 277-285

Moore W.J. (1962) Physical Chemistry 3rd ed. Prentice-Hall. pp. 368-369

Morillas M., Swietnicki W., Gambetti P., Surewicz W.K. (1999) Membrane environment alters the conformational structure of the recombinant human prion protein. *J. Biol.*

Chem. **274**: 36859-36865

Morillas M., Vanik D.L., Surewicz W.K. (2001) On the mechanism of α-helix to β-sheet transition in the recombinant prion protein. *Biochemistry* **40**: 6982-6987

Muller C.W., Schulz G.E. (1992) Structure of the complex between adenylate kinase from E.coli and the inhibitor Ap_5A refined at 1.9 A resolution. *J. Mol. Biol.* **224**: 159-177

Muller-Dieckmann H.J., Schulz G.E. (1994) The structure of uridylate kinase with its substrates, showing the transition state geometry. *J. Mol. Biol.* **236**: 361-367

Murzin A.G., Brenner S.E., Hubbard T., Chothia C. (1995) SCOP, a structural classification of proteins database for the investigation of sequence and structure. *J. Mol. Biol.* **247**: 536-540

Muzammil S., Kumar Y., Tayyab S. (2000) Anion-induced stabilization of Human Serum Albumin prevents the formation of intermediate during urea denaturation. *Proteins Str. Func. Gen.* **40**: 29-38

Nall B.T. (1994) Proline isomerization as a rate-limiting step, in *Mechanisms of Protein Folding* (Pain, R.H., ed.), IRL Press, Oxford, pp. 80-103

Nishii I., Kataoka M., Goto Y. (1995) Thermodynamic stability of the molten globule states of Apomyoglobin. *J. Biol. Chem.* **250**: 223-238

Nishimura C., Riley R., Eastman P., Fink A.L. (2000) Fluorescence energy transfer indicates similar transient and eqiulibrium intermediates in staphylococcal nuclease folding. *J. Mol. Biol.* **299**: 1133-1146

Nishimura C., Uversky V.N., Fink A.L. (2001) Effect of salts on the stability and folding of Staphylococcal Nuclease. *Biochemistry* **40**: 2113-2128

Nowak T., Maurer P.J. (1981) Fluoride inhibition of yeast enolase.II. Structural and kinetic properties of the ligand complexes determined by nuclear relaxation rate studies. *Biochemistry* **20**: 6901-6911

Nozaki Y. (1972) The preparation of guanidine hydrochloride. *Methods Enzymol.* **26**: 43-50

Nylandsted J., Rohde M., Brand K., Bastholm L., Elling F., Jaattela M. (2000) Selective depletion of heat shock protein 70 (Hsp 70) activates a tumor-specific death program that is independent of caspases and bypasses Bcl-2. *Proc. Natl. Acad. Sci. USA* **97**: 7871-7876

Oobatake M., Takahashi S., Ooi T. (1979) Conformational stability of ribonuclease T1.

II. Salt-induced renaturation. *J. Biochem (Tokyo)* **86**: 65-70

Orengo C. (1994) Classification of protein folds. *Curr. Op. Struc. Biol.* **4**: 429-440

Otzen D.E., Oliveberg M. (1999) Salt-induced detour through compact regions of the protein folding landscape. *Proc. Natl. Acad. Sci. USA* **96**: 11746-11751

Pace C.N. (1986) Determination and analysis of urea and guanidine hydrochloride denaturation curves. *Methods in Enzymol.* **131**: 266-280

Pace C.N. (1990) Conformational stability of globular proteins. *Trends Biochem. Sci.* **15**: 14-17

Pace C.N., Grimsley G.R. (1988) Ribonuclease T1 is stabilized by cation and anion binding. *Biochemistry* **27**: 3242-3246

Pace C.N., Hebert E.J., Shaw K.L., Schell D., Both V., Krajcikova D., Sevcik J., Wilson K.S., Dauter Z., Hartley R.W., Grimsley G.R. (1998) Conformational stability and thermodynamics of folding of ribonucleases Sa, Sa2 and Sa3. *J. Mol. Biol.* **279**: 271-286

Pace C.N., Schmid F.X. (1997) How to determine the molar absorbance coefficent of a protein. In *Protein Structure: a Practical Approach*. 2nd edn. Chap. 10. (Creighton T.E., ed.) pp. 253 -259 Oxford University Press, Oxford

Pace C.N., Scholtz J.M. (1997) Measuring the conformational stability of a protein. In Protein Structure: a Practical Approach. 2nd edn. Chap. 12. (Creighton T.E., ed.) pp. 299-321, Oxford University Press, Oxford

Panchenko A.R., Luthey-Schulten Z., Wolynes P.G. (1996) Foldons, protein structural modules, and exons. *Proc. Natl. Acad. Sci. USA* **93**: 2008-2013

Pande V.S., Grosberg Y., Tanaka T., Rokhsar D. (1998) Pathway for protein folding: is a new view needed? *Curr. Op. Struc. Biol.* **8**: 68-79

Paravicini G., Braus G., Hutter R. (1988) Structure of the ARO3 gene of *Saccharomyces cerevisiae*. *Mol. Gen. Genet.* **214**: 165-169

Paravicini G., Schmidheini T., Braus G. (1989) Purification and properties of the 3 - deoxy -D-*arabino*-heptulosonate 7-phosphate synthase (phenylalanine-inhibitable) of *Saccharomyces cerevisiae*. *Eur. J. Biochem.* **186**: 361-366

Pariser H.P., Zhang J., Hausman R.E. (2000) The cell adhesion molecule retina cognitin is a cell surface protein disulfide isomerase that uses disulfide exchange activity to modulate cell adhesion. *Exp. Cell Res.* **250**: 42-52

Park S., Ajrai K., Bughardt T.P. (1999) Inhibition of myosin ATP-ase by metal fluoride complexes. *Biochim. Biophys. Acta* **1430**: 127-140

Pergami P., Bramanti E., Ascoli G.A. (1999) Structural dependence of the cellular isoform of prion protein on solvent: spectroscopic characterization of an intermediate conformation. *Biochem. Biophys. Res. Comm.* **264**: 972-978

Pfeil W. (1998) Protein stability and folding: a collection of thermodynamic data. Springer, Berlin, Heidelberg, New York

Pinto J.E.B.P., Suzich J.A., Hermann K.M. (1986) 3-deoxy-D-*arabino*-heptulosonate 7-phosphate synthase from potato tuber (*Solanum tuberosum L.*). *Plant Physiol.* **82**: 1040-1044

Plapp B.V., Eklund H., Bränden C.I. (1978) Crystallography of liver alcohol dehydrogenase complexed with substrates. *J. Mol Biol.* **122**: 23-32

Plaxco K.W., Simons K.T., Baker D. (1998) Contact order, transition state placement and the refolding rates of single domain proteins. *J. Mol. Biol.* **277**: 985- 994

Pollack L., Tate M.W., Darnton N.C., Knight J.B., Gruner S.M., Eaton W.A., Austin R.H. (1999) Compactness of the denatured state of a fast-folding protein measured by submillisecond small-angle-X-ray scattering. *Proc. Natl. Acad. Sci.USA* **96**:10115-10117

Price N.C. (1972) The interaction of nucleotides with kinases, monitored by changes in protein fluorescence. *FEBS Lett.* **24**: 21-23

Price N.C. (1992) Folding and assembly of multi-subunit proteins, receptor subunits and complexes. Cambridge University press. Ed. A Barnard, A.S.V. Burgen, G.C.K. Roberts, pp. 9-37

Price N.C. (1994) Assembly of multi-subunit structures, in *Mechanisms of Protein Folding* (Pain, R.H., ed.), IRL Press, Oxford, pp. 160-193

Price N.C. (2000) Conformational issues in the characterization of proteins. *Biotechnol. Appl. Biochem.* **31**: 29-40

Price N.C., Boam D.J., Kelly S.M., Duncan D., Krell T., Gourley D.G., Coggins J.R., Virden R., Hawkins A.R. (1999) The folding and assembly of the dodecameric type II dehydroquinases. *Biochem. J.* **338**: 195-202

Price N.C., Stevens L. (1996) in *Principi di Enzimologia*.Ed. Antonio Delfino.2nd edition, pp.109-119

Privalov P.L. (1979) Stability of proteins: small globular proteins. *Adv.Protein Chem.* **33**:

167-241

Provencher S.W., Glöckner J. (1981) Estimation of globular protein secondary structure from circular dichroism. *Biochemistry* **20**: 33-37

Prusiner S.B. (1998) Prions. *Proc. Natl. Acad USA* **95**: 1363-13383

Prusiner S.B. (1997) Prion diseases and the BSE crisis. *Science* **278**: 245-251

Ptitsyn O.B. (1973) Stage mechanism of the self-organization of protein molecules. *Dokl. Acad. Nauk.* **210**: 1213-1215

Ptitsyn O.B. (1995a) Molten globule and protein folding. *Adv. Protein Chem.* **47**: 83-229

Ptitsyn O.B. (1995b) Structures of folding intermediates. *Curr. Op. Struc. Biol.* **5**: 74-78

Ptitsyn O.B. (1998) Protein folding and protein evolution: common folding nucleus in different subfamilies of c-type cytochromes? *J. Mol. Biol.* **278**: 655-666

Radford S.E. (2000) Protein folding – progress made and promise ahead. *Trends Biochem. Sci.* **25**: 611-618

Radford S.E., Dobson C.M., Evans P.A. (1992) The folding of hen lysozyme involves partially structured intermediates and mutliple pathways. *Nature* **358**: 302-307

Rahfeld J.U., Schierhorn A., Mann K., Fischer G. (1994) A novel peptidyl-prolyl *cis/trans* isomerase from *Escherichia coli*. *FEBS Lett.* **343**: 65-69

Ramjee M.N., Balasubramanian S., Abell C., Coggins J.R., Davies G.M., Hawkes T.R., Lowe D.J., Thorneley R.N.F. (1992) Reaction of (6R)-6-F-EPSP with recombinant Escherichia coli chorismate synthase generates a stable flavin mononucleotide semiquinone radical. *J. Amer. Chem. Soc.* **114**: 3151-3153

Ramjee M.N., Coggins J.R., Hawkes T.R., Lowe D.J., Thorneley R.N.F. (1991) Spectrophotometric detection of a modified flavin mononucleotide (FMN) intermediate formed during the catalytic cycle of chorismate synthase. *J. Amer. Chem. Soc.* **113**: 8566-8567

Randolph T.W., Carpenter J.F., St. John J.R. (2001) High pressure refolding of protein aggregates and inclusion bodies. International application 2000, WO 00/02 901

Ranson N.A., White H.E., Saibil H.R. (1998) Chaperonins. *Biochem. J.* **333**: 233-242

Reinstein J., Schlichting I., Wittinghofer A. (1990) Structurally and catalytically important residues in the phosphate binding loop of adenylate kinase of *Escherichia coli*. *Biochemistry* **29**: 7451-7459

Rhoads D.G., Lowenstein J.M. (1968) Initial velocity and equilibrium kinetics of myokinase. *J. Biol. Chem.* **243**: 3963-3972

Ribas de Pouplana L., Atrian S., Gonzàlez-Duarte R., Fothergill-Gilmore L.A., Kelly S.M., Price N.C. (1991) Structural properties of long-and short-chain alcohol dehydrogenases. *Biochem. J.* **276**: 433-438

Roberts C.W., Roberts F., Lyons R.E., Kirisits M.J., Mui E.J., Finnerty J., Johnson J.J., Ferguson D.J.P., Coggins J.R., Krell T., Coombs G.H., Milhous W.K., Kyle D.E., Tzipori S., Barnwell J., Dame J.B., Carlton J., McLeod R. (2002) The shikimate pathway and its branches in apicomplexan parasites. *J. Infect. Diseases* **185**: S25-36

Roberts F., Roberts C.W., Johnson J.J., Kyle D.E., Krell T., Coggins J.R., Coombs G.H., Milhous W.K., Tzipori S., Ferguson D.J.P., Chakrabarti D., McLeod R. (1998) Evidence for the shikimate pathway in apicomplexan parasites. *Nature* **39**: 3801-3805

Robinson G.W., Cho C.H. (1999) Role of Hydration Water in Protein Unfolding. *Biophysical J.* **77**: 3311-3318

Roder H., Colon W. (1997) Kinetic role of early intermediates in protein folding. *Curr. Op. Struc.Biol.* **7**: 15-28

Roder H., Elove G.A., Englander S.W. (1988) Structural characterization of folding intermediates in cytochrome c by H-exchange labelling and proton NMR. *Nature* **335**: 700-704

Roder H., Shastry M.R. (1999) Methods for exploring early events in protein folding. *Curr. Op. Struc. Biol.* **9**: 620-626

Royer C.A. (1995) Approaches to teaching fluorescence spectroscopy. *Biophysical J.* **681**:191-195

Ruddon R.W., Bedows E. (1997) Assisted protein folding. *J. Biol. Chem.* **272**: 3125-3128

Saborio G.P., Permanne B., Soto C. (2001) Sensitive detection of pathological prion protein by cyclic amplification of protein misfolding. *Nature* **411**: 810-813

Sanders C.R., Nagy J.K. (2000) Misfolding of membrane proteins in health and disease: the lady or the tiger? *Curr. Op. Struc. Biol.* **10**: 438-442

Sapan C.V., Lundblad R.L., Price N.C. (1999) Colorimetric protein assay techniques. *Biotechnol. Appl. Biochem.* **29**: 99-108

Saraste M., Sibbald P.R., Wittinghofer A. (1990) The P-loop a common motif in ATP

and GTP binding proteins. *Trends Biochem. Sci.* **15**: 430-434

Schiene-Fischer C., Yu C. (2001) Receptor accessory folding helper enzymes: the functional role of peptidyl prolyl *cis/trans* isomerases. *FEBS Lett.* **495**: 1-6

Schlauderer G.J., Proba K., Schulz G.E. (1996) Structure of mutant adenylate kinase ligated with an ATP-analogue showing domain clousure over ATP. *J. Mol. Biol.* **256**: 223-227

Schmid F.X. (1997) Optical spectroscopy to characterize protein conformation and conformational changes. In *Protein Structure: a Practical Approach.* 2nd edn. Chap. 12. (Creighton T.E., ed.) pp.261-296., Oxford University Press, Oxford

Schmid F.X., Mayr L.M., Mücke M., Schönbrunner E.R. (1993) Prolyl isomerases: role in protein folding. *Adv. Prot. Chem.* **44**: 25-66

Scholz J.M., York E.J., Stewart J.M., Baldwin R.L. (1991) *J. Amer. Chem. Soc.* **113**: 5102-5104

Schulz G.E., Muller C.W., Diederichs K. (1990) Induced-fit movements in adenylate kinases. *J. Mol. Biol.* **213**: 627-630

Scopes R.K. (1994) Separation by precipitation, in *Protein purification: principles and practice* 3rd ed. Springer, New York, pp. 71-101

Seto C.T., Bartlett P.A. (1994) (Z)-9-Fluoro-EPSP is not a substrate for SPSP synthase: implications for the enzyme mechanism. *J. Org. Chem.* **59**: 7130-7132

Shakhnovich E., Abkevich V., Ptitsyn O. (1996) Conserved residues and the mechanism of protein folding. *Nature* **379**: 96-98

Sham Y.Y., Ma B., Tsai C.J., Nussinov R. (2001) Molecular dynamics simulation of Escherichia coli dihydrofolate reductase and its protein fragments: relative stabilities of the protein fragments in experiment and simulations. *Protein Sci.* **10**: 135-148

Shapiro Y.E., Sinev A.M., Sineva E.V., Tugarinov V., Meirovitch E. (2000) Backbone dynamics of *Escherichia coli* adenylate kinase at the extreme stages of the catalytic cycle studied by ^{15}N NMR relaxation. *Biochemistry* **39**: 6634-6644

Sheehan D. (2000) Spectroscopic Techniques. In *Physical Biochemistry: Principles and Applications.* Chap. 3, pp. 74-87. John Wiley & Sons Ltd

Shinde U., Inouye M. (1995a) Folding mediated by an intramolecular chaperone: autoprocessing pathway of the precursor resolved via a substrate assisted catalysis mechanism. *J. Mol. Biol.* **247**: 390-395

Shinde U., Inouye M. (1995b) Folding Pathway mediated by an intramolecular chaperone: characterization of the structural changes in pro-substilin E coincident with autoprocessing. *J. Mol. Biol.* **252:** 25-30

Shinde U., Inouye M. (1997) Protein memory through altered folding mediated by intramolecular chaperones. *Nature* **389**: 520-522

Shinde U., Li Y., Chatterjee S., Inouye M. (1993) Folding pathway mediated by an intramolecular chaperone. *Proc. Natl. Acad. Sci. USA* **90**: 6924-6928

Shneier A., Harris J., Kleanthous C., Coggins J.R., Hawkins A.R., Abell C. (1993) Evidence for opposite stereochemical courses for the reactions catalyzed by type I and type II dehydroquinases. *Bioorg. Med. Chem. Lett.* **3**: 1399-1402

Siekierka J.J., Hung S.H., Poe M., Liu C.S., Sigal N.H. (1989) A cytosolic binding protein for the immunosuppressant FK506 has peptidyl-prolyl isomerase activity but is distinct from cyclophilin. *Nature* **341**: 755-757

Sigal I.S., Gibbs J.B., D'Alonzo J.S., Temeles G.L., Wolanski B.S., Socher S.H., Scolnick E.M. (1986) Mutant ras-encoded proteins with altered nucleotide binding exert dominant biological effects. *Proc. Natl. Acad. USA* **83**: 952-956

Sigurdsson E.M., Permanne B., Soto C., Wisniewski T., Frangione B. (2000) In vivo reversal of amyloid-beta lesions in rat brain. *J.Neuropathol. Exp. Neurol.* **59**: 11-17

Sikorski J.A., Gruys K.J. (1997) Understanding glyphosate's molecular mode of action with EPSP synthase: evidence favoring an allosteric inhibition model. *Acc. Chem.Res.* **30**: 2-8

Siligardi G., Drake A.F., Mascagni P., Rowlands D., Brown F., Gibbons W.A. (1991) Correlations between the conformations elucidated by CD spectroscopy and the antigenic properties of four peptides of the foot-and-mouth disease virus. *Eur.J. Biochem.***199**: 545-551

Sinev M.A., Sineva E.V., Ittah V., Haas E. (1996) Domain closure in adenylate kinase. *Biochemistry* **35**: 6425-6437

Singer J.S. (1962) The properties of proteins in nonaqueous solvents. *Adv. Protein Chem.* **17**:1-68

Sinha N., Kumar S., Nussinov R. (2001) Interdomain interactions in hinge-bending transitions. *Structure* **9**: 1165-1181

Sivaraman T., Kumar T.K.S., Chang D.K., Lin W.Y., Yu C. (1998) Events in the kinetic

folding pathway of a small, all beta-sheet protein. *J. Biol. Chem.* **273**: 10181-10189

Smith C.A., Rayment I. (1996) Active site comparison highlights structural similarities between myosin and other P-loop proteins. *Biophys. J.* **70**: 1590-1602

Smith C.A., Rayment I. (1995) X-ray structure of the magnesium(II)-pyrophosphate complex of the truncated head of Dictyostellium discoideum myosin to 2.7 Å resolution. *Biochemistry* **34**: 8973-8981

Soto C. (2001) Protein misfolding and disease; protein refolding and therapy *FEBS Lett.* **498**: 204-207

Soto C., Kascsak R.J., Saborio G.P., Aucouturier P., Wisniewski T., Prelli F., Kascsak R., Mendez E., Harris D.A., Ironside J., Tagliavini F., Carp R.I., Frangione B. (2000) Reversion of prion protein conformational changes by synthetic beta-sheet breaker peptide. *Lancet* **355**: 192-197

Soto C., Sigurdsson E.M., Morelli L., Kumar R.A., Castano E.M., Frangione B. (1998) Beta-sheet breaker peptides inhibit fibrillogenesis in rat brain model of amylosis: implications for Alzheimer's theraphy. *Nat. Med.* **4**: 822-826

Sreerama N., Woody R.W. (1993) A self-consistent method for the analysis of protein secondary structure from circular dichroism. *Analyt. Biochem.* **209**: 32-44.

Sreerama N., Woody R.W. (1994) Protein secondary structure from circular dichroism spectroscopy. *J. Mol. Biol.* **242**: 497-507

St. John R.J., Carpenter J.F., Randolph T.W. (1999) High pressure fostrers protein refolding from aggregates at high concentrations. *Proc. Natl. Acad. Sci. USA* **96**: 13029-13033

Staniforth R.A., Bigotti M.G., Cutruzzolà F., Travaglini Allocatelli C., Brunori M. (1998) Unfolding of apomyoglobin from aplysia limacina: the effect of salt and pH on the cooperativity of folding. *J.Mol.Biol.* **275**: 133-148

Steinrucken H.C., Amrhein N. (1980) The herbicide glyphosate is a potent inhibitor of 5-enolpyruvylshikimic acid 3-phosphate synthase. *Biochem. Biophys. Res. Commun.* **94**: 1207-1212

Stephens C.M., Bauerle R. (1991) Analysis of the metal requirement of 3-deoxy-D-*arabino* -heptulosonate 7-phosphate synthase from *Escherichia coli*. *J. Biol. Chem.* **266**: 20810-20817

Stockel J., Hartl F.U. (2001) Chaperonin-mediated de novo generation of prion protein

aggregates. *J. Mol. Biol.* **313**: 861-872

Story R.M., Steitz T.A. (1992) Structure of the recA protein-ADP complex. *Nature* **355**: 374-376

Sudarsanam S. (1998) Structural diversity of sequentially identical subsequences of proteins: identical octapeptides can have different conformations. *Proteins:Struct. Funct. Genet.* **30**:228-231

Suzich J.A., Dean J.F.D., Hermann K.M. (1985) 3-deoxy-D-*arabino*-heptulosonate 7-phosphate synthase from carrot root (*Daucus carota*) is a hysteretic enzyme. *Plant Physiol.* **79**: 765-770

Talzelt J., Voellmy R., Welch W.J. (1998) Abnormalities in stress proteins in prion diseases. *Cell. Mol. Neurobiol.* **18**: 721-729

Tams J.W., Welinder K.G. (1996) Unfolding and refolding of *Coprinus cinereus* peroxidase at high pH, in urea, and high temperature. Effect of organic and ionic additives on these processes. *Biochemistry* **35**: 7573-7579

Thatcher D.R., Hitchcock A. (1994) Protein folding in biotechnology, in *Mechanisms of Protein Folding* (Pain, R.H., ed.), IRL Press, Oxford, pp. 229-261

Timasheff S.N., Arakawa T. (1997) Stabilization of protein structure by solvents. In *Protein Structure: a Practical Approach*. 2nd edn. Chap. 14. (Creighton T.E., ed.) pp.349-364, Oxford University Press, Oxford

Todd M.J., Hausinger R.P. (2000) Fluoride inhibition of *Klebsiella aerogenes* urease: mechanistic implications of a pseudo-uncompetitive, slow-binding inhibitor. *Biochemistry* **39**: 5389-5396

Traut T.W. (1994) The functions and consensus motif of nine types of peptide segments that form different types of nucleotide-binding sites. *Eur. J. Biochem.* **222**: 9-19

Troullier A., Reinstadler D., Dupont Y., Naumann D., Forge V. (2000) Transient non-native secondary structures during the refolding of α- lactalbumin detected by infrared spectroscopy. *Nat. Struct. Biol.* **7**: 78-86

Tsai C.J., Kumar S., Ma B., Nussinov R. (1999) Folding Funnels, binding funnels and protein function. *Protein Sci.* **8**: 1181-1190

Tsai C.J., Nussinov R. (1997) Hydrophobic folding units derived from dissimilar monomer structures and their interactions. *Protein Sci.* **6**: 24-42

Tsai C.J., Xu D., Nussinov R. (1998) Protein folding via binding and vice versa. *Fold.*

Des. **3**: R71-R80

Tsou C.L. (1986) Location of the active sites of some enzymes in limited and flexible molecular regions. *Trends Biochem. Sci.* **11**: 427-429

Tsou C.L.(1993) Conformational flexibility of enzyme active sites. *Science* **262**: 380-381

Tume R., Thomas G.J. (1997) Mechanism of virus assembly probed by Raman spectroscopy: the icosahedral bacteriophage P22. *Biophys. Chem.* **68**: 17-31

Urbatsch I.L., Gimi K., Wilke-Mounts S., Senior A.E. (2000) Conserved Walker A Ser residues in the catalytic sites of P-glycoprotein are critical for catalysis and involved primarly at the transition state step. *J. Biol. Chem.* **275**: 25031-25038

Uversky V. N., Winter S., Lober G. (1996) Use of fluorescence decay times of 8-ANS-protein complexes to study the conformational transitions in proteins which unfold through the molten globule state. *Biophys. Chem.* **60**: 79-88

Uversky V. N., Winter S., Lober G. (1998a) Self-association of 8-anilino-1-naphthalene -sulfonate molecules: spectroscopic characterization and application to the investigation of protein folding. *Biochim. Biophys. Acta* **1388**: 133-144

Uversky V., Segel D.J., Doniach S., Fink A.L. (1998b) Association-induced folding of globular proteins. *Proc. Natl. Acad. Sci. USA* **95**: 5480-5483

Uversky V.N., Fink A.L. (2002) The chicken-egg scenario of protein folding revisited. *FEBS Lett.* **515**: 79-83

Valinger Z., Engel P.C., Metzler D.E. (1993) Is pyridoxal 5'-phosphate an affinity label for phosphate-binding sites in proteins? The case of bovine glutamate dehydrogenase. *Biochem. J.* **294**: 835-839

van der Goot F.G., Gonzales-Manas J.M., Lakey J.H., Pattus F. (1991) A "molten globule" membrane-insertion intermediate of the pore-forming domain of colicin A. *Nature* **354**: 408- 410

van Holde K.E., Johnson W.C., Ho P.S.(1998) Emission Spectroscopy. In *Physical Biochemistry,* ed. By Prentice-Hall, Inc. Chap. 11 pp. 452-483

Vey M., Pilkuhn S., Wille H., Nixon R., DeArmond S., Smart E.J., Anderson R.G.W., Taraboulos A., Prusiner S.B. (1996) Subcellular colocalization of the cellular and scrapie prion proteins in caveolae-like membranous domains. *Proc. Natl. Acad. USA* **93**: 14945-14949

Vinella D., Gagny B., Joselau-Petit D., D'Ari R., Cashel M. (1996) Mecillinam resistance

in *Escherichia coli* is conferred by loss of a second activity of the *aroK* protein. *J. Bacteriol.* **178**: 3818-3828

Von Hippel P.H., Schleich T. (1969) in "The effect of neutral salts on the structure of biological macromolecules" eds. Timasheff S.N., Fasman G.D., New York: Marcel Dekker Inc. pp.417-574

Vonrhein C., Schlauder G.J., Schulz G.E. (1995) Movie of the structural changes during a catalytic cycle of nucleoside monophosphate kinases. *Structure* **3**: 483-490

Walker G.E., Dunbar B., Hunter I.S., Nimmo H.G., Coggins J.R. (1996) Evidence for a novel class of microbial 3-deoxy-Darabino-heptulosonate 7-phosphate synthase in *Streptomyces coelicolor* A3(2), *Streptomyces rimosus* and *Neurospora crassa*. *Microbiology* **142**: 1973-1982

Walker J. E., Saraste M., Runswick M.J., Gay N.J. (1982). Distantly related sequences in the α- and β- subunits of ATP synthase, myosin, kinases and other ATP-requiring enzymes and a common nucleotide binding fold. *EMBO J.* **1**: 945-951

Walsh D.M., Hartley D.M., Kusumoto Y., Fezoui Y., Condron M.M., Lomakin A., Benedek G.B., Selkoe D.J., Teplow D.B. (1999) Amyloid beta-protein fibrillogenesis. *J. Biol. Chem.* **274**: 25945-25952

Walsh D.M., Klyubin I., Fadeeva J.V., Cullen W.K., Anwyl R., Wolfe M.S., Rowan M.J., Selkoe D.J. (2002) Naturally secreted oligomers of amyloid beta protein potently inhibit hippocampal long-term potentiation in vivo. *Nature* **416**: 535-539

Walter A., Kuehl G., Barnes K., VanderWaerdt G. (2000) The vesicle-to-micelle transition of phosphatidylcholine vesicles induced by nonionic detergents: effects of sodium chloride, sucrose and urea. *Biochim. Biophys. Acta* **1508**: 20-33

Wang G.F., Cao Z.F., Zhou H.M., Zhao Y.F. (2000) Comparison of inactivation and unfolding of methanol dehydrogenase during denaturation in guanidine hydrochloride and urea. *Int. J. Biochem. Cell. Biol.* **32**: 873-878

Wang Z., Feng H.P., Landry S.J., Maxwell J., Gierasch L.M. (1999) Basis of substrate binding by the chaperonin GroEL. *Biochemistry* **38**: 12537-12546

Ward L.D. (1985) Measurements of ligand binding to proteins by fluorescence spectroscopy. *Methods in Enzymol.* **117** :400-414

Washabaugh M.W., Collins K.D. (1986) The systematic characterisation by aqueous column chromatography of solutes which affect protein stability. *J. Biol. Chem.* **261**:

12477-12485

Weber G.(1997) Fluorescence in biophysics: accomplishments and deficiencies. *Methods in Enzymol.* **278**: 1-15

Weiss U., Edwards J.M. (1980) The biosynthesis of aromatic compounds, pp. 103-133. New York: John Wiley & Sons.

Weissman J.S. (1995) All roads lead to Rome? The multiple pathways of protein folding. *Chemistry & Biology* **2**: 255-260

Weissman J.S., Kim P.S. (1993) Efficient catalysis of disulphide bond rearrangements by protein disulphide isomerase. *Nature* **365**: 185-188

Westaway D., Telling G., Priola S. (1998) Prions. *Proc. Natl. Acad. Sci. USA* **95**: 11030-11031

Wetlaufer D.B. (1973) Nucleation, rapid folding, and globular interchain regions in proteins. *Proc. Natl. Acad. Sci. USA* **70**: 697-701

Wetlaufer D.B., Xie Y. (1995) Control of aggregation in protein refolding: a variety of surfactants promote renaturation of carbonic anhydrase II. *Protein Sci.* **8**: 1535-1543

Whipp M.J., Pittard A.J. (1995) A reassessment of the relationship between *aroK*- and *aroL*-encoded shikimate kinase enzymes of *Escherichia coli*. *J. Bacteriol.* **177**: 1627-1629

White P.J., Young J., Hunter I.S., Nimmo H.G., Coggins J.R. (1990) The purification and characterization of 3- dehydroquinase from *Streptomyces coelicolor*. *Biochem. J.* **265**: 735-738

Widlanski T., Bender S.L., Knowles J.R. (1989) Dehydroquinate synthase: the use of subtrate analogues to probe the late steps of the catalyzed reaction. *Biochemistry* **28**: 7572-7582

Wiggins P.M. (1997) Hydrophobic hydration, hydrophobic forces and protein folding. *Physica A* **238**: 113-128

Winter J., Klappa P., Freedman R.B., Lilie H., Rudolph R. (2002) Catalytic activity and chaperone function of human protein-disulfide isomerase are required for efficent refolding of proinsulin. *J. Biol. Chem.* **277**: 310-317

Wolynes P.G., Luthey-Schulten Z., Onuchic J.N. (1996) Fast folding experiments and the topography of protein folding energy landscapes. *Chem. Biol.* **3**: 425-432

Woody R.W. (1995) Circular dichroism. *Methods in Enzymol.* **246**: 34-71

Yonath A. (2002) The search and its outcome: High resolution structures of ribosomal particles from mesophilic, thermophilic, and halophilic bacteria at various functional states. *Annu. Rev. Biophys. Biomol. Struct.* **31**: 257-273

Yoshida M., Amano T. (1995) A common topology of proteins catalyzing ATP-triggered reactions. *FEBS Lett.* **359**: 1-5

Zhang H., Stockel J., Mehlhorn I., Groth D., Baldwin M.A., Prusiner S.B., James T., Cohen F.E. (1997) Physical studies of conformational plasticity in a recombinant prion protein. *Biochemistry* **36**: 3543-3553

Zhang H.J, Sheng X.R., Pan X.M., Zhou J.M. (1998) Refolding of urea-denatured adenylate kinase. *Biochem. J.* **333**: 401-405

Zhang J., Matthews C.R. (1998) The role of ligand binding in the kinetic folding mechanism of human $p21^{H\text{-}ras}$ protein. *Biochemistry* **37**: 14891-14899